

TWEAK-Fn14 Signalling in Acute and Chronic Skeletal Muscle Remodelling

Amy Pascoe

Bachelor of Science, Bachelor of Medical Science (Hons H1)

Submitted in fulfilment of the requirements for the Doctorate of Philosophy in Biochemistry and
Genetics

Department of Biochemistry and Genetics,

La Trobe Institute for Molecular Science

La Trobe University

Victoria, Australia

October, 2020

This document in its entirety is confidential.

Statement of Authorship

This thesis includes work by the author that has been published or accepted for publication as described in the text. Except where reference is made in the text of the thesis, this thesis contains no other material published elsewhere or extracted in whole or in part from a thesis accepted for the award of any other degree or diploma. No other person's work has been used without due acknowledgment in the main text of the thesis. This thesis has not been submitted for the award of any degree or diploma in any other tertiary institution.

All research procedures in this thesis were approved by the relevant Ethics Committee, Safety Committee, or authorised officer.

This work was supported by an Australian Government Research Training Program Scholarship.

- Amy Pascoe

14th October, 2020

Abstract

Skeletal muscle wasting is a devastating comorbidity associated with a range of acute and chronic health conditions. TWEAK-Fn14 signalling has been implicated in a number of muscle wasting models. The function of TWEAK-Fn14, and whether they can be targeted to combat atrophy or drive muscle growth, remains elusive. This thesis broadly aims to characterise the role of TWEAK-Fn14 signalling in acute and chronic muscle wasting.

This thesis consists of four results chapters as well as a two-part review of the literature. Chapter One provides a general overview of muscle homeostasis and is supplemented by a published review summarising TWEAK-Fn14 signalling in skeletal muscle with a particular emphasis on methodological inconsistencies and physiological relevance. Chapter Two is a general methods chapter. Chapter Three details development and characterisation of an agonistic α -Fn14 antibody using reporter cells and C2C12 myoblasts. Chapter Four describes unexpected adverse events observed in acute notexin-induced muscle injury model and argues for greater transparency in animal model usage. Chapter Five shows the effects of α -Fn14 antibodies on regenerating muscle following notexin-induced injury and compares these findings to muscle taken from old and chronically low-resistance trained mice. This chapter highlights the positive-feedback regulation of Fn14 by α -Fn14 antibodies with an apparent downstream effect on MyoD expression. Finally, Chapter Six explores adaptations in mitochondrial dynamics and autophagy markers as a function of low-resistance training in old and chronically low-resistance trained mice. This was pursued after TWEAK-Fn14 was not found to correlate with these markers of muscle health. Low-resistance late-in-life exercise is presented here as a promising and realistic intervention in old muscle health.

Overall, this thesis demonstrates a novel agonistic (activating) α -Fn14 antibody which is capable of activating Fn14 to drive both Fn14 and MyoD gene expression. In conjunction with *in vivo* characterisation, this provides insight into physiological roles of TWEAK-Fn14.

Acknowledgements

With the one exception of my experiments going wrong at every given opportunity, I could not have asked for a better PhD experience. Thank you so much to all the people who have made this chapter of my life so enjoyable.

To my lab mates, past and present, thank you for shaping me into the scientist that I have become with your generously shared knowledge and expertise. You have all come to feel like a second family over the years. Particular thanks to Heidy Flores and Stefan Wette, my constant coffee and lab companions who were always ready and willing to troubleshoot and commiserate over yet another disastrous western.

Thank you to Laura Jenkinson for putting up with my endless questions without ever blocking my number. Miranda Grounds, thank you of course for allowing me to raid your freezer but also for inviting me into your lab and your home. Chris van der Poel for all of your help with the animal models and the feedback over the years. The Australian Physiological Society for giving me the opportunity, time and time again, to present my work to such a friendly and receptive audience and for investing in the development of young researchers. Thank you to La Trobe, and particularly LIMS, for the financial support to travel and attend conferences and to write up my work. Thank you to all the lab animals, who sacrifice the most and get the least credit. This thesis is dedicated to all of them.

Thank you to my uni girl gang - Cristina Triffon, Rachael Impey, Cathryn Ugalde, and Tatiana Soares de Costa – I'm so proud to call this group of smart and driven women my friends and I can't wait to share a cup of tea (or gin and water) with you all soon. Thank you to my non-uni girl gang – Sophie 'Sasha' Hadden, Jess Whitby, Michelle 'Perky' Jackson, and Kate 'Pony'

Carter – you all know how much you mean to me, thanks for calling me Dr Amy well before I'd ever earned it.

To my wonderful partner, Niall Claridge, and our wonderful cat, Kitten, thank you for always making me smile. Thank you to my parents, Annette and Kevin, and my brother, Josh, who are still not entirely sure what it is I do but have always been very proud nonetheless.

Thank you to my mentor, Kaye Truscott, for going above and beyond and always reaching out to make sure I was supported and on track throughout my PhD.

To my co-supervisor, Amelia Johnston, who is a wealth of knowledge on all things Fn14, thank you for your continued support and guidance over the years.

Last but not least, thank you to my supervisor, Robyn Murphy. Thank you for cultivating a lab group that feels like home and that we all gravitate around even as we move off in different directions. Thank you for always uplifting young researchers, and particularly women in science. I truly wouldn't be where I am today without you always in my corner.

Abbreviations

001	α -Fn14 001
001X	α -Fn14 001X
2-ME	beta-mercaptoethanol
Akt	protein kinase B
AMP	adenosine monophosphate
AMPK	AMP-activated protein kinase
ANOVA	analysis of variance
ATP	adenosine triphosphate
BSA	bovine serum albumin
C2C12	mouse myoblast cell line
C57BL/6	C57 Black 6 inbred mouse strain
C57BL/10	C57 Black 10 inbred mouse strain
CD68	cluster of differentiation 68
clAP	cellular inhibitor of apoptosis
COXIV	cytochrome c oxidase subunit IV
CS	citrate synthase
DRP-1	Dynamin-1-like protein
DMEM	Dubecco's Modified Eagle Media

EDL	<i>extensor digitorum longus</i> muscle
EGTA	ethylene glycol-bis(β -aminoethyl ether)-N,N,N',N'-tetraacetic acid
FBS	foetal bovine serum
Fn14	Fibroblast growth factor-inducible 14
HEPES	4-(2-hydroxyethyl)-1-piperazineethanesulfonic acid
hFn14	human-derived Fn14
HIIT	high-intensity interval training
HR	high-resistance
LC3B	microtubule-associated proteins 1A/1B light chain 3B
IgG	immunoglobulin G
LR	low-resistance
MAPK	mitogen-activated protein kinase
MEF	mouse embryonic fibroblast
mFn14	mouse-derived Fn14
Mfn-2	Mitofusin-2
MHC	myosin heavy chain
MiD49	mitochondrial dynamics protein 49
MiD51	mitochondrial dynamics protein 51
MOPS	3-(N-morpholino)propanesulfonic acid

mOsmol	milliosmol
MRF4	myogenic regulatory factor 4
mTWEAK	membrane TWEAK
MuRF1	muscle RING-finger protein-1
Myf5	myogenic factor 5
MyoD	Myogenic differentiation 1
MyoG	Myogenin
NDUFA9	NADH:Ubiquinone Oxidoreductase Subunit A9
NFkB	Nuclear factor kappa B
NoAB	non-antibody treated
NTC	no template control
OCT	optimal cutting temperature
OPA-1	optic atrophy gene 1
p62	sequestosome 1
Pax3	paired box 3 gene
Pax7	paired box 7 gene
PBS	phosphate buffered saline
PBST	phosphate buffered saline with Tween-20
PGC-1 α	peroxisome proliferator-activated receptor gamma coactivator 1-alpha

PI3K	phosphoinositide 3-kinases
QUAD	<i>quadriceps</i> muscle
SDS	sodium dodecyl sulfate
SED	sedentary housed mice
Sulfo-SMCC	sulfosuccinimidyl 4-(N-maleimidomethyl) cyclohexane-1-carboxylate
SOL	<i>soleus</i> muscle
sTWEAK	soluble TWEAK
TA	<i>tibialis anterior</i> muscle
TBST	tris-buffered saline with Tween-20
TEMED	N,N,N',N'-tetramethylethylenediamine
TNF	Tumor necrosis factor
TNFSF	TNF superfamily
TNFRSF	TNF-receptor superfamily
TNFRSF12A	alternative name for Fn14
TWEAK	TNF α -like weak inducer of apoptosis
ULK	Unc-51-like kinase

List of Figures

Figure 1.1: Myogenic regulatory factors driving developmental and post-natal myogenesis..	6
Figure 3.1: Sulfo-SMCC crosslinking of α -Fn14 001 antibody.....	47
Figure 3.2: Efficacy of SMCC crosslinking of α -Fn14 001 to generate α -Fn14 001X.....	50
Figure 3.3: Binding of α -Fn14 001X to endogenous mouse Fn14 and induced human Fn14 in mouse embryonic fibroblast (MEF) H-Ras ^{V12} cells.....	51
Figure 3.4: NF κ B activity of α -Fn14 001 and α -Fn14 001X in soluble TWEAK (sTWEAK)-treated HEK293T NF κ B-GFP cells.....	53
Figure 3.5: Differentiation of C2C12 myotubes treated with α -Fn14 or soluble TWEAK (sTWEAK).....	55
Figure 4.1: Body weight and temperature change in C57BL/6 mice following intramuscular notexin injury.....	69
Figure 4.2: Gel electrophoresis and mass spectrometry of notexin.....	70
Figure 4.3: Representative images showing progression of tissue architecture recovery following notexin injury.....	71
Figure 4.4: Stain-free UV image of notexin injured samples.....	72
Figure 5.1: Degradation of tibialis anterior (TA) tissue architecture following notexin injury.....	89
Figure 5.2: Fn14 mRNA and protein in notexin-injured tibialis anterior (TA) muscle.....	91
Figure 5.3: Fn14 mRNA and protein in quadriceps (QUAD) from old and chronically low resistance-trained mice.....	92

Figure 5.4: TWEAK mRNA and protein in notexin-injured tibialis anterior (TA) muscle.	94
Figure 5.5: TWEAK mRNA and protein in quadriceps (QUAD) muscle from old and chronically low-resistance exercised mice.	95
Figure 5.6: Time course of myogenic regulatory factor mRNA levels in notexin-injured tibialis anterior (TA) mouse muscle.....	97
Figure 5.7: Myogenic regulatory factor mRNA in quadriceps (QUAD) muscle from old and low- resistance (LR) trained mice.	98
Figure 5.8: Correlation of MyoD and Fn14 transcripts in notexin-injury and ageing.....	99
Figure 5.9: Degradation of actin, myosin and desmin in notexin-injured tibialis anterior (TA) muscle.	101
Figure 5.10: Calpain-3 processing in notexin-injured tibialis anterior (TA) mouse muscle...	103
Figure 5.11: PGC-1 α mRNA in notexin-injured tibialis anterior (TA) mouse muscle.....	104
Figure 5.12: Endogenous IgG in notexin-injured tibialis anterior (TA) mouse muscle.....	106
Figure 5.13: CD68 in notexin-injured tibialis anterior (TA) mouse muscle.	107
Figure 5.14: MuRF1 and atrogin1 in notexin-injured tibialis anterior (TA) mouse muscle...	108
Figure 5.15: MuRF1 and atrogin1 in quadriceps (QUAD) muscle from old and low-resistance (LR) trained mice.....	109
Figure 5.16: Processing of p100-p52 in notexin-injured mouse tibialis anterior (TA) skeletal muscle.	111
Figure 5.17: Proposed positive feedback loop of Fn14 and MyoD.....	118

Figure 6.1: Mitochondrial fission and fusion.	136
Figure 6.2: Voluntary running activity levels.	143
Figure 6.3: Body weight and quadriceps muscle mass.	145
Figure 6.4: Mitochondrial protein content and activity.	147
Figure 6.5: Citrate synthase activity correlations.	148
Figure 6.6: Fibre type distribution.	149
Figure 6.7: PGC-1 α mRNA.	150
Figure 6.8: Mitochondrial fission and fusion.	152
Figure 6.9: AMPK α and ULK.	153
Figure 6.10: Phosphorylation of Acetyl-CoA.	155
Figure 6.11: LC3B conversion.	156
Figure 6.12: p62 accumulation and cleavage.	157
Figure II.1: Proliferation of C2C12 myotubes treated with α -Fn14 or soluble TWEAK (sTWEAK).	185
Figure II.2: p100-p52 in proliferation C2C12 myoblasts treated with soluble TWEAK (sTWEAK) and α -Fn14 antibodies.	186
Figure II.3: p100-p52 in differentiating C2C12 myoblasts treated with soluble TWEAK (sTWEAK) and α -Fn14 antibodies.	187
Figure III.1: Optimisation of whole muscle homogenates used for western blotting.	195

Figure III.2: Representative blot and stain-free UV image of Cell Signaling Technology 13812 α -MyoD antibody validation.	196
Figure III.3: Full western blot of TWEAK (Abcam 37170) in notexin-injured tibialis anterior (TA) mouse muscle.	198
Figure III.4: Western blot of TWEAK (Abcam 37170) below 43 kDa in notexin-injured tibialis anterior (TA) mouse muscle.....	199
Figure III.5: Western blot of suspected TWEAK bands excised for mass spectrometry.....	200
Figure III.6: TWEAK (abcam 37170) validation in mouse liver and skeletal muscle homogenates.	201
Figure III.7: TWEAK (abcam 37170) antibody testing in fractionated mouse skeletal muscle.	202
Figure IV.1: Actin and myosin content in notexin-injured tibialis anterior (TA) mouse skeletal muscle 21 days post-injury.	207
Figure IV.2: Fn14 mRNA and protein abundance following barium chloride (BaCl ₂)-induced skeletal muscle injury in mouse tibialis anterior (TA).....	208
Figure IV.3: Structural protein recovery following barium chloride (BaCl ₂)-induced skeletal muscle injury in mouse tibialis anterior (TA).....	209
Figure IV.4: Atrogin1 and MuRF1 expression following barium chloride (BaCl ₂)-induced skeletal muscle injury in mouse tibialis anterior (TA).....	210
Figure V.1: Correlation between Fn14 mRNA and normalised quadriceps muscle mass in old and chronically low-resistance (LR) trained mice.....	214

Figure V.2: Correlation between TWEAK mRNA and normalised quadriceps muscle mass in old and chronically low-resistance (LR) trained mice.....215

Figure V.3: Correlation between membrane-bound TWEAK (mTWEAK) protein and normalised quadriceps muscle mass in old and chronically low-resistance (LR) trained mice.....216

List of Tables

Table 2.1: iScript cDNA Synthesis Thermal Cycling Conditions	40
Table 2.2: iTaq Universal SYBR Green Supermix qPCR Thermal Cycling Settings.....	40
Table 5.1: Pathological scoring criteria for proteins of interest	86
Table 5.2: Samples with detectable Calpain-3.....	102
Table III.1: Antibody details. Full details of primary antibodies used for western blotting. CST, Cell Signaling Technologies; HRP, horse-radish peroxidase.	193
Table III.2: Primer sequences: Primer sequence details used for qPCR. Primer Bank ID cited where applicable (Spandidos et al., 2010).....	194
Table V.1: Pearson co-efficient tests of Fn14 mRNA correlation normalised quadriceps muscle mass in old and chronically low-resistance (LR) trained mice. Significant but weak correlation was seen only in Young Sedentary (SED) mice.	214
Table V.2: Pearson co-efficient tests of TWEAK mRNA correlation normalised quadriceps muscle mass in old and chronically low-resistance (LR) trained mice. No significant correlations were detected.	215
Table V.3: Pearson co-efficient tests of membrane-bound TWEAK (mTWEAK) protein correlation normalised quadriceps muscle mass in old and chronically low-resistance (LR) trained mice. No significant correlations were detected.....	216

Contents

Statement of Authorship	ii
Abstract.....	iii
Acknowledgements.....	v
Abbreviations.....	vii
List of Figures	xi
List of Tables	xvi
Chapter 1.....	1
Chapter Summary	2
1.1. Skeletal Muscle Homeostasis.....	3
1.1.1. Muscle Synthesis	4
1.1.2. Muscle Degradation	8
1.1.3. Fibre Type Switching.....	9
1.2. Mitochondrial Content and Function	10
References	12
Chapter 1 cont.	16
Thesis Outline and Aims.....	30
Chapter 2.....	32
Chapter Summary	33
2.1. Animals.....	34
2.1.1. Notexin Injury	34

2.1.2. Dissection.....	35
2.2. Old and Chronically Resistance-Trained Mice	35
2.3. Histology	36
2.3.1. Haemotoxylin and Eosin	36
2.4. Western Blotting.....	37
2.4.1. Sample Preparation	37
2.4.2. Immunodetection	37
2.5. Fibre Type Composition by SDS-PAGE	38
2.6. Gene Expression.....	39
2.6.1. cDNA synthesis	39
2.6.2. cDNA Quantification	40
2.6.3. qPCR.....	40
2.7. Cell Culture.....	41
2.8. Citrate Synthase Activity	41
2.9. Statistical Analyses.....	41
References	42
Chapter 3.....	43
Chapter Summary	44
3.1. Introduction	45
3.2. Methods.....	47

3.2.1.	Sulfo-SMCC cross-linkage of α -Fn14 001.....	47
3.2.1.1.	Fn14 Binding.....	47
3.2.1.2.	NF κ B Activation Assay.....	48
3.2.2.	In vitro myogenic effects of α -Fn14 001, α -Fn14 001X, and sTWEAK.....	48
3.2.2.1.	Differentiation Assay.....	49
3.3.	Results.....	50
3.3.1.	Cross-linked α -Fn14 001 Quality Control	50
3.3.2.	Fn14 Binding	51
3.3.3.	NF κ B Activation Assay in HEK293T NF κ B-GFP Reporter Cells	52
3.3.4.	Myogenic Effects in C2C12 Model Cells	53
3.3.4.1.	Differentiation Assay.....	53
3.4.	Discussion.....	56
3.4.1.	Crosslinking Efficacy and Purity.....	56
3.4.2.	Crosslinked Antibody Binds Human and Mouse Fn14	56
3.4.3.	Crosslinked α -Fn14 001 Activates Fn14 in Absence of sTWEAK	56
3.4.4.	Supraphysiological Dose sTWEAK Blunts C2C12 Differentiation	58
3.5.	Conclusions	59
	References	60
	Chapter 4.....	62
	Chapter Summary	63

Abstract.....	64
4.1. Introduction	65
4.2. Methods.....	66
4.2.1. Animals	66
4.2.1.1. Notexin Injury.....	66
4.2.1.2. Notexin Quality Control	67
4.2.2. Histology	67
4.2.3. Gel Electrophoresis.....	67
4.3. Results.....	68
4.3.1. Adverse Reactions to Notexin Injury	68
4.3.1.1. Notexin Quality Control	69
4.3.2. Tissue Architecture	70
4.3.3. Gel Electrophoresis.....	71
4.4. Discussion.....	72
References	76
Chapter 5.....	78
Chapter Summary	79
5.1. Introduction	80
5.2. Methods.....	83
5.2.1. Animals	83

5.2.1.1. Notexin Injury.....	83
5.2.1.2. Uninjured Control Animals.....	84
5.2.1.3. Old and Chronically Resistance Trained Mice.....	84
5.2.2. Histology.....	84
5.2.3. Western Blotting.....	85
5.2.3.1. Pathological Scoring.....	85
5.2.4. qPCR.....	87
5.2.5. Statistical Analyses.....	87
5.3. Results.....	88
5.3.1. Adverse Reactions to Notexin Injury.....	88
5.3.2. Fn14 mRNA and Protein Regulation.....	90
5.3.2.1. Fn14 in Notexin Injury.....	90
5.3.2.2. Fn14 mRNA and Protein in Ageing and Exercise.....	92
5.3.3. TWEAK mRNA and Protein Processing.....	93
5.3.3.1. TWEAK mRNA and Protein in Notexin Injury.....	93
5.3.3.2. TWEAK mRNA and Protein in Ageing and Exercise.....	95
5.3.4. Myogenic Regulatory Factors.....	96
5.3.4.1. Myogenic Regulatory Factors in Notexin Injury.....	96
5.3.4.2. Myogenic Regulatory Factors in Ageing and Exercise.....	98
5.3.5. Fn14 and MyoD Correlations.....	99

5.3.6.	Structural Proteins.....	100
5.3.6.1.	Actin, Myosin, and Desmin	100
5.3.6.2.	Calpain-3	102
5.3.7.	PGC-1a	104
5.3.8.	Infiltration of Immune Cells.....	105
5.3.9.	Atrogenes.....	108
5.3.9.1.	Atrogenes in Notexin Injury	108
5.3.9.2.	Atrogenes in Ageing and Exercise	109
5.3.10.	NFkB in Notexin Injury	110
5.4.	Discussion.....	112
5.4.1.	Notexin Injury Reproducibility is Unreliable.....	112
5.4.2.	Notexin Injury Induces Fn14 Expression	112
5.4.3.	Fn14 mRNA is Downregulated in Aged Muscle	113
5.4.4.	Notexin-Induced Fn14 Upregulation is Prolonged and Amplified by α -Fn14 Treatment	115
5.4.5.	MyoD is Transcriptionally Upregulated by α -Fn14 Treatment	116
5.4.6.	Soluble TWEAK is Expressed in Regenerating Tissue	120
5.4.7.	Structural Protein Recovery is Delayed by α -Fn14 Antibody Treatment.	121
5.4.8.	PGC-1 α mRNA Was Not Altered by α -Fn14 Antibody Treatment.....	122
5.4.9.	Inflammation is Prolonged by α -Fn14 Antibody Treatment	123
5.4.10.	Atrogenes Are Not Altered by α -Fn14 Antibody Treatment.....	124

5.4.11. Signalling Pathways.....	125
5.5. Conclusions	125
References	127
Chapter 6.....	132
Chapter Summary	133
6.1. Introduction	134
6.2. Methods.....	140
6.2.1. Animals	140
6.2.2. Western Blotting.....	141
6.2.3. Fibre Type Composition.....	141
6.2.4. qPCR.....	141
6.2.5. Citrate Synthase Activity Assay	141
6.2.6. Statistical Analyses and Graphs.....	142
6.3. Results.....	143
6.3.1. Running Activity Levels.....	143
6.3.2. Body Weight and Muscle Mass	144
6.3.3. Mitochondrial Content and Activity	146
6.3.4. Fibre Type	148
6.3.5. Mitochondrial Dynamics.....	150
6.3.6. Autophagy.....	153

6.4.	Discussion.....	158
6.4.1.	Mitochondrial content and activity are not reduced in old mice	158
6.4.2.	Old mice are metabolically responsive to low-resistance training	159
6.4.3.	Mitochondrial content and activity are lower in sedentary mice.....	162
6.4.4.	Autophagy is altered in old mice	163
6.4.5.	Low-resistance training is not sufficient to correct autophagy changes in old mice	165
6.5.	Conclusions	166
	References	168
	Chapter 7.....	173
	References	177
	Appendix I	178
	Appendix II	180
	Appendix Summary.....	181
II.a.	Introduction	182
II.b.	Methods.....	183
II.b.i.	C2C12 Proliferation Cell Count	183
II.b.ii.	NFκB Activation in C2C12 Cells.....	183
II.c.	Results.....	184
II.c.i.	Proliferation Assay.....	184
II.c.ii.	NFκB Activation in C2C12 Model Cells	186

II.d.	Discussion.....	188
II.d.i.	sTWEAK and α -Fn14 Treatments Do Not Prevent Proliferation	188
II.d.ii.	Supraphysiological Dose sTWEAK Strongly Activates Non-Canonical NF κ B 188	
II.d.iii.	α -Fn14 001 and α -Fn14 001X May Activate Fn14 Independently of sTWEAK 189	
	References	190
	Appendix III	191
	Appendix Summary.....	192
III.a.	Antibody details	193
III.b.	Primer details	194
III.c.	Optimisation of muscle homogenates	195
III.d.	Unsuccessful MyoD validation	196
III.e.	TWEAK antibody validation.....	197
	References	203
	Appendix IV.....	204
	Appendix Summary.....	205
IV.a.	Notexin Timeline Assessment	206
IV.a.i.	Validation of Regenerative Markers.....	207
	References	211
	Appendix V	212

Appendix Summary.....	213
V.a. Fn14 mRNA correlation with quadriceps mass.....	214
V.b. TWEAK mRNA correlation with quadriceps muscle mass.....	215
V.c. TWEAK protein correlation with quadriceps muscle mass.....	216

Chapter 1

Review of the Literature

Chapter Summary

This literature review is complementary to the published review, Pascoe *et al.* (2020), which forms part of this thesis. Pascoe *et al.* (2020) is focused on the specific purported roles of TWEAK and Fn14 signalling in muscle degeneration, growth, and repair, as well as the myogenic outcomes associated with NFκB, MAPK, and PI3K/Akt signalling. This additional review provides a brief general introduction to skeletal muscle structure, function, and homeostasis, and introduces the concept of mitochondrial dynamics. This chapter places the additional review along with the published review, Pascoe *et al.* (2020), in context with the overall thesis. The overall aims of the thesis can be found after the published review.

1.1. Skeletal Muscle Homeostasis

Skeletal muscle is one of the largest tissue types in the human body, comprising ~40% of total body weight in average healthy adults (Janssen *et al.*, 2000). Maintenance of skeletal muscle mass and function is critical for optimal locomotion, postural support, and metabolism (Jackman & Kandarian, 2004). Skeletal muscle is a highly plastic tissue, adapting dramatically to changes in stimuli. Muscles contraction produces force and allows the body to move. As part of this, a normal physiological function of skeletal muscle is to perform lengthening contractions which can result in acute micro-injuries to muscle fibres, triggering regeneration and remodelling of tissues to maintain function and they can constantly adapt to changing demands. Dysregulation of muscle damage or repair mechanisms can result in pathological muscle wasting. This dysregulation can occur due to insufficient muscle protein synthesis, excess muscle protein degradation, impaired muscle degradation resulting in accumulation of non-functional or damaged proteins, or some combination of the aforementioned (Jackman & Kandarian, 2004).

Loss of muscle mass and function is broadly categorised as muscle atrophy, or muscle wasting. Muscle atrophy is a comorbidity associated with an array of pathological and physiological conditions, including but not limited to – injury, immobilisation, malnutrition, cancer, diabetes, stroke, and ageing (Bonaldo & Sandri, 2013). Dramatic muscle atrophy can have devastating impacts on an individuals' quality of life, treatment responsiveness, and long-term health outcomes. The direct and indirect personal and healthcare burdens imposed by muscle atrophy are difficult to measure given the widespread prevalence and often secondary nature of this condition. The healthcare cost of falls in the elderly population – largely predicted by ageing-related muscle atrophy, or sarcopenia – was \$559 million in NSW, Australia alone in 2006-2007 (Watson *et al.*, 2010). Additionally, the presence of muscle

atrophy can limit the feasibility and efficacy of treatment options for the primary condition. This is observed in cancer cachexia – the loss of muscle and fat observed in up to 80% of cancer patients – which has been shown to not only predict the survival of cancer patients, but also reduce the efficacy of chemotherapy treatments (Mayr *et al.*, 2018). It is evident that therapeutics to prevent muscle atrophy and promote muscle regeneration and growth are desperately needed.

The multi-factorial nature of muscle atrophy is a significant hurdle in identifying and developing therapeutics. Despite similar clinical and functional presentation, there is a broad heterogeneity in the underlying biochemical processes and architectural characteristics observed in distinct forms of muscle atrophy (Sandri, 2013). Further, skeletal muscle is a heterogeneous tissue which does not respond uniformly to muscle wasting stimuli (Wang & Pessin, 2013). Experimental techniques that can differentiate the responses of different skeletal muscle types will be pivotal in understanding the mechanisms of muscle wasting.

1.1.1. Muscle Synthesis

Skeletal muscle synthesis, or myogenesis, occurs during development, growth, and repair. During development and regeneration, myogenesis is controlled by a tightly regulated host of transcription factors (Zammit, 2017). Amongst these are paired-box proteins 3 and 7 (Pax3 and Pax7), myogenic differentiation 1 (MyoD), myogenin (MyoG), myogenic factor 5 (Myf5), and myogenic factor 6 (MRF4), the latter four are collectively referred to as the myogenic regulatory factors, defined by their common basic helix-loop-helix motif.

In early myogenesis, muscle progenitor cells expressing *Pax3*, *Pax7*, *MyoD*, and *Myf5*, differentiate into myoblasts, which fuse to become multinucleated myotubes and develop into muscle fibres (Sabourin & Rudnicki, 2000). Post-development, a subset of progenitor cells

remain quiescent in the space between the basal lamina and sarcolemma of muscle cells (Hawke & Garry, 2001). These quiescent cells are named satellite cells and are activated in response to cellular damage. Upon activation, these satellite cells are able to undergo asymmetric division to differentiate and develop into myoblasts which fuse with existing myotubes to regenerate the muscle fibre, whilst still maintaining a pool of quiescent satellite cells (Le Grand & Rudnicki, 2007). This pro-myogenic pathway is observed following healthy recovery from muscle injury, such as that occurring with prolonged or loaded eccentric muscle contractions, which is the same mechanism which allows adaptation of muscle in response to training, e.g. hypertrophy through progressive resistance training, as in seen in body builders. Progression of the myogenic program is primarily controlled by the myogenic regulatory factors (Figure 1.1), with an apparent shift in function between development and post-natal myogenesis. A comprehensive review of myogenic regulatory factor regulation during myogenesis, both in development and mature muscle, is provided in Zammit (2017). It should be noted that hypertrophy has been observed in adult mice depleted of satellite cells in response to mechanical overload of the *plantaris* muscle, indicating that muscle growth is not entirely dependant upon generation of new myotubes (McCarthy *et al.*, 2011). Regeneration was, however, blunted in those same mice following barium chloride injury indicating that muscle regeneration is a distinct process from that of muscle growth (McCarthy *et al.*, 2011).

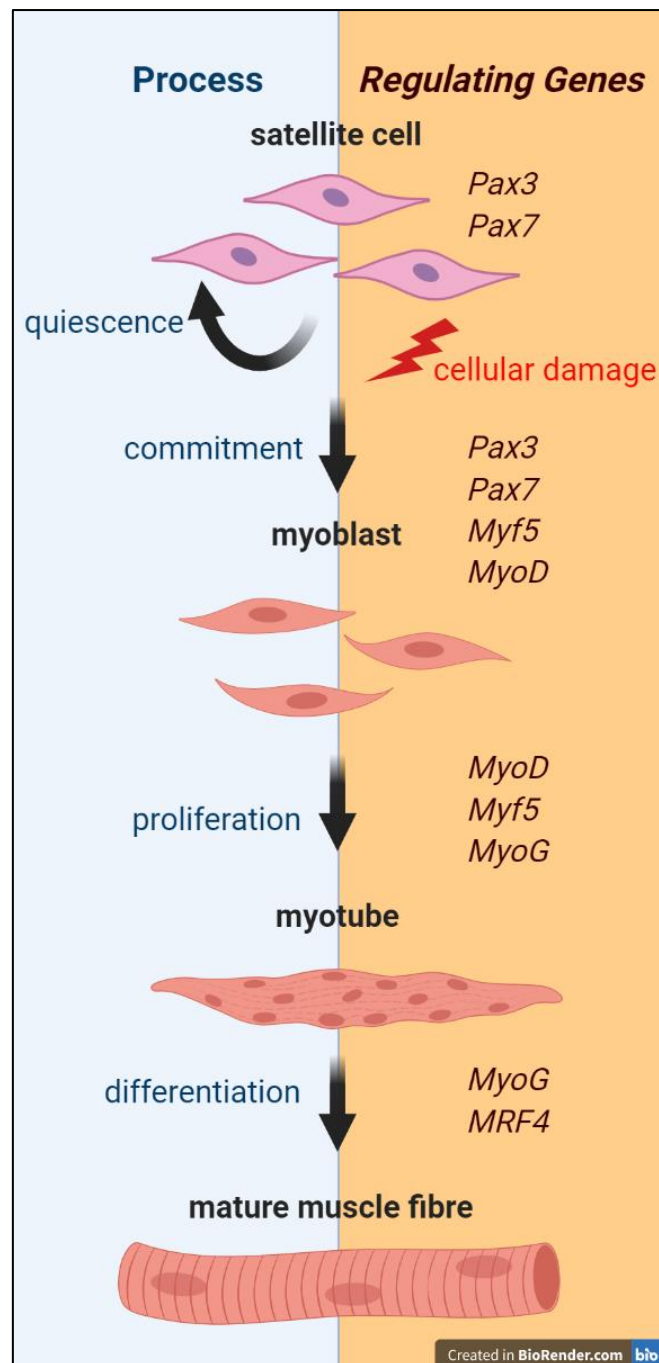


Figure 1.1. Myogenic regulatory factors driving developmental and post-natal myogenesis. Stages of the myogenic program, both developmental and post-natal, is shown with cellular processes involved in the myogenic program indicated in blue on the left and key regulatory genes in orange on the right. A population of quiescent satellite cells expressing *Pax3* and *Pax7* is maintained below the basal lamina of skeletal muscle (Sabourin & Rudnicki, 2000). When activated, by post-natal cellular damage or in the developmental program, *MyoD* is upregulated and satellite cells undergo asymmetric division, developing into myoblasts or retaining their pluripotency as satellite cells (Tapscott, 2005). Myoblasts proliferate under the influence of *MyoD*, *Myf5*, and *MyoG* before fusing into immature myotubes (Rantanen et al., 1995). Differentiation into mature muscle fibres is driven by *MyoG* and *MRF4* in the developmental stage (Hasty et al., 1993), with *MyoG* dispensable in the regeneration of mature muscle (Meadows et al., 2011). Created with BioRender.com.

Developmental myogenesis requires specification of progenitor cells to the myogenic lineage followed by differentiation and maturation into myofibers. Viable offspring have been produced in mice with the single knockdown of any one of *Myf5*, *MyoD*, and *MRF4*, whilst knockdown of all three failed to produce myoblasts and were embryonically lethal, suggesting these myogenic regulatory factors are at least partially redundant in early myogenesis (Rudnicki *et al.*, 1993; Kassam-Duchossoy *et al.*, 2004). Conversely, loss of *MyoG* during embryonic development results in failure of myoblasts to further differentiate leading to neonatal death, indicating an indispensable role of *MyoG* in embryonic myogenesis (Hasty *et al.*, 1993). This is distinct from the myogenic program observed in post-natal muscle regeneration (Figure 1.1).

Adult muscle regeneration can be studied acutely, using a range of injury models, or chronically, using degenerative phenotypes – such as the mouse model of Duchenne muscular dystrophy, the *mdx* mouse, and a range of ageing models. *Ex vivo* studies show *Myf5*-null mice are capable of entering early myogenesis, however myogenic potential is enhanced in *Myf5* heterozygotes, suggesting it may act as a primer for transcription of the other myogenic regulatory factors (Gayraud-Morel *et al.*, 2007; Gayraud-Morel *et al.*, 2012). Upregulation of the remaining myogenic regulatory factors is a temporally controlled program. Both *MyoD* and *MyoG* are transiently detectable at the protein level following acute injury – first appearing at 12 hours post-injury and persisting for several days – whilst *MRF4* plays no apparent role in the early regenerative process being undetectable until myoblasts have already fused and begun maturation (Figure 1.1; Rantanen *et al.*, 1995; Zhou & Bornemann, 2001). Loss of *MyoD* has been investigated in both acute and chronic regenerative mouse models and results in an apparent delay of regeneration (Smythe & Grounds, 2001), whilst loss of *MyoG* using a recombinant knockdown in the chronically regenerative *mdx* mouse had

no effect, suggesting that unlike embryonic myogenesis, MyoG is not essential to the mature muscle myogenic program (Meadows *et al.*, 2011).

1.1.2. Muscle Degradation

In opposition to myogenesis in the maintenance of muscle homeostasis is muscle degradation. Physiological muscle degradation is a result of increased protein turnover relative to protein synthesis. Degradation enables the removal of damaged or defective proteins and is a source of metabolic energy as breakdown products, such as amino acids, can be used to generate energy, or are lost from the intracellular environment. Protein turnover is driven by three key pathways; the ubiquitin proteasome system (UPS), the autophagy-lysosome pathway, and caspase-mediated proteolysis (Neel *et al.*, 2013; Sandri, 2013; Bell *et al.*, 2016). The UPS ubiquitinates proteins, tagging them for degradation via E3 ubiquitin ligases; ubiquitinated proteins are then recognised by the 26S proteasome, which encases the ubiquitinated protein and catalyses its degradation in an ATP-dependent process (Voges *et al.*, 1999). Pathological muscle wasting is often associated with enhanced UPS activity and an increase in the abundance of E3 ubiquitin ligase proteins (Sandri, 2013). Autophagy, or 'self-eating', is the process by which defective proteins are sequestered within membrane-bound vesicles, which, in turn, fuse with lysosomes where the defective protein is degraded and recycled (Rabinowitz & White, 2010). The autophagy-lysosome pathway is most notably upregulated in starvation-induced atrophy, as it attempts to compensate for the reduced metabolic intake by converting muscle mass into essential amino acids and ATP (Rabinowitz & White, 2010). Conversely, defects in the autophagy-lysosome pathway can result in the accumulation of defective proteins and has been observed in a number of degenerative muscle-wasting conditions, including Danon disease and Duchenne muscular dystrophy (Bell

et al., 2016). Lastly, caspase-mediated proteolysis involves a family of caspases (cysteine-aspartic proteases) involved in the apoptotic program (Bell *et al.*, 2016)

These pathways are dynamic and importantly, have described roles in myogenesis; UPS is involved in the regulation of myogenic regulatory factors in the myogenic program and the energy produced by autophagy-lysosomal degradation is a potential trigger for the activation of quiescent satellite cells in mature muscle regeneration (Gardrat *et al.*, 1997; Tang & Rando, 2014). Understanding the switch from physiological to pathological muscle degradation will be essential in targeting muscle atrophy.

1.1.3. Fibre Type Switching

In addition to muscle synthesis and degradation, skeletal muscle exhibits a high degree of plasticity with regard to fibre type composition. Skeletal muscle is broadly categorised into two main fibre types – fast and slow twitch – distinguished by their myosin type and metabolic profiles (Herbison *et al.*, 1982). Slow twitch – also classified as Type I fibres – are oxidative fibres with a high mitochondrial content. They are slow to fatigue and slow to recover, they are predominantly observed in muscles with low level but constant energy demands, such as postural support muscles in the trunk. Fast twitch fibres – further classified as Type IIA and Type IIB fibres in humans – rely on both oxidative and/or glycolytic metabolic pathways. Type II fibres are responsible for rapid and powerful movements and typically fatigue quickly but also recover rapidly, due to the different fatigue mechanisms that would occur (Allen *et al.*, 2008). The distinct profiles of fibre types will be addressed in this thesis in broad terms, though it is important to note there are nuanced differences in metabolic pathway and fatigability, particularly within the type II subtypes; a detailed overview of the metabolic profiles of each muscle fibre type is available in Herbison *et al.* (1982).

Fibre type proportion varies dramatically from species to species and muscle to muscle. In addition to this, fibre type proportion is highly plastic in response to energy demands. Type I slow twitch fibres are upregulated in endurance athletes, enabling them to sustain activity over a long duration (Fitts & Widrick, 1996). Type II glycolytic fibres are likewise upregulated in athletes with high intensity but short duration energy requirements, including sprinters and weightlifters. Fibre type shifting is a complex pathway with various triggers. A key player in fibre type composition is peroxisome proliferator-activated receptor gamma coactivator 1-alpha (PGC-1 α) (Lin *et al.*, 2002). PGC-1 α is a major driver of mitochondrial biogenesis; with mitochondrial content being a large determinant of fibre type based on its metabolic capacity, an upregulation of PGC-1 α promotes Type I biogenesis and hence fibre type switching (Lin *et al.*, 2002).

Fibre type composition is a contributing factor to muscle wasting susceptibility. Type I and Type II fibres do not respond uniformly to muscle wasting stimuli, with Type II fibres more susceptible to damage (Ciciliot *et al.*, 2013). PGC-1 α appears to have protective effects in response to damaging stimuli, with transgenic PGC-1 α expression shown to significantly reduce TWEAK-induced atrophy both *in vivo* in C57BL/6 mice and *in vitro* in cultured myotubes (refer to accompanying published literature review for further discussion of TWEAK; Brault *et al.*, 2010; Hindi *et al.*, 2014).

1.2. Mitochondrial Content and Function

As described above, mitochondrial content is a key characteristic of fibre type and plays a considerable role in dictating the functional profile of skeletal muscle with an ability to respond rapidly to training stimuli (Holloszy, 1967; Young *et al.*, 1983). Detrimental changes to mitochondrial content, as well as mitochondrial turnover (a process referred to as

mitochondrial dynamics) and function have been frequently associated with sarcopenia and dynapenia – age-associated loss of muscle mass and function respectively (Peterson *et al.*, 2012). The interaction of ageing and exercise training on the content and function of mitochondria is an emerging field with readily translatable aims. Chapter 6 explores more comprehensively the existing literature on mitochondrial content and function and examines these factors as potential correlates of ageing-associated sarcopenia distinct from the TWEAK-Fn14 pathway.

References

- Allen DG, Lamb GD & Westerblad H. (2008). Skeletal muscle fatigue: cellular mechanisms. *Physiol Rev* **88**, 287-332.
- Bell RA, Al-Khalaf M & Megeney LA. (2016). The beneficial role of proteolysis in skeletal muscle growth and stress adaptation. *Skelet Muscle* **6**, 16.
- Bonaldo P & Sandri M. (2013). Cellular and molecular mechanisms of muscle atrophy. *Disease models & mechanisms* **6**, 25-39.
- Brault JJ, Jespersen JG & Goldberg AL. (2010). Peroxisome proliferator-activated receptor gamma coactivator 1alpha or 1beta overexpression inhibits muscle protein degradation, induction of ubiquitin ligases, and disuse atrophy. *J Biol Chem* **285**, 19460-19471.
- Ciciliot S, Rossi AC, Dyar KA, Blaauw B & Schiaffino S. (2013). Muscle type and fiber type specificity in muscle wasting. *Int J Biochem Cell Biol* **45**, 2191-2199.
- Fitts RH & Widrick JJ. (1996). Muscle mechanics: adaptations with exercise-training. *Exerc Sport Sci Rev* **24**, 427-473.
- Gardrat F, Montel V, Raymond J & Azanza JL. (1997). Proteasome and myogenesis. *Mol Biol Rep* **24**, 77-81.
- Gayraud-Morel B, Chretien F, Flamant P, Gomes D, Zammit PS & Tajbakhsh S. (2007). A role for the myogenic determination gene Myf5 in adult regenerative myogenesis. *Dev Biol* **312**, 13-28.
- Gayraud-Morel B, Chrétien F, Jory A, Sambasivan R, Negroni E, Flamant P, Soubigou G, Coppée J-Y, Di Santo J, Cumano A, Mouly V & Tajbakhsh S. (2012). Myf5 haploinsufficiency reveals distinct cell fate potentials for adult skeletal muscle stem cells. *J Cell Sci* **125**, 1738-1749.
- Hasty P, Bradley A, Morris JH, Edmondson DG, Venuti JM, Olson EN & Klein WH. (1993). Muscle deficiency and neonatal death in mice with a targeted mutation in the myogenin gene. *Nature* **364**, 501-506.
- Hawke TJ & Garry DJ. (2001). Myogenic satellite cells: physiology to molecular biology. *J Appl Physiol* **91**, 534-551.
- Herbison GJ, Jaweed MM & Ditunno JF. (1982). Muscle fiber types. *Arch Phys Med Rehabil* **63**, 227-230.
- Hindi SM, Mishra V, Bhatnagar S, Tajrishi MM, Ogura Y, Yan Z, Burkly LC, Zheng TS & Kumar A. (2014). Regulatory circuitry of TWEAK-Fn14 system and PGC-1alpha in skeletal muscle atrophy program. *FASEB J* **28**, 1398-1411.

- Holloszy JO. (1967). Biochemical adaptations in muscle. Effects of exercise on mitochondrial oxygen uptake and respiratory enzyme activity in skeletal muscle. *J Biol Chem* **242**, 2278-2282.
- Jackman RW & Kandarian SC. (2004). The molecular basis of skeletal muscle atrophy. *Am J Physiol Cell Physiol* **287**, C834-843.
- Janssen I, Heymsfield SB, Wang ZM & Ross R. (2000). Skeletal muscle mass and distribution in 468 men and women aged 18-88 yr. *J Appl Physiol (1985)* **89**, 81-88.
- Kassar-Duchossoy L, Gayraud-Morel B, Gomès D, Rocancourt D, Buckingham M, Shinin V & Tajbakhsh S. (2004). Mrf4 determines skeletal muscle identity in Myf5:Myod double-mutant mice. *Nature* **431**, 466.
- Le Grand F & Rudnicki MA. (2007). Skeletal muscle satellite cells and adult myogenesis. *Curr Opin Cell Biol* **19**, 628-633.
- Lin J, Wu H, Tarr PT, Zhang CY, Wu Z, Boss O, Michael LF, Puigserver P, Isotani E, Olson EN, Lowell BB, Bassel-Duby R & Spiegelman BM. (2002). Transcriptional co-activator PGC-1 alpha drives the formation of slow-twitch muscle fibres. *Nature* **418**, 797-801.
- Mayr R, Gierth M, Zeman F, Reiffen M, Seeger P, Wezel F, Pycha A, Comploj E, Bonatti M, Ritter M, van Rhijn BWG, Burger M, Bolenz C, Fritsche HM & Martini T. (2018). Sarcopenia as a comorbidity-independent predictor of survival following radical cystectomy for bladder cancer. *J Cachexia Sarcopenia Muscle* 10.1002/jcsm.12279.
- McCarthy JJ, Mula J, Miyazaki M, Erfani R, Garrison K, Farooqui AB, Srikuea R, Lawson BA, Grimes B, Keller C, Van Zant G, Campbell KS, Esser KA, Dupont-Versteegden EE & Peterson CA. (2011). Effective fiber hypertrophy in satellite cell-depleted skeletal muscle. *Development (Cambridge, England)* **138**, 3657-3666.
- Meadows E, Flynn JM & Klein WH. (2011). Myogenin Regulates Exercise Capacity but Is Dispensable for Skeletal Muscle Regeneration in Adult mdx Mice. *PLoS One* **6**, e16184.
- Neel BA, Lin Y & Pessin JE. (2013). Skeletal Muscle Autophagy: A New Metabolic Regulator. *Trends in endocrinology and metabolism: TEM* **24**, 10.1016/j.tem.2013.1009.1004.
- Pascoe AL, Johnston AJ & Murphy RM. (2020). Controversies in TWEAK-Fn14 signaling in skeletal muscle atrophy and regeneration. *Cell Mol Life Sci* 10.1007/s00018-020-03495-x.
- Peterson CM, Johannsen DL & Ravussin E. (2012). Skeletal muscle mitochondria and aging: a review. *J Aging Res* **2012**, 194821.
- Rabinowitz JD & White E. (2010). Autophagy and metabolism. *Science* **330**, 1344-1348.

- Rantanen J, Hurme T, Lukka R, Heino J & Kalimo H. (1995). Satellite cell proliferation and the expression of myogenin and desmin in regenerating skeletal muscle: evidence for two different populations of satellite cells. *Lab Invest* **72**, 341-347.
- Rudnicki MA, Schnegelsberg PNJ, Stead RH, Braun T, Arnold H-H & Jaenisch R. (1993). MyoD or Myf-5 is required for the formation of skeletal muscle. *Cell* **75**, 1351-1359.
- Sabourin LA & Rudnicki MA. (2000). The molecular regulation of myogenesis. *Clin Genet* **57**, 16-25.
- Sandri M. (2013). Protein breakdown in muscle wasting: role of autophagy-lysosome and ubiquitin-proteasome. *Int J Biochem Cell Biol* **45**, 2121-2129.
- Smythe GM & Grounds MD. (2001). Absence of MyoD Increases Donor Myoblast Migration into Host Muscle. *Experimental Cell Research* **267**, 267-274.
- Tang AH & Rando TA. (2014). Induction of autophagy supports the bioenergetic demands of quiescent muscle stem cell activation. *EMBO J* **33**, 2782-2797.
- Tapscott SJ. (2005). The circuitry of a master switch: MyoD and the regulation of skeletal muscle gene transcription. *Development* **132**, 2685-2695.
- Voges D, Zwickl P & Baumeister W. (1999). The 26S proteasome: a molecular machine designed for controlled proteolysis. *Annu Rev Biochem* **68**, 1015-1068.
- Wang Y & Pessin JE. (2013). Mechanisms for fiber-type specificity of skeletal muscle atrophy. *Curr Opin Clin Nutr Metab Care* **16**, 243-250.
- Watson W, Clapperton A & Mitchell R. (2010). The incidence and cost of falls injury among older people in New South Wales 2006/07, ed. Health NDo. Sydney.
- Young JC, Chen M & Holloszy JO. (1983). Maintenance of the adaptation of skeletal muscle mitochondria to exercise in old rats. *Med Sci Sports Exerc* **15**, 243-246.
- Zammit PS. (2017). Function of the myogenic regulatory factors Myf5, MyoD, Myogenin and Mrf4 in skeletal muscle, satellite cells and regenerative myogenesis. *Semin Cell Dev Biol* 10.1016/j.semcdb.2017.11.011.
- Zhou Z & Bornemann A. (2001). MRF4 protein expression in regenerating rat muscle. *Journal of Muscle Research & Cell Motility* **22**, 311-316.

Chapter 1 cont.

Supplementary Review of the Literature

The following literature review, titled "Controversies in TWEAK-Fn14 signaling in skeletal muscle atrophy and regeneration.", is published in full in *Cellular and Molecular Life Sciences*, 77(17), 3369-3381, DOI: 10.1007/s00018-020-03495-x.



Controversies in TWEAK-Fn14 signaling in skeletal muscle atrophy and regeneration

Amy L. Pascoe¹ · Amelia J. Johnston¹ · Robyn M. Murphy¹ Received: 2 October 2019 / Revised: 27 January 2020 / Accepted: 24 February 2020
© Springer Nature Switzerland AG 2020

Abstract

Skeletal muscle is one of the largest functional tissues in the human body; it is highly plastic and responds dramatically to anabolic and catabolic stimuli, including weight training and malnutrition, respectively. Excessive loss of muscle mass, or atrophy, is a common symptom of many disease states with severe impacts on prognosis and quality of life. TNF-like weak inducer of apoptosis (TWEAK) and its cognate receptor, fibroblast growth factor-inducible 14 (Fn14) are an emerging cytokine signaling pathway in the pathogenesis of muscle atrophy. Upregulation of TWEAK and Fn14 has been described in a number of atrophic and injured muscle states; however, it remains unclear whether they are contributing to the degenerative or regenerative aspect of muscle insults. The current review focuses on the expression and apparent downstream outcomes of both TWEAK and Fn14 in a range of catabolic and anabolic muscle models. Apparent changes in the signaling outcomes of TWEAK-Fn14 activation dependent on the relative expression of both the ligand and the receptor are discussed as a potential source of divergent TWEAK-Fn14 downstream effects. This review proposes both a physiological and pathological model of TWEAK-Fn14 signaling. Further research is needed on the switch between these states to develop therapeutic interventions for this pathway.

Keywords NFκB · Myogenesis · Proliferation · Differentiation · Muscle loss · Cachexia

Introduction

Skeletal muscle is one of the largest tissue types in the human body, comprising between 30 and 40% of total body weight in average healthy adults [1]. Maintenance of skeletal muscle mass and function is critical for optimal locomotion, postural support, and metabolism [2]. An emerging topic in the field of muscle homeostasis is the cytokine, tumour necrosis factor (TNF)—like weak inducer of apoptosis (TWEAK), and its cognate receptor, fibroblast growth factor-inducible 14 (Fn14). The TWEAK-Fn14 pathway has been broadly implicated in the pathogenesis of multiple acute and chronic muscle wasting conditions, though the precise function remains elusive. The downstream effects of TWEAK-Fn14 signalling have been reported as both catabolic (anti-myogenic) and anabolic (pro-myogenic). Unsurprisingly, the

reported signalling pathways of TWEAK-Fn14 activity are similarly diverse. As an example, TWEAK-Fn14 has been shown to signal via both the canonical and non-canonical nuclear factor kappa-β (NFκB) pathways, as well as the mitogen-activated protein kinase (MAPK) pathways [3, 4].

This review aims to summarise some of the seemingly contradictory evidence regarding TWEAK-Fn14 signalling in the context of skeletal muscle homeostasis with a viewpoint to understanding their function in both a physiological and pathological setting.

Is TWEAK an apoptotic stimulus?

TWEAK is a TNF superfamily (TNFSF) cytokine first described in 1997 by Chicheportiche et al. [5] as a weakly pro-apoptotic ligand, as the name suggests. Since then, TWEAK has been associated with a range of physiological and pathological cellular responses including proliferation, migration, differentiation, and inflammation [6]. TWEAK has been described in two forms; a full length 26 kDa membrane bound form (mTWEAK) and a soluble circulating

✉ Robyn M. Murphy
r.murphy@latrobe.edu.au

¹ Department of Biochemistry and Genetics, La Trobe Institute for Molecular Science, La Trobe University, Melbourne, VIC 3086, Australia

18 kDa cleaved fragment (sTWEAK) [5]. Expression of TWEAK differs from that of many other TNFSF cytokines in that it is constitutively expressed in a wide array of tissues; sTWEAK protein has been detected in healthy human serum at 200–300 pg/ml and both protein and mRNA have been detected in healthy pancreas, intestine, heart, brain, lung, vascular, and skeletal muscle [7]. Transient upregulation of both mRNA and protein has been observed in response to injury; inflammatory cells including macrophages and monocytes have been identified as a major source of TWEAK protein abundance [8, 9].

TWEAK has primarily been described as a promoter of cell death, both *in vivo* and *in vitro*. The first evidence of this was in its initial identification as a cytokine capable of inducing apoptosis in human adenocarcinoma cell lines [5]. Further investigation of this has highlighted the weakness of TWEAK-induced apoptosis, with cell death occurring only under specific conditions, where it was necessary to use sensitive cell lines, prolonged incubation, or high ligand/receptor concentrations [10]. This draws into question the physiological relevance of TWEAK as an inducer of apoptosis; an argument which is supported by the lack of a death domain on its cognate receptor, Fn14. A dose-dependent effect of TWEAK is supported by the observation that relatively low doses (4–10 ng/ml) induces a proliferative phenotype in mammalian epithelial cell line, Eph4, whilst high doses (100 ng/ml) result in cell death [11]. It is worth noting

that circulating levels of sTWEAK in healthy humans more closely resemble the low dosage studies, with serum concentrations ranging from ~500–800 pg/ml [12–14]. These low dose studies are of course still considerably higher than reported physiological levels. Furthermore, pathological cohorts often show decreased levels, i.e., severely obese (~250 pg/ml), atherosclerotic (~200 pg/ml), and type II diabetic (~300 pg/ml) [12–14]. Absolute concentrations of mTWEAK, particularly in skeletal muscle tissue, have yet to be described.

Later work focusing on inflammation and repair has indicated that the physiological functions of TWEAK may instead be important for acute tissue repair and progenitor activation [5, 10]. A summary of exogenous TWEAK treatments in varying tissues and species is provided in Table 1. Jakubowski et al. [15] first suggested the role of TWEAK in progenitor regulation, demonstrating potent proliferation of oval cells (liver progenitor cells) in TWEAK transgenic mice with no effect on mature hepatocytes. Later work has demonstrated similar effects in a range of progenitor cell types. *Ex vivo* human aortic smooth muscle cells derived from the tracheal section of healthy and asthmatic human lung transplant donors and stimulated with recombinant human TWEAK showed enhanced proliferation and migration of smooth muscle cells [16]. Similarly, application of a topical TWEAK solution to experimental burns on BALB/c mice accelerated healing by enhancing production of laminin—an

Table 1 Dose and route of exogenous TWEAK administration in various tissues

Study	Tissue	Dose	Route	Outcome
Jakubowski et al. [15]	Cultured NRC-1 (rat cholangiocyte-1 cells)	25–200 ng/ml	Soluble TWEAK in serum-free media	↑Proliferation
Jakubowski et al. [15]	Oval cells from tg-TWEAK rats	Up to 14× mRNA transcripts relative to non-tg rats	Transgenic overexpression	Oval cell hyperplasia
Michaelson et al. [11]	Eph4 mammary epithelial cells	4–10 ng/ml	Fc-TWEAK in media containing 10% serum	↑Proliferation ↓Differentiation
Michaelson et al. [11]	Eph4 mammary epithelial cells	100 ng/ml	Fc-TWEAK in media containing 10% serum	Cell death
Zhu et al. [16]	Human aortic smooth muscle cells	100 ng/ml	Recombinant human TWEAK in serum-free media	↑Proliferation ↑Migration NFκB activation
Liu et al. [17]	Full-thickness burns of mouse dorsal skin	20 μg/ml	Topical application in saline	↑Inflammatory cell infiltration ↑Growth factor production ↑Extracellular matrix in wound area
Girgenrath et al. [9]	C2C12 cells	100 ng/ml	Soluble TWEAK and soluble heat-inactivated TWEAK in media containing 10, 2, or 0.2% serum	↑Proliferation ↓Terminal differentiation
Polck et al. [18]	RAW264.7 monocyte/macrophage cells NB: cells did not express Fn14	150–750 ng/ml	Glutathione <i>S</i> -transferase-TWEAK fusion protein in media containing 10% serum	↑Differentiation

extracellular matrix component believed to drive proliferation of skin cells—and differentiation of myofibroblasts [17]. In both those studies, the effects were eliminated by silencing Fn14 with siRNA or genetic depletion. One exception to the proliferative effects of TWEAK are seen in RAW264.7 monocyte/macrophage cells, where high doses of TWEAK (> 150 ng/ml) induced differentiation [18]. Notably, these cells were shown to be negative for Fn14, suggesting an alternative receptor may be responsible for these TWEAK-mediated differentiation effect [18]. Tissue-specific outcomes of TWEAK-Fn14 activation are highlighted in a study of ginkgo flavanol glycosides and ginkgolides—the active components of *Ginkgo biloba*—and their ability to mitigate ischemic reperfusion injury in both the heart and brain [19]. Interestingly, the *Ginkgo biloba* downregulated Fn14 in the heart but upregulated Fn14 in the brain, both of which were associated with reduced ischemic reperfusion injury, suggesting that alternate mechanisms were involved [19]. The possibility of alternative ligands for Fn14, which may explain the differential responses of Fn14, has been raised; however, there are currently no putative ligands identified in the literature. This notion is discussed further in “Is TWEAK necessary for Fn14 activation?”. Moving into a skeletal muscle cellular setting, Girgenrath et al. [9] demonstrated that TWEAK administration enhanced proliferation of C2C12 myoblasts whilst inhibiting their terminal differentiation.

The underlying mechanisms of the described effects have been partially attributed to activation of the NFκB pathway (discussed further in “What are the signaling pathways of TWEAK-Fn14?”) [16]. The net effect of this is a blockade of myogenesis. This enhanced proliferative, but impaired differentiation, effect is likely dose-dependent and tissue-specific and may partially explain the atrophic or anti-myogenic effects frequently associated with prolonged TWEAK signalling seen in chronic inflammatory states.

Dogra et al. [20] further investigated the myogenic outcomes of TWEAK signalling both in vivo and in vitro, again demonstrating that enhanced or chronic upregulation of TWEAK resulted in impaired growth, albeit at levels likely above physiological relevance. Working in C2C12 cultured myotubes, TWEAK was shown to reduce myotube diameter and enhance ubiquitination of myosin heavy chain in cultured myotubes. Similarly in vivo; both chronic administration (100 µg/kg per week for 4 weeks starting at 3 weeks) and muscle-specific transgenic overexpression of TWEAK resulted in reduced muscle mass in C57Bl/6 mice [20].

Further evidence that overexpressed TWEAK is a negative regulator of myogenesis is seen in a number of chronic human atrophic disease states. Inclusion-body myositis (IBM) is the most common acquired inflammatory myopathy observed in elderly populations, marked by a failure of progenitor cells to differentiate, leading to progressive

muscle weakness [21]. Morosetti et al. [21] investigated the expression and modulation of both TWEAK and Fn14 in human ex vivo mesoangioblast cell culture; mesoangioblasts isolated from IBM patients were shown to have increased TWEAK and Fn14 relative to healthy controls. Inhibition of TWEAK by siRNA interference was able to restore myogenic differentiation in the same IBM mesoangioblasts, whilst treatment of mesoangioblasts derived from patients with dermatomyositis—an inflammatory myopathy without reduced differentiation potential—with 100 ng/ml human recombinant TWEAK, resulted in reduced differentiation rate [21].

Myotonic dystrophy type 1 (DM1) represents a phenotypically similar condition to IBM with a distinct biochemical mechanism. DM1 muscle wasting is known to be linked to an expanded allele in the DM protein kinase gene resulting in an accumulation of RNA; the downstream pathways between this toxic RNA accumulation and the clinical myopathy are poorly understood [22]. Using a DM5 mouse model of RNA toxicity, Yadava et al. [22] investigated the effects of TWEAK using both a TWEAK-null/DM5 hybrid, and by intraperitoneally administering TWEAK, albeit the shorter soluble form (see “What are the signaling pathways of TWEAK-Fn14?” for further detail). As with IBM, TWEAK-deficiency was shown to reduce pathology and enhance muscle function, whilst TWEAK administration exacerbated the DM5 phenotype.

Finally, Mittal et al. [23] reported similar effects of TWEAK modulation in the acute atrophy model of denervation-induced wasting, with transgenic overexpression of TWEAK exacerbating muscle-specific protein degradation, and genetic ablation of TWEAK sparing muscle loss in denervated C57Bl/6 mouse *tibialis anterior* muscle. Importantly, Mittal et al. [23] note that it is the receptor, Fn14, rather than TWEAK itself, which is most dramatically upregulated in this injury model as measured at the mRNA level, suggesting a receptor-driven enhancement of the TWEAK-Fn14 pathway may be driving muscle atrophy.

Is TWEAK necessary for Fn14 activation?

Fn14, first identified by Wiley et al. [24], currently remains the only known binding partner of TWEAK. Fn14 belongs to the TNF receptor superfamily (TNFRSF), containing the distinctive motif of cysteine-rich repeats in the extracellular domain. Whilst most TNFRSF members contain three to four of these cysteine-rich repeats, Fn14 contains only one and is the smallest described family member at 102 amino acids [24]. An additional distinction between Fn14 and other TNFRSF members is the lack of a death domain—a cytoplasmic motif which enables the induction of apoptosis—an

observation which has confounded and undermined the supposed apoptotic actions of its ligand TWEAK [24].

Fn14 is a constitutively expressed receptor under normal physiological conditions in most cell and tissue types, and is highly inducible under a range of acute and chronic pathological conditions (Table 2) [6, 25]. Induction of Fn14 in damaged tissues is poorly understood but has been linked to a number of growth factors and cytokines, including TWEAK [10]. Changes in receptor trafficking dynamics have been proposed to play a role in the apparent upregulation of Fn14. Gurunathan et al. [4] investigated the post-translational regulation of Fn14 in HeLa cells. As with most TNFRSF members, turnover of Fn14 was accelerated in the presence of its ligand—in this instance, TWEAK—as the TWEAK-Fn14 complex was internalised and degraded by the lysosome. In addition to this ligand-dependent turnover, Gurunathan et al. [4] reported a distinct and additive ligand-independent turnover mechanism, wherein unliganded Fn14 is rapidly shed from the cell surface, or internalised and degraded. The half-life of unliganded Fn14 was measured using cycloheximide to inhibit protein synthesis, with a

half-life of approximately 74 min, indicating a rapid turnover relative to the average measured half-life of proteins in HeLa cells of 20 h. These findings indicate a constitutive down-regulatory mechanism may be pivotal in dynamic Fn14 signalling. Winer et al. [26] have since identified GABARAP-mediated autophagy as the likely primary negative-regulator of Fn14 under basal conditions in HeLa cells.

The one-to-one nature of TWEAK and Fn14 as a ligand-receptor pair is thrown into question by several studies highlighting effects of both TWEAK and Fn14 in the absence of their counterpart. TWEAK-induced differentiation of RAW264.7 monocyte/macrophage cells in the absence of Fn14 described in “Is TWEAK an apoptotic stimulus?” suggests an alternative receptor for TWEAK, or TWEAKR2 as described by Polek et al. [18]. Whilst no alternative ligand has been identified for Fn14, there is growing evidence of TWEAK-independent activation of Fn14. Whether this is strictly due to self-association or a putative ligand remains to be determined.

Dramatic upregulation of Fn14 as described above may result in TWEAK-independent signalling via self-association

Table 2 Inducible changes of TWEAK and Fn14 in a range of human and mouse disease models

Disease model	TWEAK	Fn14	Tissues used
TWEAK-tg	fourfold increase in protein levels [23] fivefold increase in mRNA levels [23]	Unchanged at mRNA level [23]	C57Bl/6 mouse model, gastrocnemius and tibialis anterior muscles
TWEAK-KO		1.5-fold increase in mRNA [23]	C57Bl/6 mouse model, tibialis anterior muscle
Cancer and cachexia		Upregulated on solid tumours [27]	Observed in human tumour samples [27] Human Fn14-expressing tumours on C57Bl/6 mice induced cachexia [28] C26-tumour bearing mice treated with α -Fn14 did not develop cachexia [28]
Denervation	Unchanged [23]	Six to sevenfold increase in mRNA [23] Upregulated protein [23]	C57Bl/6 mouse model, gastrocnemius muscle
Cardiotoxin	Increased mRNA Remained elevated for longer in Fn14-deficient animals [9]	Increased mRNA [9]	129/sv mouse model, wild-type and Fn14-deficient
Unloading		Twofold increase in mRNA [29] Unchanged in NF κ B-KO mice [29]	B6129PF2/J mouse model, gastrocnemius muscle
Fasting/ starvation		15-fold increased mRNA [30] Sixfold increased mRNA in muscle-specific TRAF6-KO [30]	Floxed TRAF6 and muscle specific TRAF6-KO mouse model, gastrocnemius muscle
Diabetes	Circulating TWEAK ~20% lower in type II diabetics [13]	Unchanged in adipose tissue of type II diabetes but increased in adipose tissue of severely obese subjects [31]	Human subjects
Adeno-associated virus-based vector expressing activin A		mRNA increased [25] Tenfold increase in protein [25]	C57Bl/6 mouse model

of the trans-membrane and C-terminal regions of the Fn14 receptor (see Fig. 1). Brown et al. [32] demonstrated this using HEK293/NF κ B-luciferase reporter cells transfected with an Fn14 mutant unable to bind TWEAK, reporting activation of the NF κ B pathway and dimerisation of the receptor detectable on a non-reducing SDS-PAGE. Ligand-independent signalling is suggested as a possible mechanism underlying Fn14-associated cachexia—the dramatic muscle and fat loss often developed in cancer patients. Johnston et al. [28] investigated the effects of Fn14 antibodies on the development of cachexia in tumour bearing mice, reporting a complete blockade of cachexia with the administration of an antagonistic Fn14 antibody. Interestingly, they were unable to replicate these results via inhibition of TWEAK with TWEAK antibodies, indicating that the role of Fn14 in the development of cachexia is likely TWEAK-independent. It is worth noting that the Fn14 targeted in this disease model was present on the tumour itself, as opposed to the skeletal muscle. Administration of the same Fn14 antibody in an activin-A induced mouse skeletal muscle atrophy model was

unable to prevent wasting—and in fact may have slightly inhibited the regenerative process—indicating that Fn14 may have tissue-specific functions which vary between distinct atrophy models, namely muscle atrophy due to cachexia or due to direct muscle injury [28]. It is unclear what factors dictate the balance of TWEAK-dependant Fn14 signalling vs TWEAK-independent self-association or if they are mutually exclusive; however, it is likely that these events co-exist *in vivo* with dose and tissue-specific responses.

Does TWEAK-independent Fn14 signalling promote myogenesis?

Similar to its ligand, Fn14 has been associated with both pro- and anti-myogenic pathways. Given the atrophic phenotypes frequently associated with TWEAK overexpression, it should follow that activation of its cognate receptor will also correlate with atrophy; however, this is not the case in the current literature, which will be discussed below. Whilst Fn14 is frequently upregulated in acute and chronic muscle

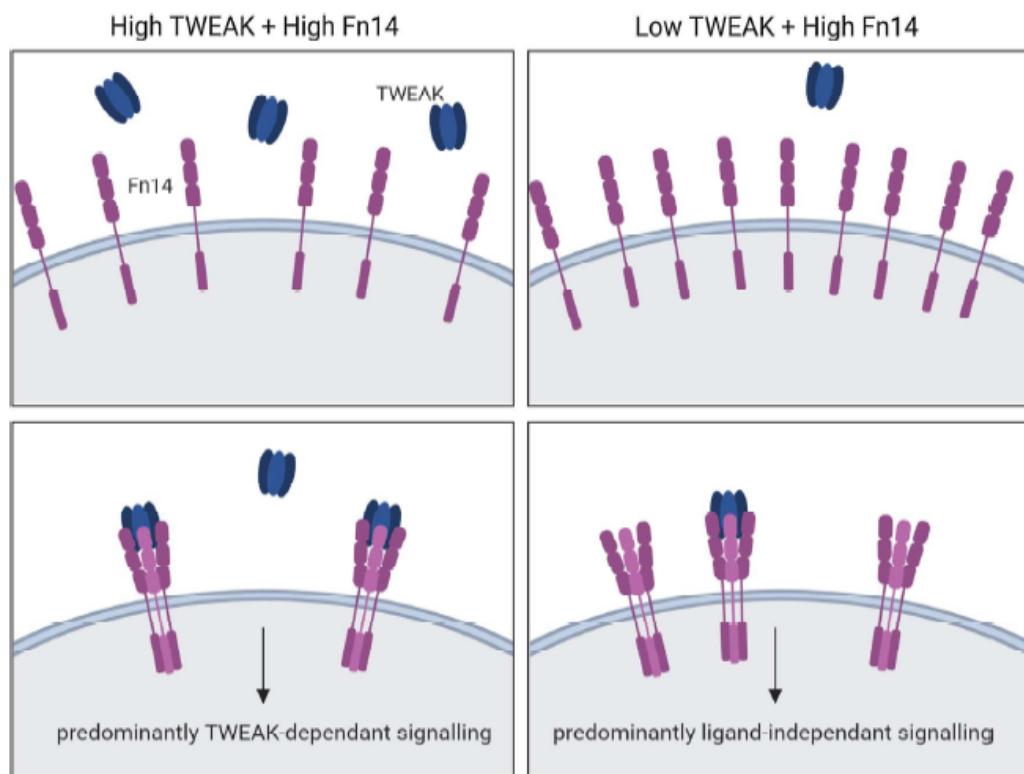


Fig. 1 Ligand-dependant and ligand-independent Fn14 activation: When both TWEAK and Fn14 are highly expressed, e.g., in chronic inflammatory disease states, trimeric TWEAK is able to bind the extracellular domain of Fn14, bringing the C-terminal domains of Fn14 together and triggering a ligand-dependant activation of the TWEAK-Fn14 pathway [24]. When Fn14 is highly expressed with-

out overexpression of TWEAK, Fn14 clustering occurs due to the high density of Fn14 receptors present on the cell membrane [32]. The close proximity of Fn14 receptors leads to self-association of the trans-membrane and C-terminal domains of Fn14 leading to ligand-independent activation of the Fn14 pathway [32]

wasting conditions, there is growing evidence that rather than driving atrophy, it may in fact play an important role in regenerative signalling via TWEAK-independent self-association. An overview of human skeletal muscle-based evidence of TWEAK-Fn14 alteration is provided in Table 3. Variability in the species and muscle type samples, particularly given the fibre-type specificity of Fn14, is a further complication in directly comparing evidence across studies.

Early evidence of Fn14 involvement in regeneration was observed in the delayed recovery of *Fn14*-null mice following a localised muscle injury created by intramuscular cardiotoxin injection [9]. Girgenrath et al. [9] reported a defective inflammatory response with a delayed peak of inflammatory cell infiltration, along with a reduced proliferative capacity indicated by a decrease in centrally nucleated muscle fibres and reduced embryonic myosin heavy chain expression. Depletion of Fn14 using RNA interference was similarly shown to impair myogenesis in C2C12 myoblast cells [38]. Under normal conditions, C2C12 myoblasts express high levels of Fn14 protein which is downregulated upon differentiation into myotubes [38]. RNAi knockdown of Fn14 resulted in decreased expression of the myogenic regulatory factors (MRFs)—a set of transcription factors essential for myogenic progression—specifically, MyoD and myogenin, resulting in a significant reduction in myotube formation and expression of muscle-specific proteins including myosin heavy chains and creatine kinase [38]. Dogra et al. [38] concluded that whilst TWEAK-dependant Fn14 signalling appeared to inhibit differentiation, Fn14 was able to act independently of TWEAK and was in fact required for the expression of MRFs and by extension, myogenic differentiation.

A review of TWEAK-Fn14 signalling by Burkly et al. [39] highlights the potential regenerative role of Fn14 by comparing the Fn14 mRNA expression profiles of muscle

biopsies taken from Duchenne's muscular dystrophy (DMD) patients aged 1.5 months to 5 years. DMD is a progressive muscle wasting condition, wherein absence of the dystrophin protein renders the sarcolemma fragile and vulnerable to damage resulting in repeated rounds of damage and repair [40]. The regenerative capacity of skeletal muscle is reduced as the patient ages leading to progressive muscle wasting. The younger cohort investigated in that dataset (GEO dataset GSE6011) would likely be considered pre-symptomatic with the older individuals representing early onset of the disease. Burkly et al. [39] note that Fn14 mRNA expression was highest in younger DMD patients, suggesting it correlates with regenerative capacity rather than muscle wasting. A striking longitudinal study of fat-free muscle mass retention in young, healthy, human males following a 21-day period of energy-deficit at high altitude identified high baseline levels of Fn14 mRNA measured from a muscle biopsy of the *vastus lateralis* as a correlate of muscle mass retention [34]. Whilst only correlative, the authors went on to suggest high levels of Fn14 may in fact be a protective factor against muscle atrophy.

Further support for Fn14 upregulation as a correlate of remodelling and regeneration is observed in response to resistance exercise. Healthy muscle readily adapts to changes to stimuli; the most physiologically relevant example of this is the micro-injuries and remodelling which occur following resistance exercise. A study of monozygotic twins with self-reported divergent exercise habits reported increased expression of Fn14 mRNA in skeletal muscle of the twin with a history of chronic endurance training [35]. It is interesting to note that despite having higher markers of cardiovascular and pulmonary health, the endurance trained twin did exhibit lower muscle size and strength, an effect likely due to the nature of the cardiovascular endurance training favoured by the trained twin over a more resistance-heavy program.

Table 3 Human skeletal muscle responses of TWEAK and Fn14 in various pathologies and exercise interventions

Study	Intervention/cohort	TWEAK	Fn14	Tissues used
Burkly, Dohi [33]	Duchenne's muscular dystrophy (DMD) patients aged 1.5 months to 5 years	NA	Fn14 mRNA higher in youngest DMD patients	<i>Quadriceps</i> biopsy
Pasiakos et al. [34]	Healthy young men exposed to 21-day energy-deficit at high altitude	NA	High Fn14 mRNA correlated with fat-free mass retention	<i>Vastus lateralis</i> biopsy
Bathgate et al. [35]	Monozygotic twins with divergent activity levels	NA	Fn14 mRNA higher in chronically active twin	<i>Vastus lateralis</i> biopsy
Raue et al. [36]	Acute resistance exercise, young untrained adults	Unchanged	12-fold mRNA increase 4 h post-exercise	<i>Vastus lateralis</i> biopsy
	Acute resistance exercise, old untrained adults	Unchanged	fourfold mRNA increase 4 h post-exercise	<i>Vastus lateralis</i> biopsy
Rauc et al. [37]	Acute treadmill running	Unchanged	Fn14 protein detected in some participants 12- and 24 h post-exercise	<i>Vastus lateralis</i> biopsy
	Acute resistance training	Unchanged	Fn14 protein detected in all participants 12- and 24 h post-exercise; higher levels than treadmill running	<i>Vastus lateralis</i> biopsy

Raue et al. [36] investigated the transcriptome of human skeletal muscle following acute and chronic resistance exercise training. Fn14 was shown to be upregulated ~12-fold 4 h post-resistance exercise in young untrained adults. Old adults showed a similar yet blunted response to resistance exercise, with a ~fourfold change detected. This blunted response correlated with reduced muscle adaptations in old adults and was common to many pre/post resistance exercise transcriptomic changes. Notably, TWEAK mRNA was not altered in response to resistance exercise, suggesting that Fn14 levels are the primary regulator of TWEAK-Fn14 signalling in exercise-induced muscle adaptation. Raue et al. [36] also describe activation of the NF κ B pathway, marked by induction of the NF κ B-inducing kinase (NIK) and degradation of NF κ B inhibitory molecule, I κ B α , and suggested that induction of this pathway was via upregulation of Fn14 with downstream effects including the normal physiological remodelling of muscle. A follow-up study by the same group comparing the regulation of both TWEAK and Fn14 following either resistance exercise or treadmill running similarly showed Fn14, but not TWEAK, was responsive to training in human muscle [37]. Interestingly, treadmill running produced a smaller Fn14 response at the mRNA level; Fn14 protein was sporadically detected in two of six participants at 8 h post-run and in a different two participants at 12 and 24 h post-run. In comparison, resistance exercise produced

a more robust Fn14 mRNA response which was also detectable at the protein level in all six participants, peaking 12 h post-exercise. The stronger response elicited by resistance exercise – a training mode characterised by micro-injury and adaptive growth – provides further evidence of Fn14 as a regulator of normal physiological remodelling in healthy skeletal muscle.

What are the signaling pathways of TWEAK-Fn14?

NF κ B, MAPK, and PI3K/Akt signalling have all been implicated as downstream targets of TWEAK-Fn14 activity (Fig. 2) [3, 20, 41]. NF κ B is broadly categorised into two pathways—the canonical (classical) and non-canonical (alternative). Comprehensive reviews of the distinct role in muscle homeostasis each pathway plays are provided in Bakkar, Guttridge [42] and Enwere et al. [3]; a general consensus in the literature points to canonical signalling as a promoter of early myogenic proliferation and inhibitor of differentiation, whilst non-canonical signalling enhances differentiation and fusion. The balance between canonical vs non-canonical NF κ B, MAPK, and PI3K/Akt signalling are likely dose and tissue specific and temporally regulated. Delineating the specific conditions, wherein each pathway is

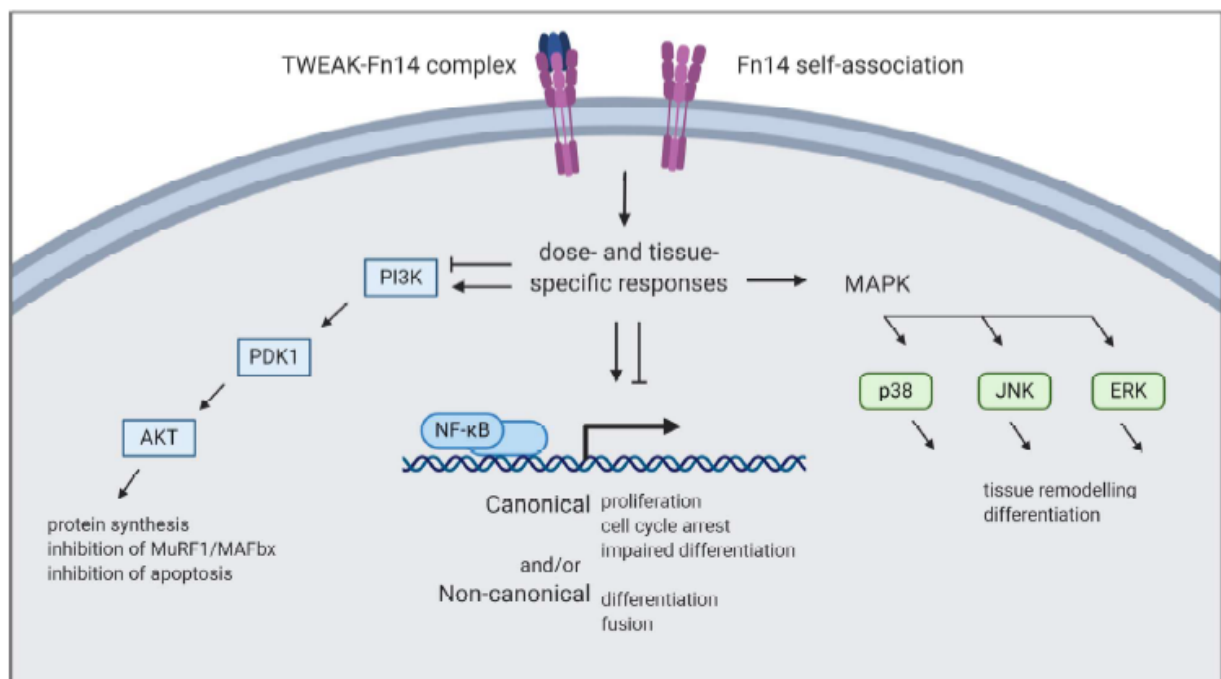


Fig. 2 Signalling pathways of Fn14 activation. TWEAK-dependent and TWEAK-independent Fn14 signalling has been associated with MAPK, PI3K/Akt, and both canonical and non-canonical NF κ B [3,

20, 41]. Each of these pathways appear to be activated or inhibited in a dose- and tissue-specific manner with specific and often opposing outcomes associated with each pathway

active may aid in understanding the role in a switch between physiological and pathological TWEAK-Fn14 signalling.

TWEAK is expressed as a type II transmembrane protein with an N-terminal cytosolic domain, a transmembrane domain, and an extracellular C-terminal TNF homology domain (THD). When initially describing TWEAK, Chicheportiche et al. [5] reported a smaller, soluble form of TWEAK detected in cell culture medium, indicating the possibility that TWEAK is proteolytically cleaved. Furin, a pro-protein convertase, was later identified as the TWEAK-processing enzyme, binding specifically to the 90–93 amino acid residues of a subset of TWEAK within the Golgi apparatus and cleaving off the C-terminal THD, which is in turn secreted into the extracellular environment [43]. This secreted THD domain of TWEAK is referred to as sTWEAK, whilst the full-length membrane bound form is referred to as mTWEAK. Both sTWEAK and mTWEAK have been shown to bind Fn14 and trigger signal transduction; however, there is evidence that the two forms differentially activate the NF κ B and MAPK pathways in HT29 and HeLa TNFR2 cell cultures [44].

Balance between sTWEAK and mTWEAK signalling is one possible basis for the diverse outcomes of TWEAK-Fn14 signalling although little work has been done to adequately address the roles of each TWEAK form in skeletal muscle degeneration and regeneration. Morosetti et al. [21] reported increased TWEAK abundance in human inclusion-body myositis skeletal muscle biopsies using both immunohistochemistry and western blotting. It is unclear; however, if there was a shift in the proportions of mTWEAK and sTWEAK and if this has any bearing on the pathology. Standard western blotting practice includes the centrifugation and fractionation of samples to remove ‘cellular debris’, the pitfalls of which include the discarding of significant but inconsistent quantities of protein, and are addressed fully in Murphy, Lamb [45] and Murphy et al. [46].

Canonical pathway

The canonical arm of the NF κ B pathway is characterised largely by the proteolysis of p105 to p50; the p50 active subunit is able to form homo- or heterodimers with several NF κ B family members, with p65 (also called RelA) being the most extensively described binding partner [42]. Interestingly, homodimerisation of p50, and likewise p52 in the non-canonical arm, appear to have inhibitory effects on gene transcription [47]. Downstream effects of canonical NF κ B signalling are also influenced by a host of post-translational modifications, co-activators, and co-repressors. It is, therefore, not surprising that canonical NF κ B signalling has a diverse range of cellular outcomes.

Despite this, there is evidence of canonical NF κ B signalling as a negative regulator of myogenesis. Bakkar et al.

[48] generated p65-null mice and noted a two-fold increase in fibre number and increased myogenic activity relative to wild-type or p50-null mice, indicating p65 is a repressor of myogenesis. The p65 subunit has also been linked with degradation of peroxisome proliferator-activated receptor γ coactivator 1- α (PGC-1 α), a key driver of mitochondrial biogenesis, and by extension, a regulator of fibre type conversion [49]. It has been suggested that this inhibitory mechanism is a driver of slow to fast fibre type conversion [50]; given the enhanced susceptibility of fast fibres to muscle wasting this may represent a predisposition to muscle atrophy in settings with prolonged canonical NF κ B signalling.

Blockade of myogenesis is further supported by canonical NF κ B interactions with MyoD—an early myogenic regulatory factor [51]. Degradation of MyoD protein, and thus reduced myogenic progression, was observed in C2C12 myoblasts following the administration of TWEAK; of course, extrapolation of this in vitro study to a physiological in vivo model of TWEAK-Fn14 signalling should be approached with care [51].

The apparent inhibitory effect of canonical NF κ B has also been suggested as a requisite precursor of myogenic differentiation by promoting myoblast proliferation [48]. It has been proposed that a shift in canonical to non-canonical NF κ B may be involved in normal physiological TWEAK-Fn14 mediated myogenesis. Enwere et al. [52] reported primarily non-canonical NF κ B activation under physiological (low) levels of TWEAK stimulation in newly forming myoblasts, suggesting that the primary physiological function of TWEAK is via the non-canonical pathway. Overall, it appears that aberrations in the canonical to non-canonical switch may underlie pathological chronic TWEAK-Fn14 signalling.

Non-canonical pathway

Non-canonical NF κ B signalling, also known as the alternative pathway, has also been implicated in TWEAK-Fn14 signalling, albeit largely as a positive regulator of myogenesis. As described above, there is evidence of non-canonical signalling promoting differentiation and fusion of myoblasts in later stage myogenesis.

Under basal conditions, NF κ B-inducing kinase (NIK) is constitutively degraded by a complex of cellular inhibitor of apoptosis (cIAP) and TNF-receptor associated factors 2 and 3 (TRAF2/3) [42]. Activation of the non-canonical pathway in HT1080 human fibrosarcoma cells and Daudi human Burkitt’s lymphoma cells resulted in translocation from the cytosol to the membrane and subsequent degradation of the cIAP-TRAF2/3 complex [53]. In the absence of cIAP, NIK is stabilised which in turn enables downstream proteolysis of p100 to p52 [42, 53]. Similar to the canonical arm, p52 is able to form homo- or heterodimers with other

NFκB family members, in this instance preferentially binding RelB to drive transcription [42].

Interactions between the canonical and non-canonical arms of the NFκB pathway further complicate the delineation of their actions. It should be noted that whilst cIAP is degraded upon activation of the non-canonical arm, it has been shown to be necessary for the activation of canonical NFκB. Varfolomeev et al. [53] showed that pre-treatment of HT1080 cells, Ramos human Burkitt's lymphoma cells, and HT29 and Ku812F human chronic myelogenous leukemia cells with IAP antagonist, BV6, blunted activation of the canonical signalling pathway. Varfolomeev et al. [53] went on to conclude that cIAP was essential for activation of the canonical NFκB pathway by TNFR family members, including TWEAK.

Constitutive non-canonical NFκB activation is believed to be present in both *cIAP*-null mice and *cIAP*-null cultured myotubes, as indicated by enhanced proteolysis of p100 to p52 [52]. Interestingly, *cIAP*-null cultured myotubes exhibited an increase in fusion and fibre size, whilst the *in vivo* model demonstrated enhanced markers of regenerating fibres following cardiotoxin injury, namely an increase in centralised nuclei. In contrast to Varfolomeev et al. [53] assertion that cIAP degradation inhibits canonical NFκB activation, Enwere et al. [52] describe a simultaneous activation of both canonical and non-canonical pathways when cIAP is deficient. The actions of the canonical pathway are believed to delay cell cycle exit and downstream maturation; however, a small subset of proliferating cells appear to be capable of overcoming this blockade and are then able to respond to the differentiation-promoting non-canonical stimulation resulting in a net pro-myogenic response. The interplay between these two pathways, particularly in *in vivo* models, is clearly more extensive than once thought. These findings indicate that in certain circumstances, both canonical and non-canonical NFκB signalling can be pro-myogenic.

Whilst the anti-myogenic effects of TWEAK have been previously discussed, there has been evidence to suggest that at physiological levels, TWEAK signals preferentially via the non-canonical pro-myogenic pathway. The phenotype described in *cIAP*-null myotubes was recapitulated in cultured myoblasts stimulated with low doses (10 ng/ml) recombinant mouse TWEAK, indicating a similar effect—stimulation of the non-canonical NFκB pathway [52].

In addition to cIAP, NIK can also be cleaved and inactivated by the cysteine-aspartic acid protease, caspase 8 [54]. Caspase 8 is involved in the apoptotic complex called the ripoptosome, which, in some models has been induced in TWEAK-Fn14 signalling [55]. It should be noted; however, many models of TWEAK implicating the ripoptosome are cell-based and involve non-physiological concentrations of ligand. Regardless, activation of caspase 8, and thereby inhibition of the non-canonical NFκB pathway is one more

consideration to be made when investigating the downstream signalling events of TWEAK-Fn14 activation.

MAPK pathway

The MAPK pathway has also been implicated in TWEAK-Fn14 signalling (Fig. 2); albeit with more limited work available on muscle-specific models. Similar to NFκB, the MAPK pathway consists of distinct arms—ERK1/2, p38, and JNK—with similarly diverse downstream outcomes [56]. Which of these three pathways is activated by TWEAK-Fn14 again appears to be a tissue- and dose-specific response.

The myogenic outcomes of MAPK signalling are still an emerging field; however, there is evidence of temporal regulation of ERK1/2, p38, and JNK at distinct stages of myogenesis. ERK1/2 is likely to be involved the early proliferative phase of myogenesis. Jones et al. [57] describe dominant-negative mutants of Raf-1, resulting in inactivation of the ERK1/2 pathway, as having a deleterious effect on proliferation in MM14 muscle satellite cells with no impact on their fusion and maturation. A similar study looking at inhibition of the ERK1/2 pathway in L6A1 myoblasts was in fact shown to enhance differentiation, suggesting that not only is ERK1/2 not required for differentiation, it is a negative regulator of late-stage myogenesis [58]. The different conclusions on the ability of ERK1/2 to regulate differentiation may be attributed at least partially to the use of distinct cellular models.

JNK has likewise been linked to early myogenic proliferation. Xie et al. [59] describe a double-negative feedback loop in C2C12 cells, wherein JNK signalling was both down-regulated by microRNAs associated with terminal differentiation, whilst also negatively regulating differentiation. The net effect indicates that JNK is a negative regulator which must be inhibited for skeletal muscle terminal differentiation.

Finally, the p38 cascade has been identified as an essential regulator of myogenesis, with involvement at several steps of the myogenic program. A thorough review of the p38 pathway in myogenesis is provided in Keren et al. [60]. Cabane et al. [61] generated several mutants at different stages of the p38 kinase pathway and noted that without a fully functional p38 pathway, C2C12 cells were unable to undergo terminal differentiation, with significant reductions observed in MyoD and the skeletal muscle specific structural protein, troponin T. In contrast to this, Jin, Li [62] identified p38 as a promoter of atrogen-1—an ubiquitin ligase associated with muscle atrophy—in a lipopolysaccharide-induced mouse model of muscle atrophy. Keren et al. [60] note that the role of p38 may be dual, with distinct effects pre- and post-differentiation, which may explain the somewhat

counter-intuitive outcomes of p38 signalling in the injury model described by Jin, Li [62].

Li et al. [41] investigated the effects of TWEAK administration on C2C12 myotubes which had been previously differentiated for 96 h, reporting enhanced activation of ERK1/2, p38, and JNK. Whilst these results indicate that TWEAK signals via all three arms of the MAPK pathway, it should be noted that the dose, 100 ng/ml is again far above the likely physiological range and should be interpreted with caution. The specific aims of this study were to determine the mechanism of TWEAK-induced activation of MMP-9—a matrix metalloproteinase implicated in muscle atrophy [41]. Whilst all three MAPK pathways and both NFκB pathways were activated in response to TWEAK, only inhibition of the p38 and NFκB were sufficient to prevent TWEAK-induced MMP-9 activation, indicating that these may be the primary signalling cascades of TWEAK. Given the diverse outcomes of p38 activation previously described, and the non-physiological dose of TWEAK, it is likely that MAPK involvement in physiological TWEAK-Fn14 signalling is again dose- and tissue-specific.

PI3K/Akt pathway

Activation of the PI3 kinase (PI3K) pathway and its downstream kinase, Akt, have been identified as potent inducers of skeletal muscle hypertrophy by two key mechanisms; enhancing mTOR-induced protein synthesis and inhibiting the expression of atrophy-associated genes, MuRF1 and MAFbx (also called Atrogin-1) [63, 64].

Interaction of TWEAK-Fn14 activation and the PI3K/Akt pathway again appears to be a dose- or tissue-dependant response. A review of TWEAK-Fn14 as a druggable target by Wajant [65] highlights some of the inconsistencies in the described PI3K/Akt signalling outcomes of TWEAK-induced signalling in various tissues. Dogra et al. [20] describe reduced phosphorylation of Akt and enhanced MuRF1/MAFbx expression in C2C12 myotubes as early as 3 h following administration of 10 ng/ml sTWEAK. Synthesis of MyHC was not reduced by TWEAK; however, the overall diameter of the TWEAK-treated myotubes was shown to be reduced, potentially due to the increased catabolic effects of MuRF1 and MAFbx [20]. Interestingly, denervation of the *gastrocnemius* muscle of wild-type, TWEAK-tg, and TWEAK-KO C57Bl/6 mice showed comparable reduction of Akt phosphorylation, indicating that TWEAK was not modulating the PI3K/Akt response in vivo, potentially due to redundancy in signalling pathways [23]. Mittal et al. [23] did, however, indicate that TWEAK induced upregulation of MuRF1 but MAFbx, albeit via NFκB signalling, and that this was a primary mechanism of TWEAK in exacerbating denervation atrophy.

In further contrast to the effects observed in C2C12 myotubes, TWEAK has been shown to activate, rather than inhibit, PI3K/Akt in renal tubular cells, glioma, and osteoblastic cells [66–68]. It should be noted that each of these studies implemented a dose of 100 ng/ml, tenfold greater than the dose which elicited inhibitory effects in C2C12 myotubes and well above any described physiological levels. It is possible that the contradictory effects of TWEAK on PI3K/Akt are largely dose dependant. This notion is supported by a study on the use of TWEAK as a therapeutic intervention in cardiac reperfusion injury [69]. Yang et al. [69] describe a dose-dependent reduction in apoptosis and caspase-3 activity in hypoxic and then re-oxygenated H9C2 cells (rat cardiomyocytes) when treated with 0–1000 ng/ml recombinant human TWEAK. This effect was attributed to enhanced activation of the PI3K/Akt pathway at 100 ng/ml, although unfortunately no dose–response data is shown for Akt phosphorylation. Yang et al. [69] went on to describe a significant reduction in cardiac reperfusion injury, apoptosis, and caspase-3 activity in Sprague–Dawley rats pre-treated with 1 μg TWEAK/100 μl PBS injected directly into the myocardium.

The outcomes of TWEAK-Fn14 activation on the PI3K/Akt pathway are in need of further investigation to identify the mechanistic nature of the diverse outcomes described; however, the preliminary evidence indicates that the distinct actions of supraphysiological levels of TWEAK may be useful in certain therapeutic settings.

Concluding remarks

It is apparent that the signalling pathways and outcomes of TWEAK and Fn14 in the context of muscle injury, atrophy, and repair, are diverse with dose and tissue specific effects. There is mounting evidence that Fn14 is indeed an important regulator of myogenesis, with high levels of Fn14 serving as a protective factor against a range of muscular insults and driving cellular differentiation. Conversely, TWEAK has been frequently associated with atrophic and inflammatory phenotypes, and often exacerbates models of muscle wasting and tissue injury. The most likely explanation for these opposing actions of a putative one-to-one ligand and receptor pair is dose- and tissue-specific responses and post-translation processing of TWEAK; however, the possibility of undescribed secondary receptors or ligands should not be discounted.

Understanding the regulation and binding of both TWEAK and Fn14, particularly in settings of acute and chronic inflammation, will provide further insight into their physiological and pathological roles, and aid in the development of therapeutics targeting this pathway.

Acknowledgements This research was supported by an Australian Government Research Training Program (RTP) Scholarship to ALP. Figures created with BioRender.com.

References

- Janssen I, Heymsfield SB, Wang ZM, Ross R (2000) Skeletal muscle mass and distribution in 468 men and women aged 18–88 yr. *J Appl Physiol* 89(1):81–88
- Jackman RW, Kandarian SC (2004) The molecular basis of skeletal muscle atrophy. *Am J Physiol Cell Physiol* 287(4):C834–C843. <https://doi.org/10.1152/ajpcell.00579.2003>
- Enwere EK, Lacasse EC, Adam NJ, Korneluk RG (2014) Role of the TWEAK-Fn14-cIAP1-NF-kappaB signaling axis in the regulation of myogenesis and muscle homeostasis. *Front Immunol* 5:34. <https://doi.org/10.3389/fimmu.2014.00034>
- Gurunathan S, Winkles JA, Ghosh S, Hayden MS (2014) Regulation of fibroblast growth factor-inducible 14 (Fn14) expression levels via ligand-independent lysosomal degradation. *J Biol Chem* 289(19):12976–12988. <https://doi.org/10.1074/jbc.M114.563478>
- Chicheportiche Y, Bourdon PR, Xu H, Hsu YM, Scott H, Hession C, Garcia I, Browning JL (1997) TWEAK, a new secreted ligand in the tumor necrosis factor family that weakly induces apoptosis. *J Biol Chem* 272(51):32401–32410
- Winkles JA (2008) The TWEAK-Fn14 cytokine-receptor axis: discovery, biology and therapeutic targeting. *Nat Rev Drug Discov* 7(5):411–425. <https://doi.org/10.1038/nrd2488>
- Chen T, Guo ZP, Li MM, Li JY, Jiao XY, Zhang YH, Liu HJ (2011) Tumour necrosis factor-like weak inducer of apoptosis (TWEAK), an important mediator of endothelial inflammation, is associated with the pathogenesis of Henoch-Schonlein purpura. *Clin Exp Immunol* 166(1):64–71. <https://doi.org/10.1111/j.1365-2249.2011.04442.x>
- Nakayama M, Kayagaki N, Yamaguchi N, Okumura K, Yagita H (2000) Involvement of tweek in interferon γ -stimulated monocyte cytotoxicity. *J Exp Med* 192(9):1373–1380
- Girgenrath M, Weng S, Kostek CA, Browning B, Wang M, Brown SAN, Winkles JA, Michaelson JS, Allaire N, Schneider P, Scott ML, Hsu YM, Yagita H, Flavell RA, Miller JB, Burkly LC, Zheng TS (2006) TWEAK, via its receptor Fn14, is a novel regulator of mesenchymal progenitor cells and skeletal muscle regeneration. *EMBO J* 25(24):5826–5839. <https://doi.org/10.1038/sj.emboj.7601441>
- Burkly LC, Michaelson JS, Hahn K, Jakubowski A, Zheng TS (2007) TWEAKing tissue remodeling by a multifunctional cytokine: role of TWEAK/Fn14 pathway in health and disease. *Cytokine* 40(1):1–16. <https://doi.org/10.1016/j.cyto.2007.09.007>
- Michaelson JS, Cho S, Browning B, Zheng TS, Lincecum JM, Wang MZ, Hsu Y-M, Burkly LC (2005) Tweak induces mammary epithelial branching morphogenesis. *Oncogene* 24(16):2613–2624. <https://doi.org/10.1038/sj.onc.1208208>
- Blanco-Colio LM, Martin-Ventura JL, Munoz-Garcia B, Orbe J, Paramo JA, Michel JB, Ortiz A, Meilhac O, Egido J (2007) Identification of soluble tumor necrosis factor-like weak inducer of apoptosis (sTWEAK) as a possible biomarker of subclinical atherosclerosis. *Arterioscler Thromb Vasc Biol* 27(4):916–922. <https://doi.org/10.1161/01.ATV.0000258972.10109.ff>
- Kralisch S, Ziegelmeier M, Bachmann A, Seeger J, Lossner U, Bluher M, Stumvoll M, Fasshauer M (2008) Serum levels of the atherosclerosis biomarker sTWEAK are decreased in type 2 diabetes and end-stage renal disease. *Atherosclerosis* 199(2):440–444. <https://doi.org/10.1016/j.atherosclerosis.2007.10.022>
- Maymó-Masip E, Vendrell J, Garrifo-Sanchez L, Fernández-Veledo S, Chacón MR, Vázquez-Carballo A, García España A, Tinahones FJ, García-Fuentes E, Rodríguez MdM (2013) The rise of soluble TWEAK levels in severely obese subjects after bariatric surgery may affect adipocyte-cytokine production induced by TNF α . *J Clin Endocrinol Metab* 98(8):E1323–E1333. <https://doi.org/10.1210/jc.2012-4177>
- Jakubowski A, Ambrose C, Parr M, Lincecum JM, Wang MZ, Zheng TS, Browning B, Michaelson JS, Baetscher M, Wang B, Bissell DM, Burkly LC (2005) TWEAK induces liver progenitor cell proliferation. *J Clin Invest* 115(9):2330–2340. <https://doi.org/10.1172/jci23486>
- Zhu C, Zhang L, Liu Z, Li C, Bai Y (2017) TWEAK/Fn14 interaction induces proliferation and migration in human airway smooth muscle cells via activating the NF-kappaB pathway. *J Cell Biochem*. <https://doi.org/10.1002/jcb.26525>
- Liu J, Peng L, Liu Y, Wu K, Wang S, Wang X, Liu Q, Xia Y, Zeng W (2018) Topical TWEAK accelerates healing of experimental burn wounds in mice. *Front Pharmacol* 9:660. <https://doi.org/10.3389/fphar.2018.00660>
- Polek TC, Talpaz M, Darnay BG, Spivak-Kroizman T (2003) TWEAK mediates signal transduction and differentiation of RAW264.7 cells in the absence of Fn14/TweakR. Evidence for a second TWEAK receptor. *J Biol Chem* 278(34):32317–32323. <https://doi.org/10.1074/jbc.M302518200>
- Xiao G, Lyu M, Wang Y, He S, Liu X, Ni J, Li L, Fan G, Han J, Gao X, Wang X, Zhu Y (2019) Ginkgo flavonol glycosides or ginkgolides tend to differentially protect myocardial or cerebral ischemia-reperfusion injury via regulation of TWEAK-Fn14 signaling in heart and brain. *Front Pharmacol* 10:735. <https://doi.org/10.3389/fphar.2019.00735>
- Dogra C, Changotra H, Wedhas N, Qin X, Wergedal JE, Kumar A (2007) TNF-related weak inducer of apoptosis (TWEAK) is a potent skeletal muscle-wasting cytokine. *FASEB J* 21(8):1857–1869. <https://doi.org/10.1096/fj.06-7537com>
- Morosetti R, Gliubizzi C, Sanerica C, Broccolini A, Gidaro T, Lucchini M, Mirabella M (2012) TWEAK in inclusion-body myositis muscle: possible pathogenic role of a cytokine inhibiting myogenesis. *Am J Pathol* 180(4):1603–1613. <https://doi.org/10.1016/j.ajpath.2011.12.027>
- Yadava RS, Foff EP, Yu Q, Gladman JT, Zheng TS, Mahadevan MS (2016) TWEAK regulates muscle functions in a mouse model of RNA toxicity. *PLoS ONE* 11(2):e0150192. <https://doi.org/10.1371/journal.pone.0150192>
- Mittal A, Bhatnagar S, Kumar A, Lach-Trifilieff E, Wauters S, Li H, Makonchuk DY, Glass DJ, Kumar A (2010) The TWEAK-Fn14 system is a critical regulator of denervation-induced skeletal muscle atrophy in mice. *J Cell Biol* 188(6):833–849. <https://doi.org/10.1083/jcb.200909117>
- Wiley SR, Cassiano L, Lofton T, Davis-Smith T, Winkles JA, Lindner V, Liu H, Daniel TO, Smith CA, Fanslow WC (2001) A novel TNF receptor family member binds TWEAK and is implicated in angiogenesis. *Immunity* 15(5):837–846. [https://doi.org/10.1016/S1074-7613\(01\)00232-1](https://doi.org/10.1016/S1074-7613(01)00232-1)
- Chen JL, Walton KL, Winbanks CE, Murphy KT, Thomson RE, Makanji Y, Qian H, Lynch GS, Harrison CA, Gregorevic P (2014) Elevated expression of activins promotes muscle wasting and cachexia. *FASEB J* 28(4):1711–1723. <https://doi.org/10.1096/fj.13-245894>
- Winer H, Fraiberg M, Abada A, Dadosh T, Tamim-Yecheskel BC, Elazar Z (2018) Autophagy differentially regulates TNF receptor Fn14 by distinct mammalian Atg8 proteins. *Nat Commun* 9(1):3744. <https://doi.org/10.1038/s41467-018-06275-1>
- Culp PA, Choi D, Zhang Y, Yin J, Seto P, Ybarra SE, Su M, Sho M, Steinle R, Wong MHL, Evangelista F, Grove J, Cardenas M, James M, Hsi ED, Chao DT, Powers DB, Ramakrishnan V, Dubridge R (2010) Antibodies to TWEAK receptor inhibit human tumor growth through dual mechanisms. *Clin*

- Cancer Res 16(2):497–508. <https://doi.org/10.1158/1078-0432.ccr-09-1929>
28. Johnston AJ, Murphy KT, Jenkinson L, Laine D, Emmrich K, Faou P, Weston R, Jayatilake KM, Schloegel J, Talbo G, Casey JL, Levina V, Wong WW, Dillon H, Sahay T, Hoogenraad J, Anderton H, Hall C, Schneider P, Tanzer M, Foley M, Scott AM, Gregorevic P, Liu SY, Burkly LC, Lynch GS, Silke J, Hoogenraad NJ (2015) Targeting of Fn14 prevents cancer-induced cachexia and prolongs survival. *Cell* 162(6):1365–1378. <https://doi.org/10.1016/j.cell.2015.08.031>
 29. Wu CL, Kandarian SC, Jackman RW (2011) Identification of genes that elicit disuse muscle atrophy via the transcription factors p50 and Bcl-3. *PLoS ONE* 6(1):e16171. <https://doi.org/10.1371/journal.pone.0016171>
 30. Paul PK, Bhatnagar S, Mishra V, Srivastava S, Darnay BG, Choi Y, Kumar A (2012) The E3 ubiquitin ligase TRAF6 intercedes in starvation-induced skeletal muscle atrophy through multiple mechanisms. *Mol Cell Biol* 32(7):1248–1259. <https://doi.org/10.1128/mcb.06351-11>
 31. Vendrell J, Maymo-Masip E, Tinahones F, Garcia-Espana A, Megia A, Caubet E, Garcia-Fuentes E, Chacon MR (2010) Tumor necrosis-like weak inducer of apoptosis as a proinflammatory cytokine in human adipocyte cells: up-regulation in severe obesity is mediated by inflammation but not hypoxia. *J Clin Endocrinol Metab* 95(6):2983–2992. <https://doi.org/10.1210/jc.2009-2481>
 32. Brown SA, Cheng E, Williams MS, Winkles JA (2013) TWEAK-independent Fn14 self-association and NF-kappaB activation is mediated by the C-terminal region of the Fn14 cytoplasmic domain. *PLoS ONE* 8(6):e65248. <https://doi.org/10.1371/journal.pone.0065248>
 33. Burkly LC, Dohi T (2011) The TWEAK/Fn14 Pathway in tissue remodeling: for better or for worse. In: Wallach D, Kovalenko A, Feldmann M (eds) *Advances in TNF family research: proceedings of the 12th International TNF conference, 2009*. Springer New York, New York, NY, pp 305–322. doi: 10.1007/978-1-4419-6612-4_32
 34. Pasiakos SM, Berryman CE, Carbone JW, Murphy NE, Carrigan CT, Bamman MM, Ferrando AA, Young AJ, Margolis LM (2018) Muscle Fn14 gene expression is associated with fat-free mass retention during energy deficit at high altitude. *Physiol Rep* 6(14):e13801. <https://doi.org/10.14814/phy2.13801>
 35. Bathgate KE, Bagley JR, Jo E, Talmadge RJ, Tobias IS, Brown LE, Coburn JW, Arevalo JA, Segal NL, Galpin AJ (2018) Muscle health and performance in monozygotic twins with 30 years of discordant exercise habits. *Eur J Appl Physiol*. <https://doi.org/10.1007/s00421-018-3943-7>
 36. Raue U, Trappe TA, Estrem ST, Qian H-R, Helvering LM, Smith RC, Trappe S (2012) Transcriptome signature of resistance exercise adaptations: mixed muscle and fiber type specific profiles in young and old adults. *J Appl Physiol* 112(10):1625–1636. <https://doi.org/10.1152/jappphysiol.00435.2011>
 37. Raue U, Jemiolo B, Yang Y, Trappe S (2015) TWEAK-Fn14 pathway activation after exercise in human skeletal muscle: insights from two exercise modes and a time course investigation. *J Appl Physiol* 118(5):569–578. <https://doi.org/10.1152/jappphysiol.00759.2014>
 38. Dogra C, Hall SL, Wedhas N, Linkhart TA, Kumar A (2007) Fibroblast growth factor inducible 14 (Fn14) is required for the expression of myogenic regulatory factors and differentiation of myoblasts into myotubes. Evidence for TWEAK-independent functions of Fn14 during myogenesis. *J Biol Chem* 282(20):15000–15010. <https://doi.org/10.1074/jbc.M608668200>
 39. Burkly LC, Michaelson JS, Zheng TS (2011) TWEAK/Fn14 pathway: an immunological switch for shaping tissue responses. *Immunol Rev* 244(1):99–114. <https://doi.org/10.1111/j.1600-065X.2011.01054.x>
 40. Darras BT, Miller DT, Urion DK (1993) Dystrophinopathies. In: Pagon RA, Adam MP, Ardinger HH et al. (eds) *GeneReviews(R)*. University of Washington, Seattle, WA, USA. All rights reserved.
 41. Li H, Mittal A, Paul P, Kumar M, Srivastava D, Tyagi S, Kumar A (2009) Tumor necrosis factor-related weak inducer of apoptosis augments matrix metalloproteinase 9 (MMP-9) production in skeletal muscle through the activation of nuclear factor-kappa B-inducing kinase and p38 mitogen-activated protein kinase A potential role of MMP-9 in myopathy. *J Biol Chem* 284:4439–4450. <https://doi.org/10.1074/jbc.M805546200>
 42. Bakkar N, Guttridge DC (2010) NF-kappaB signaling: a tale of two pathways in skeletal myogenesis. *Physiol Rev* 90(2):495–511. <https://doi.org/10.1152/physrev.00040.2009>
 43. Brown SAN, Ghosh A, Winkles JA (2010) Full-length, membrane-anchored TWEAK can function as a juxtacrine signaling molecule and activate the NF-kB pathway. *J Biol Chem* 285(23):17432–17441. <https://doi.org/10.1074/jbc.M110.131979>
 44. Roos C, Wicovsky A, Muller N, Salzmann S, Rosenthal T, Kalthoff H, Trauzold A, Seher A, Henkler F, Kneitz C, Wajant H (2010) Soluble and transmembrane TNF-like weak inducer of apoptosis differentially activate the classical and noncanonical NF-kappa B pathway. *J Immunol* 185(3):1593–1605. <https://doi.org/10.4049/jimmunol.0903555>
 45. Murphy RM, Lamb GD (2013) Important considerations for protein analyses using antibody based techniques: down-sizing western blotting up-sizes outcomes. *J Physiol* 591(Pt 23):5823–5831. <https://doi.org/10.1113/jphysiol.2013.263251>
 46. Murphy RM, Mollica JP, Beard NA, Knollmann BC, Lamb GD (2011) Quantification of calsequestrin 2 (CSQ2) in sheep cardiac muscle and Ca²⁺-binding protein changes in CSQ2 knockout mice. *Am J Physiol Heart Circ Physiol* 300(2):H595–604. <https://doi.org/10.1152/ajpheart.00902.2010>
 47. Tong X, Yin L, Washington R, Rosenberg DW, Giardina C (2004) The p50-p50 NF-kappaB complex as a stimulus-specific repressor of gene activation. *Mol Cell Biochem* 265(1–2):171–183
 48. Bakkar N, Wang J, Ladner KJ, Wang H, Dahlan JM, Carathers M, Acharyya S, Rudnicki MA, Hollenbach AD, Guttridge DC (2008) IKK/NF-kappaB regulates skeletal myogenesis via a signaling switch to inhibit differentiation and promote mitochondrial biogenesis. *J Cell Biol* 180(4):787–802. <https://doi.org/10.1083/jcb.200707179>
 49. Alvarez-Guardia D, Palomer X, Coll T, Davidson MM, Chan TO, Feldman AM, Laguna JC, Vazquez-Carrera M (2010) The p65 subunit of NF-kappaB binds to PGC-1alpha, linking inflammation and metabolic disturbances in cardiac cells. *Cardiovasc Res* 87(3):449–458. <https://doi.org/10.1093/cvr/cvq080>
 50. Sato S, Ogura Y, Kumar A (2014) TWEAK/Fn14 signaling axis mediates skeletal muscle atrophy and metabolic dysfunction. *Front Immunol* 5:18. <https://doi.org/10.3389/fimmu.2014.00018>
 51. Dogra C, Changotra H, Mohan S, Kumar A (2006) Tumor necrosis factor-like weak inducer of apoptosis inhibits skeletal myogenesis through sustained activation of nuclear factor-kappaB and degradation of MyoD protein. *J Biol Chem* 281(15):10327–10336. <https://doi.org/10.1074/jbc.M51131200>
 52. Enwere EK, Holbrook J, Lejmi-Mrad R, Vineham J, Timusk K, Sivaraj B, Isaac M, Uehling D, Al-awar R, LaCasse E, Korneluk RG (2012) TWEAK and cIAP1 regulate myoblast fusion through the noncanonical NF-kappaB signaling pathway. *Sci Signal* 5(246):ra75. <https://doi.org/10.1126/scisignal.2003086>
 53. Varfolomeev E, Goncharov T, Maecker H, Zobel K, Komuves LG, Deshayes K, Vucic D (2012) Cellular inhibitors of apoptosis are global regulators of NF-kappaB and MAPK activation by members of the TNF family of receptors. *Sci Signal* 5(216):ra22. <https://doi.org/10.1126/scisignal.2001878>
 54. Hu WH, Johnson H, Shu HB (2000) Activation of NF-kappaB by FADD, Casper, and caspase-8. *J Biol Chem* 275(15):10838–10844

Controversies in TWEAK-Fn14 signaling in skeletal muscle atrophy and regeneration

55. Ikner A, Ashkenazi A (2011) TWEAK induces apoptosis through a death-signaling complex comprising receptor-interacting protein 1 (RIP1), Fas-associated death domain (FADD), and caspase-8. *J Biol Chem* 286(24):21546–21554. <https://doi.org/10.1074/jbc.M110.203745>
56. Cargnello M, Roux PP (2011) Activation and function of the MAPKs and their substrates, the MAPK-activated protein kinases. *Microbiol Mol Biol Rev* 75(1):50–83. <https://doi.org/10.1128/mmr.00031-10>
57. Jones NC, Fedorov YV, Rosenthal RS, Olwin BB (2001) ERK1/2 is required for myoblast proliferation but is dispensable for muscle gene expression and cell fusion. *J Cell Physiol* 186(1):104–115. [https://doi.org/10.1002/1097-4652\(200101\)186:1%3c104:aid-jcp1015%3e3.0.co;2-0](https://doi.org/10.1002/1097-4652(200101)186:1%3c104:aid-jcp1015%3e3.0.co;2-0)
58. Coolican SA, Samuel DS, Ewton DZ, McWade FJ, Florini JR (1997) The mitogenic and myogenic actions of insulin-like growth factors utilize distinct signaling pathways. *J Biol Chem* 272(10):6653–6662
59. Xie S-J, Li J-H, Chen H-F, Tan Y-Y, Liu S-R, Zhang Y, Xu H, Yang J-H, Liu S, Zheng L-L, Huang M-B, Guo Y-H, Zhang Q, Zhou H, Qu L-H (2018) Inhibition of the JNK/MAPK signaling pathway by myogenesis-associated miRNAs is required for skeletal muscle development. *Cell Death Differ* 25(9):1581–1597. <https://doi.org/10.1038/s41418-018-0063-1>
60. Keren A, Tamir Y, Bengal E (2006) The p38 MAPK signaling pathway: a major regulator of skeletal muscle development. *Mol Cell Endocrinol* 252(1–2):224–230. <https://doi.org/10.1016/j.mce.2006.03.017>
61. Cabane C, Englaro W, Yeow K, Ragno M, Derijard B (2003) Regulation of C2C12 myogenic terminal differentiation by MKK3/p38alpha pathway. *Am J Physiol Cell Physiol* 284(3):C658–666. <https://doi.org/10.1152/ajpcell.00078.2002>
62. Jin B, Li YP (2007) Curcumin prevents lipopolysaccharide-induced atrogin-1/MAFbx upregulation and muscle mass loss. *J Cell Biochem* 100(4):960–969. <https://doi.org/10.1002/jcb.21060>
63. Bodine SC, Stitt TN, Gonzalez M, Kline WO, Stover GL, Bauerlein R, Zlotchenko E, Scrimgeour A, Lawrence JC, Glass DJ, Yancopoulos GD (2001) Akt/mTOR pathway is a crucial regulator of skeletal muscle hypertrophy and can prevent muscle atrophy in vivo. *Nat Cell Biol* 3(11):1014–1019. <https://doi.org/10.1038/ncb1101-1014>
64. Stitt TN, Drujan D, Clarke BA, Panaro F, Timofeyeva Y, Kline WO, Gonzalez M, Yancopoulos GD, Glass DJ (2004) The IGF-1/PI3K/Akt pathway prevents expression of muscle atrophy-induced ubiquitin ligases by inhibiting FOXO transcription factors. *Mol Cell* 14(3):395–403. [https://doi.org/10.1016/s1097-2765\(04\)00211-4](https://doi.org/10.1016/s1097-2765(04)00211-4)
65. Wajant H (2013) The TWEAK-Fn14 system as a potential drug target. *Br J Pharmacol* 170(4):748–764. <https://doi.org/10.1111/bph.12337>
66. Sanz AB, Sanchez-Niño MD, Carrasco S, Manzarbeitia F, Ruiz-Andres O, Selgas R, Ruiz-Ortega M, Gonzalez-Enguita C, Egido J, Ortiz A (2012) Inflammatory cytokines and survival factors from serum modulate tweak-induced apoptosis in PC-3 prostate cancer cells. *PLoS ONE* 7(10):e47440–e47440. <https://doi.org/10.1371/journal.pone.0047440>
67. Fortin SP, Ennis MJ, Savitch BA, Carpentieri D, McDonough WS, Winkles JA, Loftus JC, Kingsley C, Hostetter G, Tran NL (2009) Tumor necrosis factor-like weak inducer of apoptosis stimulation of glioma cell survival is dependent on Akt2 function. *Mol Cancer Res* 7(11):1871–1881. <https://doi.org/10.1158/1541-7786.mcr-09-0194>
68. Ando T, Ichikawa J, Wako M, Hatsushika K, Watanabe Y, Sakuma M, Tasaka K, Ogawa H, Hamada Y, Yagita H, Nakao A (2006) TWEAK/Fn14 interaction regulates RANTES production, BMP-2-induced differentiation, and RANKL expression in mouse osteoblastic MC3T3-E1 cells. *Arthritis Res Ther* 8(5):R146. <https://doi.org/10.1186/ar2038>
69. Yang B, Yan P, Gong H, Zuo L, Shi Y, Guo J, Guo R, Xie J, Li B (2016) TWEAK protects cardiomyocyte against apoptosis in a PI3K/AKT pathway dependent manner. *Am J Transl Res* 8(9):3848–3860

Publisher's Note Springer Nature remains neutral with regard to jurisdictional claims in published maps and institutional affiliations.

Thesis Outline and Aims

The current thesis aims to investigate the role of TWEAK-Fn14 in both acute and chronic muscle homeostasis as well as the efficacy of targeting the TWEAK-Fn14 pathway in the prevention or treatment of acute muscle injury with the following studies and aims:

Study One (Chapter 3)

1. To generate and characterise the binding, activity, and myogenic outcomes of a crosslinked α -Fn14 antibody (α -Fn14 001X):
 - a. Generate α -Fn14 001X via sulfosuccinimidyl 4-(N-maleimidomethyl) cyclohexane-1-carboxylate (Sulfo-SMCC) crosslinking;
 - b. Confirm the ability of α -Fn14 001X to bind human and mouse derived Fn14;
 - c. Characterise the ability of α -Fn14 001X to stimulate NF κ B activity;
 - d. Determine the pro- or anti-myogenic outcomes of α -Fn14 001X relative to α -Fn14 001 and varying concentrations of sTWEAK on proliferating and differentiating C2C12 mouse myoblasts.

Study Two (Chapter 4 and Chapter 5)

1. Investigate the effects of Fn14 stimulation in an acute injury model
 - a. Perform, and characterise the recovery from, a notexin-induced acute myogenic injury in C57BL/6 mice;
 - b. Determine the effects of α -Fn14 001 and α -Fn14 001X on:
 - i. Myogenic recovery;
 - ii. Fn14 and TWEAK expression;
 - iii. Atrophic and inflammatory markers.

Study Three (Chapter 5 and Chapter 6)

2. To determine whether TWEAK-Fn14 is a viable target in the prevention or management of age-associated muscle atrophy
 - a. Characterise the myogenic and metabolic profiles of old and chronically low-resistance trained mouse muscle by examining muscle mass, fibre type composition, activity level, mitochondrial content and dynamics, and atrophic markers;
 - b. Determine Fn14 and TWEAK correlations with the described myogenic and metabolic profiles of these mice.

Chapter 2

General Methods and Materials

Chapter Summary

Methods outlined here are techniques or protocols repeated throughout the thesis. Where a method is used only in one chapter, the full details are outlined within the methods section of the relevant chapter.

2.1. Animals

All procedures were approved by, and conducted in accordance with, the Animal Ethics Committee of La Trobe University (AEC 15-32, 16-70, 17-68). Additional retrospective samples were provided by Emer. Prof. Miranda Grounds and Dr Zoe White (University of Western Australia), Dr Chris van der Poel (La Trobe University), and Dr Alex Addinsall (Deakin University).

2.1.1. Notexin Injury

Male C57BL/6 mice (16 weeks old, n=36) were used for notexin injury protocol. Mice were housed in littermate groups prior to injury and individually post-injury as per the NHMRC 'Guide for the Care and Use of Laboratory Animals' (National Research Council, 2011) and local AEC and veterinary advice. Notexin injury was performed by Dr Chris van der Poel (School of Life Sciences, La Trobe University). C57BL/6 mice (n=36) were placed under isoflurane anaesthesia (flow rate 2-5%, recovery within 5 minutes) and a small incision (2-3 mm) was made to expose the left and right *tibialis anterior* (TA) muscles. 40 µL of notexin (10 µg/ml, total 0.4 µg notexin, Latoxan, France) was injected intramuscularly in the right TA muscle and 40 µL saline injected in the left TA as an internal control. Incisions were closed with reflex wound clips and mice were subcutaneously administered with buprenorphine (0.05 mg/kg body weight) whilst still under anaesthesia. Mice were placed on heat pads during the initial recovery period (average time on heat pad was 10-15 minutes). Additional buprenorphine and saline fluids were administered subcutaneously throughout the recovery period in response to the poor body and behavioural condition observed, as prescribed by

the supervising veterinarians, Dr John Inns and Dr Tara Egan (La Trobe Animal Research and Training Facility, La Trobe University).

Mice were IP injected with either α -Fn14 001, α -Fn14 001X (20 mg/kg – see Chapter 3 for details of antibody generation; n = 12 for each treatment), or no antibody injection control (NoAB; n = 12) at 6-hours post-injury, and again at 7 days post-injury, if applicable. Mouse body weights were recorded daily and core temperatures were monitored in select animals until stabilised.

Animals were culled by CO₂ asphyxiation with a secondary kill method of cervical dislocation at 3-, 7-, or 14 days post-procedure (n = 4 for each treatment at each time point except α -Fn14 001X 14 days post-injury group where n = 3) and both TA muscles and blood (via cardiac puncture immediately post-mortem) were collected. Post-injury time points were selected following assessment of previous notexin and barium chloride injured mouse muscle samples (see Appendix IV). Blood was centrifuged (16,000g, 10 minutes, 4°C) to separate plasma from blood cells; plasma was snap frozen in liquid nitrogen.

2.1.2. Dissection

Hind legs were surgically exposed post-mortem and *tibialis anterior* (TA), *extensor digitorum longus* (EDL), *soleus* (SOL), and *gastrocnemius* (GAS) were removed as close to the tendon as possible. Excised muscles were placed in cryotubes and frozen directly in liquid nitrogen, or coated in OCT (TissueTek) and frozen in 2-methylbutane over liquid nitrogen. Frozen samples were stored at -80°C until required.

2.2. Old and Chronically Resistance-Trained Mice

Samples from old and chronically resistance-trained mice were provided by Emer. Professor Miranda Grounds and Dr Zoe White with full experimental and morphological information

published in Softe *et al.* (2016). Young (13 weeks) and old (105 weeks) C57BL/6 mice were housed in either standard cages (sedentary controls – YOUNG SED $n = 9$, OLD SED $n = 9$) or voluntary access resistance running wheels under a progressive low resistance training (low resistance (LR) group – YOUNG LR $n = 7$, OLD LR $n = 7$) or progressive high resistance training (high resistance (HR) group – YOUNG HR $n = 7$) program for 10 weeks. Quadriceps (QUAD) muscles were collected and stored whole at -80°C .

2.3. Histology

OCT mounted frozen muscles were bisected at the widest point and serial $10\ \mu\text{m}$ cryosections were taken at -20°C and mounted on 1.0-1.2 mm glass microscope slides (Livingstone, Australia; Knittel, Germany). Slides were stored at -20°C until required.

2.3.1. Haematoxylin and Eosin

Tissue architecture was assessed using Haematoxylin and Eosin (H+E) staining. Slides were brought to room temperature and rinsed under running tap water before H+E staining. Sections were stained with Mayer's haematoxylin for 40 seconds, rinsed under running tap water until water ran clear, Scott's tap water for 15 seconds, standing tap water for 30 seconds, 1% aqueous eosin for 35 seconds, and rinsed again under running tap water until water ran clear. Slides were dried in 75% ethanol then twice in 100% ethanol, followed by 2 x 2 minutes in xylene, and then mounted with DPX mounting medium. Stained sections were examined microscopically for markers of injury. Markers of injury were defined as centralised nuclei, loss of muscle fibre size uniformity, proportion of non-contractile, and infiltration of inflammatory cells (Spasov *et al.*, 2010).

2.4. Western Blotting

2.4.1. Sample Preparation

Frozen muscle samples were bisected at the widest point at -20°C and $\sim 20 \times 10 \mu\text{m}$ cryosections from the widest point of the muscle were collected. Excess OCT was removed when applicable. Sections were placed directly in $150 \mu\text{l}$ relaxing buffer with SDS loading buffer (2:1 v/v relaxing buffer: SDS loading buffer; relaxing buffer: 129 mM K^+ , 36 mM Na^+ , $1 \text{ mM free Mg}^{2+}$ ($10.3 \text{ mM total Mg}^{2+}$), 90 mM HEPES , 50 mM EGTA , osmolality $295 \pm 10 \text{ mOsmol/kg H}_2\text{O}$; SDS loading buffer: 0.125 M Tris-HCL , $4\% \text{ SDS}$, $10\% \text{ glycerol}$, 4 M urea , $10\% \text{ beta-mercaptoethanol (2-ME)}$, $0.001\% \text{ bromophenol blue}$). To aid solubilisation, samples were incubated at room temperature for one hour, and vortexed for five seconds every 20 minutes during incubation. Resulting solubilised samples, herein after referred to as homogenates, were frozen at -80°C and thawed before further use. Homogenates were normalised for total protein content and diluted to approximately $2.5 \mu\text{g wet weight}/\mu\text{l}$ with SDS loading buffer (see above). A muscle calibration mix was created by combining equal volumes of homogenates for all samples within a given study. This calibration curve was run on all gels for the given study to allow comparison across gels. Normalised homogenates and muscle calibration mixes were stored at -80°C .

2.4.2. Immunodetection

Homogenates were run on Criterion TGX 4-15% or 10% stain-free gels (BioRad) in Tris/Glycine/SDS running buffer (BioRad) at 200V for 45 or 60 minutes respectively unless specified otherwise. All gels included a 4- or 5-point calibration curve ranging from 1 to $16 \mu\text{l}$ and PageRuler Plus Prestained Protein Ladder molecular weight markers (ThermoFisher, Melbourne, Australia). Proteins were transferred to $0.45 \mu\text{m}$ nitrocellulose membrane filter

using a BioRad transfer system (100 V, 30 minutes) in Tris/Glycine transfer buffer (BioRad) with 20% (v/v) methanol. Total protein was visualised using UV detection on the gel pre- and post-transfer, and the nitrocellulose membrane filter post transfer, to confirm successful and even transfer. nitrocellulose membrane filters were treated with Miser Antibody Extender (ThermoFisher) for 10 minutes and blocked for at least 1 hour in 5% (w/v) skim milk in tris-buffered saline with Tween-20 (TBST) with constant rocking before immunodetection. Primary antibodies were diluted in 1% BSA/ PBST + 0.02% NaN₃ and incubated at 4°C overnight with constant rocking. Secondary antibodies were goat α-rabbit (PIE31460, ThermoFisher), goat α-mouse (PIE31430, ThermoFisher), or goat α-mouse intact (ab97023, Abcam) conjugated with horse radish peroxidase diluted in 5% skim milk/ PBST, incubated at room temperature for 45-60 minutes with constant rocking. Full antibody details are provided in Appendix III. Chemiluminescent detection was performed using SuperSignal West Femto Maximum Sensitivity Substrate (BioRad) on either a ChemiDoc Touch or Chemidoc MP detection system (BioRad). Relative protein quantification was performed using the low concentration western blotting technique as described and validated in Murphy *et al.* (2011). Quantification was performed only on bands which fell within the calibration curve. Full details of antibodies used can be found in Appendix III.

2.5. Fibre Type Composition by SDS-PAGE

Muscle sections were diluted in myosin heavy chain (MHC) loading buffer (1:1 v/v MHC 2X loading buffer: relaxing buffer; 2X MHC loading buffer: 0.125 M Tris-HCL, 25% glycerol, 4.6% SDS, 10% 2-ME, 25% sucrose, 0.001% bromophenol blue; relaxing buffer: 129 mM K⁺, 36 mM Na⁺, 1 mM free Mg²⁺ (10.3 mM total Mg²⁺), 90 mM HEPES, 50 mM EGTA, osmolality 295 ± 10 mOsmol/kg H₂O). Resultant homogenates were normalised for total protein content as

described in Chapter 2, Section 2.4.1. Normalised homogenates were run on SDS-PAGE MHC Separating Gels (stacking gel: 30% glycerol, 4% acrylamide, 50:1 acrylamide: N'ethlyenebisacrylamide, 70 mM Tris-HCL pH 6.7, 0.4% SDS, 4 mM EDTA, 0.1% ammonium persulfate, 0.05% N,N,N',N'-tetramethylethylenediamine (TEMED); separating gel: 32% glycerol, 8% acrylamide, 50:1 acrylamide: N'ethlyenebisacrylamide, 0.2 M Tris-HCL pH 8.8, 0.4% SDS, 0.1 M glycine, 0.1% ammonium persulfate, 0.05% TEMED). Gels were run using MHC gel lower running buffer (0.05 M Tris, 75 mM glycine, 0.05% w/v SDS) and MHC gel upper running buffer (6X MHC gel lower running buffer with 0.12% w/v 2-ME). Gels were run at 150 V at 4°C for 24 hours then stained with coomassie brilliant blue G250 (Bio-Rad, Gladesville, NSW, Australia) and imaged using a Chemidoc MP detection system (BioRad).

2.6. Gene Expression

2.6.1. cDNA synthesis

RNA was extracted from cryosections of muscles. Cryosections (~50, wet weight ~2-5 mg) were placed directly in 250 µl ice cold TRI reagent (Molecular Research Centre, Ohio US) and homogenised by pipetting then incubated at room temperature for 5 minutes. Phase separation was induced with 12.5 µl 4-bromoanisole (Molecular Research Centre) and tubes centrifuged at 12,000 *g* for 15 minutes at 4°C. Supernatant was removed and added to 125 µl isopropanol to precipitate RNA. Samples were incubated at room temperature for 15 minutes then centrifuged at 12,000 *g* for 10 minutes at 4°C. Pellets were washed twice in ice cold ethanol before being centrifuged at 8,000 *g* for 5 minutes at 4°C. Excess ethanol was removed and pellets air dried for 2-5 minutes before resuspending in 20 µl nuclease-free H₂O. Final RNA concentration and purity was assessed by NanoDrop (ThermoFisher) spectrophotometry. cDNA was synthesised using an iScript cDNA synthesis kit (BioRad) with

1 ng of RNA template on a Takara PCR Thermal Cycler with the manufacturers thermal cycling conditions (Table 2.1).

Table 2.1: iScript cDNA Synthesis Thermal Cycling Conditions

priming	5 minutes at 25°C
reverse transcription (RT)	20 minutes at 46°C
RT inactivation	1 minute at 95°C
hold	4°C

2.6.2. cDNA Quantification

cDNA was quantified using an OliGreen ssDNA Quantification Kit (BioRad) according to manufacturer's instructions and used for normalisation of qPCR results.

2.6.3. qPCR

qPCR was performed using iTaq Universal SYBR Green Supermix (BioRad). Approximately 1 ng cDNA template was added to 20 µl reactions and run on a CFX96 Real Time PCR Detection System (BioRad) using the manufacturers thermal cycling conditions (Table 2.2). A no template control (NTC) contained mastermix reagent with no cDNA template. Results were analysed using the 2^{-Ct} method normalised to the total cDNA content as determined by OliGreen ssDNA assay.

Table 2.2: iTaq Universal SYBR Green Supermix qPCR Thermal Cycling Settings

Polymerase Activation	30 seconds at 95°C	} x 40 cycles
DNA Denaturation	5 seconds at 95°C	
Annealing/Extension and Plate Read	30 seconds at 60°C	
Melt Curve Analysis	65°C to 95°C, 0.5°C increments for 5 seconds and plate read	

2.7. Cell Culture

Cell culture methods are described in full in Chapter 3.

2.8. Citrate Synthase Activity

Assay protocol is described in full in Chapter 6.

2.9. Statistical Analyses

Results are presented as mean \pm standard deviation or standard error of mean unless stated otherwise. Data was analysed using one-way ANOVA, two-way ANOVA, two-tailed paired t-test, or Pearson r correlation as appropriate and detailed in specific figure legends. Significance was declared at $p \leq 0.05$. All statistical tests were performed using Prism v8 (GraphPad).

References

- Murphy RM, Mollica JP, Beard NA, Knollmann BC & Lamb GD. (2011). Quantification of calsequestrin 2 (CSQ2) in sheep cardiac muscle and Ca²⁺-binding protein changes in CSQ2 knockout mice. *Am J Physiol Heart Circ Physiol* **300**, H595-604.
- National Research Council. (2011). *Guide for the Care and Use of Laboratory Animals: Eighth Edition*, doi:10.17226/12910. The National Academies Press, Washington, DC.
- Soffe Z, Radley-Crabb HG, McMahon C, Grounds MD & Shavlakadze T. (2016). Effects of loaded voluntary wheel exercise on performance and muscle hypertrophy in young and old male C57Bl/6J mice. *Scand J Med Sci Sports* **26**, 172-188.
- Spasov A, Gredes T, Gedrange T, Lucke S, Pavlovic D & Kunert-Keil C. (2010). Histological changes in masticatory muscles of mdx mice. *Arch Oral Biol* **55**, 318-324.

Chapter 3

Generation and *in vitro* Characterisation of α -Fn14 Antibodies

Chapter Summary

The following chapter describes the rationale and method of generating a cross-linked α -Fn14 antibody. It details the validation and characterisation of the newly generated antibody in reporter cell lines and in C2C12 myoblasts. This work lays the foundations for moving forward with an *in vitro* assessment of the antibody and attempts investigation of downstream signalling pathways which are activated in C2C12 myoblasts which could not be confidently assessed in whole muscle homogenates from notexin-injured mice due to limitations of commercially available antibodies (see Chapter 4 and Appendix III). Whilst these assessments were again limited, they were sufficient to determine that α -Fn14 treatment is able to activate Fn14 independently of sTWEAK and provide a basis for ongoing *in vivo* work. Please refer to the supplementary COVID-19 Impact Statement (Appendix I) for further clarification of limitations in this chapter and Appendix II for preliminary data.

3.1. Introduction

A pivotal study by Johnston *et al.* (2015) demonstrated the efficacy of an α -Fn14 antibody in preserving muscle mass in a cachectic mouse model. Whilst cachexia presents as progressive skeletal muscle wasting, the underlying basis is rooted in the comorbidity of terminal cancer. Use of the same antibody intervention in a direct skeletal muscle insult – namely the muscle-specific upregulation of activin A using a recombinant adeno-associated virus-based vector to induce atrophy – failed to preserve muscle mass (Johnston *et al.*, 2015). The antibody in question, α -Fn14 001, has been characterised *in vitro* as an antagonistic (blocking) antibody, blocking the activation of the TWEAK-Fn14 signalling pathway in HEK293T NF κ B-GFP reporter cells (Johnston *et al.*, 2015). Previous work both *in vitro* and *in vivo* has demonstrated that genetic depletion of Fn14 is in fact detrimental to the development and regeneration of muscle (Girgenrath *et al.*, 2006; Dogra *et al.*, 2007). C2C12 myoblasts and mouse primary myoblasts treated with short interfering RNA to suppress Fn14 both showed marked reductions in the ability to differentiate into mature myotubes (Dogra *et al.*, 2007). Likewise, Fn14-deficient 129/sv mice showed delayed recovery following an acute cardiotoxin-induced injury, marked by a reduction in centrally nucleated fibres and embryonic myosin expression (Girgenrath *et al.*, 2006). It is apparent from these studies that rather than perpetuating atrophy, Fn14 may play an important role in the pro-myogenic program.

The conclusions drawn by Johnston *et al.* (2015) suggest that whilst α -Fn14 001 is an effective anti-cachectic treatment, it likely acts by blocking Fn14 present on the tumour itself, thus blocking the release of an unknown factor(s) which in turn induces atrophy. This is in contrast to exerting effects by directly interacting with Fn14 present on the skeletal muscle. Given the apparent role of Fn14 in promoting muscle development, it is hypothesised that an

agonistic (activating) α -Fn14 antibody – in contrast with the likely antagonistic α -Fn14 001 – may prove beneficial in the direct treatment of injured or atrophic muscle.

The experiments in this chapter aim to generate and characterise an agonistic α -Fn14 antibody. Fn14 belongs to the TNF receptor superfamily (TNFRSF), and is otherwise known as TNFRSF12A. Antibodies against TNFRSF members are reported to have strong agonistic properties when oligomerised, whilst their dimeric forms generally exhibit little to no agonistic activity (Wajant, 2015). In the current study, an oligomeric form of α -Fn14 001, referred to hereafter as α -Fn14 001X, was generated and characterised *in vitro* for binding ability, NF κ B activity, and downstream myogenic outcomes in the presence or absence of the endogenous Fn14 ligand, soluble TWEAK (sTWEAK).

3.2. Methods

3.2.1. Sulfo-SMCC cross-linkage of α -Fn14 001

The α -Fn14 001 antibody previously generated and described by Johnston *et al.* (2015) was cross-linked using SMCC and Sulfo-SMCC (ThermoScientific, USA) cross-linking protocol to create cross-linked α -Fn14 001 (001X; Figure 3.1). Efficiency of the cross-linking procedure was assessed using a 4-12% bis-tris NuPAGE gel with MOPS buffer under non-reducing conditions. Both α -Fn14 001 and α -Fn14 001X were assessed for endotoxin contamination using Charles River Endosafe PTS (Charles River).

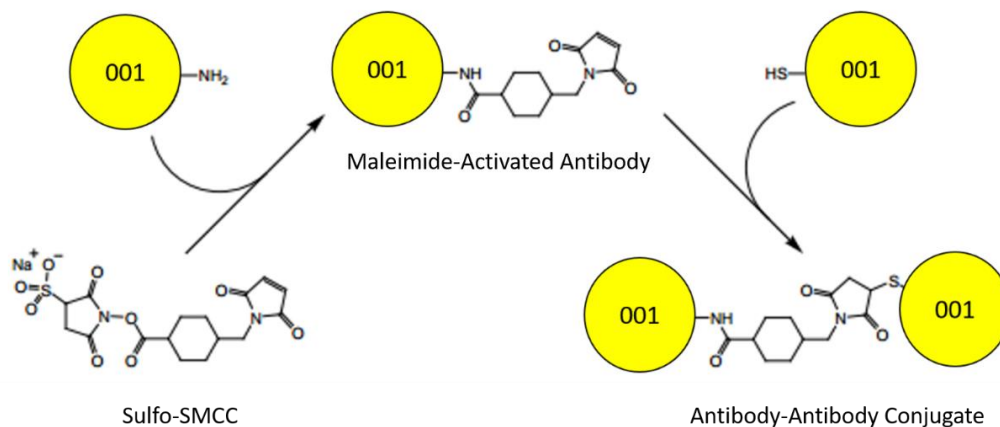


Figure 3.1: Sulfo-SMCC crosslinking of α -Fn14 001 antibody. Amide-containing α -Fn14 001 is conjugated to Sulfo-SMCC to generate maleimide-activated α -Fn14 001. The maleimide-activated 001 is then reacted with sulfhydryl-containing α -Fn14 001 to generate the cross-linked antibody, α -Fn14 001X. Figure adapted from SMCC and Sulfo-SMCC Protocol (ThermoFisher).

3.2.1.1. Fn14 Binding

Binding of α -Fn14 001 to human and mouse Fn14 (hFn14 and mFn14, respectively) has previously been shown in Johnston *et al.* (2015). Retention of α -Fn14 001X ability to bind hFn14 and mFn14 was assessed using mouse embryonic fibroblast (MEF) H-Ras^{V12} cells expressing endogenous mFn14 and inducible hFn14.

Induced or non-induced MEF H-Ras^{V12} cells (1×10^5) in 1% BSA/PBS were added to 96-well tissue culture plates and centrifuged at 250 *g* for 3 minutes to pellet cells. Supernatant was aspirated and α -Fn14 001X at concentrations ranging from 0.01-0.5 μ g/ml (data shown only for 0.5 μ g/ml) were added and incubated for 30 minutes on ice. Plates were centrifuged at 250 *g* for 3 minutes and supernatant aspirated followed by three washes with PBS. Secondary antibody (goat anti-mouse Alexafluor647™, 1:200 in 1% BSA/PBS) was added and incubated for 30 minutes on ice. Plates were centrifuged at 250 *g* for 3 minutes and washed three times with PBS. Pellets were resuspended in 100 μ l PBS and assessed by flow cytometry.

3.2.1.2. NF κ B Activation Assay

NF κ B activation of α -Fn14 001 and α -Fn14 001X was assessed in HEK293T cells that endogenously express hFn14 with a stably introduced NF κ B-GFP reporter construct (Vince *et al.*, 2008). Flat-bottom 96 well tissue culture-treated plates were seeded with 1×10^4 cells/well and allowed to attach for 24 hours. Cells were then incubated overnight at 37°C in 5% CO₂, with either no antibody, α -Fn14 001, or α -Fn14 001X at 0.1 μ g/ml or 1 μ g/ml, and in the presence of sTWEAK (0-200 ng/ml). Post-incubation, cells were gently resuspended and transferred to round bottom 96-well plates for flow cytometry analysis.

3.2.2. In vitro myogenic effects of α -Fn14 001, α -Fn14 001X, and sTWEAK

Myogenic outcomes of α -Fn14 001, α -Fn14 001X, and varying concentrations of sTWEAK were determined in C2C12 myoblasts. A combination of α -Fn14 001 and protein-G was used as a substitute for α -Fn14 001X in cell culture experiments due to limited availability of SMCC-crosslinked α -Fn14 001. C2C12 mouse myoblast cells were maintained in Gibco Dubecco's Modified Eagle Media (DMEM; ThermoFisher, Australia) containing 1% penicillin-streptomycin and 10% foetal bovine serum (FBS).

For differentiation assay, 3.5×10^5 cells were seeded in 6 well plates and grown to ~80% confluence. Differentiation was triggered by replacing 10% FBS with 2% horse serum. Cell cultures were treated with either 1 $\mu\text{g/ml}$ $\alpha\text{-Fn14 001}$, 1 $\mu\text{g/ml}$ $\alpha\text{-Fn14 001}$ with 1 $\mu\text{g/ml}$ protein-G (ThermoFisher), 1 ng/ml sTWEAK, 100 ng/ml sTWEAK, or 500 ng/ml sTWEAK. Cells were imaged using light microscopy at 40X magnification to assess myotube growth and fusion, and subsequently harvested at 48, 72, and 96 hours. Culture media was changed every two days throughout the assay period.

Lysates were prepared by resuspending cell pellets in SDS loading buffer (0.125 M Tris-HCl, 4% SDS, 10% glycerol, 4 M urea, 10% β -mercaptoethanol (2-ME), 0.001% bromophenol blue). Lysates were stored at room temperature for 1 hour, vortexing for 5 seconds every 20 minutes, before storing at -80°C prior to use. A master mix containing equal volumes of lysate from all samples was created and used as an internal calibration curve run on all western blots to allow comparison across gels.

3.2.2.1. Differentiation Assay

Differentiation was assessed qualitatively by light microscopy as described above as well as semi-quantitatively by western blotting of cell lysates for myosin (MF-20, DSHB). Lysates were subjected to SDS-PAGE using Criterion TGX 4-15% Stain-Free gels (BioRad, Hercules, CA, USA) in Tris/Glycine/SDS running buffer (BioRad) at 200 V for 45 minutes at room temperature as per methods described in Chapter 2, Section 2.4. Total protein was visualised using UV activation followed by light detection and measured with ImageLab v 5.2.1 software (BioRad). Specific protein density was measured on ImageLab v 5.2.1 and expressed normalised to total protein.

3.3. Results

3.3.1. Cross-linked α -Fn14 001 Quality Control

Efficacy of SMCC crosslinking of α -Fn14 001 to produce α -Fn14 001X was confirmed by subjecting samples to non-reducing SDS-PAGE using bis-tris NuPAGE gels (Figure 3.2). A prominent band was observed in α -Fn14 001 at ~91 kDa (monomer) along with some faint lower molecular weight bands at ~64 and ~51kDa, identified as SMCC fragments. The crosslinked α -Fn14 001X exhibited two prominent bands at ~91 kDa (monomer) and above the largest marker of 191 kDa (dimer, polymer), in addition to some faint higher and lower molecular weight bands, identified as SMCC fragments. In addition, the level of contaminating endotoxin was assessed and determined to be less than the level of assay detection (< 0.05 EU/mg; data not shown).

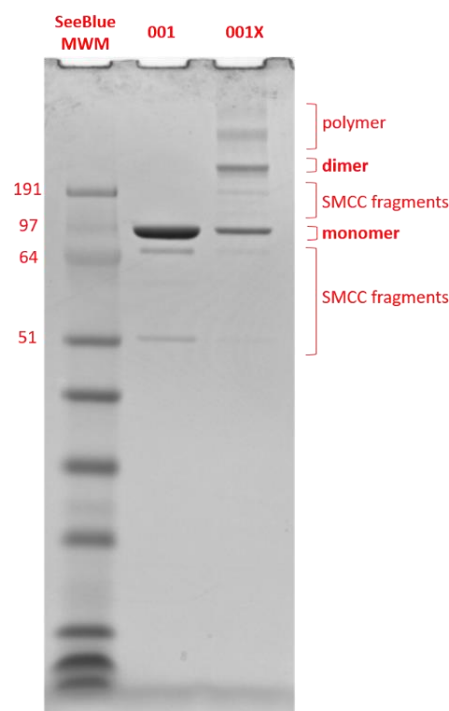


Figure 3.2: Efficacy of SMCC crosslinking of α -Fn14 001 to generate α -Fn14 001X. SMCC crosslinking was assessed by gel electrophoresis under non-reducing conditions. α -Fn14 001 showed a large band close to the 97 kDa marker with some faint bands detected close to the 64 and ~51 kDa markers. α -Fn14 001X showed similar bands to α -Fn14 001 with additional higher molecular weight bands band above the largest molecular weight marker of 191 kDa. The density of the presumed monomer and dimer was approximately equal in the α -Fn14 001X sample. Monomer, dimer, polymer all indicated, in addition to SMCC fragments.

3.3.2. Fn14 Binding

Binding of α -Fn14 001X to both hFn14 and mFn14 was observed (Figure 3.3). Shift in Alexa-647A signal was detected in both populations with a greater shift, indicating antibody binding, detected in induced cells expressing hFn14 as well as endogenous mFn14. Binding was dose-dependent with greatest shift detected in 0.5 μ g/ml antibody (data shown only for 0.5 μ g/ml). Binding of α -Fn14 001 to hFn14 and mFn14 has previously been shown in Johnston *et al.* (2015).

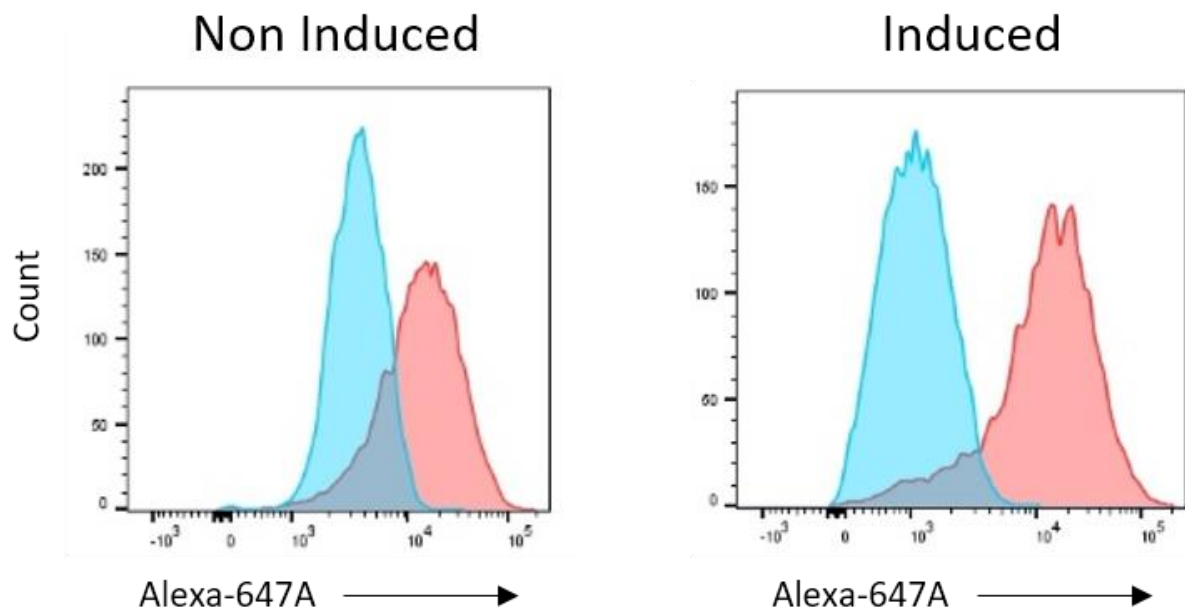


Figure 3.3: Binding of α -Fn14 001X to endogenous mouse Fn14 and induced human Fn14 in mouse embryonic fibroblast (MEF) H-Ras^{V12} cells. MEF H-Ras^{V12} cells were induced to express human Fn14 (hFn14). Non-induced cells express endogenous mouse Fn14 (mFn14) only. Blue histogram shows cells stained with secondary antibody only, red histogram shows cells stained with α -Fn14 001X (0.5 μ g/ml). The shift to the right in the induced situation indicates a higher degree of antibody binding.

3.3.3. NFκB Activation Assay in HEK293T NFκB-GFP Reporter Cells

HEK293T NFκB-GFP reporter cells expressing endogenous hFn14 were treated with a range of sTWEAK concentrations (0, 50, 100, 200 ng/ml), and NFκB activation by addition of α-Fn14 001 and α-Fn14 001X was assessed (Figure 3.4). sTWEAK alone was shown to induce dose-dependent NFκB activation, observed as an increase in GFP expression and indicated by a shift in the blue histograms (Figure 3.4). Red histograms represent the same condition with the addition of the specified antibody concentration. Activation was effectively countered by α-Fn14 001 at a dose of 1 µg/ml. Baseline activity of α-Fn14 001X showed moderate increase in GFP expression in the absence of sTWEAK, addition of sTWEAK failed to induce further activity.

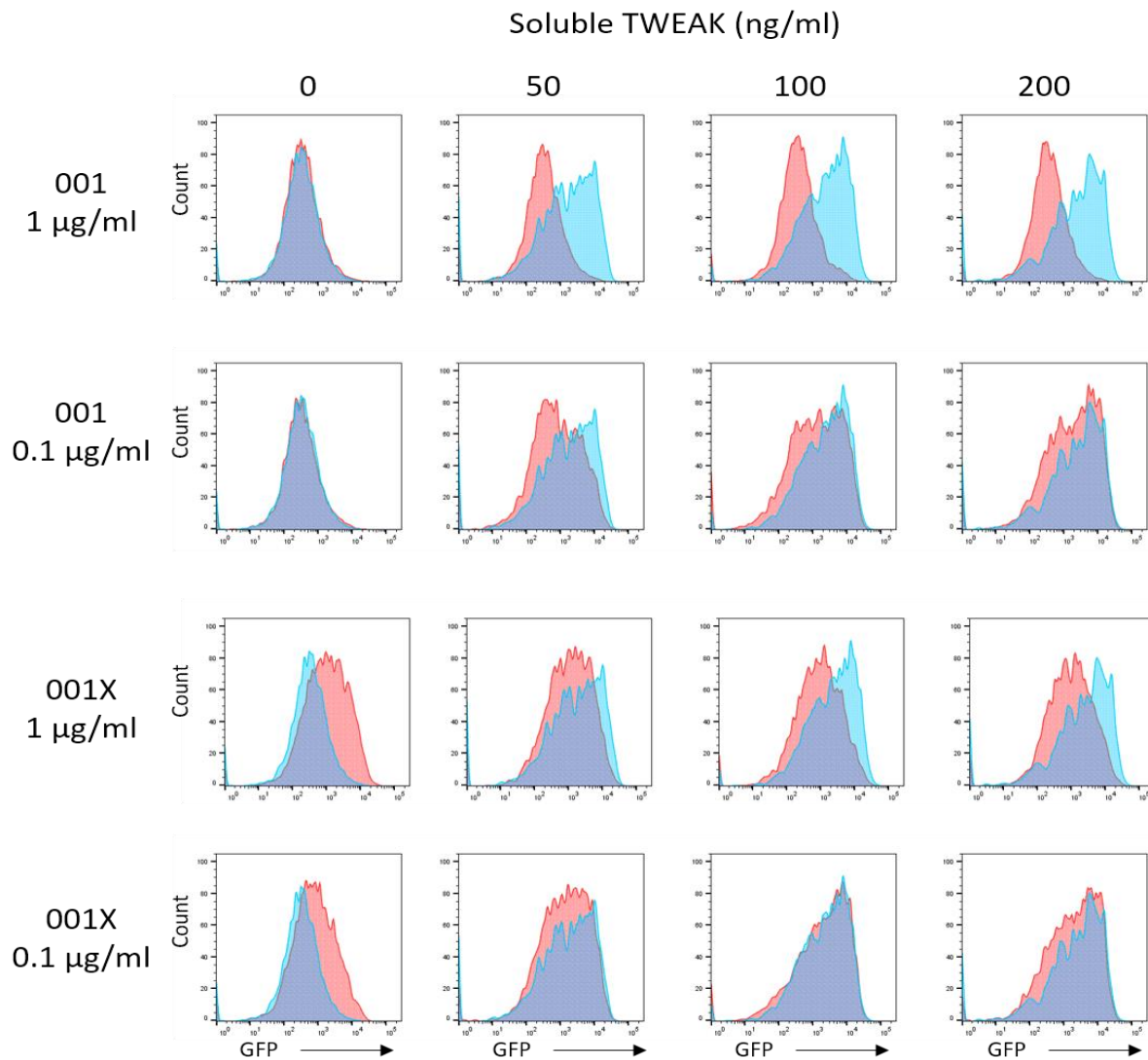


Figure 3.4: *NFκB* activity of α -Fn14 001 and α -Fn14 001X in soluble TWEAK (sTWEAK)-treated HEK293T *NFκB*-GFP cells. HEK293T cells with an *NFκB*-promoter driving GFP expression were treated with varying doses of sTWEAK, α -Fn14 001, and α -Fn14 001X. Blue histograms show cells plus sTWEAK in the absence of antibody treatments. Red histograms show α -Fn14 001 or α -Fn14 001X-coincubated populations superimposed over equivalent sTWEAK-only treated populations.

3.3.4. Myogenic Effects in C2C12 Model Cells

3.3.4.1. Differentiation Assay

Differentiation of myoblast cells was assessed using light microscopy of cell cultures and western blotting for the detection of myosin in cell lysates (Figure 3.5). Formation of myotubes was detected in media only controls, α -Fn14 001 (1 $\mu\text{g/ml}$), and the α -Fn14 001X

mimetic, α -Fn14 (1 $\mu\text{g/ml}$) with Protein G (1 $\mu\text{g/ml}$; Figure 3.5A). Myotube formation was also detected in sTWEAK-treated cell cultures at 1 ng/ml and 100 ng/ml, however 500 ng/ml showed negligible myotube formation (Figure 3.5B). The differentiation marker, myosin, was detected in a time-dependent manner in all cell cultures except those treated with sTWEAK at 100 and 500 ng/ml (Figure 3.5C,D).

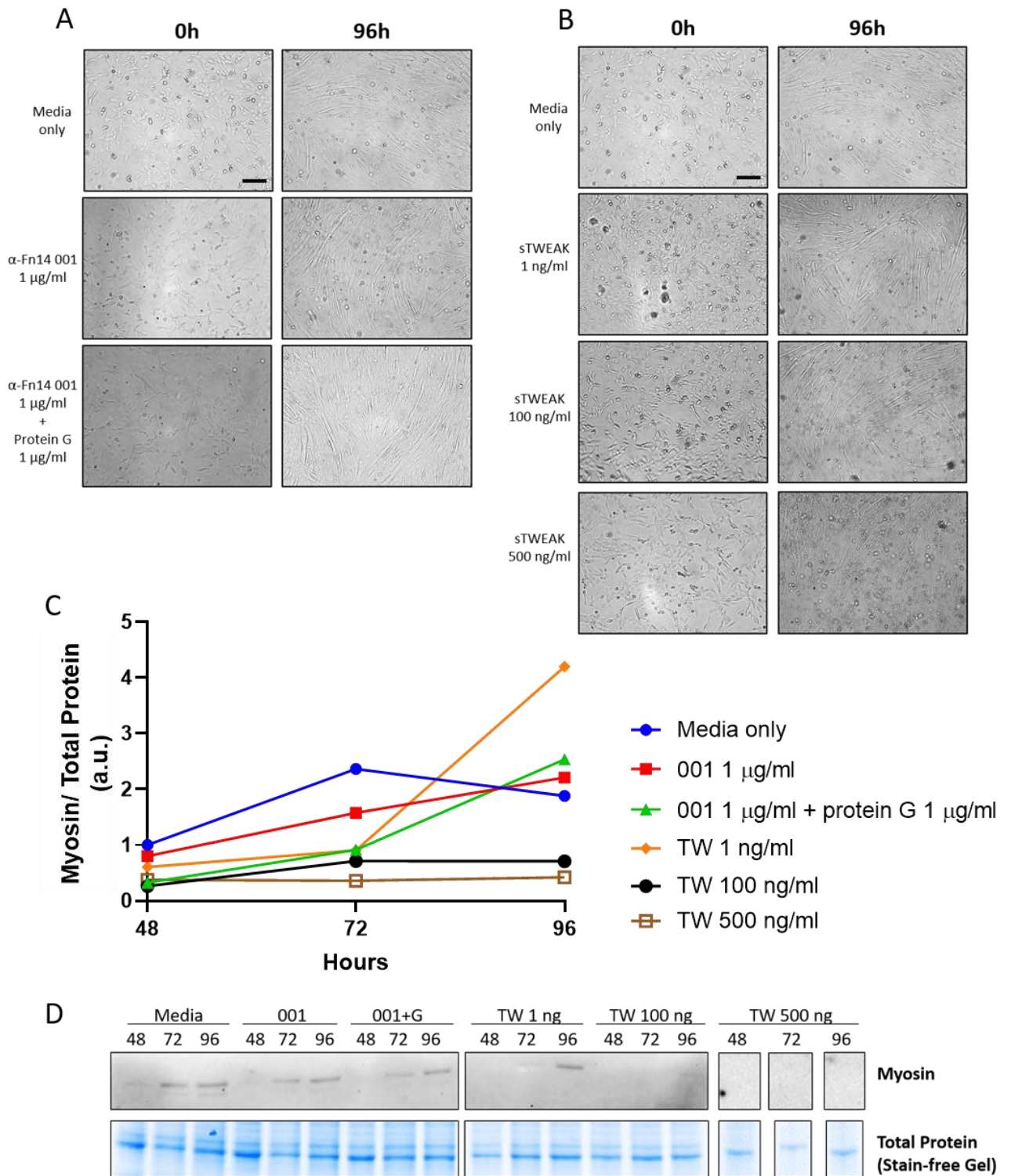


Figure 3.5: Differentiation of C2C12 myotubes treated with α -Fn14 or soluble TWEAK (sTWEAK). Light microscopy images of myotube formation in α -Fn14 (A) and sTWEAK (B) treated cell cultures. 0 hour images show primary myoblasts whilst 96 hour post-differentiation cultures show myotube formation in all cultures except high dose sTWEAK (500 ng/ml). (C) Myosin expression was detected and expressed relative to total protein content over 48-, 72-, and 96 hours post-differentiation ($n = 1$). Myosin expression was observed in a time-dependent manner in all cultures except 100 ng/ml and 500 ng/ml sTWEAK. (D) Representative blot of myosin western blot and stain-free image of total protein content. A prominent band was detected above 200 kDa (MF-20, DSHB, expected molecular weight 223 kDa). Scale bar 450 μ m.

3.4. Discussion

3.4.1. Crosslinking Efficacy and Purity

The crosslinked antibody α -Fn14 001X was generated successfully, albeit with less than 100% efficiency. In-gel analysis of the crosslinked product indicates the presence of monomeric products which were not removed by further purification, as well as bands at ~50 kDa potentially indicating release of antibody heavy chain (Liu *et al.*, 2007). *In vitro* analysis of the binding and activity profiles of α -Fn14 001X (described below) were determined to be sufficiently distinct from α -Fn14 001 to proceed with the antibody *in vivo* without further optimisation of the cross-linking protocol. Future studies may find that increasing the efficiency and purity of α -Fn14 001X generation may produce more pronounced agonistic effects.

3.4.2. Crosslinked Antibody Binds Human and Mouse Fn14

Monomeric α -Fn14 001 has previously been shown to bind with comparable efficiency to both hFn14 and mFn14 (Johnston *et al.*, 2015). Retention of this binding ability was confirmed using MEF H-Ras^{V12} cells expressing endogenous mFn14 with inducible hFn14. The crosslinked α -Fn14 001X showed a greater level of binding in induced cells, although it is not immediately clear whether this represents greater affinity for hFn14 or simply the greater abundance of overall Fn14 in the induced cells. These results allow us to move to an *in vivo* mouse model with relative confidence that the antibody is intact and retains the Fn14 binding capability.

3.4.3. Crosslinked α -Fn14 001 Activates Fn14 in Absence of sTWEAK

Activity of α -Fn14 001 and α -Fn14 001X were assessed in comparison to the activity of endogenous ligand, sTWEAK. Baseline activity of sTWEAK was as expected, with a dose-dependent response in NF κ B activation in HEK293T NF κ B-GFP reporter cells. It is important

to note that the TWEAK stimulant used was in the form of sTWEAK, and in doses ascending above and beyond physiological levels. Although physiological serum measurements of sTWEAK are in the range 500-800 pg/ml in serum of healthy adults (Blanco-Colio *et al.*, 2007; Kralisch *et al.*, 2008; Maymó-Masip *et al.*, 2013), the higher concentrations used here are reflective of the ranges used in the literature and aim to recapitulate acute inflammatory responses, which though not absolutely quantified are often stated in the literature as transiently upregulated (Nakayama *et al.*, 2000; Girgenrath *et al.*, 2006). Additionally, the presence of membrane-bound TWEAK (mTWEAK), which remains poorly characterised in the literature, is not accounted for in serum concentrations of TWEAK.

Both α -Fn14 001 and the crosslinked variant, α -Fn14 001X, showed considerable inhibition of sTWEAK-induced NF κ B activity. This indicates that both variants are in some way preventing sTWEAK from binding with Fn14, potentially via spatial inhibition that is enhanced in the cross-linked form. Monomeric α -Fn14 001 did not show induction of NF κ B activity in the absence of sTWEAK, suggesting that the monomeric form is acting as expected as an antagonistic antibody. As anticipated, the oligomeric α -Fn14 001X did show a dose-dependent induction of GFP expression. This is consistent with the previously described phenomenon of oligomerised antibodies creating agonistic effects in TNFRSF members (Wajant, 2015). Whether the monomeric form, α -Fn14 001, naturally oligomerises *in vivo* is a possibility that cannot be ruled out from these *in vitro* experiments, however this ability of the crosslinked form to activate signalling in the absence of sTWEAK presents an attractive target for downstream optimisation and use *in vivo* as an agonistic Fn14 antibody.

3.4.4. Supraphysiological Dose sTWEAK Blunts C2C12 Differentiation

The impact of sTWEAK administration on C2C12 differentiation was assessed using qualitative visualisation and semi-quantitative analysis of MHC density. Given that cell cultures represent an n of 1, it is not feasible to perform statistical assessment on these results and instead they are presented as semi-quantitative markers of differentiation. Low level dose of sTWEAK (1 ng/ml) showed robust formation of myotubes and high levels of MHC expression at both 72- and 96-hours post-differentiation. The highest dose of sTWEAK (500 ng/ml) displayed negligible differentiation in both assays. Interestingly, whilst the intermediate dose (100 ng/ml) appeared to display myotube formation under light microscopy, this cell lysate was found to contain negligible MHC protein. Assuming this finding is reproducible, it is an important consideration when interpreting prior studies on TWEAK effects in myotubes; whilst the development may appear morphologically normal, the myotubes may be in some way immature or defective.

As described above, the doses of sTWEAK found to inhibit differentiation and maturation of myotubes in the current study represent supraphysiological doses, though these are frequently cited in the literature when describing potential physiological roles of TWEAK (Pascoe *et al.*, 2020). Indeed, the 1 ng/ml dose is the closest approximation to previously described sTWEAK concentrations *in vivo*, and under these conditions we see a normal, or even enhanced, differentiation and maturation of myotubes. These findings indicate that the role of TWEAK-Fn14 signalling under normal physiological conditions may indeed be as a promoter of myogenesis.

3.5. Conclusions

The evidence presented here shows that the generation of a crosslinked variant of α -Fn14 001 was achieved via SMCC crosslinking, however with a portion of monomer remaining in the preparation. The crosslinked variant, dubbed α -Fn14 001X, retained its ability to bind both hFn14 and mFn14. Preliminary *in vitro* reporter assays indicate that α -Fn14 001X activates NF κ B in a manner distinct from both α -Fn14 001 or sTWEAK alone, with α -Fn14 001X activating NF κ B signalling whilst also preventing sTWEAK-induced activity. Future studies would benefit from refined purification of this crosslinked product to enhance purity, however given this antibody in its unrefined form was able to elicit activating effects *in vitro*, it was determined that this product was sufficient to proceed with for *in vivo* characterisation.

C2C12 myoblasts treated with an α -Fn14 001X mimetic (α -Fn14 001 plus Protein G), tolerated higher doses of antibody than sTWEAK ligand, with myotube formation and MHC expression retained. We also demonstrate here that physiologically relevant levels of sTWEAK do not interfere with C2C12 differentiation and maturation as has been previously asserted and attribute this mischaracterisation of sTWEAK as an apoptotic ligand to the use of supraphysiological doses. Whilst further characterisation of downstream signalling pathways was limited (Appendix II), we were able to demonstrate that α -Fn14 001X is able to bind and activate Fn14 of human and mouse origin in the absence of sTWEAK and proceed with *in vivo* works to determine the myogenic outcomes of this activity.

References

- Blanco-Colio LM, Martin-Ventura JL, Munoz-Garcia B, Orbe J, Paramo JA, Michel JB, Ortiz A, Meilhac O & Egido J. (2007). Identification of soluble tumor necrosis factor-like weak inducer of apoptosis (sTWEAK) as a possible biomarker of subclinical atherosclerosis. *Arterioscler Thromb Vasc Biol* **27**, 916-922.
- Dogra C, Hall SL, Wedhas N, Linkhart TA & Kumar A. (2007). Fibroblast growth factor inducible 14 (Fn14) is required for the expression of myogenic regulatory factors and differentiation of myoblasts into myotubes. Evidence for TWEAK-independent functions of Fn14 during myogenesis. *J Biol Chem* **282**, 15000-15010.
- Girgenrath M, Weng S, Kostek CA, Browning B, Wang M, Brown SAN, Winkles JA, Michaelson JS, Allaire N, Schneider P, Scott ML, Hsu YM, Yagita H, Flavell RA, Miller JB, Burkly LC & Zheng TS. (2006). TWEAK, via its receptor Fn14, is a novel regulator of mesenchymal progenitor cells and skeletal muscle regeneration. *EMBO Journal* **25**, 5826-5839.
- Johnston AJ, Murphy KT, Jenkinson L, Laine D, Emmrich K, Faou P, Weston R, Jayatilleke KM, Schloegel J, Talbo G, Casey JL, Levina V, Wong WW, Dillon H, Sahay T, Hoogenraad J, Anderton H, Hall C, Schneider P, Tanzer M, Foley M, Scott AM, Gregorevic P, Liu SY, Burkly LC, Lynch GS, Silke J & Hoogenraad NJ. (2015). Targeting of Fn14 Prevents Cancer-Induced Cachexia and Prolongs Survival. *Cell* **162**, 1365-1378.
- Kralisch S, Ziegelmeier M, Bachmann A, Seeger J, Lossner U, Bluher M, Stumvoll M & Fasshauer M. (2008). Serum levels of the atherosclerosis biomarker sTWEAK are decreased in type 2 diabetes and end-stage renal disease. *Atherosclerosis* **199**, 440-444.
- Liu H, Gaza-Bulseco G, Chumsae C & Newby-Kew A. (2007). Characterization of lower molecular weight artifact bands of recombinant monoclonal IgG1 antibodies on non-reducing SDS-PAGE. *Biotechnol Lett* **29**, 1611-1622.
- Maymó-Masip E, Vendrell J, Garrifo-Sanchez L, Fernández-Veledo S, Chacón MR, Vázquez-Carballo A, Garcia España A, Tinahones FJ, García-Fuentes E & Rodríguez MdM. (2013). The Rise of Soluble TWEAK Levels in Severely Obese Subjects After Bariatric Surgery May Affect Adipocyte-Cytokine Production Induced by TNF α . *J Clin Endocrinol Metab* **98**, E1323-E1333.
- Nakayama M, Kayagaki N, Yamaguchi N, Okumura K & Yagita H. (2000). Involvement of Tweak in Interferon γ -Stimulated Monocyte Cytotoxicity. *J Exp Med* **192**, 1373-1380.
- Pascoe AL, Johnston AJ & Murphy RM. (2020). Controversies in TWEAK-Fn14 signaling in skeletal muscle atrophy and regeneration. *Cell Mol Life Sci* 10.1007/s00018-020-03495-x.
- Vince JE, Chau D, Callus B, Wong WW-L, Hawkins CJ, Schneider P, McKinlay M, Benetatos CA, Condon SM, Chunduru SK, Yeoh G, Brink R, Vaux DL & Silke J. (2008). TWEAK-FN14 signaling induces lysosomal degradation of a cIAP1-TRAF2 complex to sensitize tumor cells to TNF α . *J Cell Biol* **182**, 171-184.

Wajant H. (2015). Principles of antibody-mediated TNF receptor activation. *Cell Death Differ* **22**, 1727-1741.

Chapter 4

Adverse Events Encountered in Notexin-Induced Mouse Model of Skeletal Muscle Injury

Chapter Summary

The following chapter is presented as an unpublished manuscript describing the unexpected adverse events which arose following the use of notexin for inducing acute localised necrotic skeletal muscle injury. These observations and subsequent quality control investigations are included to provide context for the limitations encountered in downstream analyses of these samples, as well as to highlight the variability in animal injury model outcomes and reporting. These variations, in addition to harming animal welfare, are a potential source of confounding results frequently described in the literature regarding skeletal muscle degradation and regeneration. This work warrants further examination of the mechanisms behind batch variability and injury reproducibility, however due to the nature of the concerns, these experiments must be performed by an external investigator. This collaboration is being pursued with Dr Peter Houweling (Murdoch Childrens Research Institute) to perform independent injuries using current notexin and distinct batches using a range of approved analgesics to examine the consistency of this injury model.

Abstract

Muscle wasting is a devastating comorbidity associated with an array of chronic and acute conditions including, but not limited to, injury, diabetes, immobilisation, cancer, ageing, and muscular dystrophies. The use of animal models which accurately and consistently recapitulate the clinical and biochemical signatures of human disease is an essential step in understanding muscle wasting and regeneration.

Notexin is a potent phospholipase A2 toxin derived from Australian Tiger snake venom, commonly used to induce an acute necrotic phenotype. The current study implemented a relatively low dose intramuscular injection of notexin solution (40 µl, 10 µg/ml in saline) in the right *tibialis anterior* (TA) and 40 µl saline injected in the left TA of C57BL/6 mice. Injuries were performed under isoflurane anaesthesia (2-5% flow rate, recovery within 5 minutes) with buprenorphine (0.05mg/kg) injected subcutaneously as analgesic immediately post-injury, and during recovery as prescribed by the supervising veterinarian.

Despite apparent recovery immediately post-injury, all mice exhibited poor body and behavioural condition by 24-hours post-injury, necessitating constant ongoing surveillance and remedial care. Mice were culled by CO₂ asphyxiation at days 3, 7, and 14 post-injury and both TA muscles collected (n=3-4 for each treatment and time point). Tissue architecture and western blot analyses indicated severe and prolonged muscle necrosis.

The adverse events observed in the current study are incongruous with previously reported notexin injury models. These results suggest batch variability in the potency of notexin, as well as highlighting potential shortcomings in the current reporting of animal injury protocols, with important implications for scientific reproducibility and animal ethics.

4.1. Introduction

Mature muscle regeneration is studied using a range of acute injury models. Commonly used experimental models include mechanical injuries – such as cryoinjury (freezing) or crushing – including denervation or immobilisation, and inducing injury using myotoxic agents – such as notexin or cardiotoxin. The use of varying injury mechanisms has been shown to alter the course of regeneration, with distinct biochemical pathways activated in different injury models (Mahdy *et al.*, 2015). Varied use of animal injury models can produce confounding data when studying muscle regeneration. It is therefore important to choose an injury model which accurately and reliably recapitulates the clinical and biochemical signatures of the human disease being investigated.

Notexin is a basic phospholipase A2 toxin purified from *Notechis scutatus* (Australian Tiger snake) venom. Notexin exerts damage by binding to, and hydrolysing, the sarcolemmal membranes of muscle fibres causing a dysregulation of ionic gradients and pathological hyper-contraction of the sarcolemma (Dixon & Harris, 1996). This hyper-contraction creates an uneven increase in tension on surrounding fibres, which in combination with the hydrolytic weakening of membranes, ultimately leads to widespread degeneration of the muscle architecture (Dixon & Harris, 1996). This injury model presents a severe traumatic necrotic phenotype. The regenerative profile of notexin injury has been characterised in several studies (Whalen *et al.*, 1990; Harris *et al.*, 2000; Brigitte *et al.*, 2010; Head *et al.*, 2014).

The current study implements a dosage of notexin well within the range utilised in previously published studies. An antibody treatment was administered as part of a larger study; delineation of these groups is included for full transparency of animal treatment, however the aims of this treatment are unrelated to the current results and did not impact

the adverse reactions observed so will not be discussed further. The adverse reactions encountered highlight potential issues with batch variability in notexin as well as shortcomings in current reporting of animal injury protocols with implications for scientific reproducibility and animal welfare.

4.2. Methods

4.2.1. Animals

All procedures were approved by, and conducted in accordance with, the Animal Ethics Committee of La Trobe University (AEC: 16-70). Male C57BL/6 mice (16 weeks old, n=36) were used for notexin injury protocol. Mice were housed in littermate groups prior to injury and individually post-injury.

4.2.1.1. Notexin Injury

C57BL/6 mice (n=36) were placed under isoflurane anaesthesia (flow rate 2-5%, recovery within 5 minutes) and a notexin injury was performed as per Chapter 2, Section 2.1.1. 40 μ L of notexin (10 μ g/ml, total 0.4 μ g notexin, Latoxan, France) was injected intramuscularly in the right TA muscle and 40 μ L saline injected in the left TA as an internal control. Injuries were performed by Dr Chris van der Poel (Department of Life Sciences, La Trobe University) with assistance from Ms Laura Jenkinson (Department of Biochemistry and Genetics, La Trobe University).

Mice were IP injected with either antibody A, antibody B (20 mg/kg; n=12 for each treatment), or no antibody injection control (n=12) at 6-hours post-injury, and again at 7 days post-injury where applicable. Mouse body weights were recorded daily; core temperatures were monitored in select animals until stabilised.

4.2.1.2. Notexin Quality Control

Quality control was performed on notexin stock solution after unexpected adverse reactions were observed in treatment mice. Identity and concentration of notexin solution were confirmed with mass spectrometry, gel electrophoresis (NuPAGE 4-12% bis-tris gel, MES running buffer), and NanoDrop (ThermoFisher) spectrophotometry. Mass spectrometry was performed by Dr Pierre Faou of the La Trobe Comprehensive Proteomics Platform.

4.2.2. Histology

Frozen TA muscles were bisected at the widest point and serial 10 µm cryosections were taken at -20°C and mounted on 1.0-1.2 mm glass microscope slides (Livingstone, Australia; Knittel, Germany). Slides were stored in the dark at -20°C until required. H+E staining was performed as per Chapter 2, Section 2.3.1 to assess markers of injury, which were defined as centralised nuclei, loss of muscle fibre size uniformity, proportion of non-contractile, and infiltration of inflammatory cells (Spasov *et al.*, 2010).

4.2.3. Gel Electrophoresis

Whole muscle homogenates were prepared and subjected to SDS-PAGE as per Chapter 2, Section 2.4. Details of antibodies used can be found in Appendix III.

4.3. Results

4.3.1. Adverse Reactions to Notexin Injury

All mice recovered from anaesthesia within 5 minutes; all mice with the exception of one returned to normal behaviour and activity within 10 minutes and were able to be removed from heat pads and returned to normal individual housing. One mouse with persistent reduced activity remained on the heated pad and was administered with additional buprenorphine and saline fluids (subcutaneous injection route) as prescribed by the supervising veterinarians. Reflex wound clips were found to have fallen off or been manually removed by several mice; mice with absent wound clips did not appear to exhibit different activity or behaviours from remaining mice and as such clips were not reattached. By 24 hours post-injury all mice were experiencing substantial weight and core temperature losses (Figure 4.1). Majority of mice were exhibiting behaviours associated with pain or distress i.e. hunched posture, poor grooming, reduced exploratory behaviour. Despite having hypothermic core temperatures, mice did not exhibit shivering. Remedial treatment was provided for all mice in the form of ongoing buprenorphine analgesia, saline fluids, heat packs, and high caloric dietary supplement gels under the ongoing supervision of veterinarians, and animal technician staff (La Trobe Animal Research and Training Facility, La Trobe University). One mouse was culled for humane reasons on day 2 with a recorded body temperature of 24°C (normal core temperature 36-38°C). Weight and temperature losses peaked at 1-3 days post-injury and steadily recovered thereafter; however few animals recovered fully to baseline. Temperature was not anticipated as an observational metric in the current study, and as such, the data is an incomplete representation of the hypothermic response.

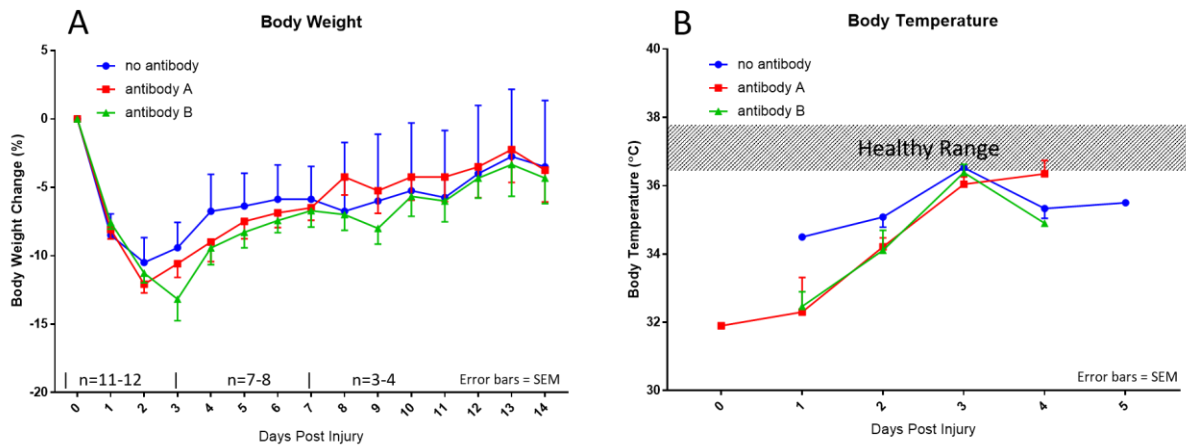


Figure 4.1: Body weight and temperature change in C57BL/6 mice following intramuscular notexin injury. All notexin-injured mice experienced dramatic weight loss (A) and hypothermia (B) that was not correlated with a specific antibody treatment. Weight loss was most apparent at 2-4 days post-injury and gradually recovered throughout the remaining experimental period. Temperature monitoring was limited, however, drastic decreases in core temperature were recorded for all treatment groups at days 1 and 2 post-injury with one mouse euthanised on day 2 for humane reasons. Remedial care was provided to increase and stabilise body temperature.

Notexin-injured legs exhibited substantial swelling, as anticipated, and upon dissection appeared discoloured with yellowish white granular deposits which extended beyond the TA into the surrounding muscles. Granular tissue was most notable at seven days post-injury, persisting to a lesser extent in the 14-day post-injury group.

4.3.1.1. Notexin Quality Control

Concentration of notexin stock solution was measured by NanoDrop (ThermoFisher) spectrophotometer at 120 $\mu\text{g}/\text{ml}$, indicating that the working 1 in 10 dilution used for injections was $\sim 12 \mu\text{g}/\text{ml}$; given the retrospective nature of measuring the notexin quality, a working solution was not available for analysis. Mass spectrometry detected a single species at 13,579.5 Da with no notable contaminants; the expected molecular weight of notexin, as provided by the supplier Latoxan, is 13,574 Da (see Figure 4.2). Confirmation was also provided by the manufacturer that their internal quality control testing detected no

anomalies or impurities in the batch used. Electrophoresis under both reducing and non-reducing conditions likewise showed notexin to resolve slightly above the expected molecular weight with two smaller products detected under reducing conditions (Figure 4.2).

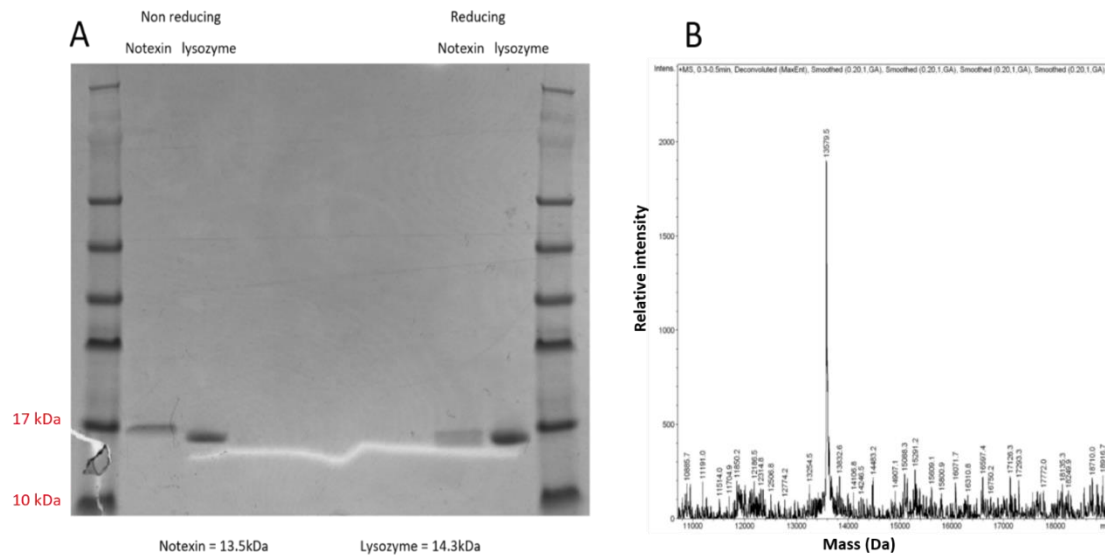


Figure 4.2: Gel electrophoresis and mass spectrometry of notexin. Identity of notexin toxin was confirmed using both gel electrophoresis (A) under reducing and non-reducing conditions, and mass spectrometry (B). Notexin migrated at approximately the predicted molecular weight with a slightly higher mass observed under non-reducing conditions. Lysozyme with a known molecular mass of 14.3 kDa is included as an additional marker. No notable contaminants were detected by mass spectrometry.

4.3.2. Tissue Architecture

H+E staining showed considerable loss of tissue architecture at 3 days post-injury relative to saline-treated control, with substantial extra-cellular debris and non-contractile tissue (Figure 4.3A, B). Extra-cellular debris was persistent at 7 days post-injury with an increase in infiltration by suspected inflammatory cells (Figure 4.3C). By day 14 post-injury, muscle fibres were apparent with heterogeneity in shape and size and ongoing centralised nuclei and infiltrating inflammatory cells (Figure 4.3D). All notexin-injured muscle remained pathological relative to saline-treated controls by 14 days post-injury.

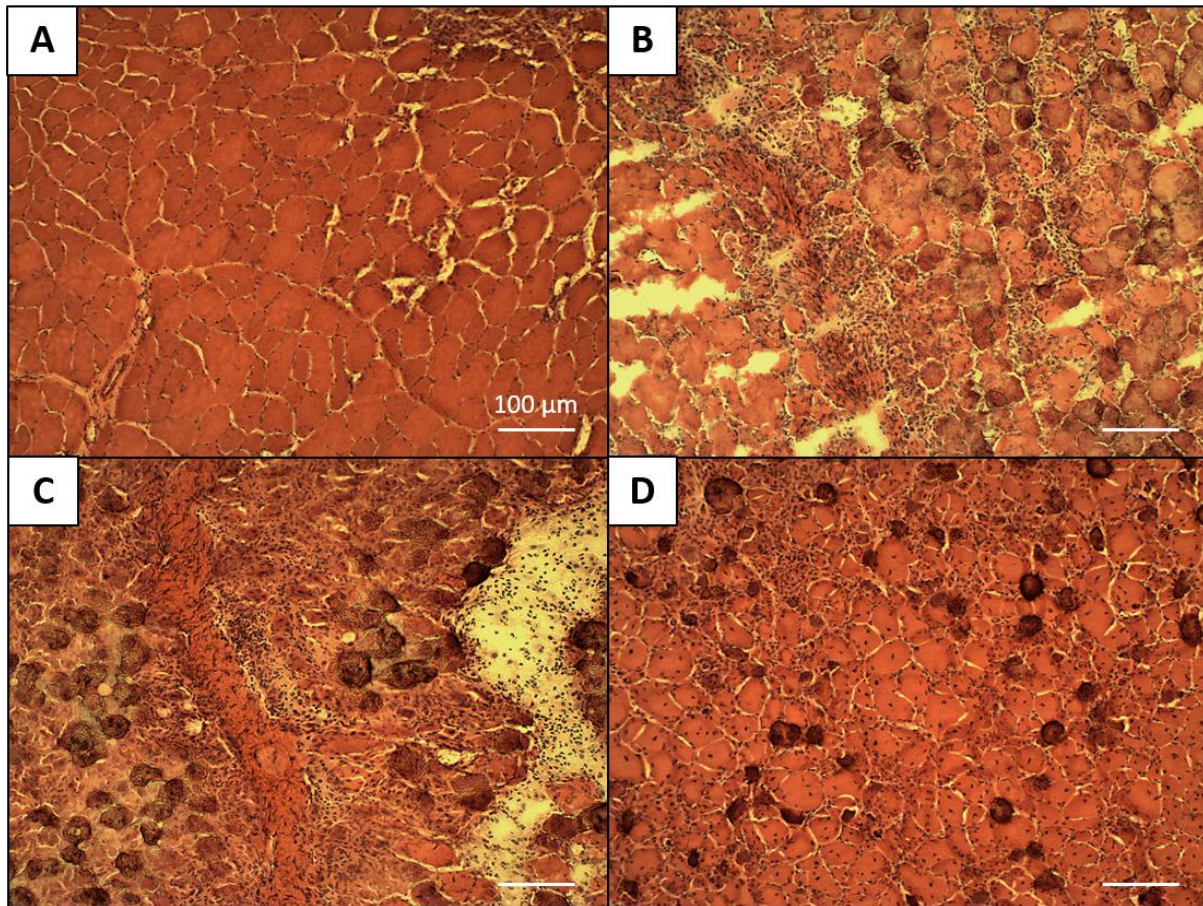


Figure 4.3: Representative images showing progression of tissue architecture recovery following notexin injury. (A) uninjured saline-injected TA muscle at 3 days post-injection. (B) Notexin-injured TA 3 days post-injury shows high degree non-contractile tissue and extensive extracellular debris. (C) 7 days post-injury shows infiltration of suspected inflammatory cells and persistent regions of non-contractile tissue and extracellular debris. (D) 14 days post-injury shows primarily centralised nuclei with persistent infiltration of suspected inflammatory cells.

4.3.3. Gel Electrophoresis

Notexin-injured TA samples were likewise evidently degraded when run on SDS-PAGE and visualised on a UV imager for total protein content (see Figure 4.4). Whilst saline control TA muscle homogenates show clear banding of proteins, with characteristic dense bands indicative of high myosin and actin content apparent at ~200 and 43 kDa respectively, notexin-injured samples were frequently lacking these distinct bands and instead appeared streaky with some apparent low molecular weight bands (see Figure 4.4). This apparent

degradation was not specific to any antibody treatment and remained persistent at 14 days post-injury. Loss of total protein compromised the ability to perform further quantitative immunoblotting for specific proteins in these samples.

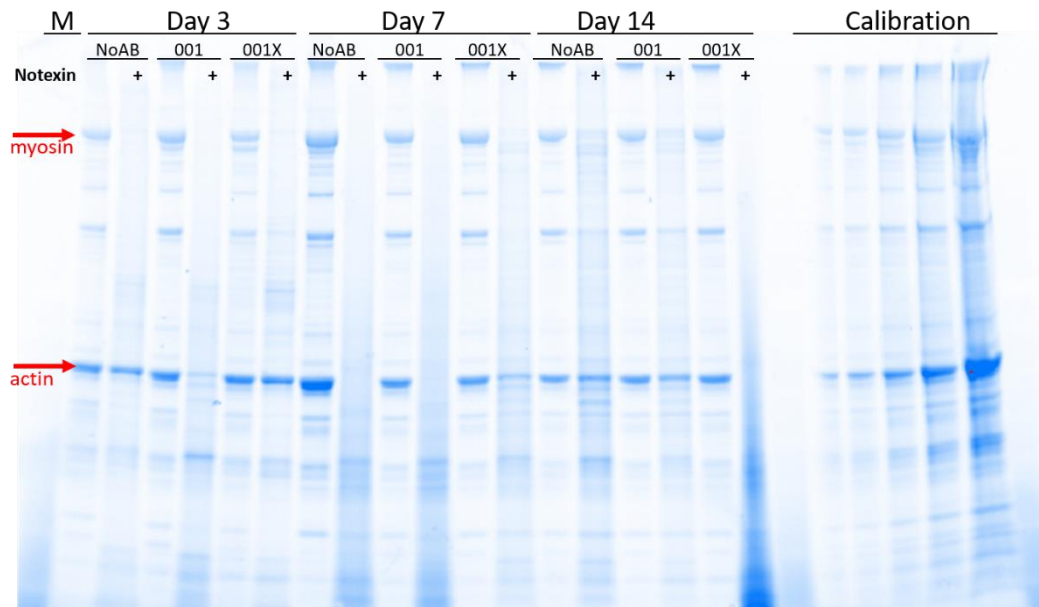


Figure 4.4: Stain-free UV image of notexin injured samples. A representative UV image of total protein at 3, 7, and 14 days post-saline or post-notexin injury. Notexin injured samples exhibited a loss of characteristic myosin and, less frequently actin, bands. Degradation was not confined to a specific antibody treatment and was persistent in some samples at 14 days post-injury.

4.4. Discussion

The severe adverse reaction of experimental mice to a localised notexin muscle injury was both unexpected and inconsistent with previously published protocols. The dosage and administration of notexin was well within the parameters of the literature, and in fact much a smaller dosage (0.4 μg) than many described protocols that used between 0.2 and 8.5 μg intramuscular injections of notexin (Brigitte *et al.*, 2010; Head *et al.*, 2014; Hardy *et al.*, 2016; Swiderski *et al.*, 2016). One of the highest doses reported in the literature was used by Hardy *et al.* (2016), injecting up to 50 μl of 12.5 μmol (total 8.5 μg) notexin solution in 0.9% PBS into

the TA muscle of C57Bl/6 mice. No unexpected adverse reactions were reported with tissue architecture mostly recovered by 12 days post-injury. The current study used a much lower dose of 0.4 µg from the same supplier (Latoxan), which not only almost completely degraded the tissue architecture, as evident in both H+E staining and total protein visualisation of western blot and largely persistent at 14 days post-injury, but resulted in the euthanasia of one mouse and extensive ongoing remedial care for the remaining cohort. A similar dose to the current study was used by Head *et al.* (2014) who injected 0.2 µg into the *extensor digitorum longus* (EDL), a muscle roughly half the size of the TA, of C57BL/6 mice in an attempt to replicate muscular dystrophy tissue architecture. Again, no adverse reactions were reported and by 21 days post-injury these mice were no more susceptible to stretch-induced injuries than uninjured muscle, suggesting minimal persistent damage.

It is worth noting that assessment of tissue regeneration may be varied depending on the metric used. Hardy *et al.* (2016) highlighted this issue in a comparative study of four distinct injury models in C57/Bl6 mice. Cryoinjury in that study was performed by exposing the TA muscle with a small incision and freezing the muscle directly three times for 15 seconds with a liquid nitrogen cooled rod; whilst the cryoinjury produced the most dramatic injury phenotype of the tested models, as indicated by histological examination of tissue architecture, it is interesting to note that satellite cell activation had returned to baseline one month post-injury but was still elevated three months post-injury in the other models (Hardy *et al.*, 2016). This is in contrast to other damage markers, such as fibrosis and infiltration of inflammatory cells, which remained elevated for longer in cryoinjury relative to other models. These findings highlight the potential to report different recovery progression depending upon the injury markers measured. Given the specific emphasis of the studies implementing notexin injury varies, this is a potential source of confounding data around this injury model.

The hypothermia observed in the current study, coupled with the apparent lack of shivering response, indicates a potential systemic neurotoxic effect in addition to the localised muscle injury. Notexin is a known neurotoxin, acting at the presynaptic terminal to inhibit acetylcholine release (Mollier *et al.*, 1990); acetylcholine has in turn been implicated in hypothalamic thermoregulation, i.e. shivering (Díaz & Becker, 2010). Notexin is frequently presented as a localised myotoxic agent; failure to consider the off-target neurotoxic effects may have profound impacts on the welfare of experimental animals.

A possible source of variation between prior literature and the current study is the anaesthesia and analgesia employed. Autopsy report provided by Cerberus (Adelaide, Australia) and interpreted by supervising veterinarian, Dr Tara Egan, on the euthanised mouse suggested possible insufficient analgesia prior to the injury leading to a 'wind-up' phenomenon – a perceived increase in pain perception in response to a chronic pain stimuli, in this instance muscle necrosis (Herrero *et al.*, 2000). Hardy *et al.* (2016) and Head *et al.* (2014) both performed injuries using an intraperitoneal injection of Ketamine® and Xylazine®, whilst the current study implemented gaseous isoflurane as per local animal ethics committee and veterinarian recommendations. Other studies fail to describe any specific anaesthetic or analgesic usage (Dixon & Harris, 1996; Brigitte *et al.*, 2010; Liu *et al.*, 2015). The intraperitoneal Ketamine® and Xylazine® may have provided stronger initial analgesia and prevented the 'wind-up' phenomenon which may have contributed to the extreme events seen in the current study. This is of course a speculative notion based on discussions with veterinary staff and would require specific testing to confirm. Ongoing administration of analgesia is not described in either of the aforementioned studies and it is unclear whether this additional analgesia was not required or simply not reported. Given that muscle necrosis was present for at least 4 days post-injury in Hardy *et al.* (2016), it is unlikely that further pain

management beyond the initial anaesthesia was not required. This omission is a common trend in the literature and represents a shortcoming in the reporting of animal injury model protocols.

The use of more than 20-fold greater notexin in prior studies leads us to believe that pain management was not the sole contributor to the adverse reactions in the current study. Prior literature and personal correspondence with other researchers experienced in notexin-injury suggests that natural variation in potency between batches of notexin are at least partially responsible for the dramatically different responses observed. If varying potency between equivalent doses of notexin is in fact occurring, then notexin-injury presents an injury model that is poorly reproducible and is best avoided for both scientific integrity and animal welfare concerns.

References

- Brigitte M, Schilte C, Plonquet A, Baba-Amer Y, Henri A, Charlier C, Tajbakhsh S, Albert M, Gherardi RK & Chretien F. (2010). Muscle resident macrophages control the immune cell reaction in a mouse model of notexin-induced myoinjury. *Arthritis Rheum* **62**, 268-279.
- Díaz M & Becker DE. (2010). Thermoregulation: Physiological and Clinical Considerations during Sedation and General Anesthesia. *Anesthesia Progress* **57**, 25-33.
- Dixon RW & Harris JB. (1996). Myotoxic activity of the toxic phospholipase, notexin, from the venom of the Australian tiger snake. *J Neuropathol Exp Neurol* **55**, 1230-1237.
- Hardy D, Besnard A, Latil M, Jouvion G, Briand D, Thepenier C, Pascal Q, Guguin A, Gayraud-Morel B, Cavallion JM, Tajbakhsh S, Rocheteau P & Chretien F. (2016). Comparative Study of Injury Models for Studying Muscle Regeneration in Mice. *PLoS One* **11**, e0147198.
- Harris JB, Grubb BD, Maltin CA & Dixon R. (2000). The neurotoxicity of the venom phospholipases A(2), notexin and taipoxin. *Exp Neurol* **161**, 517-526.
- Head SI, Houweling PJ, Chan S, Chen G & Hardeman EC. (2014). Properties of regenerated mouse extensor digitorum longus muscle following notexin injury. *Exp Physiol* **99**, 664-674.
- Herrero JF, Laird JM & Lopez-Garcia JA. (2000). Wind-up of spinal cord neurones and pain sensation: much ado about something? *Prog Neurobiol* **61**, 169-203.
- Liu X, Wu G, Shi D, Zhu R, Zeng H, Cao B, Huang M & Liao H. (2015). Effects of nitric oxide on notexin-induced muscle inflammatory responses. *Int J Biol Sci* **11**, 156-167.
- Mahdy MA, Lei HY, Wakamatsu J, Hosaka YZ & Nishimura T. (2015). Comparative study of muscle regeneration following cardiotoxin and glycerol injury. *Ann Anat* **202**, 18-27.
- Mollier P, Brochier G & Morot Gaudry-Talarmain Y. (1990). The action of notexin from tiger snake venom (*Notechis scutatus scutatus*) on acetylcholine release and compartmentation in synaptosomes from electric organ of *Torpedo marmorata*. *Toxicon* **28**, 1039-1052.
- Spassov A, Gredes T, Gedrange T, Lucke S, Pavlovic D & Kunert-Keil C. (2010). Histological changes in masticatory muscles of mdx mice. *Arch Oral Biol* **55**, 318-324.
- Swiderski K, Thakur SS, Naim T, Trieu J, Chee A, Stapleton DI, Koopman R & Lynch GS. (2016). Muscle-specific deletion of SOCS3 increases the early inflammatory response but does not affect regeneration after myotoxic injury. *Skelet Muscle* **6**, 36.
- Whalen RG, Harris JB, Butler-Browne GS & Sesodia S. (1990). Expression of myosin isoforms during notexin-induced regeneration of rat soleus muscles. *Dev Biol* **141**, 24-40.

Chapter 5

Myogenic Effects of α -Fn14 Antibodies in Acute Skeletal Muscle

Injury

Chapter Summary

The following chapter describes changes in TWEAK-Fn14 in the acute notexin injury model following a range of Fn14-targeting antibody interventions, generated and characterised *in vitro* in Chapter 3. The primary outcomes of this study were the injury and regenerative phenotypes following injury, however given the severity of the injury model (described in Chapter 4), secondary outcomes have been used to approximate the regeneration process and identify potential targets of the TWEAK-Fn14 axis. Myogenic regulatory factors, mitochondrial biogenesis, atrogenes, and structural proteins were each assessed to establish an overall picture of muscle recovery.

The key finding of these experiments is the positive-feedback loop of Fn14 when stimulated by our antibody, α -Fn14 001X, and to a lesser extent, α -Fn14 001. Upregulation of Fn14 was correlated with significant transcriptional upregulation of the master myogenic regulator, MyoD. Evidence is also provided of prolonged sarcomeric remodelling in α -Fn14 001X-treated mice. Whilst the limitations of the current injury model prevent us from determining whether this phenomenon results in downstream enhancement of the myogenic program, it provides valuable insight into the potential mechanistic actions of Fn14 as a positive regulator of muscle mass and indicates that therapeutic stimulation of Fn14 may be possible.

Additional samples of 13- and 105-week old and chronically resistance-trained mice obtained from Emeritus Professor Miranda Grounds (University of Western Australia) and morphologically described in Soffe *et al.* (2016) are also included to provide contrast for the observations made in the primary notexin study and highlight the context-dependent role of Fn14 in muscle homeostasis.

5.1. Introduction

TWEAK-Fn14 signalling has been implicated widely in both acute and chronic muscle wasting phenotypes (Tajrishi *et al.*, 2014b). Given the opposing outcomes associated with TWEAK-Fn14 activity, there is reason to believe that the effects of TWEAK-Fn14 are largely tissue- and dose-dependent and signal via diverse pathways (Pascoe *et al.*, 2020). In addition to diverse TWEAK-Fn14 signalling outcomes, there is a possibility that Fn14 is able to self-associate in conditions of high receptor density to initiate TWEAK-independent Fn14 activity (Brown *et al.*, 2013). Differential effects have been observed in TWEAK-inhibition versus antagonistic α -Fn14 antibodies; Johnston *et al.* (2015) describe an antagonistic α -Fn14 antibody which is able to prevent cachexia in tumour-bearing mice which could not be achieved by inhibition of TWEAK. These findings are supportive of a distinct role for TWEAK-independent Fn14 activity.

The evidence of TWEAK-dependent Fn14 signalling as a negative regulator of myogenesis is considerable. Activation of ubiquitination and other catabolic pathways downstream of TWEAK-dependent Fn14 activity have been shown in a range of models. Dogra *et al.* (2007a) investigated the effects of 10 ng/ml TWEAK administration – a reasonably high dose, albeit still on the lower range of exogenous TWEAK utilised in the literature – on C2C12 myotubes over the course of 24 hours. TWEAK administration was shown to result in smaller diameter myotubes with increased ubiquitination of muscle-specific proteins, such as MHC, and enhanced transcript levels of E3 ubiquitin ligases, atrogen1 and MuRF2 – also referred to as atrogenes – that peaked after 12 hours TWEAK administration (Dogra *et al.*, 2007a). Moving to an *in vivo* model, Mittal *et al.* (2010a) examined the effects of denervation of the *gastrocnemius* muscle of C57BL/6 TWEAK-Transgenic (Tg) or TWEAK-knockout (KO) mice. TWEAK was found to exacerbate the effects of denervation-induced atrophy via modulation specifically of MuRF1, with transcript levels elevated in TWEAK-Tg mice and blunted in

TWEAK-KO mice when compared to wild-type littermate controls (Mittal *et al.*, 2010b). Interestingly, when genetic ablation of Fn14 itself, rather than the ligand, is performed, the results vary. Tajrishi *et al.* (2014a) described an Fn14-KO mouse which showed reduced sarcopenia – ageing-related muscle atrophy – at 18-months of age relative to wild-type controls. Whilst it appears that the overall outcome of Fn14 ablation is similar to that of TWEAK ablation, Tajrishi *et al.* (2014a) reported no changes to either atrogen1 or MuRF1 transcripts in their Fn14-KO model, suggesting that the effects of TWEAK are distinct from those of Fn14.

In contrast to the catabolic actions associated with TWEAK administration, there is a growing body of evidence to support a pro-myogenic role of Fn14. RNA interference-based depletion of Fn14 in C2C12 myotubes – which endogenously express high levels of Fn14 during proliferation that is downregulated upon differentiation – results in reduction of myogenic progression and smaller myotubes (Dogra *et al.*, 2007b). This effect appeared to be modulated by a reduction in the expression of myogenic regulatory factors – a host of basic helix-loop-helix transcription factors that drive myogenic progression (Dogra *et al.*, 2007b). Of the myogenic regulatory factors, MyoD and Myogenin appeared to be the most drastically impacted (Dogra *et al.*, 2007b). Similar results are again seen in an *in vivo* setting. Girgenrath *et al.* (2006) examined the recovery of Fn14-KO mice following an intramuscular cardiotoxin injury. When Fn14 was absent, the innate inflammatory response and proliferative capacity of regenerating muscle was found to be blunted, resulting in a delay of muscle recovery (Girgenrath *et al.*, 2006).

Interaction of the TWEAK-Fn14 axis with peroxisome proliferator-activated receptor γ coactivator 1 α (PGC-1 α) has also been reported and may have impact on TWEAK-dependent

or TWEAK-independent Fn14-associated muscle outcomes. PGC-1 α is a primary driver of mitochondrial biogenesis and may in turn influence fibre-type composition of skeletal muscle, promoting fast-to-slow switching of fibre types (Lin *et al.*, 2002). Given the increased susceptibility of fast fibre types to muscle atrophy, potential modulation of PGC-1 α is an important consideration (Ciciliot *et al.*, 2013). Mutually inhibitory roles of PGC-1 α with both TWEAK and Fn14 have been described, wherein TWEAK-KO and Fn14-KO mice show increased PGC-1 α mRNA and were partially spared from denervation-induced atrophy (Hindi *et al.*, 2014). Overexpression of PGC-1 α protein also spared muscle wasting in TWEAK-Tg mice and reduced expression of Fn14, as well as the atrogenes, MuRF1 and atrogin1 (Hindi *et al.*, 2014).

Previous studies have focused on TWEAK-Fn14 modulation in the context of skeletal muscle atrophy by TWEAK administration, antagonistic α -Fn14 antibodies, or genetic depletion of either receptor or ligand. To the best of our knowledge, there is no description of an agonistic α -Fn14 antibody being used to stimulate TWEAK-independent Fn14 activity. The α -Fn14 001X antibody generated and characterised in Chapter 3 presents a viable candidate to investigate the therapeutic outcomes of an agonistic Fn14 antibody.

The current study aims to stimulate Fn14 whilst blocking TWEAK via the use of an agonistic α -Fn14 antibody, α -Fn14 001X, and assess the potential regenerative effects of TWEAK-independent Fn14 activation in a notexin-induced acute skeletal muscle injury. Muscle architecture, muscle-specific structural proteins, and mRNA expression of myogenic regulatory factors, atrogenes, and PGC-1 α were assessed to help determine potential myogenic or catabolic effects of α -Fn14 001X. Putative downstream signalling molecules, namely substrates of the NF κ B pathway, were also measured in an attempt to delineate the signalling outcomes of Fn14 activation. A descriptive study of Fn14 in old and chronically

exercised mouse samples was also investigated to compare and contrast the effects of Fn14 modulation in models of acute injury versus chronic atrophy.

5.2. Methods

5.2.1. Animals

All procedures were conducted in accordance with the National Health and Medical Research Council and approved by either the Animal Ethics Committee of La Trobe University (AEC: 16-70) or University of Western Australia.

5.2.1.1. Notexin Injury

This is as described in Chapter 2, Section 2.1.1 of this thesis. For completeness, it is repeated here. Male C57BL/6 mice (n=36) were placed under isoflurane anaesthesia (flow rate 2-5%, recovery within 5 minutes) and a notexin injury was performed. 40 μ L of notexin (10 μ g/ml, total 0.4 μ g notexin, Latoxan, France) was injected intramuscularly in the right TA muscle and 40 μ L saline injected in the left TA as an internal control. Injuries were performed by Dr Chris van der Poel (School of Life Sciences, La Trobe University) with assistance from Ms Laura Jenkinson (Dept of Biochemistry and Genetics, La Trobe University).

Mice were IP injected with either α -Fn14 001, α -Fn14 001X (20 mg/kg – see Chapter 3 for details of antibody generation; n = 12 for each treatment), or no antibody injection control (NoAB; n = 12) at 6-hours post-injury and again at 7 days post-injury for mice in the latest time point.

Animals were culled by CO₂ asphyxiation with a secondary kill method of cervical dislocation at 3, 7, or 14 days post-procedure (n = 4 for each treatment at each time point

except α -Fn14 001X 14 days post-injury group where n = 3) and both TA muscles were collected and stored at -80°C.

5.2.1.2. Uninjured Control Animals

In addition to internal controls of saline-injected contralateral TAs from animals described above, uninjured control TA muscle was obtained from 6-month old healthy male C57BL/6 mice (n = 5). Muscles were collected as described above and stored at -80°C.

5.2.1.3. Old and Chronically Resistance Trained Mice

Additional samples were provided by Emeritus Professor Miranda Grounds and Dr Zoe White with full experimental and morphological information published in Soffe *et al.* (2016).

Young (13 weeks) and old (105 weeks) C57BL/6 mice were housed in either standard cages (sedentary controls – YOUNG SED n = 9, OLD SED n = 9) or voluntary access resistance running wheels under a progressive low resistance training program (low resistance (LR) group – YOUNG LR n = 7, OLD LR n = 7) for 10 weeks. *Quadriceps* (QUAD) muscles were collected and stored whole at -80°C.

5.2.2. Histology

Frozen TA muscles were bisected at the widest point and serial 10 μ m cryosections were taken at -20°C and mounted on 1.0-1.2 mm glass microscope slides (Livingstone, Australia; Knittel, Germany). Slides were stored in the dark at -20°C until required. H+E staining was performed as per Chapter 2, Section 2.3.1 to assess markers of injury, which were defined as centralised nuclei, loss of muscle fibre size uniformity, proportion of non-contractile, and infiltration of inflammatory cells (Spasov *et al.*, 2010).

5.2.3. Western Blotting

Whole muscle homogenates were prepared from frozen QUAD and TA samples and subjected to SDS-PAGE as per Chapter 2, Section 2.4. Fn14 was detected using Criterion™ 16.5% Tris/Tricine gels run in Tris/Tricine/SDS running buffer (BioRad). Transfer was as per Chapter 2, Section 2.4 and post-transfer gel was stained with Coomassie Blue R-250 (ThermoFisher) to detect total protein. Details of antibodies used can be found in Appendix III. A muscle calibration mix was created by combining equal volumes of homogenates from each sample and used to run the same calibration curve on all subsequent gels. Normalised homogenates and muscle calibration mix were stored at -80°C.

5.2.3.1. Pathological Scoring

Degradation of total protein in notexin-injured TA muscles rendered typical quantitative analysis of western blots for all proteins not possible (see Chapter 4, Figure 4.4). Where necessary, samples were instead assigned qualitative scores based on their densitometry or the appearance of proteolysis products. Samples visually similar to healthy saline controls scored at 0 with increasing scores corresponding to increasing abnormality. Table 5.3 details the pathological scoring criteria used.

Table 5.3: Pathological scoring criteria for proteins of interest

Protein	Pathological Score			
	0	1	2	3
Fn14	No Fn14 detected	Fn14 detected		
Actin	Single band detected at 43 kDa	Band detected at 43 kDa plus one proteolytic product	Band detected at 43 kDa plus two proteolytic products	No actin detected
Myosin	Clear band detected in UV Stain Free gel	Smear band detected in UV Stain Free gel	No band detected in UV Stain Free gel	
Desmin	Single band detected at 57 kDa	Bands detected at 57 kDa and ~45 kDa	Single band detected at ~45 kDa	No desmin detected
IgG light chain	No IgG detected	IgG detected		
CD68	No CD68 detected	Faint CD68 band detected at ~110 kDa	Strong CD68 band detected at ~110 kDa	Strong, smeared CD68 band detected at ~110 kDa
p100-p52	No p52 detected	Faint p52 band detected	Clear p52 band detected	

5.2.4. qPCR

qPCR was performed as per protocol described in Chapter 2, Section 2.6. Results were analysed using the 2^{-Ct} method normalised to the total cDNA content as determined by OliGreen ssDNA assay. This method means that a housekeeping gene is not required, because the absolute amount of single-stranded cDNA used in each assay was known.

Notexin-injured TA samples were expressed relative to the mean of uninjured control muscle from C57BL/6 mice; QUAD muscle from old and LR trained animals were expressed relative to the mean of YOUNG SED samples. Fn14 primers were designed by Dr Amelia Johnston (Dept of Biochemistry and Genetics, La Trobe University); MyoD, Myogenin, MRF4, Myf5, and PGC-1 α primers were sourced from PrimerBank (see Appendix III for full primer details and relevant optimisation and validation; Spandidos *et al.*, 2008; Spandidos *et al.*, 2010)

5.2.5. Statistical Analyses

Statistical analyses were performed in Prism v8 (GraphPad). TWEAK and calpain-3 ratios for notexin-injured samples were analysed by paired Student's t-test with time-matched contralateral saline TA from the same animal as an internal control. Proteins which were assessed with pathological scores were handled as qualitative data and graphed for visualisation but were not analysed statistically. mRNA was assessed only in notexin-injured samples by two-way ANOVA with Dunnett's multiple comparisons post-hoc analyses and time-matched NoAB used as a control. Old and LR trained mice protein and mRNA samples were analysed by two-way ANOVA. All two-way ANOVA main effects are annotated alongside graphs.

5.3. Results

5.3.1. Adverse Reactions to Notexin Injury

Acute reactions to notexin were severe and unpredicted. Tissues collected from these animals were severely degraded as observed at both the histological level and SDS-PAGE total protein content analysis (Figure 5.1; same cohort as mice described and shown in Chapter 4, Figure 4.3, however different representative H+E images are shown here to demonstrate each antibody condition). H+E staining showed extensive centralisation of nuclei, loss of fibre size uniformity, regions of non-contractile tissue, and infiltration of inflammatory cells which remained persistent at 14 days post-injury in all treatment groups (Figure 5.1A). Stain-free in gel UV imaging of total protein content showed prolonged degradation of cellular proteins as indicated by a streaking pattern in contrast to the typical banded appearance of whole muscle homogenates which is seen in saline-injected controls; absence of typical actin and myosin bands was evident in many injured samples across time points and treatment groups (Figure 5.1B). Full quantitative analysis by western blotting was not possible in these conditions; qualitative and semi-quantitative western blotting has been used where appropriate. Full description of these adverse events are detailed in Chapter 4.

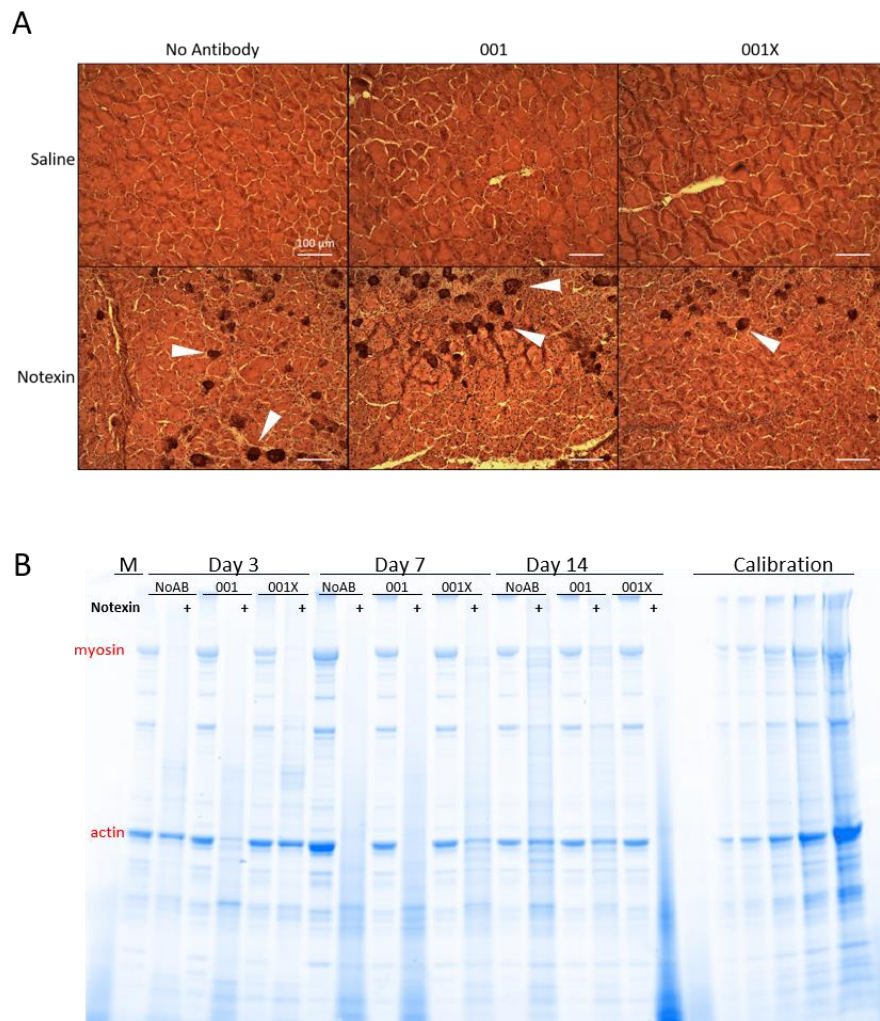


Figure 5.1: Degradation of tibialis anterior (TA) tissue architecture following notexin injury. (A) H+E stains of saline and notexin-treated (+) TA muscle 14 days post-injury. Tissue architecture remained pathological in notexin-injured TA across all treatment groups (NoAB = No Antibody; 001 = α -Fn14 001; 001X = α -Fn14 001X) with persistent centralised nuclei, loss of fibre size uniformity, and infiltration of inflammatory cells (examples indicated by white arrows). (B) Stain-Free UV image of total protein content on SDS-PAGE gel. Characteristic myosin and actin bands evident in saline-treated samples are frequently degraded in notexin-injured samples across time points and treatment groups.

5.3.2. Fn14 mRNA and Protein Regulation

5.3.2.1. Fn14 in Notexin Injury

Fn14 was measured at both the protein and mRNA level using semi-quantitative western blotting and qPCR, respectively (Figure 5.2).

Fn14 mRNA transcript levels in notexin-injured TA from NoAB, 001, or 001X groups were each assessed using qPCR, normalised to total cDNA and expressed relative to the mean of uninjured control (uninjured controls excluded from statistical analyses; time-matched NoAB used as statistical control, Figure 5.2A). Fn14 was transcriptionally upregulated in all groups at 3 days post-injury, with levels returning towards baseline at 7 days. At 14 days post-injury, Fn14 mRNA was significantly upregulated in 001X relative to time-matched NoAB (two-way ANOVA with Dunnett's multiple comparisons, $p < 0.0001$). 001 also showed a spike in mRNA at 14 days post-injury, albeit with a large spread in biological replicates and was not statistically different from NoAB (two-way ANOVA with Dunnett's multiple comparisons, $p = 0.066$).

Fn14 protein was measured qualitatively due to the severe degradation of total protein content. Results are expressed as a binary present or absent result coded as present = 1 and absent = 0 (Figure 5.2B, C). These results are presented cautiously and without statistical analyses. Fn14 at the protein level is presented to indicate that there was a detectable increase of protein in notexin-injured muscle.

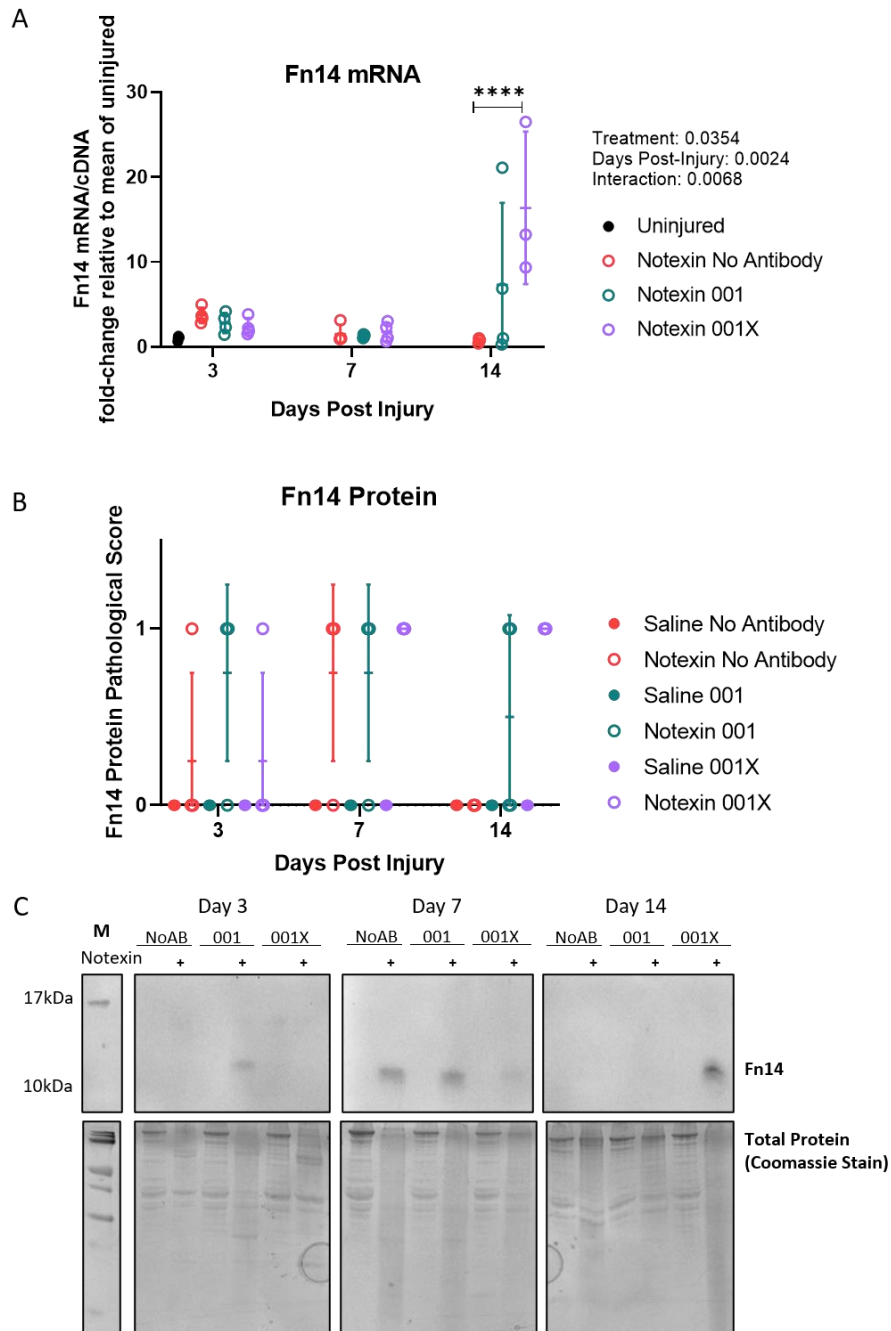


Figure 5.2: Fn14 mRNA and protein in notexin-injured tibialis anterior (TA) muscle. (A) Fn14 mRNA was detected in all notexin-injured samples at all time points. α -Fn14 001X (001X)-treated mice showed significantly greater Fn14 mRNA at 14 days post-injury relative to time-matched No Antibody (NoAB)-treated mice (two-way ANOVA with Dunnett's multiple comparisons, $p < 0.0001$). α -Fn14 001 (001)-treated mice showed a similar upregulation at 14 days post-injury, however greater biological variability meant this was not statistically significant. $n = 3-4$ per time per treatment (B) Fn14 protein was measured qualitatively by western blot using pathological criteria outlined in Table 5.3 (where 0 = absent and 1 = present). Fn14 was detected only in notexin-injured TA; no statistical analyses were performed due to degradation of total protein. (C) Representative blot of Fn14 and Coomassie stain of total protein content. A band at ~ 14 kDa was detected for Fn14, notably, only in notexin-injured muscle (Cell Signaling Technology 4403, expected molecular weight – 14 kDa).

5.3.2.2. Fn14 mRNA and Protein in Ageing and Exercise

Fn14 was also assessed in old and chronically low resistance-trained mice (Figure 5.3). Fn14 mRNA (Figure 5.3A) was shown to be reduced as a result of ageing and in response to LR training (two-way ANOVA age effect, $p = 0.0028$, activity effect, $p = 0.0060$). No Fn14 protein was detected in any group (Figure 5.3B, C).

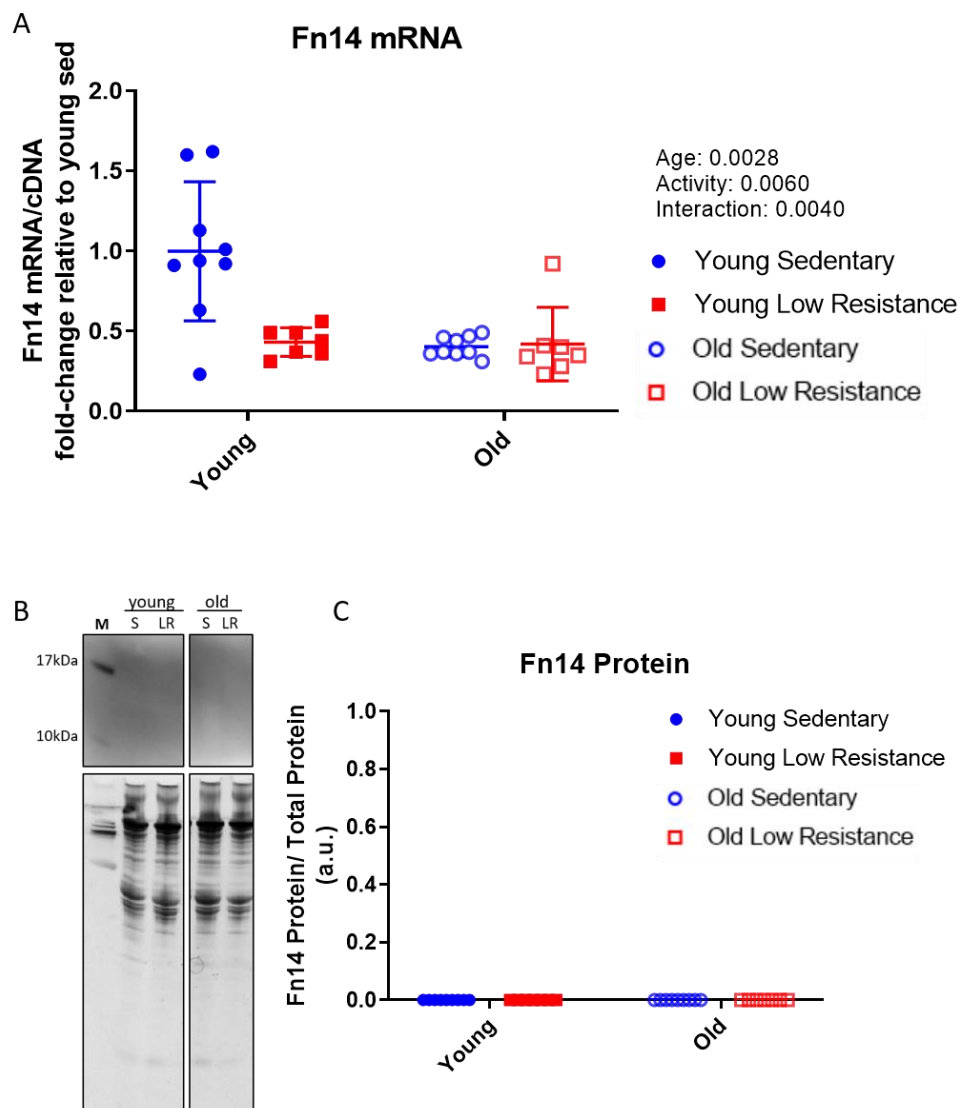


Figure 5.3: Fn14 mRNA and protein in quadriceps (QUAD) from old and chronically low resistance-trained mice. (A) Fn14 mRNA was expressed relative to the mean of young sedentary mice and found to be reduced in old (two-way ANOVA age effect, $p = 0.0028$) and low-resistance trained mice (two-way ANOVA activity effect, $p = 0.0060$). $n = 7-9$, as indicated by separate data points. (B) Representative blot for Fn14 and Coomassie stain of total protein content. (C) No Fn14 bands were detected in any group (Cell Signaling Technology 4403, expected molecular weight – 14 kDa). $n = 7-9$ as indicated by separate data points.

5.3.3. TWEAK mRNA and Protein Processing

5.3.3.1. TWEAK mRNA and Protein in Notexin Injury

Details of TWEAK antibody validation are provided in Appendix III. TWEAK mRNA was shown to be elevated in α -Fn14 001X treated mice at 7 days post-injury relative to time-matched NoAB controls (two-way ANOVA with Dunnett's multiple comparison, $p = 0.0009$), however the absolute transcript level of TWEAK in uninjured controls was found to be low in abundance with considerable biological variability (Figure 5.4A). Protein bands for membrane bound TWEAK (mTWEAK) and soluble TWEAK (sTWEAK) were detected with sTWEAK appearing primarily in notexin-injured samples (Figure 5.4B, C). sTWEAK:mTWEAK ratio was shown to be elevated in NoAB and 001X mice at 7 days post-injury relative to contralateral saline controls (paired t-test, $p = 0.0053$ and 0.0042 respectively).

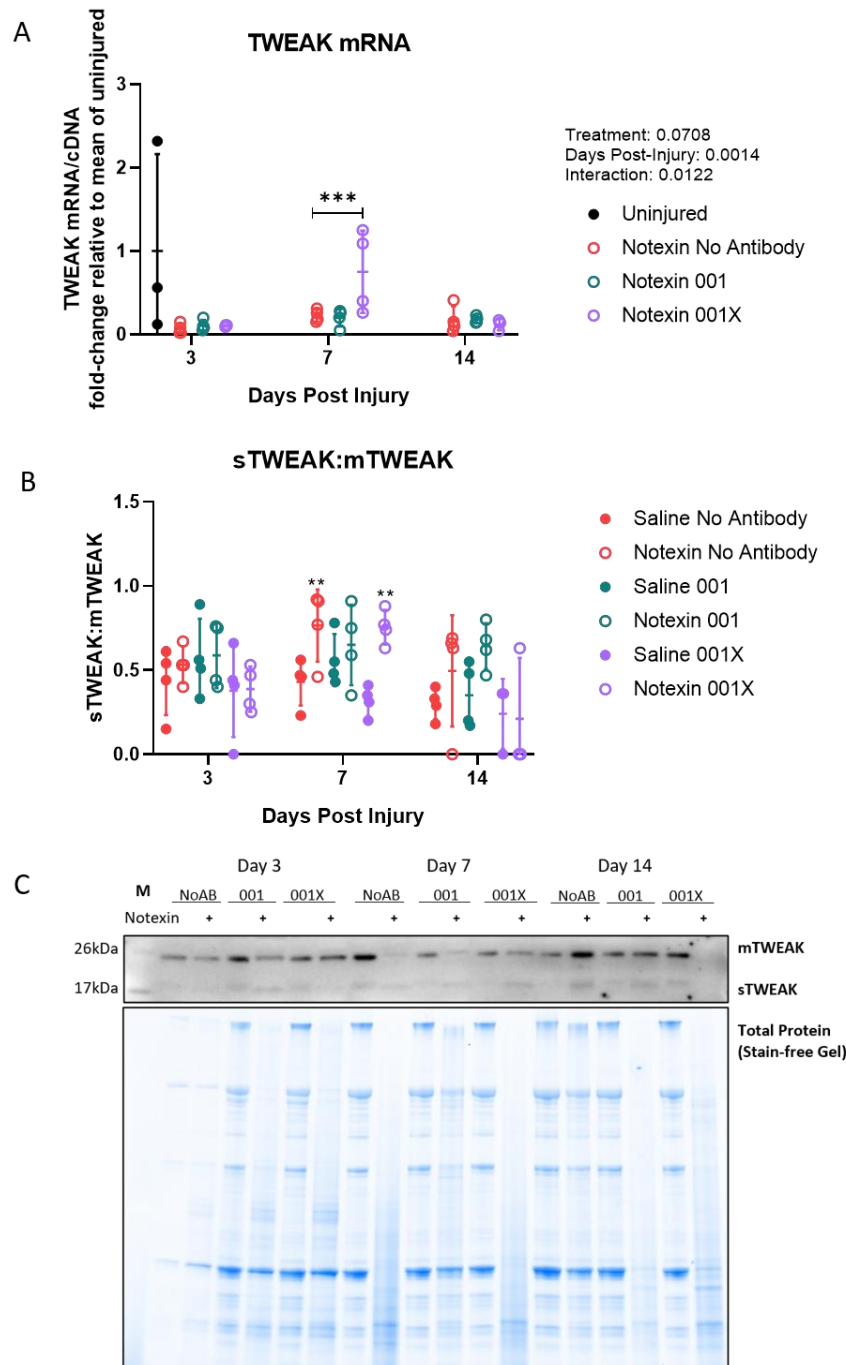


Figure 5.4: TWEAK mRNA and protein in notexin-injured tibialis anterior (TA) muscle. (A) TWEAK mRNA was elevated in 7 days post-injury α -Fn14 001X (001X) treated notexin-injured TA relative to time-matched No Antibody (NoAB) treatment mice (two-way ANOVA with Dunnett's multiple comparisons, $p = 0.0009$), however all samples were within the range of uninjured TA controls (shown in black). No changes were detected in α -Fn14 001 (001) treated mice at any time point. (B) Ratio of sTWEAK to mTWEAK proteins was elevated in No Antibody and 001X treated mice at 7 days post-injury relative to contralateral saline-injected TA controls (paired t-test, $p = 0.0053$ and 0.0042 respectively). (C) Representative blot of TWEAK and Stain-Free UV image of total protein content. Bands were detected at ~ 26 kDa (mTWEAK) and ~ 18 kDa (sTWEAK; Abcam 37170, expected molecular weight – 26, 18 kDa). The total protein was not used for analyses, as here the internal ratio could be assessed regardless of the total protein present.

5.3.3.2. TWEAK mRNA and Protein in Ageing and Exercise

TWEAK mRNA was decreased in muscle from old mice relative to young mice (two-way ANOVA age effect, $p = 0.0368$) but no effects of exercise were detected (Figure 5.5A). Overall abundance of TWEAK mRNA was low in all samples with CT values greater than 30 in all but two uninjured samples. TWEAK protein was detected only in the form of mTWEAK (Figure 5.5B) which was not found to be altered by age or LR training in mice (Figure 5.5C).

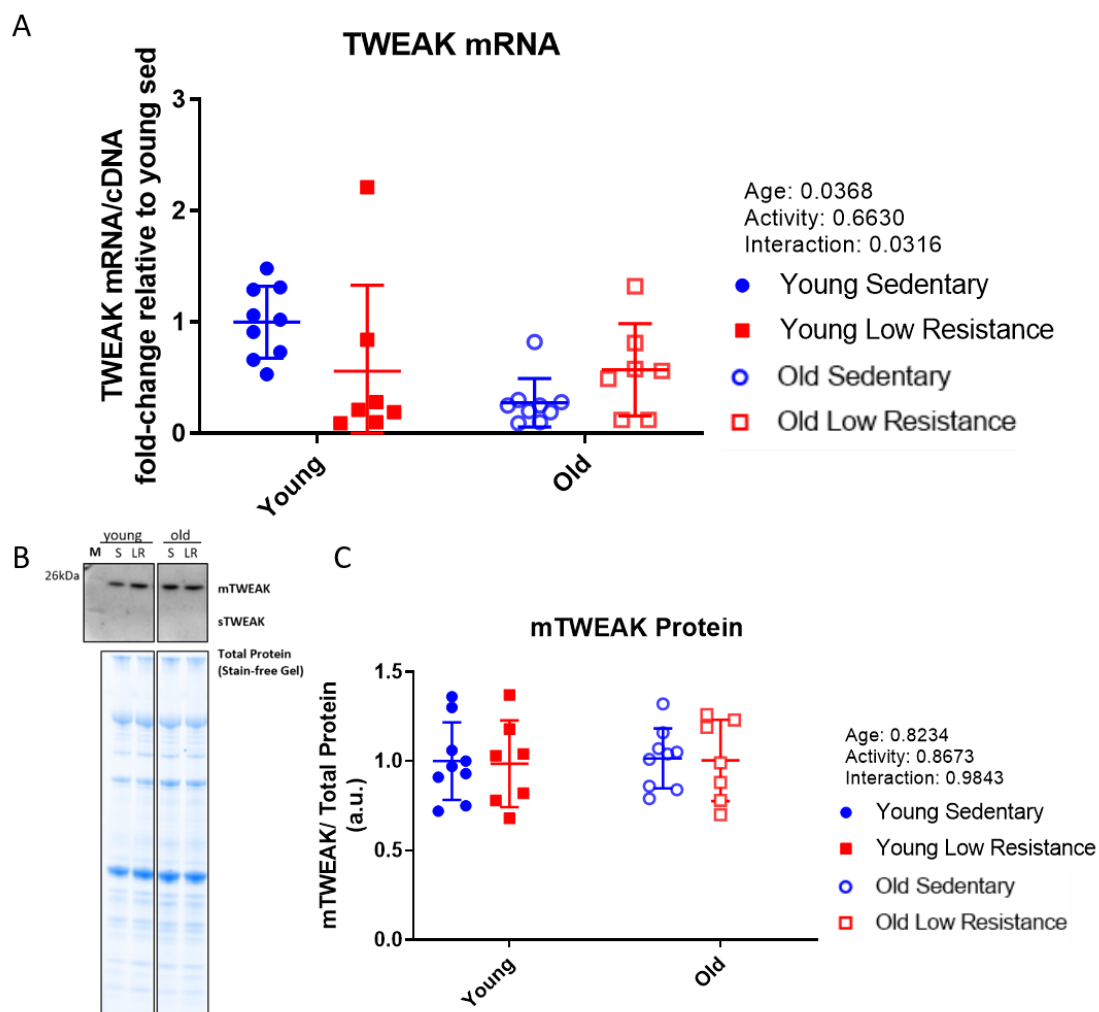


Figure 5.5: TWEAK mRNA and protein in quadriceps (QUAD) muscle from old and chronically low-resistance exercised mice. (A) TWEAK mRNA was overall of low abundance and was found to be decreased in old mice (two-way ANOVA age effect, $p = 0.0368$). (B) Representative blot of TWEAK with Stain-Free UV image of total protein content. A band was detected for mTWEAK at 26 kDa but no sTWEAK was detected in any group (Abcam 37170, expected molecular weight – 26, 18 kDa). (C) No effects of age or LR training were detected in mTWEAK. $n = 7-9$ as indicated by separate data points.

5.3.4. Myogenic Regulatory Factors

5.3.4.1. Myogenic Regulatory Factors in Notexin Injury

Western blotting of all myogenic regulatory factors at the protein level failed to generate reliable and quantifiable specific bands (see Appendix III). MRF4, Myf5, Myogenin, and MyoD mRNA transcript levels in notexin injured TA NoAB, 001, or 001X groups were each assessed using qPCR with specific mRNA normalised to total cDNA and expressed relative to the mean of uninjured control TA as a means of assessing myogenesis (uninjured controls excluded from statistical analyses; time-matched NoAB used as statistical control; Figure 5.6).

Myf5, MRF4, and Myogenin each showed peaks at 7 days post-injury which returned towards baseline at 14 days post-injury. α -Fn14 001X-treated mice showed significant upregulation of Myf5 and Myogenin relative to time-matched NoAB controls at 7 days post-injury (two-way ANOVA with Dunnett's multiple comparison, $p = 0.0490$ and 0.0024 respectively).

MyoD was significantly downregulated in α -Fn14 001X-treated mice relative to time-matched NoAB controls at 3 days post-injury (two-way ANOVA with Dunnett's multiple comparison, $p = 0.0468$) but upregulated at 14 days post-injury (two-way ANOVA with Dunnett's multiple comparison, $p = 0.0027$). α -Fn14 001-treated mice also showed upregulation of MyoD relative to NoAB time-matched controls at 14 days post-injury (two-way ANOVA with Dunnett's multiple comparison, $p = 0.0182$).

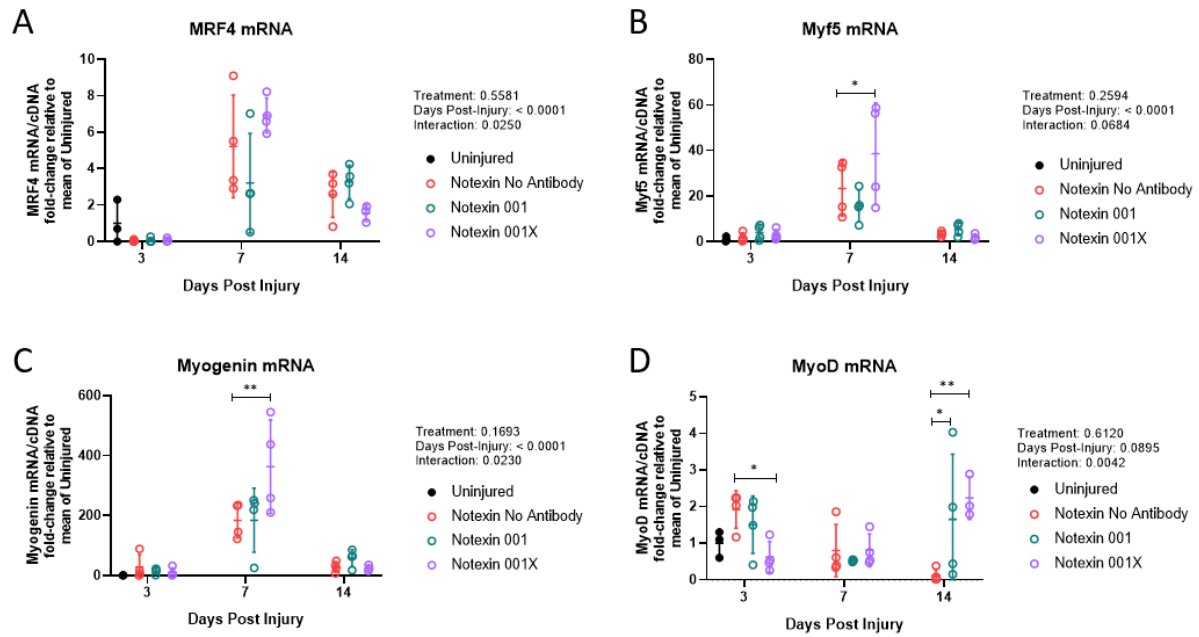


Figure 5.6: Time course of myogenic regulatory factor mRNA levels in notexin-injured tibialis anterior (TA) mouse muscle. (A) MRF4 peaked at 7 days post-injury in all treatment groups, no differences were detected between treatments. (B) Myf5 and (C) Myogenin were upregulated in α -Fn14 001X (001X)-treated mice relative to time-matched No Antibody (NoAB) at 7 days post-injury (two-way ANOVA with Dunnett's multiple comparison, $p = 0.0490$ and 0.0024 respectively). (D) MyoD was downregulated in 001X-treated mice relative to time-matched NoAB controls at 3 days post-injury (two-way ANOVA with Dunnett's multiple comparison, $p = 0.0468$) but upregulated at 14 days post-injury (two-way ANOVA with Dunnett's multiple comparison, $p = 0.0027$). α -Fn14 001 (001)-treated mice also showed upregulated MyoD relative to time-matched NoAB controls at 14 days post-injury, albeit with greater biological variability (two-way ANOVA with Dunnett's multiple comparison, $p = 0.0182$). $n=3-4$ mice per treatment, per time-point, indicated as individual data points throughout.

5.3.4.2. Myogenic Regulatory Factors in Ageing and Exercise

Myogenic regulatory factor transcript levels for MRF4, Myf5, Myogenin, and MyoD were measured in old and LR trained mice (Figure 5.7). Overall effects of age were detected for MRF4 (Figure 5.7A) and MyoD (Figure 5.7D; two-way ANOVA age effect, $p = 0.0009$ and 0.0076 respectively). Myf5 (Figure 5.7B) and Myogenin (Figure 5.7C) showed no effects of age. No effects of LR training were detected for any myogenic regulatory factor.

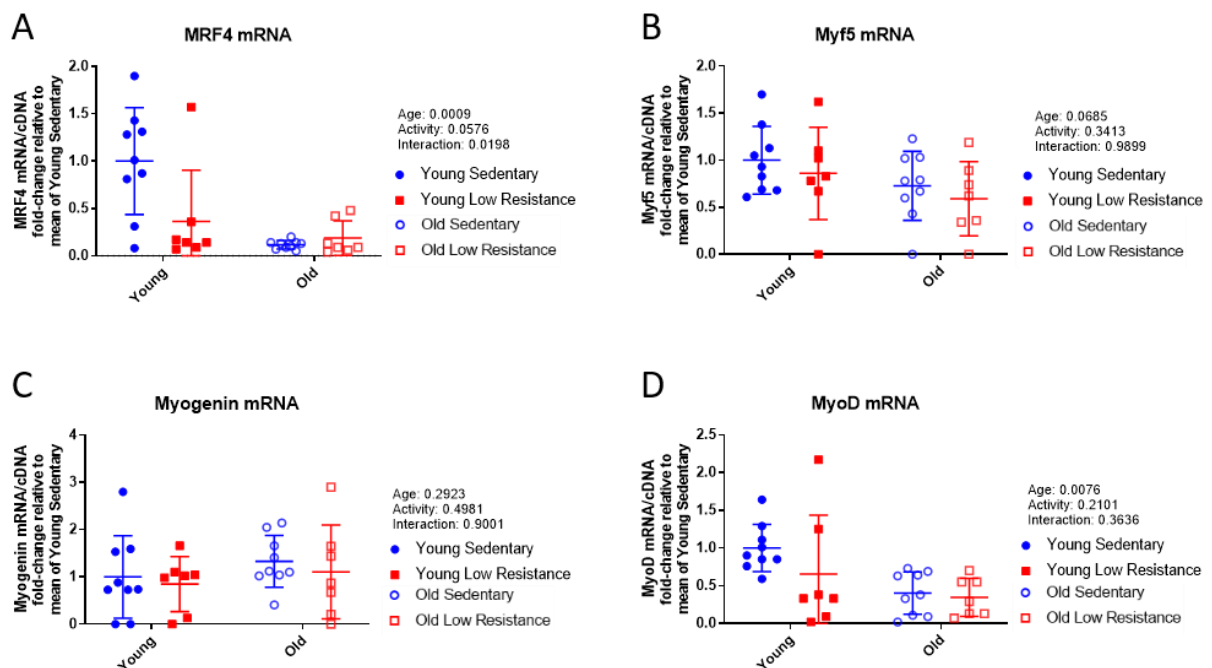


Figure 5.7: Myogenic regulatory factor mRNA in quadriceps (QUAD) muscle from old and low-resistance (LR) trained mice. MRF4 (A) and MyoD (D) were downregulated in old mice relative to young controls (two-way ANOVA age effect, $p = 0.0009$ and 0.0076 respectively). No effects of age or LR training were detected for Myf5 (B) or Myogenin (C). $n=7-9$ mice per treatment, per time-point, indicated as individual data points.

5.3.5. Fn14 and MyoD Correlations

MyoD and log transform of Fn14 transcripts were found to be positively correlated for all treatment groups in notexin-injured TA muscle (Figure 5.8A). Log transform was used to linearise exponential distribution. No such correlation was observed in QUAD muscle from ageing and LR training cohorts (Figure 5.8B).

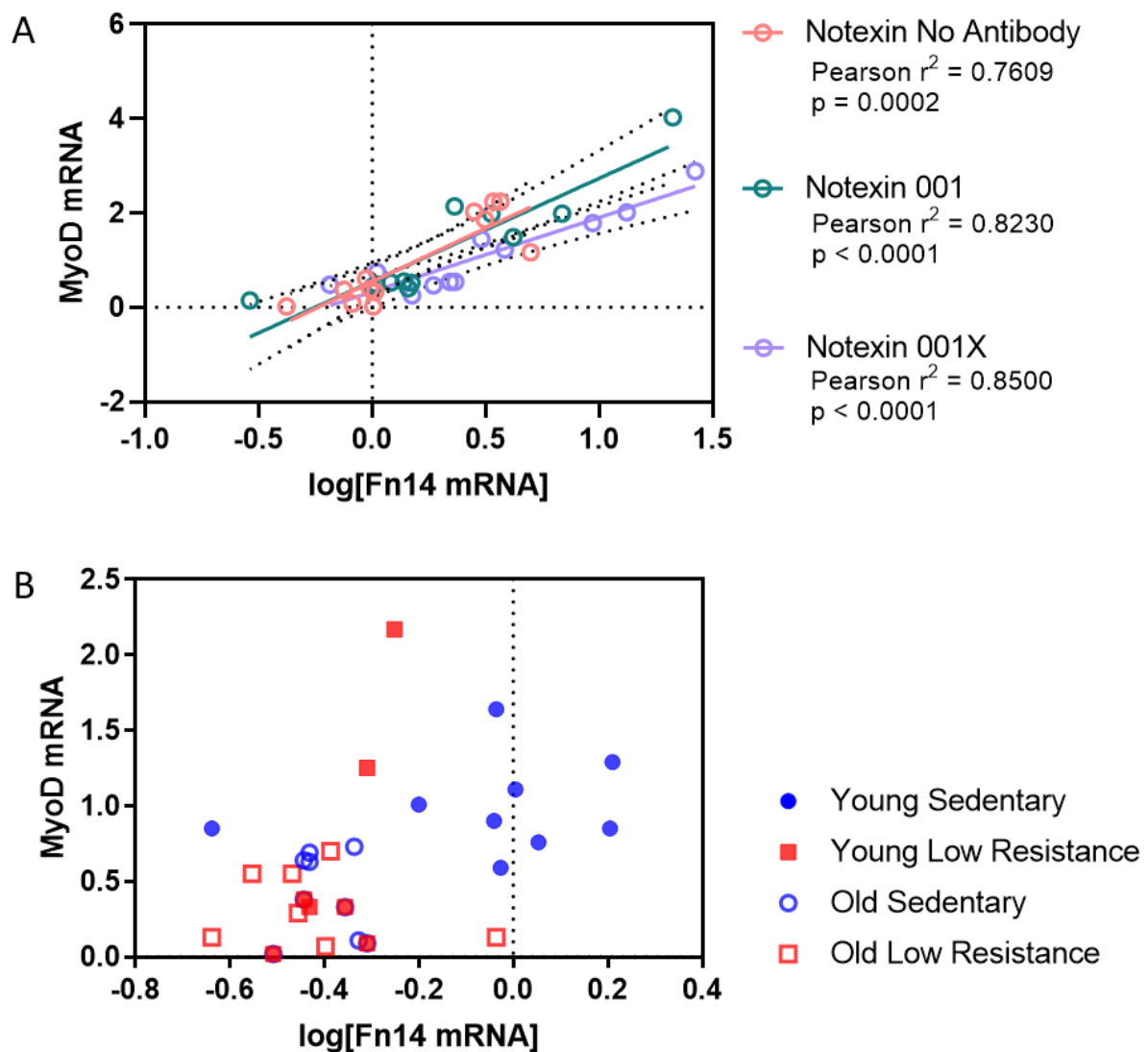


Figure 5.8: Correlation of MyoD and Fn14 transcripts in notexin-injury and ageing. (A) MyoD mRNA was found to positively correlate with log transform of Fn14 mRNA in No Antibody (NoAB), α -Fn14 001 (001), and α -Fn14 001X (001X) treatment groups for notexin-injured tibialis anterior (TA) muscle (Each group analysed separately; Pearson r correlation, $r^2 = 0.7609$, 0.8230 , and 0.8500 respectively, $p = 0.0002$, < 0.0001 , and < 0.0001 respectively and individual lines of best fit shown as per the legend). (B) No correlation was observed in quadriceps (QUAD) muscle from young or old, sedentary or low-resistance (LR) trained mice.

5.3.6. Structural Proteins

5.3.6.1. Actin, Myosin, and Desmin

Structural proteins – actin, myosin, and desmin – were assessed qualitatively to determine regeneration of muscle structure. Actin (Figure 5.9A), myosin (Figure 5.9B), and desmin (Figure 5.9C) were each shown to be degraded in notexin-injured TA at 3 days post-injury across all treatments. Whilst NoAB and 001 were largely returned to baseline by 14 days post-injury, all structural proteins remained pathological, as outlined in Table 5.1, in 001X mice.

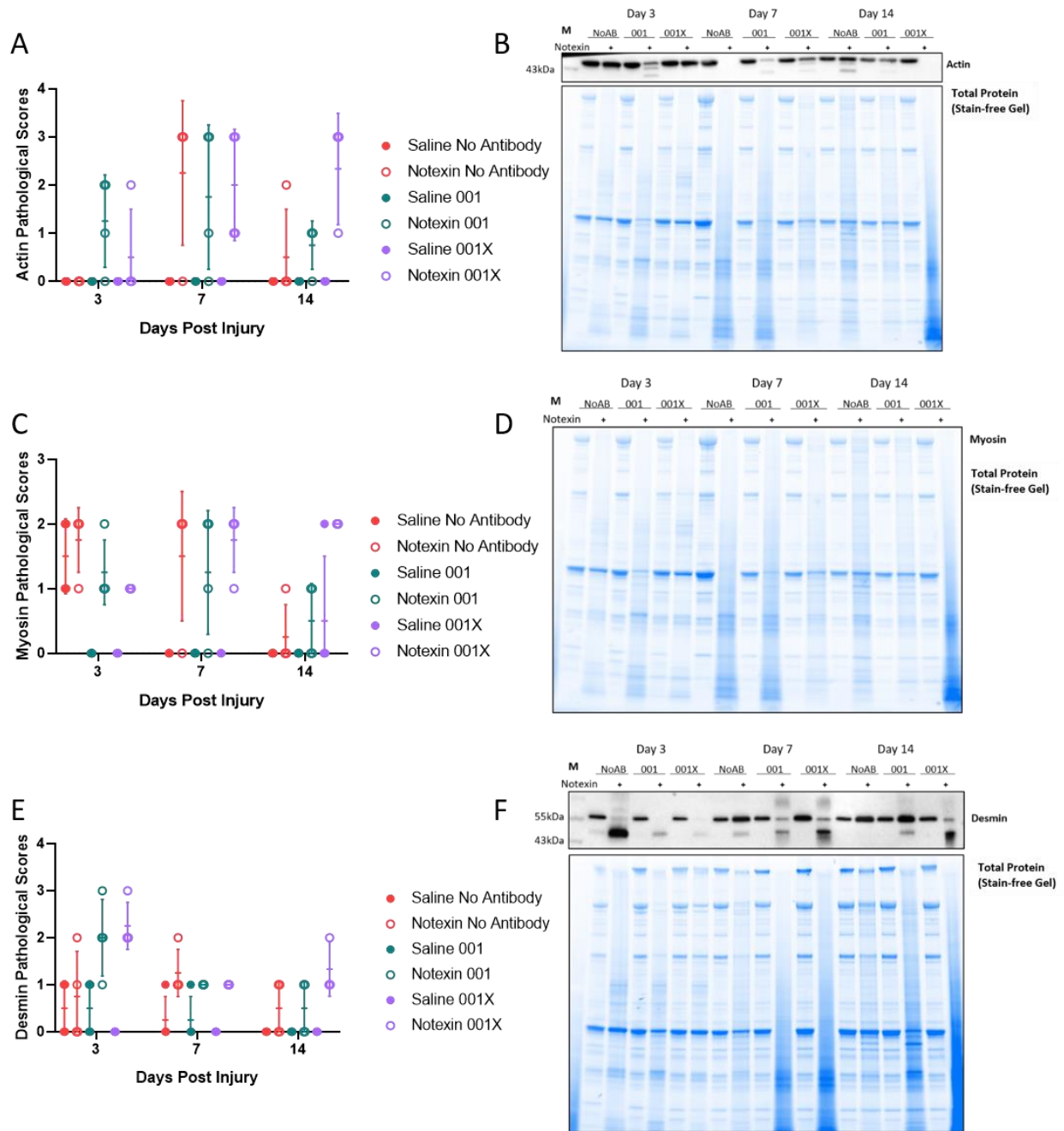


Figure 5.9: Degradation of actin, myosin and desmin in notexin-injured tibialis anterior (TA) muscle. Pathological scores, using criteria outlined in Table 5.3, of actin (A), myosin (C), and desmin (E) remained above zero at 14 days post-injury in all α -Fn14 001X (001X)-treated mice whilst mice given no antibody treatment (NoAB) or α -Fn14 001 (001) had partially returned to baseline. (B) Representative blot of Actin and Stain-Free UV image of total protein content. Up to 3 bands were detected between 40 and 45 kDa (Sigma A2066, expected molecular weight – 42 kDa). (D) Representative Stain Free gel with apparent degradation of myosin band. (F) Representative blot of Desmin and Stain-Free UV image of total protein content. Two prominent bands were detected at 45 and 57 kDa (Novocastra NCL-L-DES-DERII, expected molecular weight – 57 kDa). $n=3-4$ mice per treatment, per time-point, indicated as individual data points throughout

5.3.6.2. Calpain-3

Calpain-3 autolysis was measured in all samples where calpain-3 could be detected. Presence or absence of calpain-3 is represented in Table 5.4, where those treatments and time-points shown in blue having 1 sample where calpain-3 was not present. Specifically, calpain-3 was absent from 1 of 4 NoAB notexin-injured samples at 3 days post-injury, 1 of 4 from each treatment group at 7 days post-injury, and 1 of 3 from 001X at 14 days post-injury.

Table 5.4: Samples with detectable Calpain-3.

Treatment Days Post Injury	No Antibody		α -Fn14 001		α -Fn14 001X	
	Saline	Notexin	Saline	Notexin	Saline	Notexin
Day 3	4 of 4	3 of 4	4 of 4	4 of 4	4 of 4	4 of 4
Day 7	4 of 4	3 of 4	4 of 4	3 of 4	4 of 4	3 of 4
Day 14	4 of 4	4 of 4	4 of 4	4 of 4	4 of 4	2 of 3

Of the samples with detectable Calpain-3, percentage of overall Calpain-3 present in the autolysed form was measured (Figure 5.10). Calpain-3 autolysis was increased in notexin-injured TA relative to time- and treatment-matched saline controls for 001 and 001X at 3 days post-injury, all groups at 7 days post-injury, and only in 001X at 14 days post-injury.

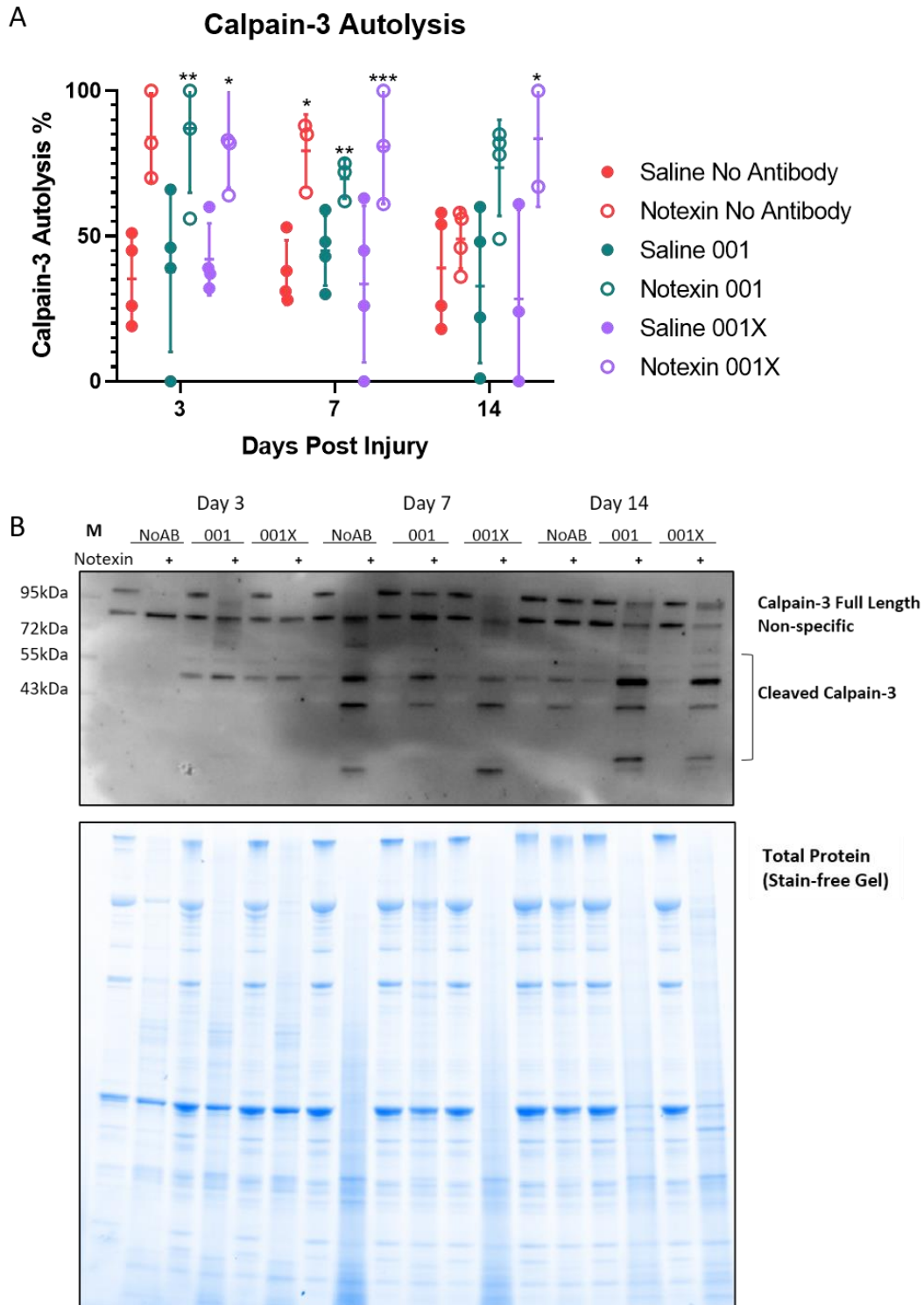


Figure 5.10: Calpain-3 processing in notexin-injured tibialis anterior (TA) mouse muscle. (A) Extent of calpain-3 autolysis in samples with detectable Calpain-3. Calpain-3 autolysis was elevated in notexin-injured samples relative to time-matched saline controls. *, **, *** indicate $p < 0.05$, 0.01 , 0.001 respectively in paired t-test. (B) Representative blot of Calpain-3 and Stain-Free UV image of total protein content. Full-length Calpain-3 was detected above 95 kDa with a non-specific Calpain-2 band just below. Multiple cleaved Calpain-3 isoforms were detected below 72 kDa (Novocastra, NCL-CALP2-12A2, expected molecular weight = 94 kDa). The total protein was not used for any analyses, and so the internal ratio could be assessed regardless of the total protein present.

5.3.7. PGC-1 α

PGC-1 α was assessed as a potential downstream target of α -Fn14 antibody treatments and a measure of mitochondrial biogenesis and precursor to fibre-type switching (Figure 5.11). Antibodies against PGC-1 α have not been reliably validated in our hands so only mRNA transcript data are presented. Uninjured controls are included as a representative baseline and were excluded from statistical analyses. A time-effect was detected with transcripts lowest at 3 days post-injury in notexin-injured TA muscle and returning towards baseline levels at 7- and 14 days post-injury (two-way ANOVA, days post-injury effect, $p < 0.0001$). No significant changes were detected between treatment groups at any time point. There was considerable biological variability of PGC-1 α transcripts, including in the uninjured controls and there was low overall abundance with CT values most greater than 30.

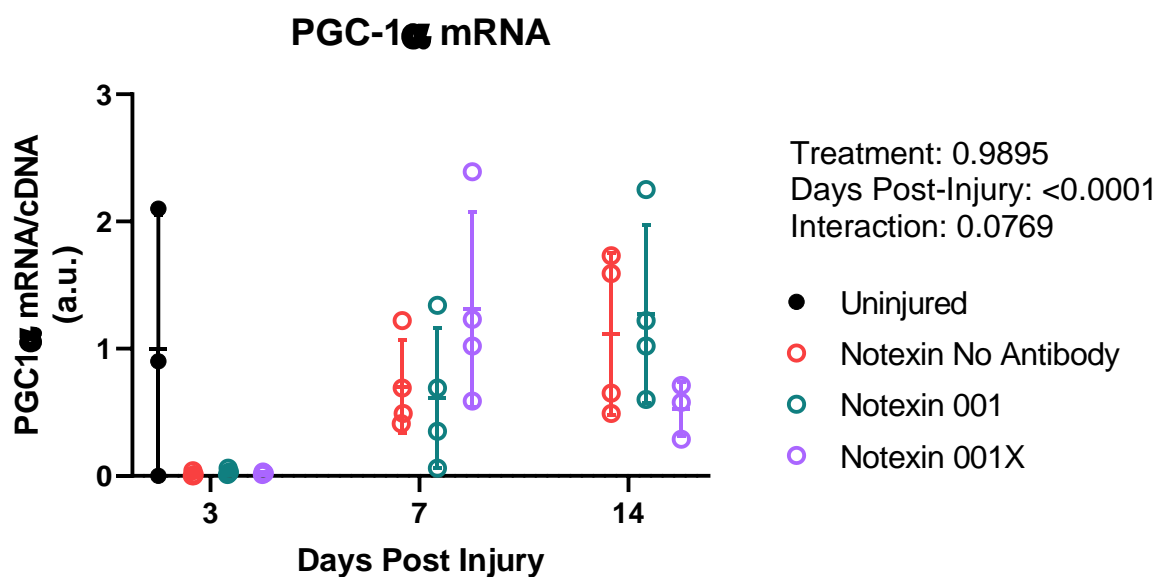


Figure 5.11: PGC-1 α mRNA in notexin-injured tibialis anterior (TA) mouse muscle. PGC-1 α mRNA was assessed by qPCR and expressed relative to the mean of uninjured controls. Overall abundance was low and considerable biological variability was observed in uninjured controls. Negligible levels were detected in all treatment groups at 3 days post-injury with all groups appearing normal at 7 and 14 days post-injury (two-way ANOVA, days post-injury effect, $p < 0.0001$). No statistically significant differences were detected between treatment groups (two-way ANOVA, treatment effect, $p = 0.9895$).

5.3.8. Infiltration of Immune Cells

Results obtained from several mouse primary antibodies in combination with a goat α -mouse IgG secondary not specific to intact IgG showed a distinct and repeated non-specific binding pattern in the notexin-injured samples (Figure 5.12A). These bands were interpreted as probable non-specific binding to endogenous IgG light and heavy chains. Probing with secondary goat α -mouse IgG only with no primary antibody confirmed the identity of these non-specific bands as endogenous IgG (Figure 5.12C). No statistical analyses were performed due to the qualitative nature of the results, and protein was measured as being present or absent. IgG appears to be persistent with more intense staining in 001 and 001X mice at 14 days post-injury relative to NoAB controls (Figure 5.12B).

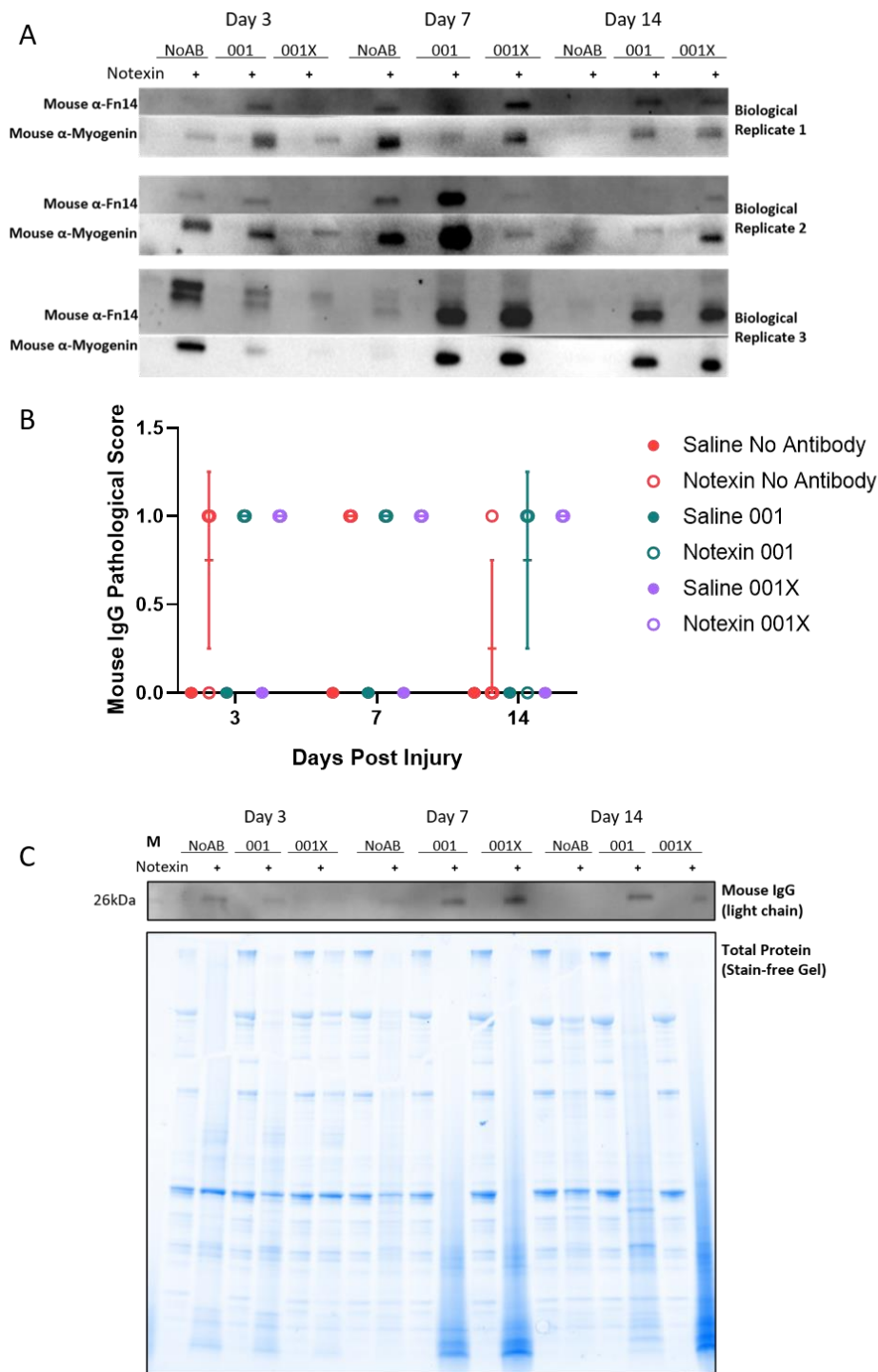


Figure 5.12: Endogenous IgG in notexin-injured tibialis anterior (TA) mouse muscle. (A) Representative blot of non-specific band at ~25 kDa (additional band at ~50 kDa not shown) obtained when using several primary antibodies raised in mouse host in combination with goat α -mouse IgG secondary. (B) Qualitative results of endogenous IgG detected; IgG present in notexin-injured samples only, with No Antibody and α -Fn14 001-treated mice returning towards baseline at 14 days post-injury. IgG remained present in all α -Fn14 001X-treated mice at 14 days post-injury. Pathological criteria outlined in Table 5.3. (C) Representative blot of goat α -mouse IgG secondary with no primary antibody and Stain Free UV gel of total protein content. Band at ~25 kDa (light chain IgG) shown only, second band at ~50 kDa (heavy chain IgG) also detected. $n = 3-4$ as indicated by individual data points.

Infiltration of macrophages was assessed using western blot analysis of CD68 (Figure 5.13). Given the qualitative analysis of total protein, no statistical analyses of CD68 were performed. No discernible difference was detected between NoAB, 001, or 001X, when scored using the pathological criteria in Table 5.1.

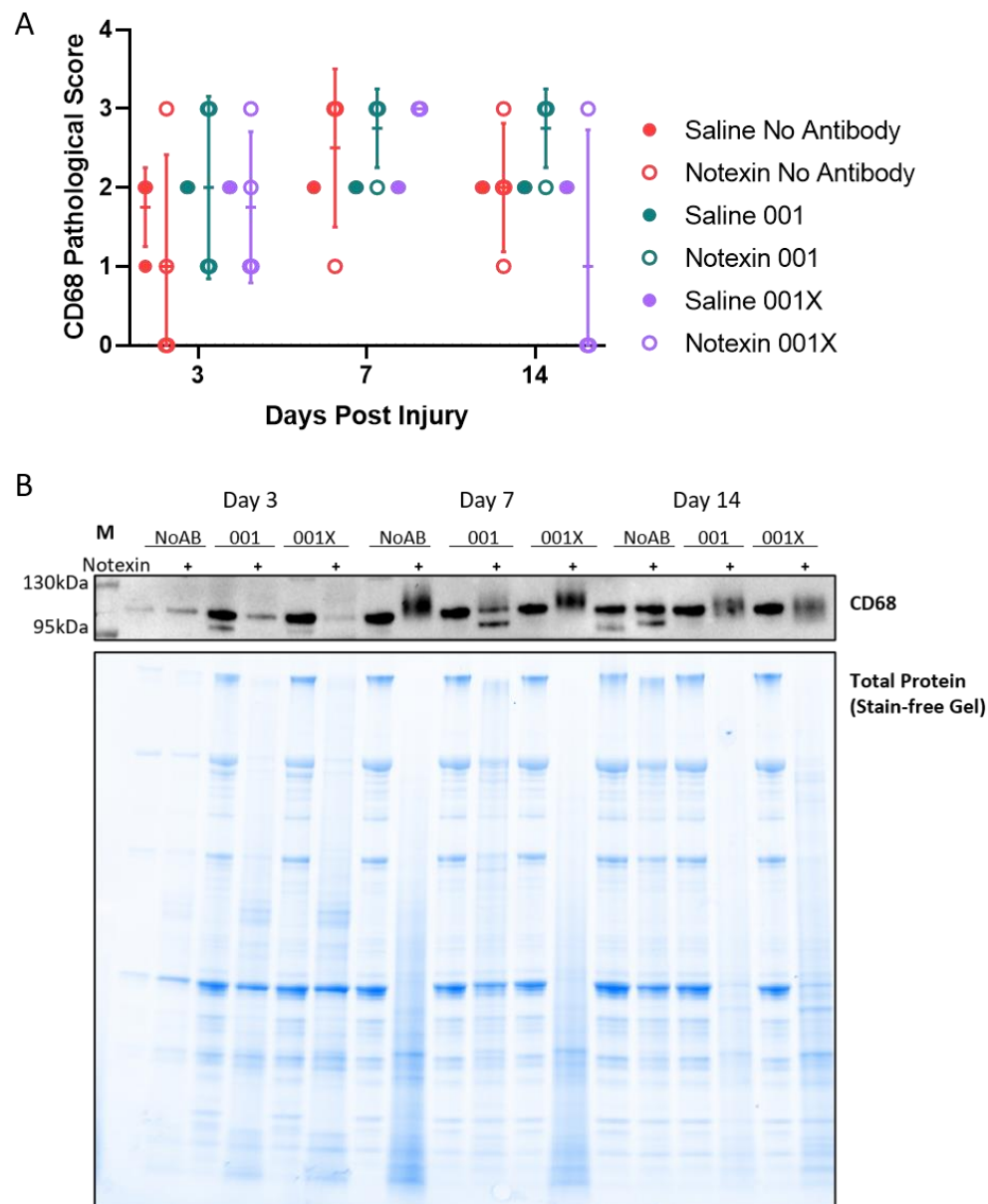


Figure 5.13: CD68 in notexin-injured tibialis anterior (TA) mouse muscle. (A) Qualitative results of CD68 showed greater variability in notexin-injured samples across No Antibody (NoAB) and α -Fn14 001-treated mice (001) and α -Fn14 001X-treated mice (001X), compared with saline at all time points. Pathological criteria outlined in Table 5.3. (B) Representative blot of CD68 and Stain-Free UV image of total protein content. Two bands were detected at \sim 110 kDa (Abcam 125212, expected molecular weight – 75 - 110 kDa). $n = 3-4$ as indicated by individual data points, although these cannot be discerned in some samples as they are all the same value (indicated by no error bars).

5.3.9. Atrogenes

5.3.9.1. Atrogenes in Notexin Injury

MuRF1 and atrogenin1 each showed a time effect (two-way ANOVA, days post-injury effect, $p < 0.0001$) with transcript levels lowest at 3 days post-injury, and resembling baseline uninjured controls by 7 and 14 days post-injury, however all transcript levels were within the range of uninjured controls (Figure 5.14). Uninjured controls were used as a representative baseline and were not included in the statistical analyses.

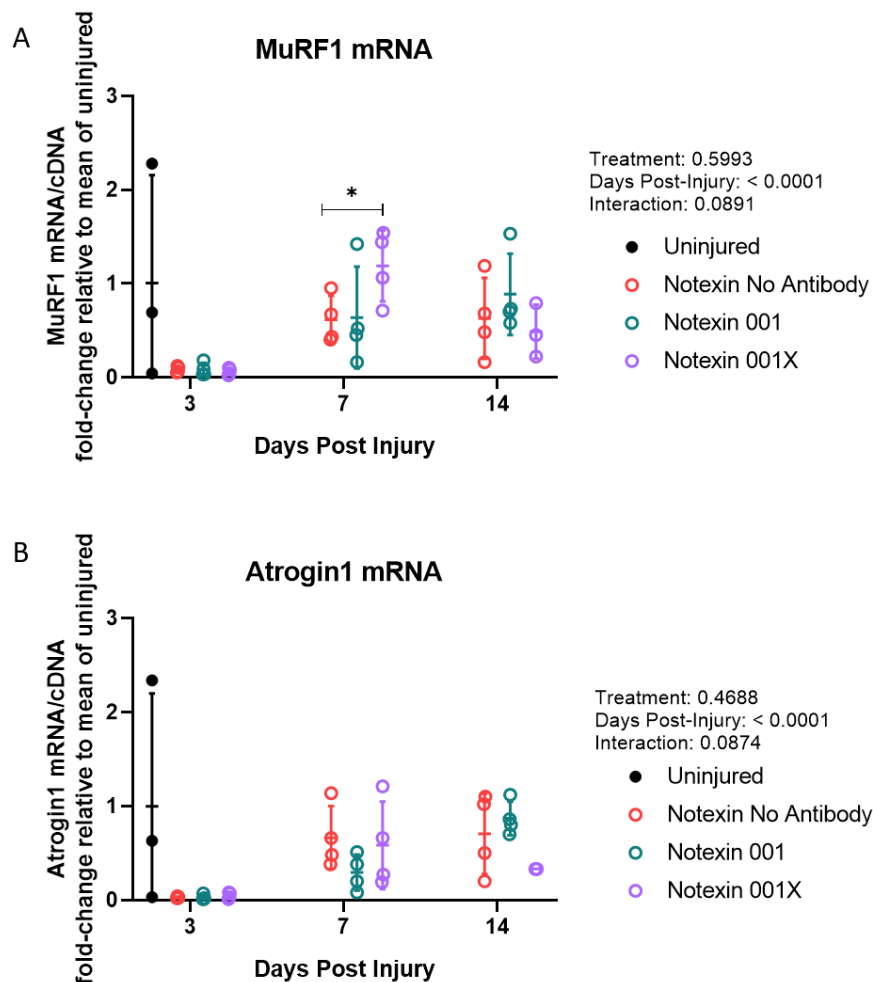


Figure 5.14: MuRF1 and atrogenin1 in notexin-injured tibialis anterior (TA) mouse muscle. MuRF1 (A) and atrogenin1 (B) transcripts were temporally regulated, with levels depleted at 3 days post-injury and returning throughout the time-course of the study (two-way ANOVA days post-injury effect, $p < 0.0001$). MuRF1 was upregulated in α -Fn14 001X-treated mice at 7 days post-injury relative to No Antibody time-matched controls (two-way ANOVA with Dunnett's multiple comparison, $p = 0.0381$). All transcripts were found to be within the range of uninjured controls. $n = 3-4$ animals per treatment, per time point and indicated by individual data points.

5.3.9.2. *Atrogenes in Ageing and Exercise*

MuRF1 and atrogen1 each showed considerable biological variability in young sedentary controls and were found to be downregulated in muscle from old mice (two-way ANOVA age effect, $p = 0.0010$ and 0.0011 respectively; Figure 5.15). MuRF1 was additionally found to be downregulated in muscle from LR trained mice (two-way ANOVA activity effect, $p = 0.0302$; Figure 5.15A).

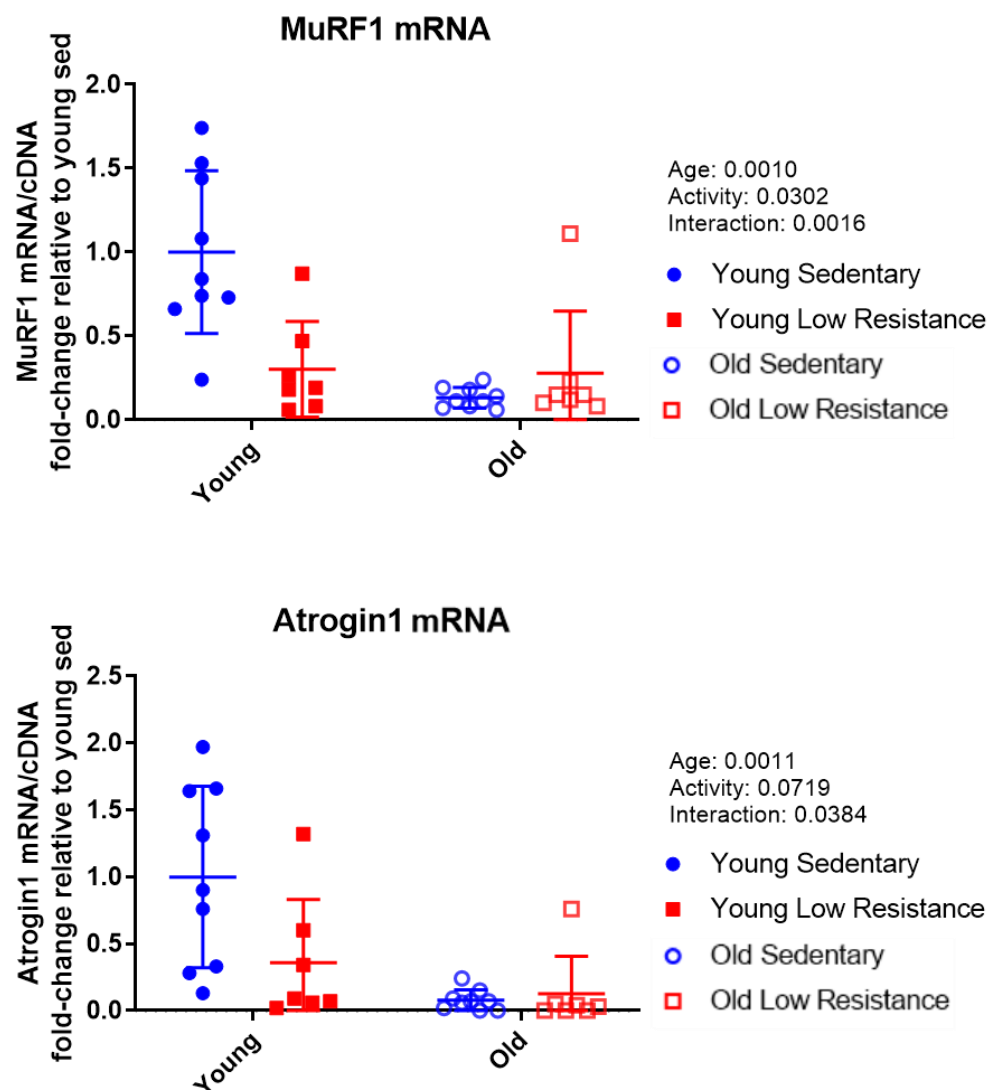


Figure 5.15: MuRF1 and atrogen1 in quadriceps (QUAD) muscle from old and low-resistance (LR) trained mice. MuRF1 (A) and atrogen1 (B) were found to be lower in muscle from old mice relative to young (two-way ANOVA age effect, $p = 0.0010$ and 0.0011 respectively). MuRF1 was also shown to be lower with low-resistance training (two-way ANOVA activity effect, $p = 0.0302$).

5.3.10. NFκB in Notexin Injury

An NFκB1 antibody capable of detecting p105 precursor and processed p50 subunits failed to detect validated bands in whole muscle homogenate. NFκB2 was assessed with an antibody capable of detecting p100 precursor subunit and the processed p52 subunit. Whilst both subunits could be detected in whole muscle, the presence of strongly reactive non-specific bands rendered detection of the fainter p100 subunit unreliable. For this reason, qualitative scoring was instead performed on the p52 subunit (see Section 5.2.3.1 and Table 5.1). Detection of p52 was primarily in notexin-injured TA and absent from saline-injected contralateral controls (Figure 5.16). p52 remained pathological across all time points with no apparent changes in p52 detection between treatment groups.

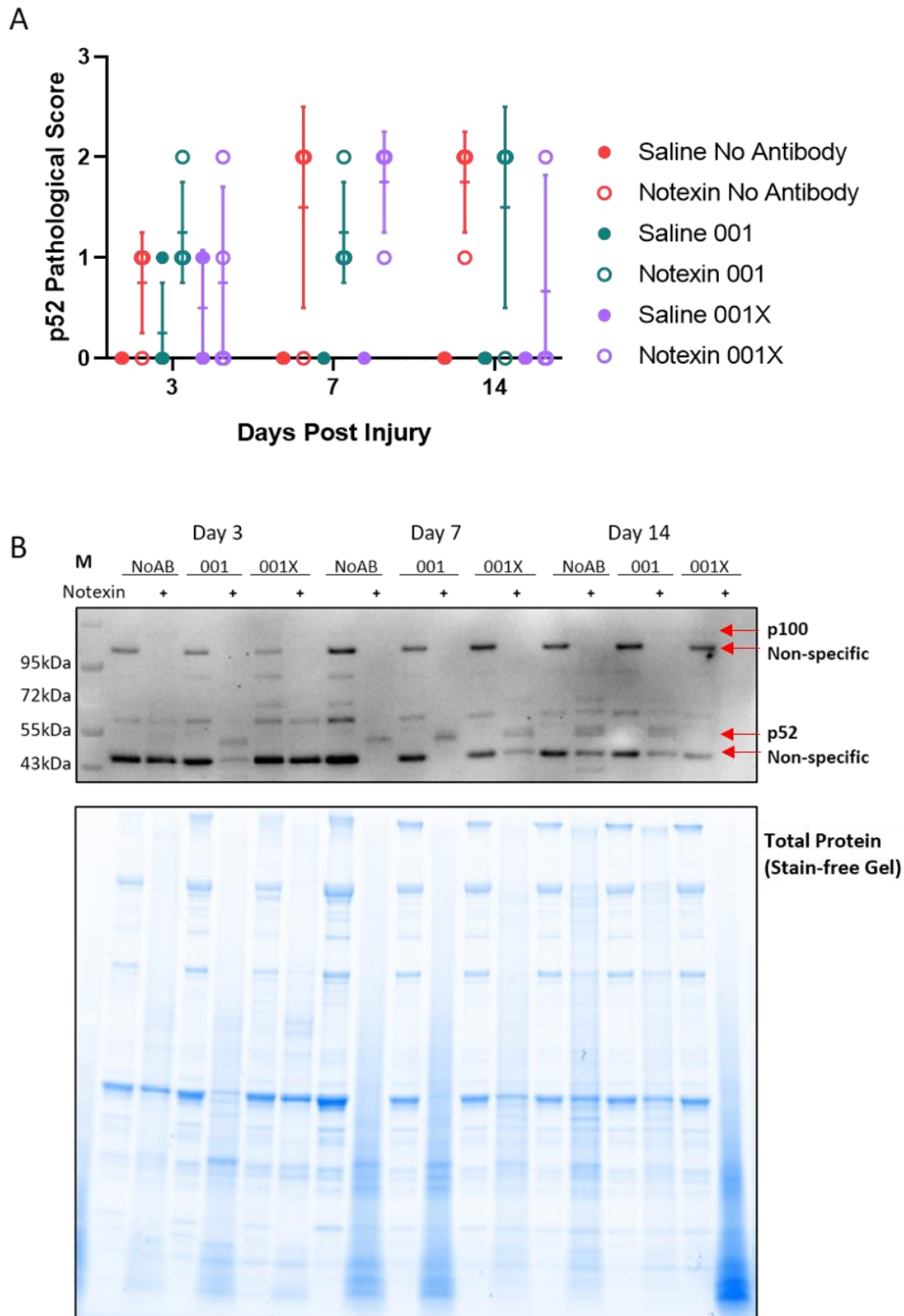


Figure 5.16: Processing of p100-p52 in notexin-injured mouse tibialis anterior (TA) skeletal muscle. (A) Pathological scoring of p100-p52 in notexin-injured mice treated with no antibody (NoAB), α -Fn14 001 (001), or α -Fn14 001X (001X) using pathological criteria outlined in Table 5.3. (B) Representative blot of p100-p52 western blot and stain-free image of total protein content. Multiple non-specific bands were detected in addition to the p100 band above the 95 kDa marker and a p52 band between the 43 and 55 kDa markers (Cell Signaling Technology 4882, expected molecular weight – 100 and 52 kDa). Specific and prominent non-specific bands are indicated by red arrows. $n = 3-4$ as indicated by individual data points.

5.4. Discussion

5.4.1. Notexin Injury Reproducibility is Unreliable

The advanced and prolonged tissue degradation observed in the current study when viewed in comparison with the published literature indicates a pressing issue in the reproducibility of notexin injuries. This possibility is discussed at length in Chapter 4 and is reiterated here to provide context for the limitations on performing quantitative protein analyses in the current study. Samples of notexin-injured *extensor digitorum longus* (EDL) mouse muscle provided by Associate Professor Brad Launikonis (University of Queensland; see Appendix IV) indicated no lasting biochemical changes at 21 days post-injury, and in combination with the protocols and time points described in the literature informed the selection of time points in the current study. It should be noted that the dose administered in the comparative samples described in Appendix IV was half the dose administered in the current study. Given the TA muscle is approximately 2-4 times larger than the EDL muscle it is unlikely that this larger muscle is unable to tolerate a higher dose and as such is not considered to be the sole cause of the observed discrepancy in injury. Further investigation of batch variability in notexin as well as adoption of best practice ARRIVE guidelines of animal model reporting in the literature is needed to resolve this issue (Kilkenny *et al.*, 2010).

5.4.2. Notexin Injury Induces Fn14 Expression

The current study indicates that a localised notexin injury can induce transcriptional and translational upregulation of Fn14. This is important to establish given the variability of muscle injury and regeneration models and provides a basis for targeting Fn14 in the pathogenesis of an acute notexin-injury (Hardy *et al.*, 2016). Quantification of protein level data for the current study was limited by the unexpected severity of total protein

degradation, as discussed above and in Chapter 4. A band believed to be Fn14 was clearly detected in notexin-injured samples with apparent temporal regulation, wherein Fn14 peaks at 7 days post-injury and returns towards baseline as regeneration progresses at day 14. mRNA measurements provide a more robust quantitative measure of Fn14 regulation in these samples. In this instance it appears that mRNA and protein do not correlate directly. This is not unusual given complexities in the transcription, translation, and turnover of these molecules (Maier *et al.*, 2009). Although a relationship between Fn14 mRNA and protein was not evident, the specific presence of Fn14 protein only in notexin-injured samples provides reasonable confidence that upregulation or stabilisation of Fn14 protein is occurring in addition to mRNA upregulation.

5.4.3. Fn14 mRNA is Downregulated in Aged Muscle

Fn14 mRNA was also detected in QUAD samples taken from young and old, sedentary or low-resistance trained mice, however no protein was detected in any group suggesting the proposed continual turnover of Fn14 protein by autophagy renders its abundance transient, or that it may be present in amounts below the detection limit in these contexts. In contrast to prior studies, we showed lower Fn14 mRNA levels in old (24-month old) mice relative to young (3-month old) controls. Tajrishi *et al.* (2014a) reported higher Fn14 mRNA from TA muscle of 18-month old mice relative to 3-month old controls when transcripts were normalised to glyceraldehyde-3-phosphate dehydrogenase (GAPDH). While we cannot rule out a difference between 18- and 24-month old mice, which may explain the discrepancy between studies, it is important to note that normalisation of target mRNA to GAPDH – a commonly used housekeeping control for both protein and mRNA analyses – may be a flawed methodology, particularly in aged populations. Wyckelsma *et al.* (2016) highlight the age and fibre-type specific differences in GAPDH protein content from human muscle samples. Whole

muscle homogenates from healthy adults aged 69.4 ± 3.5 years contained 30% less GAPDH than younger counterparts (aged 25.5 ± 2.8 years) when normalised to total protein content (Wyckelsma *et al.*, 2016). When examined as single fibres, type II (fast-twitch) fibres from both young and old participants expressed more GAPDH than type I muscle fibre types (slow-twitch; Wyckelsma *et al.*, 2016). This is particularly relevant when comparing results from muscles with different fibre-type proportions. The authors concluded that normalisation to GAPDH may artificially skew findings and total protein or cDNA content should instead be measured wherever possible.

Ribeiro *et al.* (2017) also reported higher Fn14 mRNA in *soleus* muscle from 20-month old relative to 3-month old control rats. These data were also normalised to GAPDH mRNA abundance and should be interpreted with caution. The higher Fn14 mRNA in old rat *soleus* – a primarily type I muscle – reported by Ribeiro *et al.* (2017) may in fact reflect an age-associated loss of type II fibres – which are known to be more susceptible to atrophy (Lexell, 1995) – and therefore reduced GAPDH (Wyckelsma *et al.*, 2016) artificially elevating normalised Fn14 mRNA levels.

In addition to normalisation issues, fibre-type specificity of Fn14 mRNA itself should also be noted when considering discrepancies between studies. Murach *et al.* (2014) describe the distribution and inducibility of Fn14 mRNA in *gastrocnemius* muscle from young cross-country runners following a tapered running regime and showed that type II fibres had the highest degree of inducibility. Trappe *et al.* (2015) report the same high-level inducibility of Fn14 mRNA in type II fibres from an elite sprint runner and concluded that Fn14 played an important role in muscle growth and remodelling. The specificity of Fn14 upregulation in type II fibres indicates that effects of Fn14 modulation are likely to be more physiologically relevant

in predominantly type II or mixed fibre muscles. The proposed role of Fn14 as a positive regulator muscle growth is consistent with the findings presented here, wherein old mice with reduced mass and hypertrophic potential (Soffe *et al.*, 2016), showed lower Fn14 mRNA expression.

5.4.4. Notexin-Induced Fn14 Upregulation is Prolonged and Amplified by α -Fn14

Treatment

Fn14 mRNA was found to be significantly higher in α -Fn14 001X-treated mice at 14 days post-injury relative to NoAB time-matched controls. Although no statistical analyses could be performed on Fn14 protein levels, there was persistent Fn14 protein detected in α -Fn14 001X at 14 days post-injury, whilst NoAB showed no detectable protein at this time point. Together these findings suggest that stimulation of the Fn14 receptor, which is transiently upregulated in all notexin-injured muscle, results in a positive feedback loop of ongoing transcriptional and translational expression of Fn14.

Persistent Fn14 mRNA and protein may be explained by two-fold mechanisms. Protein turnover rates for Fn14 in HeLa cells have been described by Gurunathan *et al.* (2014) and by mechanistic computational modelling in Khetan and Barua (2019). Gurunathan *et al.* (2014) describe the half-life of unliganded Fn14 protein in HeLa cells to be 74 minutes, relatively short compared to the average protein half-life of 20 hours in that model. This turnover rate was accelerated by the addition of TWEAK, as the TWEAK-Fn14 complex is internalised and degraded (Gurunathan *et al.*, 2014). This may explain the lack of Fn14 protein detectable in saline-treated TA muscle as well as QUAD samples from young and old, sedentary or low-resistance trained mice, as the constitutive downregulation of both liganded and unliganded Fn14 maintains baseline levels below detection threshold. It is feasible that the inhibition of

TWEAK-Fn14 binding by α -Fn14 001X (as described in Chapter 3) and crosslinking of receptors may help stabilise the Fn14 present on the cell membrane, allowing it to accumulate to a detectable level. In Khetan and Barua (2019) with computational modelling of TWEAK-Fn14 signalling, they report that both TWEAK-dependent and TWEAK-independent cross-linking of the Fn14 receptor are able to generate a positive feedback loop to perpetuate Fn14 receptor expression, and by extension, activation. Both mRNA and protein level data in the current study support the notion that α -Fn14 001X can crosslink Fn14 and stimulate a positive feedback loop of Fn14 upregulation. This has implications not only for development of potential therapeutic interventions but also provides support for the notion of positive feedback regulation and how this may contribute to the signalling events associated with TWEAK-dependent or TWEAK-independent Fn14 stimulation in a range of disease settings.

5.4.5. MyoD is Transcriptionally Upregulated by α -Fn14 Treatment

The myogenic outcomes of the proposed Fn14 positive feedback loop described above unfortunately could not be directly ascertained from the current study. The severity of the injury model rendered the later time points of this study earlier in the regenerative process than desired, meaning no groups exhibited full recovery. In the absence of histological evidence of altered recovery, examination of myogenic regulatory factors served as a proxy of myogenesis given the known temporal regulation of specific myogenic regulatory factors throughout myogenesis (Chapter 1, Figure 1.1; Zammit, 2017). Higher mRNA levels of myogenin and Myf5 in α -Fn14 001X-treated mice relative to time-matched NoAB controls at 7 days post-injury suggest an enhancement of muscle differentiation. More strikingly, MyoD was higher in both α -Fn14 001X, and to a lesser extent α -Fn14 001, relative to time-matched NoAB at 14 days post-injury. It is possible that the α -Fn14 001 antibody is able to partially

form multimeric antibodies *in vivo* and exert similar agonistic effects as α -Fn14 001X (refer to Chapter 3 for further details).

MyoD plays a broad role in gene expression both during development and in maturity (Bergstrom *et al.*, 2002), though it is frequently cited as the master regulator of myogenesis (Wardle, 2019) and has been shown to be indispensable in the shift from proliferation to differentiation in mouse satellite cells (Yablonka-Reuveni *et al.*, 1999). Further, overexpression of MyoD in cultured mesoangioblasts taken from human donors with inclusion body myositis – an ageing-associated muscle wasting disorder characterised by impaired differentiation – was able to restore myogenic differentiation (Morosetti *et al.*, 2006). Here, changes in MyoD mRNA were shown to be tightly correlated with changes in Fn14 mRNA following notexin-injury. Interestingly, no correlations were observed between Fn14 mRNA transcripts and MyoD mRNA in QUAD muscle taken from young and old, sedentary or low-resistance trained mice. This may be due to the lack of detectable Fn14 protein in these samples. It should also be noted that muscle fibre type differences may contribute given the different muscles utilised in each study, although given that Fn14 was not detectable in any samples, this would not be influenced by any potential fibre type shift.

The possibility of TWEAK-independent Fn14 as a positive regulator of myogenesis is not a novel hypothesis. In addition to the cell and mouse models discussed in the introduction, high levels of Fn14 mRNA have been correlated with retention of muscle mass in healthy young men subjected to 21 days of high-altitude and energy-deficient conditions (Pasiakos *et al.*, 2018). The underlying mechanism of how Fn14 may be protective in these circumstances is not elucidated, however taken in conjunction with the prior and current evidence, it is likely

that TWEAK-independent Fn14 is an important regulator of MyoD expression in muscle from challenged mice or humans.

We propose a model wherein Fn14 is transiently upregulated by an acute muscle insult, in this instance notexin-injury. TWEAK-independent stimulation of Fn14, either by an agonistic α -Fn14 antibody such as 001X or high receptor density, then initiates a positive feedback loop of Fn14 itself and downstream MyoD. A schematic of this feedback loop is seen in Figure 5.17.

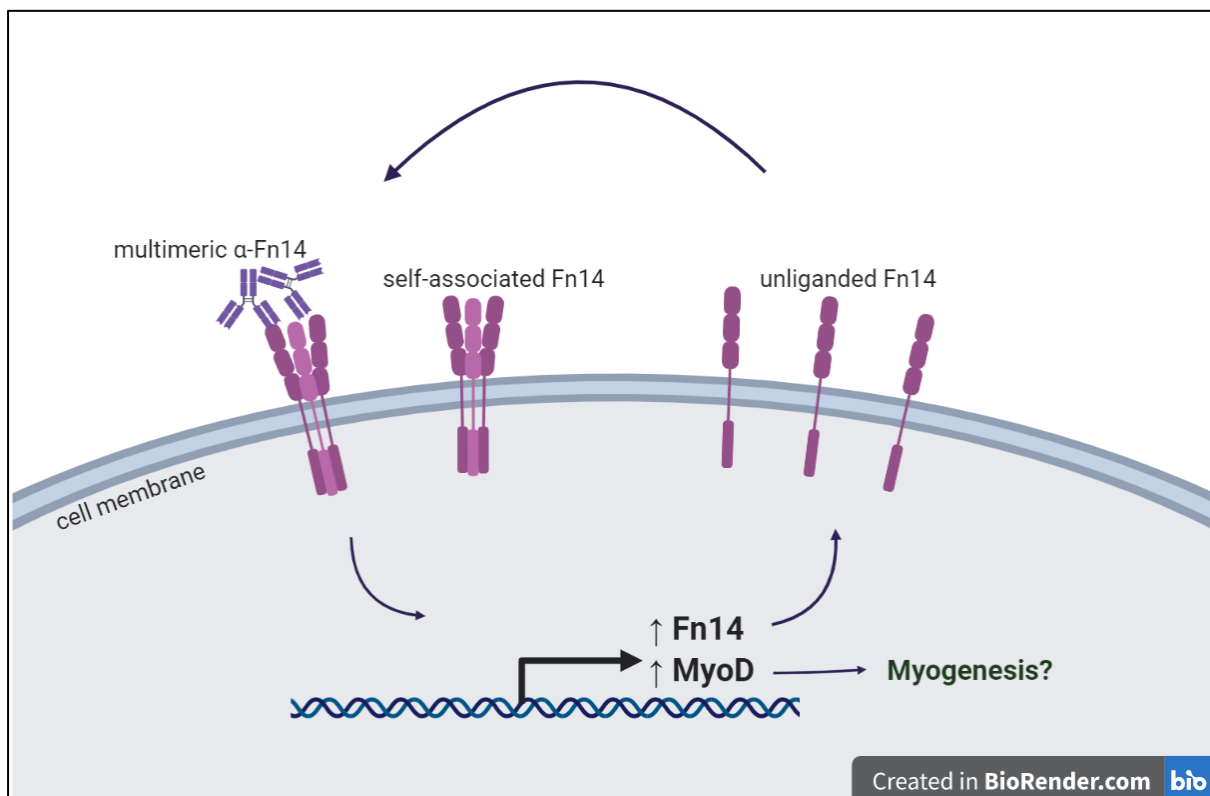


Figure 5.17: Proposed positive feedback loop of Fn14 and MyoD. Acute injury results in endogenous upregulation of the Fn14 receptor, which can exist as monomeric unliganded Fn14, or under high density conditions, may cluster to initiate self-associated signalling. α -Fn14 001 and α -Fn14 001X are able to bind multiple Fn14 receptors, indicated as multimeric α -Fn14 bound to Fn14, leading to a downstream upregulation of both Fn14 itself at the mRNA and protein level, and MyoD at the mRNA levels. Self-associated Fn14 may also signal via this TWEAK-independent pathway. This perpetuates a positive-feedback loop which may in turn drive further self-association and TWEAK-independent signalling as well as a myogenic response driven by MyoD.

It is important to note that TWEAK-dependent stimulation of Fn14 has, conversely, been associated with a blockade of myogenic differentiation via the degradation of MyoD protein

in C2C12 cells (Dogra *et al.*, 2006). It is possible that when this has been described in previous studies, the effects were due to the supraphysiological doses of TWEAK that were administered, being 500 ng/ml, three orders of magnitude higher than reported serum levels that range 250 – 800 pg/ml, and so that work may not be presenting a physiologically relevant phenomenon (Blanco-Colio *et al.*, 2007; Kralisch *et al.*, 2008; Maymó-Masip *et al.*, 2013). Whilst the degradation of MyoD and downstream myogenic differentiation under those circumstances should be interpreted with caution, it is possible that TWEAK-dependent degradation of MyoD serves as a protective mechanism to preserve a pool of quiescent satellite cells, as is the case with calpain-3 mediated degradation of MyoD (Stuelsatz *et al.*, 2010). It should also be noted that calpain-3 shows prolonged autolytic activation in α -Fn14 001X-treated samples (discussed further in Section 5.4.7) and the possibility of calpain-3 mediated degradation of MyoD protein cannot be ruled out. Instances where TWEAK is overexpressed, either experimentally or in settings of chronic inflammation, may skew this potentially protective mechanism towards a pathological inhibition of myogenic progression.

An unfortunate limitation of the current study was the inability to validate an α -MyoD antibody for use in whole muscle homogenate. This prevented examination of MyoD protein stability following α -Fn14 001 or α -Fn14 001X treatment and is a valid question for future research. Should the MyoD mRNA upregulation result in increased MyoD protein expression, agonistic α -Fn14 antibodies may present a useful therapeutic for diseases such as inclusion body myositis, where TWEAK and Fn14 are both upregulated but MyoD is deficient (Morosetti *et al.*, 2012).

5.4.6. Soluble TWEAK is Expressed in Regenerating Tissue

Both mTWEAK, and its furin-cleaved form, sTWEAK (Brown *et al.*, 2010), were detected in notexin-injured samples. Differential effects of sTWEAK and mTWEAK have been described, with both forms able to activate the non-canonical NF κ B pathway but only mTWEAK or an experimentally oligomerised version of sTWEAK shown to strongly activate the canonical NF κ B pathway in HT29 (human adenocarcinoma), HT1080 (human fibrosarcoma), and HeLa-TNFR2 cells (Roos *et al.*, 2010). sTWEAK was detected primarily in notexin-injured samples with only low amounts detected in contralateral saline-injected control muscles. Enwere *et al.* (2012) have postulated that the effects of low levels (10 ng/ml) of sTWEAK on C2C12 myoblasts preferentially activate the non-canonical NF κ B pathway with the outcome of enhanced myoblast fusion. When taken in conjunction with the observation that Fn14-inhibition via RNA interference impairs C2C12 myotube formation (Dogra *et al.*, 2007b), it seems probable that sTWEAK activation of Fn14 is involved in the development of newly formed myotubes. Given the presence of sTWEAK in acutely injured samples and not in the mature and uninjured samples utilised in the ageing and low-resistance training study, it appears that this developmental program is recapitulated in regenerating muscle following acute notexin-injury. Furin, the protease which cleaves mTWEAK to generate sTWEAK, has also been shown to be involved in pathological vascular remodelling in cardiac atherosclerosis in mice (Yakala *et al.*, 2019) lending further support to the role of sTWEAK in tissue remodelling.

QUAD samples taken from young and old, sedentary or low-resistance trained mice, which are not acutely injured, had detectable mTWEAK but not sTWEAK. mTWEAK levels in these samples were stable with no effects of ageing or low-resistance exercise training,

leading us to believe skeletal muscle TWEAK levels are not directly involved in age-associated loss of muscle mass or low-resistance training induced muscle adaptations.

High levels of circulating sTWEAK have previously been reported in samples from humans with sarcopenia, which were reduced following lifestyle intervention of whey protein supplementation and high-resistance training (Li *et al.*, 2019). The authors postulated that in this model, sTWEAK was exerting a pro-inflammatory effect. There was no report of the abundance of muscle TWEAK in that study. The old mice utilised in the current study showed reduced muscle mass suggesting the animals were sarcopenic, and whilst not measured in these mice, it is possible that circulating sTWEAK was also higher than in young mice. Regardless, the mice did not show an upregulation of intramuscular sTWEAK suggesting that if circulating sTWEAK is elevated it may not infiltrate muscle. Examination of serum and muscle from sarcopenic and non-sarcopenic individuals may further elucidate this.

5.4.7. Structural Protein Recovery is Delayed by α -Fn14 Antibody Treatment

Whilst examination of H+E stains of notexin-injured samples showed no clear differences between the degeneration or regeneration of muscle across treatment groups, there is an apparent alteration in the temporal dynamics of key muscle-specific structural proteins – namely actin, myosin, and desmin – with delayed recovery of these proteins in α -Fn14 001X-treated mice at 14 days post-injury. These results are of course qualitative and should be interpreted with caution, particularly given the small sample size of the treatment groups, however it may be indicative of a prolonged remodelling response in α -Fn14 001X-treated mice. This is supported by the prolonged autolysis (activation) of calpain-3 in these mice. Calpain-3 is a cysteine protease which has been implicated in sarcomere remodelling via activation of the ubiquitin proteasome (Kramerova *et al.*, 2005). Mutation of the calpain-3

gene, CAPN3, is a hallmark of Limb Girdle Muscular Dystrophy type 2A (LGMD2A), with individuals lacking functional calpain-3 showing the most severe phenotype with aberrant sarcomere regeneration (Hauerslev *et al.*, 2012). As with assessment of myogenic regulatory factors, due to the severity of the injury model, it is difficult to ascertain whether the net outcome in this instance is an enhancement of skeletal muscle regeneration. Investigation of the α -Fn14 001 and α -Fn14 001X antibody in a less aggressive model over a longer time course is needed to determine myogenic outcomes, however the results presented here suggest modification of the remodelling response by Fn14 targeting and it was determined that repeating the current study with additional mice was not required for this conclusion.

5.4.8. PGC-1 α mRNA Was Not Altered by α -Fn14 Antibody Treatment

Given the reported involvement of PGC-1 α as a downstream target of both TWEAK-dependent and TWEAK-independent Fn14 signalling, transcript levels were assessed to determine potential effects of α -Fn14 001 or α -Fn14 001X on mitochondrial biogenesis in regenerating tissue. Baseline levels of PGC-1 α mRNA were shown to vary considerably in uninjured TA controls, possibly reflective of the likely higher dependence of this muscle on glycolytic metabolism given it is predominantly comprised of Type II glycolytic muscle fibres. Although notexin-injury initially depleted PGC-1 α transcript levels, they recovered to baseline by 7 days post-injury with all levels remaining within the range of uninjured controls and no differences detected between treatment groups. Measuring PGC-1 α protein is complicated by the lack of validated antibodies able to measure endogenous PGC-1 α in muscle and the transient nature of mRNA transcripts means a single point-in-time may miss a biologically relevant change. Assessment of fibre-type in these mice may provide greater insight into the mitochondrial biogenesis, however prolonged degradation of myosin, discussed above, renders this unviable in the current study. From the current evidence it appears that neither

α -Fn14 001 nor α -Fn14 001X treatment affected mitochondrial biogenesis via PGC-1 α modulation in an acute injury setting.

5.4.9. Inflammation is Prolonged by α -Fn14 Antibody Treatment

Markers of inflammatory cells, specifically macrophages and B-cells, were investigated due to the known secretion of TWEAK from macrophages (Nakayama *et al.*, 2000) and the detection of suspected endogenous IgG bands when using α -mouse secondary antibody in western blotting. Macrophage marker, CD68, was measured in a limited qualitative capacity and did not show marked changes in response to α -Fn14 antibody treatment, which is consistent with the lack of altered TWEAK profiles in these samples. The presence of endogenous IgG was, however, found to be persistent in α -Fn14 001 and α -Fn14 001X-treated notexin-injured TA at 14 days post-injury, suggesting a prolonged infiltration of B-cells. This effect has previously been demonstrated as a result of TWEAK-dependent Fn14 activity. TWEAK administration (0.1 ng/ml) was shown to upregulate B-cell maturation and IgG secretion in cultured B-cells derived from mouse spleen, whilst Fn14 inhibition with an Fn14-Fc construct attenuated maturation and secretion in a mouse model of the autoimmune disease, systemic lupus erythematosus (Min *et al.*, 2016). Autosomal dominant mutations of TWEAK have also been linked to antibody-deficiency (Wang *et al.*, 2013). Interestingly, B-cells themselves express high levels of Fn14 (Min *et al.*, 2016) which may contribute to the positive-feedback loop detected in the current study. Given the activity of α -Fn14 001X is independent of TWEAK (Chapter 3), with α -Fn14 001 appearing to function similarly *in vivo*, the current study suggests that Fn14 may also modulate B-cell development and IgG secretion independent of TWEAK stimulation.

5.4.10. Atrogenes Are Not Altered by α -Fn14 Antibody Treatment

Atrogenes, MuRF1 and atrogen1 were not found to be modified by either α -Fn14 treatment in notexin-injured TA muscle. Whilst a temporal regulation of these transcripts was observed, all transcripts were within the range of uninjured controls. Further, even though the range of biological variability in these controls was large, it was within the variability observed in the QUAD samples from young sedentary mice investigated, indicating that these atrogenes are variably expressed at rest.

Modulation of atrogenes, particularly MuRF1, have largely been associated with TWEAK-dependent Fn14 signalling (Mittal *et al.*, 2010b) and are not always recapitulated in TWEAK-independent Fn14 models (Tajrishi *et al.*, 2014a). The lack of atrogene involvement in the current study suggests that the effects of both α -Fn14 001 and α -Fn14 001X are distinct from those of TWEAK and adds to the evidence presented in Chapter 3.

Both atrogen1 and MuRF1 were found to be downregulated in QUAD muscle from old relative to young control mice. This finding was counterintuitive given the role of these transcription factors in age-associated muscle loss, however a review by Gumucio and Mendias (2013) highlights inconsistencies in the literature in regards to MuRF1 and atrogen1 levels in muscle from old rodents, with some studies reporting increases whilst others report no change or decreases. MuRF1 mRNA was additionally found to be downregulated in response to low-resistance training in the current study. Again, the effects of resistance training on MuRF1 and atrogen1 gene expression are widely varied in the literature (Gumucio & Mendias, 2013). The modulation of atrogene gene expressions seen only in old and chronically trained mice and not in the acutely notexin-injured mice, suggests these genes are

responsive on a longer timescale and may not play a substantial role in tissue remodelling following acute muscle injury.

5.4.11. Signalling Pathways

Of the proposed signalling pathways of TWEAK-Fn14 activation – canonical and non-canonical NFκB, PI3K/Akt, and the JNK, p38, and ERK1/2 arms of MAPK – we were unable to validate antibodies in these samples, largely due to the profound degradation of total protein in muscle homogenates (results shown only for NFκB2, the non-canonical arm). Investigation of downstream signalling pathways of Fn14 activation in a whole muscle setting was severely limited by both the degradation of total protein and the availability of validated antibodies for use in whole muscle western blots. We have taken a conservative approach in the interpretation of signalling pathways from these antibodies in whole muscle; whilst further detail of the activation profiles of varied Fn14 stimulation is discussed in Chapter 3, it should be noted that those results taken from a C2C12 model may not be relevant to the *in vivo* activity. Further investigation in a less traumatic *in vivo* model are warranted to delineate the involvement of each pathway in the modulation of both MyoD and Fn14 itself, however given the present limitations, it is neither feasible nor meaningful to further pursue investigation of signalling pathways in the current study.

5.5. Conclusions

Whilst the current study was limited by the unexpected severity of the injury phenotype and the validation of several antibodies in whole muscle homogenates, we were able to demonstrate that notexin-injury is capable of inducing Fn14 upregulation at the mRNA and protein level. This upregulation appears to be stabilised and further upregulated in a positive-feedback loop (Figure 5.17) by the use of α-Fn14 001 and α-Fn14 001X and may recapitulate

physiological TWEAK-independent Fn14 signalling (Khetan & Barua, 2019). Whilst the injury severity prevented full regeneration of the tissue in the timeframe of the current study, MyoD mRNA was shown to be significantly upregulated and positively correlated with Fn14 mRNA expression in antibody-treated mice. Whilst these results need further validation in a milder injury model, they support the notion of Fn14 driving myogenic progression in regenerating muscle. The current study does indicate a potentially delayed recovery timeline in the α -Fn14 001 and α -Fn14 001X-treated mice, possibly representing a prolonging of the early myogenic cycle. Whilst there does appear to be a myogenic component of TWEAK-independent Fn14 stimulation, the timing and dose of therapeutic interventions will need refinement. Investigation of muscle from old and chronically exercised mice showed a reduction of Fn14 mRNA in muscle from old mice that was not reversed by chronic low-resistance training. Given the failure of this exercise regime to reverse age-associated loss of muscle mass, the reduced Fn14 is consistent with reduced myogenic potential. No modulation of either PGC-1 α or atrogenes (atrogen1 and MuRF1) mRNA was detected in response to these interventions, further indicating a distinct signalling pathway to TWEAK-dependent Fn14 activity.

To the best of our knowledge, these Fn14 antibodies represent the first instance of an Fn14 targeting molecule which opposes the actions of TWEAK whilst retaining agonistic activity against Fn14. Although previous research has demonstrated the inhibition of these apparent Fn14-associated pro-myogenic pathways (Girgenrath *et al.*, 2006; Dogra *et al.*, 2007b), this is a novel approach to stimulate Fn14 and potentially drive myogenic progression.

References

- Bergstrom DA, Penn BH, Strand A, Perry RL, Rudnicki MA & Tapscott SJ. (2002). Promoter-specific regulation of MyoD binding and signal transduction cooperate to pattern gene expression. *Mol Cell* **9**, 587-600.
- Blanco-Colio LM, Martin-Ventura JL, Munoz-Garcia B, Orbe J, Paramo JA, Michel JB, Ortiz A, Meilhac O & Egidio J. (2007). Identification of soluble tumor necrosis factor-like weak inducer of apoptosis (sTWEAK) as a possible biomarker of subclinical atherosclerosis. *Arterioscler Thromb Vasc Biol* **27**, 916-922.
- Brown SA, Cheng E, Williams MS & Winkles JA. (2013). TWEAK-independent Fn14 self-association and NF-kappaB activation is mediated by the C-terminal region of the Fn14 cytoplasmic domain. *PLoS One* **8**, e65248.
- Brown SAN, Ghosh A & Winkles JA. (2010). Full-length, Membrane-anchored TWEAK Can Function as a Juxtacrine Signaling Molecule and Activate the NF- κ B Pathway. *J Biol Chem* **285**, 17432-17441.
- Ciciliot S, Rossi AC, Dyar KA, Blaauw B & Schiaffino S. (2013). Muscle type and fiber type specificity in muscle wasting. *Int J Biochem Cell Biol* **45**, 2191-2199.
- Dogra C, Changotra H, Mohan S & Kumar A. (2006). Tumor necrosis factor-like weak inducer of apoptosis inhibits skeletal myogenesis through sustained activation of nuclear factor-kappaB and degradation of MyoD protein. *J Biol Chem* **281**, 10327-10336.
- Dogra C, Changotra H, Wedhas N, Qin X, Wergedal JE & Kumar A. (2007a). TNF-related weak inducer of apoptosis (TWEAK) is a potent skeletal muscle-wasting cytokine. *FASEB J* **21**, 1857-1869.
- Dogra C, Hall SL, Wedhas N, Linkhart TA & Kumar A. (2007b). Fibroblast growth factor inducible 14 (Fn14) is required for the expression of myogenic regulatory factors and differentiation of myoblasts into myotubes. Evidence for TWEAK-independent functions of Fn14 during myogenesis. *J Biol Chem* **282**, 15000-15010.
- Enwere EK, Holbrook J, Lejmi-Mrad R, Vineham J, Timusk K, Sivaraj B, Isaac M, Uehling D, Al-awar R, LaCasse E & Korneluk RG. (2012). TWEAK and cIAP1 regulate myoblast fusion through the noncanonical NF-kappaB signaling pathway. *Sci Signal* **5**, ra75.
- Girgenrath M, Weng S, Kostek CA, Browning B, Wang M, Brown SAN, Winkles JA, Michaelson JS, Allaire N, Schneider P, Scott ML, Hsu YM, Yagita H, Flavell RA, Miller JB, Burkly LC & Zheng TS. (2006). TWEAK, via its receptor Fn14, is a novel regulator of mesenchymal progenitor cells and skeletal muscle regeneration. *EMBO Journal* **25**, 5826-5839.
- Gumucio JP & Mendias CL. (2013). Atrogin-1, MuRF-1, and sarcopenia. *Endocrine* **43**, 12-21.

- Gurunathan S, Winkles JA, Ghosh S & Hayden MS. (2014). Regulation of fibroblast growth factor-inducible 14 (Fn14) expression levels via ligand-independent lysosomal degradation. *J Biol Chem* **289**, 12976-12988.
- Hardy D, Besnard A, Latil M, Jouvion G, Briand D, Thepenier C, Pascal Q, Guguin A, Gayraud-Morel B, Cavaillon JM, Tajbakhsh S, Rocheteau P & Chretien F. (2016). Comparative Study of Injury Models for Studying Muscle Regeneration in Mice. *PLoS One* **11**, e0147198.
- Hauerslev S, Sveen M-L, Duno M, Angelini C, Vissing J & Krag TO. (2012). Calpain 3 is important for muscle regeneration: Evidence from patients with limb girdle muscular dystrophies. *BMC Musculoskelet Disord* **13**, 43.
- Hindi SM, Mishra V, Bhatnagar S, Tajrishi MM, Ogura Y, Yan Z, Burkly LC, Zheng TS & Kumar A. (2014). Regulatory circuitry of TWEAK-Fn14 system and PGC-1alpha in skeletal muscle atrophy program. *FASEB J* **28**, 1398-1411.
- Johnston AJ, Murphy KT, Jenkinson L, Laine D, Emrich K, Faou P, Weston R, Jayatilleke KM, Schloegel J, Talbo G, Casey JL, Levina V, Wong WW, Dillon H, Sahay T, Hoogenraad J, Anderton H, Hall C, Schneider P, Tanzer M, Foley M, Scott AM, Gregorevic P, Liu SY, Burkly LC, Lynch GS, Silke J & Hoogenraad NJ. (2015). Targeting of Fn14 Prevents Cancer-Induced Cachexia and Prolongs Survival. *Cell* **162**, 1365-1378.
- Khetan J & Barua D. (2019). Analysis of Fn14-NF-kappaB Signaling Response Dynamics Using a Mechanistic Model. *J Theor Biol* 10.1016/j.jtbi.2019.07.016.
- Kilkenny C, Browne WJ, Cuthill IC, Emerson M & Altman DG. (2010). Improving Bioscience Research Reporting: The ARRIVE Guidelines for Reporting Animal Research. *PLOS Biology* **8**, e1000412.
- Kralisch S, Ziegelmeier M, Bachmann A, Seeger J, Lossner U, Bluher M, Stumvoll M & Fasshauer M. (2008). Serum levels of the atherosclerosis biomarker sTWEAK are decreased in type 2 diabetes and end-stage renal disease. *Atherosclerosis* **199**, 440-444.
- Kramerova I, Kudryashova E, Venkatraman G & Spencer MJ. (2005). Calpain 3 participates in sarcomere remodeling by acting upstream of the ubiquitin-proteasome pathway. *Hum Mol Genet* **14**, 2125-2134.
- Lexell J. (1995). Human aging, muscle mass, and fiber type composition. *J Gerontol A Biol Sci Med Sci* **50 Spec No**, 11-16.
- Li C-w, Yu K, Shyh-Chang N, Li G-x, Jiang L-j, Yu S-l, Xu L-y, Liu R-j, Guo Z-j, Xie H-y, Li R-r, Ying J, Li K & Li D-j. (2019). Circulating factors associated with sarcopenia during ageing and after intensive lifestyle intervention. *J Cachexia Sarcopenia Muscle* **10**, 586-600.

- Lin J, Wu H, Tarr PT, Zhang CY, Wu Z, Boss O, Michael LF, Puigserver P, Isotani E, Olson EN, Lowell BB, Bassel-Duby R & Spiegelman BM. (2002). Transcriptional co-activator PGC-1 alpha drives the formation of slow-twitch muscle fibres. *Nature* **418**, 797-801.
- Maier T, Guell M & Serrano L. (2009). Correlation of mRNA and protein in complex biological samples. *FEBS Lett* **583**, 3966-3973.
- Maymó-Masip E, Vendrell J, Garrifo-Sanchez L, Fernández-Veledo S, Chacón MR, Vázquez-Carballo A, Garcia España A, Tinahones FJ, García-Fuentes E & Rodríguez MdM. (2013). The Rise of Soluble TWEAK Levels in Severely Obese Subjects After Bariatric Surgery May Affect Adipocyte-Cytokine Production Induced by TNF α . *J Clin Endocrinol Metab* **98**, E1323-E1333.
- Min HK, Kim SM, Park JS, Byun JK, Lee J, Kwok SK, Park YW, Cho ML & Park SH. (2016). Fn14-Fc suppresses germinal center formation and pathogenic B cells in a lupus mouse model via inhibition of the TWEAK/Fn14 Pathway. *J Transl Med* **14**, 98.
- Mittal A, Bhatnagar S, Kumar A, Lach-Trifilieff E, Wauters S, Li H, Makonchuk DY, Glass DJ & Kumar A. (2010a). The TWEAK-Fn14 system is a critical regulator of denervation-induced skeletal muscle atrophy in mice. *J Cell Biol* **188**, 833-849.
- Mittal A, Bhatnagar S, Kumar A, Paul PK, Kuang S & Kumar A. (2010b). Genetic Ablation of TWEAK Augments Regeneration and Post-Injury Growth of Skeletal Muscle in Mice. *Am J Pathol* **177**, 1732-1742.
- Morosetti R, Gliubizzi C, Sancricca C, Broccolini A, Gidaro T, Lucchini M & Mirabella M. (2012). TWEAK in inclusion-body myositis muscle: possible pathogenic role of a cytokine inhibiting myogenesis. *Am J Pathol* **180**, 1603-1613.
- Morosetti R, Mirabella M, Gliubizzi C, Broccolini A, De Angelis L, Tagliafico E, Sampaolesi M, Gidaro T, Papacci M, Roncaglia E, Rutella S, Ferrari S, Tonali PA, Ricci E & Cossu G. (2006). MyoD expression restores defective myogenic differentiation of human mesoangioblasts from inclusion-body myositis muscle. *Proc Natl Acad Sci U S A* **103**, 16995-17000.
- Murach K, Raue U, Wilkerson B, Minchev K, Jemiolo B, Bagley J, Luden N & Trappe S. (2014). Single Muscle Fiber Gene Expression with Run Taper. *PLoS One* **9**, e108547.
- Nakayama M, Kayagaki N, Yamaguchi N, Okumura K & Yagita H. (2000). Involvement of Tweak in Interferon γ -Stimulated Monocyte Cytotoxicity. *J Exp Med* **192**, 1373-1380.
- Pascoe AL, Johnston AJ & Murphy RM. (2020). Controversies in TWEAK-Fn14 signaling in skeletal muscle atrophy and regeneration. *Cell Mol Life Sci* 10.1007/s00018-020-03495-x.
- Pasiakos SM, Berryman CE, Carbone JW, Murphy NE, Carrigan CT, Bamman MM, Ferrando AA, Young AJ & Margolis LM. (2018). Muscle Fn14 gene expression is associated with fat-free mass retention during energy deficit at high altitude. *Physiol Rep* **6**, e13801.

- Ribeiro MBT, Guzzoni V, Hord JM, Lopes GN, Marqueti RC, de Andrade RV, Selistre-de-Araujo HS & Durigan JLQ. (2017). Resistance training regulates gene expression of molecules associated with intramyocellular lipids, glucose signaling and fiber size in old rats. *Sci Rep* **7**, 8593.
- Roos C, Wicovsky A, Muller N, Salzmann S, Rosenthal T, Kalthoff H, Trauzold A, Seher A, Henkler F, Kneitz C & Wajant H. (2010). Soluble and transmembrane TNF-like weak inducer of apoptosis differentially activate the classical and noncanonical NF-kappa B pathway. *J Immunol* **185**, 1593-1605.
- Soffe Z, Radley-Crabb HG, McMahon C, Grounds MD & Shavlakadze T. (2016). Effects of loaded voluntary wheel exercise on performance and muscle hypertrophy in young and old male C57Bl/6J mice. *Scand J Med Sci Sports* **26**, 172-188.
- Spandidos A, Wang X, Wang H, Dragnev S, Thurber T & Seed B. (2008). A comprehensive collection of experimentally validated primers for Polymerase Chain Reaction quantitation of murine transcript abundance. *BMC Genomics* **9**, 633.
- Spandidos A, Wang X, Wang H & Seed B. (2010). PrimerBank: a resource of human and mouse PCR primer pairs for gene expression detection and quantification. *Nucleic Acids Res* **38**, D792-D799.
- Spassov A, Gredes T, Gedrange T, Lucke S, Pavlovic D & Kunert-Keil C. (2010). Histological changes in masticatory muscles of mdx mice. *Arch Oral Biol* **55**, 318-324.
- Stuelsatz P, Pouzoulet F, Lamarre Y, Dargelos E, Poussard S, Leibovitch S, Cottin P & Veschambre P. (2010). Down-regulation of MyoD by calpain 3 promotes generation of reserve cells in C2C12 myoblasts. *J Biol Chem* **285**, 12670-12683.
- Tajrishi MM, Sato S, Shin J, Zheng TS, Burkly LC & Kumar A. (2014a). The TWEAK-Fn14 dyad is involved in age-associated pathological changes in skeletal muscle. *Biochem Biophys Res Commun* **446**, 1219-1224.
- Tajrishi MM, Zheng TS, Burkly LC & Kumar A. (2014b). The TWEAK-Fn14 pathway: A potent regulator of skeletal muscle biology in health and disease. *Cytokine Growth Factor Rev* **25**, 215-225.
- Trappe S, Luden N, Minchev K, Raue U, Jemiolo B & Trappe TA. (2015). Skeletal muscle signature of a champion sprint runner. *J Appl Physiol* **118**, 1460-1466.
- Wang HY, Ma CA, Zhao Y, Fan X, Zhou Q, Edmonds P, Uzel G, Oliveira JB, Orange J & Jain A. (2013). Antibody deficiency associated with an inherited autosomal dominant mutation in TWEAK. *Proc Natl Acad Sci U S A* **110**, 5127-5132.
- Wardle FC. (2019). Master control: transcriptional regulation of mammalian Myod. *J Muscle Res Cell Motil* 10.1007/s10974-019-09538-6.

- Wyckelsma VL, McKenna MJ, Levinger I, Petersen AC, Lambole CR & Murphy RM. (2016). Cell specific differences in the protein abundances of GAPDH and Na(+),K(+)-ATPase in skeletal muscle from aged individuals. *Exp Gerontol* **75**, 8-15.
- Yablonka-Reuveni Z, Rudnicki MA, Rivera AJ, Primig M, Anderson JE & Natanson P. (1999). The Transition from Proliferation to Differentiation Is Delayed in Satellite Cells from Mice Lacking MyoD. *Dev Biol* **210**, 440-455.
- Yakala GK, Cabrera-Fuentes HA, Crespo-Avilan GE, Rattanasopa C, Burlacu A, George BL, Anand K, Mayan DC, Corlianò M, Hernández-Reséndiz S, Wu Z, Schwerk AMK, Tan ALJ, Trigueros-Motos L, Chèvre R, Chua T, Kleemann R, Liehn EA, Hausenloy DJ, Ghosh S & Singaraja RR. (2019). FURIN Inhibition Reduces Vascular Remodeling and Atherosclerotic Lesion Progression in Mice. *Arterioscler Thromb Vasc Biol* **39**, 387-401.
- Zammit PS. (2017). Function of the myogenic regulatory factors Myf5, MyoD, Myogenin and Mrf4 in skeletal muscle, satellite cells and regenerative myogenesis. *Semin Cell Dev Biol* 10.1016/j.semcdb.2017.11.011.

Chapter 6

Changes to Mitochondrial Function and Markers of Autophagy in Skeletal Muscle of Aged and Chronically Resistance-Trained Mice

Chapter Summary

The following chapter details changes in the mitochondrial content and function, fibre type, and autophagic intermediates of old and chronically resistance-trained mice obtained from Emeritus Professor Miranda Grounds (University of Western Australia) and morphologically described in Softe *et al.* (2016). These changes were initially investigated as a function of altered TWEAK-Fn14 signalling which was anticipated in old and exercised skeletal muscle. Alterations of Fn14 and TWEAK, as described in Chapter 5, were not found to correlate with changes described in this chapter. Statistical analyses detailing these tests can be found in Appendix V. For this reason, no further investigation was performed on the interaction of the TWEAK-Fn14 axis with mitochondrial function or autophagic intermediates in the context of ageing and resistance training. The changes that were detected in these animals are instead described here as a function of resistance training as a positive intervention in skeletal muscle dynapenia – the loss of muscle function associated with ageing.

6.1. Introduction

Sarcopenia and dynapenia are defined as age-related declines in muscle mass and function, respectively, which are not a secondary result of a concurrent disease or disability (Brzezczynska et al., 2017). The biochemical mechanisms underlying sarcopenia and dynapenia are not well-defined and are likely multifactorial and modified by a number of environmental factors, including activity level. Reduction in mitochondrial content and dynamics is one phenomenon that has been frequently associated with age-related muscle declines (Joseph et al., 2012; Peterson et al., 2012a), although this may be dependent on the fitness level of aged individuals as a decline is not always evident, at least in humans (Wyckelsma et al., 2017).

Skeletal muscle mitochondrial content refers to the total pool of mitochondria and is closely linked with muscle fibre type (Pette & Spamer, 1986). Slow twitch – also classified as Type I fibres – primarily utilise oxidative metabolic pathways and have a high mitochondrial content (Pette & Spamer, 1986). Fast twitch fibres – further classified as Type IIA, IIB, or IIX fibres – rely on both oxidative and/ or glycolytic metabolic pathways (Pette & Spamer, 1986). Fibre type composition is responsive to various triggers, such as age, activity level, and training status and as such is considered dynamic over prolonged periods of weeks to years (Qaisar et al., 2016).

A key player in fibre type switching is peroxisome proliferator-activated receptor gamma coactivator 1-alpha (PGC-1 α) (Lin et al., 2002). As mentioned in previous chapters, PGC-1 α is a major driver of mitochondrial biogenesis and a promoter of fast to slow type fibre switching (Lin et al., 2002). Previous reviews have concluded that ageing has been associated with reductions in mitochondrial content in both rodent and human skeletal muscle (Peterson

et al., 2012b), however there is considerable disagreement in the literature which may be explained at least in part by the widely varied methodologies that have been implemented. The precise role of PGC-1 α in the context of sedentary or active ageing is still poorly defined. This is likely due to the difficulty in validating antibodies for α -PGC-1 α and measuring endogenous levels of PGC-1 α protein levels in muscle. Reduced PGC-1 α protein has been reported in muscle from sedentary aged humans (Safdar *et al.*, 2010; Joseph *et al.*, 2012), however a direct comparison of *vastus lateralis* muscle from young (18-30 years) and aged (59-76 years) sedentary humans showed no change in PGC-1 α protein abundance (Lanza *et al.*, 2008). Given the increased susceptibility of fast twitch fibres to atrophy (Ciciliot *et al.*, 2013), reductions in PGC-1 α – and thus reductions in the relative content of slow-twitch muscle fibres – may present a risk factor for muscle wasting. In a cross-over study, Lanza *et al.* (2008) went on to describe a higher abundance of PGC-1 α protein in age-matched endurance-trained adults in both young and aged population, albeit with a more pronounced difference in muscle from young adults. These findings indicate that sedentary behaviour may have a larger impact on PGC-1 α protein abundance than age. A concise review of the potential implications of PGC-1 α alteration in sarcopenia is provided in Ji and Kang (2015), who concluded that aged individuals may still benefit from physical activity to drive mitochondrial biogenesis via PGC-1 α . It must be noted, however, that endogenous measures of PGC-1 α protein in muscle are notoriously difficult and must be interpreted with caution. Given these limitations and that PGC-1 α is under transcriptional control (Knutti *et al.*, 2001), assessment of mRNA may provide good insight into PGC-1 α in the context of ageing and exercise.

Maintenance of a healthy mitochondrial pool underpins mitochondrial function and occurs via the process of fusion and fission, collectively known as mitochondrial dynamics (Chen & Chan, 2004). Fusion refers to the merging of mitochondria to exchange contents and

compensate for damaged mitochondrial proteins, whilst fission allows division of a mitochondrion with a specific outcome being segregation of damaged components for reuse via fusion or disposal via mitophagy (Figure 6.1) (Chen & Chan, 2004).

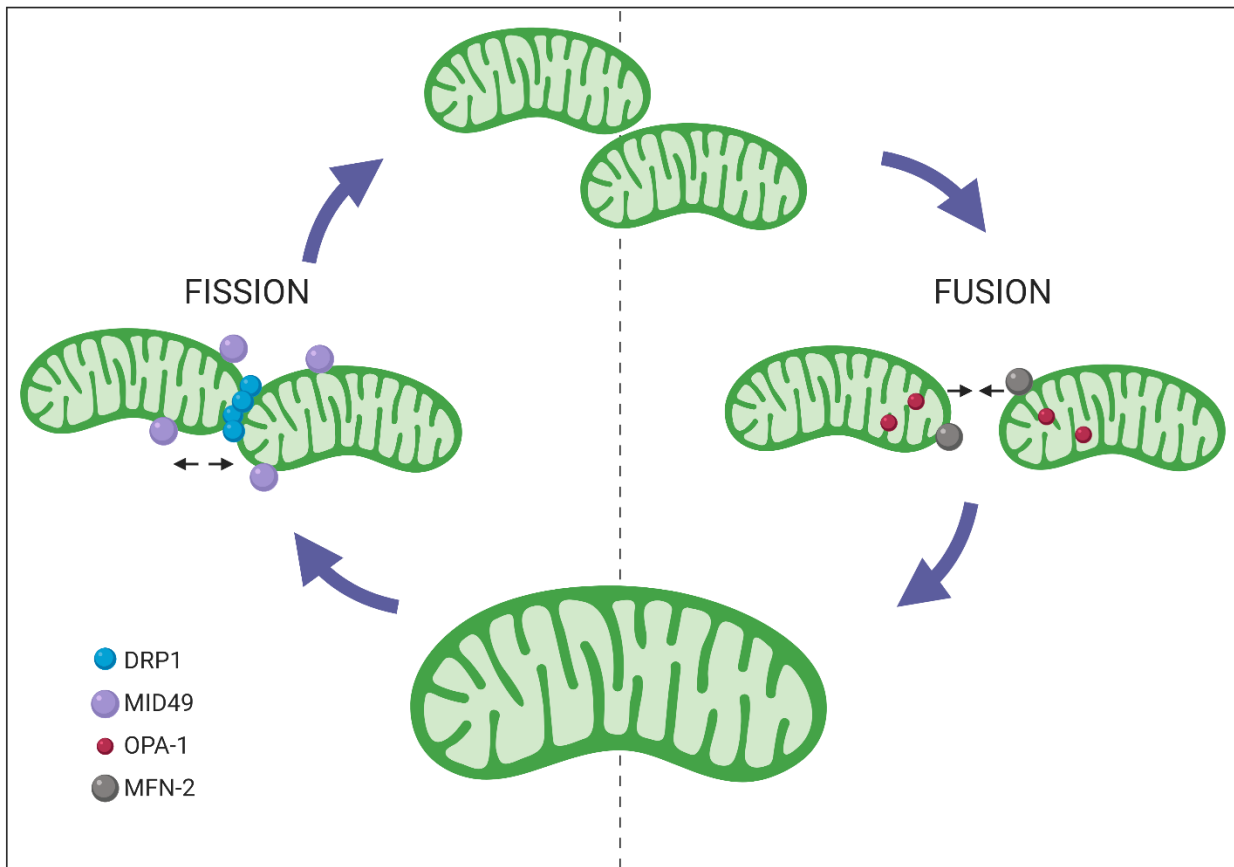


Figure 6.1: Mitochondrial fission and fusion. Fusion refers to the merging of mitochondria to form single larger organelles. The outer membrane fusion is mediated by MFN-2 and the inner membrane by OPA-1 (Koshiba *et al.*, 2004; Chan, 2006). Fission refers to the splitting of mitochondria, primarily to remove damaged components for downstream mitophagy. The process is mediated by DRP-1 which is recruited by a host of proteins including MiD49 (Palmer *et al.*, 2011) (figure created with BioRender.com).

Mitochondrial fusion is orchestrated by several dynamin-like GTPase proteins. Mitofusin-2 (MFN-2) is the predominant mitofusin protein expressed in skeletal muscle, which facilitates the fusion of the mitochondrial outer membrane (Koshiba *et al.*, 2004). Fusion of the inner membrane is in turn facilitated by optic atrophy-1 (OPA-1) (Chan, 2006). Mitochondrial dynamics proteins, MiD49 and MiD51, have been identified as recruiting proteins which

facilitate the fission of mitochondria by dynamin-related protein 1 (DRP1) (Palmer *et al.*, 2011).

It has been previously reported that MFN-2 is downregulated in muscle from aged rodents and may indicate a reduced ability to maintain a healthy mitochondrial pool (Sebastian *et al.*, 2016). Human studies have demonstrated the opposite effect whereby a greater abundance of both MFN-2 and MiD49 in whole skeletal muscle homogenates from active older adults was reported, which interestingly decreased in response to 12 weeks of high intensity interval training (HIIT) (Wyckelsma *et al.*, 2017). HIIT was also shown to enhance mitochondrial content in active older adults as measured by mitochondrial markers, cytochrome c oxidase subunit IV (COXIV) and NADH dehydrogenase [ubiquinone] 1 α subcomplex subunit 9 (NDUFA9), as well as Blue Native PAGE analysis of the individual complexes (Wyckelsma *et al.*, 2017). Together these findings suggest overall mitochondrial function may be improved with exercise training in aged humans. The authors interpreted these results to indicate that a compensatory mechanism of upregulating mitochondrial dynamics to maintain a healthy mitochondria pool is present in active but untrained older adults (Wyckelsma *et al.*, 2017). In addition to these markers of mitochondrial content, the enzymatic activity of citrate synthase – regulating a key step in the citric acid cycle – can be assayed to help determine the overall mitochondrial content and oxidative capacity of muscle. Mice subjected to voluntary resistance wheel running initiated at 15 months of age for 34 weeks were shown to have greater citrate synthase activity relative to their sedentary counterparts (White *et al.*, 2016).

Another factor to consider when discussing mitochondrial content and turnover in skeletal muscle is the role of autophagy and mitophagy. Autophagy, or ‘self-eating’, is the

system by which damaged and degraded proteins and organelles are broken down and their components recycled, thus protecting the cell against harmful accumulation of damaged proteins and preserving energy and nutrients (Glick *et al.*, 2010). Mitophagy specifically refers to the autophagy of mitochondria (Ashrafi & Schwarz, 2013).

Assembly of the autophagosome is an initial step in autophagy and is a tightly regulated process controlled by numerous regulatory and binding proteins and results in a vesicle forming around targeted proteins (Glick *et al.*, 2010). AMP-activated protein kinase (AMPK) serves as a primary energy-sensing molecule detecting when a cell is undergoing periods of stress including starvation or hypoxia and is implicated in formation of autophagosome (Herzig & Shaw, 2018). AMPK phosphorylates Unc-51-like kinase (ULK), a key regulatory protein in autophagosome assembly that has been described as a requisite step in autophagosome formation (Lee *et al.*, 2010; Egan *et al.*, 2011). Acute, intense exercise, sufficient to utilise ATP stores at a greater rate than they can be repleted and thus elevating levels of AMP, is able to activate AMPK (Hardie & Carling, 1997). This exercise-induced response has been shown to be blunted in *extensor digitorum longus* (EDL) muscle from aged rats indicating an impairment of this energy-sensing system (Reznick *et al.*, 2007).

Autophagy is often assessed by measuring the conversion of LC3BI to LC3BII (Mizushima & Yoshimori, 2007). LC3B (microtubule-associated protein light chain 3) is proteolytically cleaved by Atg4 to LC3BI, which is then further processed by Atg7 to produce LC3BII which assists in autophagosome formation (Maruyama & Noda, 2018). Measuring LC3BII accumulation is complicated by the fact that it too is degraded by autophagy and is not a measure of autophagic flux (Mizushima & Yoshimori, 2007). Measurement of the accumulation of p62 – a substrate of LC3BII – in addition to LC3BII itself provides a more

concise measure of autophagic flux, or alternatively, in animal studies, the use of lysosomal protease inhibitors can be used in conjunction with LC3B and p62 measurements to more accurately assess autophagy flux (Mizushima & Yoshimori, 2007). It should be noted that inhibitors are not without their limitations. Some inhibitors, such as leupeptin, work by inhibiting proteases including calpains and it is therefore difficult to be certain what effects they have on autophagy alone or with other cellular processes (Yang *et al.*, 2013).

The mixed effects of ageing and exercise on autophagic flux are briefly reviewed in Kim *et al.* (2017). Whilst some studies indicate an accumulation of LC3BII and p62 in sedentary 29 month old rats (Baehr *et al.*, 2016), others indicate no change in these measures in skeletal muscle from humans aged 78 ± 5 years (Distefano *et al.*, 2017) or in mice aged 23 months (White *et al.*, 2016). Compared to a group of aged-matched in 18-20 month old Sprague-Dawley rats, late-life chronic resistance exercise intervention in the form of nine weeks of weight-loaded ladder climbing was shown to both have lower loss of muscle mass as well as lower LC3BII:LC3BI ratios and p62 accumulation (Luo *et al.*, 2013). These findings again suggest that sedentary behaviour, as opposed to ageing solely, may be a greater risk factor for defective autophagy and possibly autophagic flux.

The link between exercise and maintaining, or even restoring, mitochondrial content and function during ageing is not new. Holloszy (1967) first described the use of a strenuous forced treadmill running program to enhance mitochondrial content and enzymatic activity in 9-month old rats, and later showed a similar effect in 24-month old rats using a forced swimming regime (Young *et al.*, 1983). Ongoing work in this field is comprehensively reviewed in Kim *et al.* (2017) and indicates that whilst exercise is commonly accepted as an important factor in healthy ageing, the exact mechanisms and more practically, the sufficient

prescription of type, intensity, and duration require further investigation. The individuals who stand to benefit the most from these kinds of exercise interventions often have a history of sedentary behaviour, exhibit reduced muscle mass, and have reduced propensity or tolerance for exercise. For these reasons, understanding the threshold of exercise required to induce positive adaptations is essential.

The current study aims to determine whether a late-life intervention of voluntary resistance wheel running in C57BL/6 mice, previously described in Soffe *et al.* (2016) as insufficient to restore muscle mass, is sufficient to independently restore or preserve mitochondrial content, function, and dynamics and autophagic intermediates.

6.2. Methods

6.2.1. Animals

All experiments were conducted in accordance with the National Health and Medical Research Council, Australia and approved by the Animal Ethics Committee of University of Western Australia. Samples for the current study were provided by Emer. Professor Miranda Grounds and Dr Zoe White with full experimental and morphological information published in Soffe *et al.* (2016). Young (13 weeks) and old (105 weeks) C57BL/6 mice were housed in either standard cages (sedentary controls – YOUNG SED $n = 9$, OLD SED $n = 9$) or voluntary access resistance running wheels under a progressive low resistance training (low resistance (LR) group – YOUNG LR $n = 7$, OLD LR $n = 7$) or progressive high resistance training (high resistance (HR) group – YOUNG HR $n = 7$) program for 10 weeks. Quadriceps (QUAD) muscles were collected and stored whole at -80°C .

6.2.2. Western Blotting

Whole muscle homogenates were prepared from frozen QUAD samples and subjected to SDS-PAGE as per Chapter 2, Section 2.4. Full details of antibodies used can be found in Appendix III. Mitochondrial abundance was determined using COXIV (Cell Signaling Technology 4844), fusion and fission were assessed with OPA-1 (BD Biosciences), MFN-2 (generated by Prof. Mike Ryan – Monash University), and MiD49 (Prof. Mike Ryan). Autophagy was assessed using LC3BI and LC3BII (Sigma L7543), p62 (Abcam 56416), pAcetyl-CoA (Cell Signaling Technology 3661), Acetyl-CoA (Cell Signaling Technology 3676), AMPK α (Cell Signaling Technology 2532), and ULK (Abcam 128859). A muscle calibration mix was created by combining equal volumes of homogenates from each sample and used to run the same calibration curve on all subsequent gels. Normalised homogenates and muscle calibration mix were stored at -80°C.

6.2.3. Fibre Type Composition

Muscle fibre type composition was assessed using a method previously described (Xu *et al.*, 2017) and detailed in Chapter 2, Section 2.5.

6.2.4. qPCR

qPCR was performed as per protocol described in Chapter 2, Section 2.6. Full primer details are found in Appendix III. Results were analysed using the 2^{-Ct} method normalised to the total cDNA content as determined by OliGreen ssDNA assay. This method means that a housekeeping gene is not required, because the absolute amount of single stranded cDNA used in each assay was known.

6.2.5. Citrate Synthase Activity Assay

Citrate synthase activity was assayed in whole muscle homogenates. Cryosections from QUAD muscle were collected as described in Chapter 2 and placed directly in 200 μ l relaxing buffer

(see Chapter 2, Section 2.2.1.). Homogenates (equivalent to ~ 0.5 mg wet weight tissue) were added to 200 μ l final volume citrate synthase activity assay solution (100 mM Tris-HCl, 100 μ M 5,5'-dithiobis-2-nitrobenzoic acid (DTNB), 30 μ M Acetyl CoA lithium salt, 500 μ M oxaloacetic acid, pH 8.3) in Corning® 96-well flat bottomed clear plates (Sigma-Aldrich, Australia). Absorbance at 412 nm was measured every 15 seconds for 3 minutes and reagents only samples used as a baseline.

Given that reliable muscle weight could not be determined from cryosections, it was necessary to determine mass used via total protein measurement against a calibration curve of known muscle mass. Total protein was measured by adding 2:1 v:v SDS loading buffer (see Chapter 2, Section 2.2.1) to homogenates and run on a 4-15% Criterion TGX Stain-Free gel alongside a calibration curve with known amounts of whole muscle homogenate with UV images analysed in ImageLab.

Citrate synthase activity was calculated with the following formula.

$$\frac{\text{Units}}{\text{mg}} = \frac{\Delta\text{Abs} \times \text{min}^{-1}}{\varepsilon \times L(\text{cm}) \times \text{mg tissue}} \quad \text{where } \varepsilon = 13.6 \text{ mM}^{-1} \text{ cm}^{-1}$$

6.2.6. Statistical Analyses and Graphs

Results are presented as mean \pm standard deviation unless stated otherwise. Effects of age and LR exercise were analysed using two-way ANOVA; effects of LR and HR in young mice were assessed using a one-way ANOVA as HR training was not performed on old mice. This statistical approach is in line with previously published methodologies for this cohort of animals (Soffe *et al.*, 2016) Significance was declared at $p \leq 0.05$. All statistical tests were performed using Prism v8 (GraphPad). Individual mice are consistently colour-coded across separate graphs.

6.3. Results

6.3.1. Running Activity Levels

Data from pooled weekly running distances for each exercise cohort showed decreased voluntary exercise capacity in old LR animals relative to young LR and a reduction in running distance for all groups as the study progressed (Figure 6.2A). Young HR animals also showed reduced running distance compared to young LR. The area under the curve (AUC) was calculated for individual mice in the young and old LR cohorts with young mice running further than their old counterparts (unpaired t-test $p = 0.0093$; Figure 6.2B).

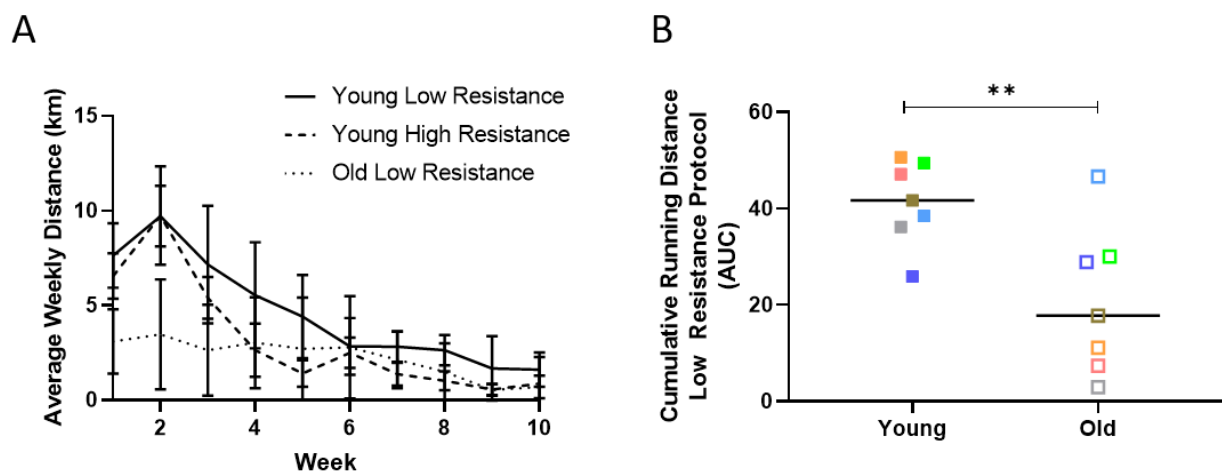


Figure 6.2: Voluntary running activity levels. (A) Average weekly distance (km) for each training intervention throughout the time course of the study (figure adapted from Soffe et al. (2016)). Older low-resistance training mice ran consistently shorter distances than young low-resistance mice. All groups ran shorter distances as the study progressed and resistance increased. Young high-resistance mice ran comparable distances to young low-resistance mice but demonstrated steeper drop-off rate in average distance as the study progressed. (B) Area under curve of individual mouse cumulative running distance from young and old low-resistance-trained mice (data adapted from Soffe et al. (2016)). Old mice ran significantly less than younger counterparts (unpaired t-test, $p = 0.0093$).

6.3.2. Body Weight and Muscle Mass

Body weight and QUAD muscle mass were each measured and expressed relative to the length of the tibia bone to account for age and biological variability in animal size (Figure 6.3). Normalised body weight (Figure 6.3A) was not altered in old mice relative to younger counterparts; LR exercise resulted in a reduction in body weight at both ages (two-way ANOVA activity effect, $p = 0.0014$). HR training resulted in greater reductions in body mass in young mice (one-way ANOVA linear trend, slope = -2.093 , $p < 0.0001$). Normalised QUAD mass (Figure 6.3B) showed an overall reduction in muscle mass in old mice (two-way ANOVA age effect, $p < 0.0001$) which was not reversed by LR exercise. Young mice showed a linear increase in muscle mass in response to LR and HR training (one-way ANOVA linear trend, slope = 9.17 , $p = 0.0044$).

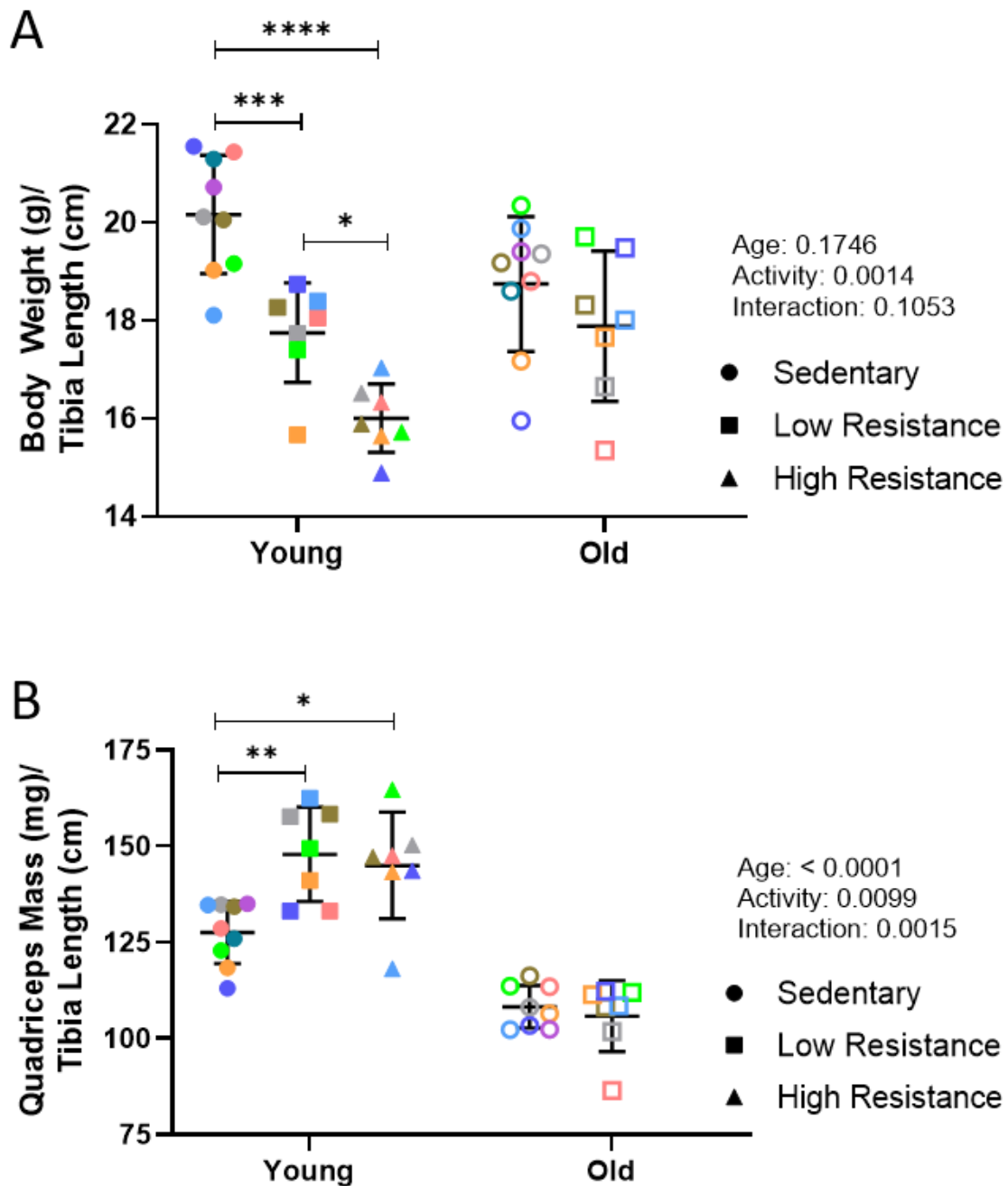


Figure 6.3: Body weight and quadriceps muscle mass. (A) Body weight normalised to tibia bone length (figure adapted from Soffe et al. (2016)). Body weight was reduced in low-resistance-trained mice relative to sedentary controls (two-way ANOVA activity effect, $p = 0.0014$). Body weight reduction was enhanced in high-resistance-trained young mice (one-way ANOVA test for linear trend, slope = -2.093 , $p < 0.0001$). (B) Quadriceps muscle mass normalised to tibia bone length was reduced in old mice (two-way ANOVA age effect, $p < 0.0001$). An overall effect of low-resistance training was detected, however no post-hoc changes were detected in old sedentary vs. old low-resistance muscle mass. A linear trend in young mice relative to increasing resistance level was detected (one-way ANOVA test for linear trend, slope = 9.171 , $p = 0.0044$).

6.3.3. Mitochondrial Content and Activity

Mitochondrial content was assessed by analysing the relative abundance of COXIV protein in QUAD muscle (Figure 6.4). Two-way ANOVA showed both young and old mice had increased COXIV abundance in LR groups relative to SED ($p = 0.0052$). This effect was more pronounced in response to higher resistance training, with young HR significantly higher than young SED ($p = 0.028$), and a linear trend detected between young SED, LR, and HR animals (slope = 0.237, $p = 0.011$). Citrate synthase activity as a measure of overall mitochondrial content was unchanged in young LR and HR animals relative to age-matched SED controls, with no linear trend detected (Figure 6.4). An overall effect of LR exercise was, however, observed in young and old animals, with citrate synthase increased in LR-trained mice (Figure 6.4). Ageing showed no overall effect on citrate synthase activity.

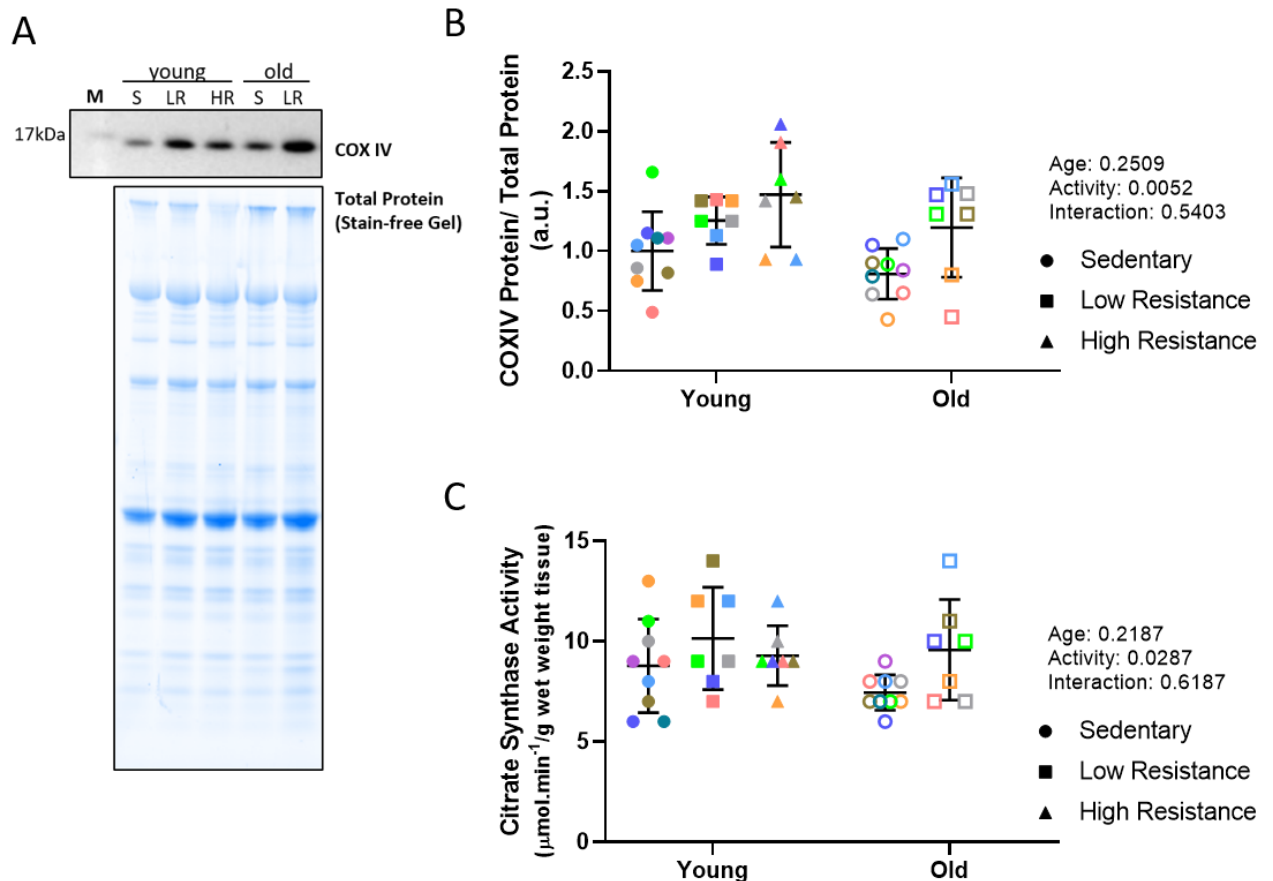


Figure 6.4: Mitochondrial protein content and activity. (A) Representative blot of COXIV western blot and stain-free image of total protein content. A single band was detected just below 17 kDa (Cell Signaling Technology 4844, expected molecular weight – 17 kDa). (B) COXIV protein normalised to total protein content. An overall effect of low-resistance (LR) training was seen relative to sedentary (S) controls (two-way ANOVA activity effect, $p = 0.0052$); this effect was enhanced in young high-resistance (HR)-trained mice (one-way ANOVA test for linear trend, slope = 0.2365, $p = 0.011$). (C) Citrate synthase activity showed an overall increase following LR training (two-way ANOVA activity effect, $p = 0.029$) but no effect of ageing or HR training in young mice (one-way ANOVA, $p = 0.476$).

Correlations were performed between citrate synthase activity and either cumulative running distance or COXIV protein abundance for both young and old LR mice (Figure 6.5). Significant correlation was only detected between citrate synthase activity and cumulative running distance for old mice (Pearson $r^2 = 0.848$, $p = 0.0032$).

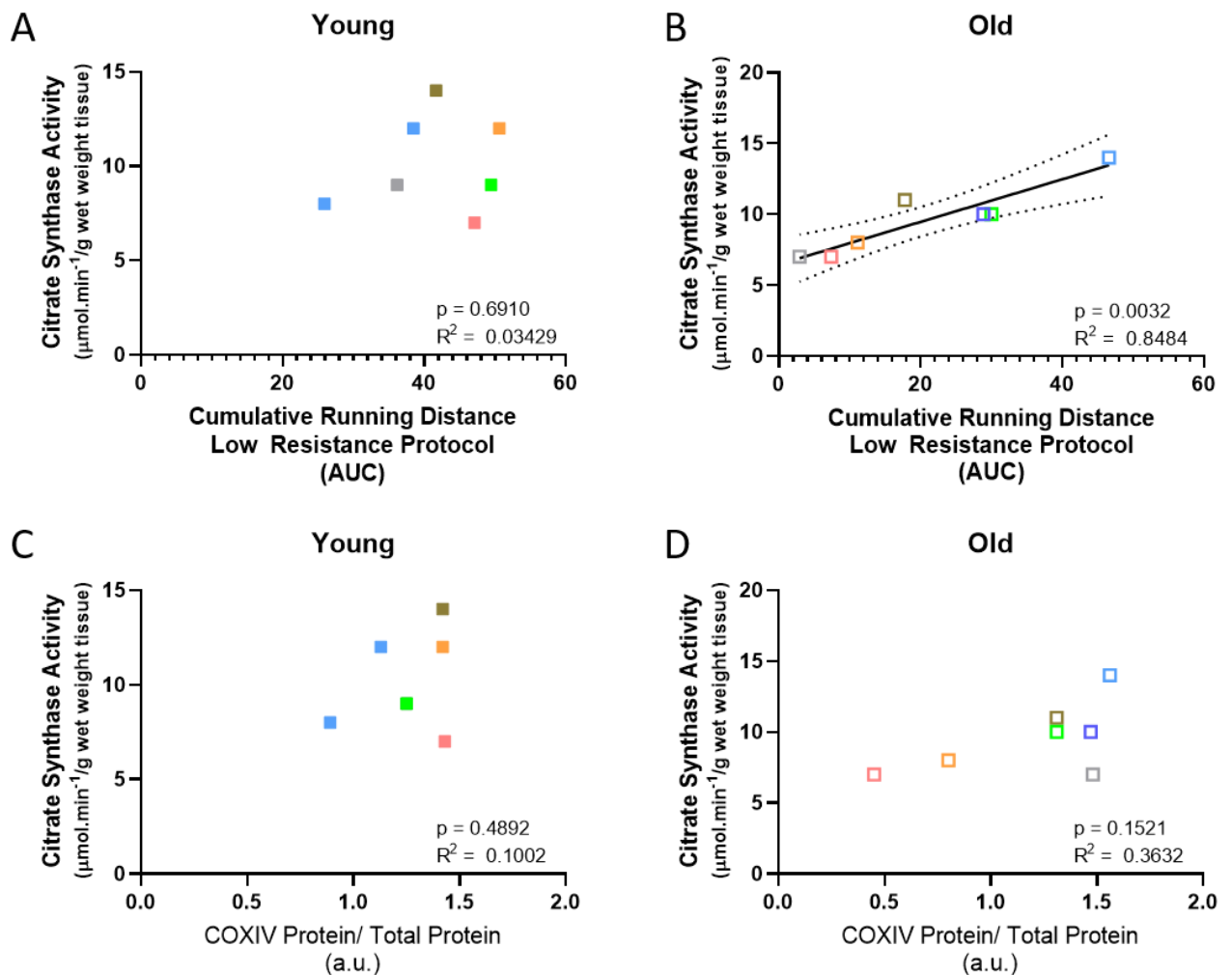


Figure 6.5: Citrate synthase activity correlations. Citrate synthase activity correlation with cumulative running distance in young (A) and old (B) low-resistance (LR)-trained mice. Significant positive correlation was seen only in old mice (Pearson $r^2 = 0.8484$, $p = 0.0032$). Citrate synthase activity correlation with COXIV protein abundance in young (C) and old (D) mice showed no significant correlations.

6.3.4. Fibre Type

QUAD muscle from all groups was found to be predominantly type IIB, with a shift towards the more oxidative IIA/IIX phenotype in response to resistance exercise (Figure 6.6). Types IIA and IIX showed poor resolution and were grouped together for analyses. Type I fibres were below detection limits. Young mice showed a more oxidative phenotype (more IIA/IIX fibres)

following resistance training (one-way ANOVA with Tukey's multiple comparisons young SED v young LR $p = 0.0010$, young SED v young HR $p < 0.0001$), with a linear trend (slope -7.533 , $p < 0.0001$ for type IIB fibre content) corresponding to higher resistance. No effects of ageing were detected by two-way ANOVA, however an overall effect of LR exercise was seen across both age groups ($p < 0.0001$).

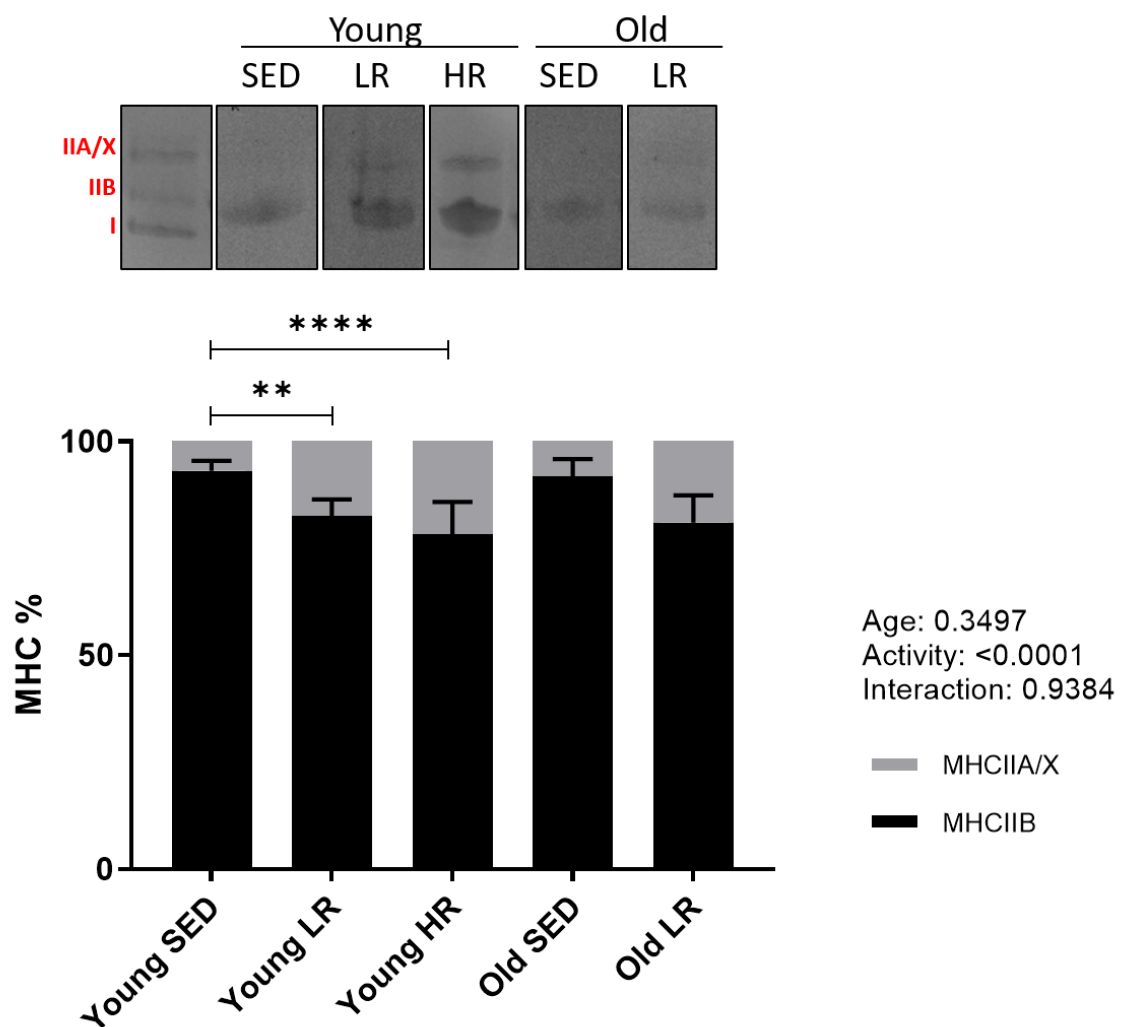


Figure 6.6: Fibre type distribution. Fibre type was assessed using Coomassie gel staining of individual MHC isoforms. Representative blot positive control sample demonstrates achievable resolution; type I was below detection limits in these quadriceps samples and types IIA and IIX were not able to be fully resolved. No overall changes in fibre type distribution were detected between age groups. Low-resistance (LR) training produced an overall shift towards type IIA/X relative to sedentary (SED) controls (two-way ANOVA activity effect, $p < 0.0001$). A linear trend was detected in young mice relative to resistance level (HR = high-resistance; one-way ANOVA test for linear trend, slope = -7.533 , $p < 0.0001$ for type IIB fibre content).

Transcript levels of PGC-1 α were assessed by qPCR and expressed relative to the mean of young sedentary controls (Figure 6.7). Considerable biological variability was detected in young LR mice that was not seen in other groups. An overall reduction was detected in old mice (two-way ANOVA activity effect, $p = 0.0091$) that was not prevented or reversed by LR training.

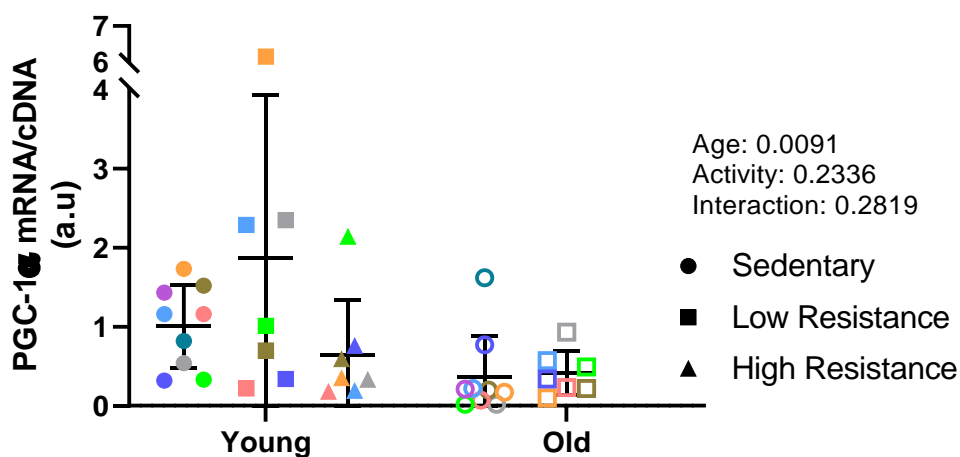


Figure 6.7: PGC-1 α mRNA. PGC-1 α was assessed by qPCR. An overall reduction in old mice was detected (two-way ANOVA age effect, $p = 0.0091$), however no effects of exercise were detected in any group. Young low-resistance-trained mice showed considerable biological variability relative to other groups.

6.3.5. Mitochondrial Dynamics

Mitochondrial fission protein, MiD49, was found to be higher in young LR animals relative to age-matched SED controls ($p = 0.035$; Figure 6.8A, B). Interestingly, this was not the case in young HR mice, with no changes detected between young SED and young HR. Young LR mice also had higher abundance MiD49 than age-matched HR training animals ($p = 0.024$). No linear trend was detected in young animals in response to increasing resistance training. No

effects of ageing were detected, however an overall greater response to LR training was detected in both age groups (two-way ANOVA activity effect, $p = 0.0066$; Figure 6.8A, B).

Mitochondrial fusion marker, OPA-1, showed a linear increase in response to resistance exercise in young mice (slope = 0.243, $p = 0.031$; Figure 6.8C, D). OPA-1 was lower in old animals (two-way ANOVA age effect, $p = 0.0138$), however LR training resulted in higher OPA-1 in both young and old mice (two-way ANOVA activity effect, $p = 0.0042$). MFN-2 showed no effects of ageing or exercise across all groups and resistance levels (Figure 6.8E, F).

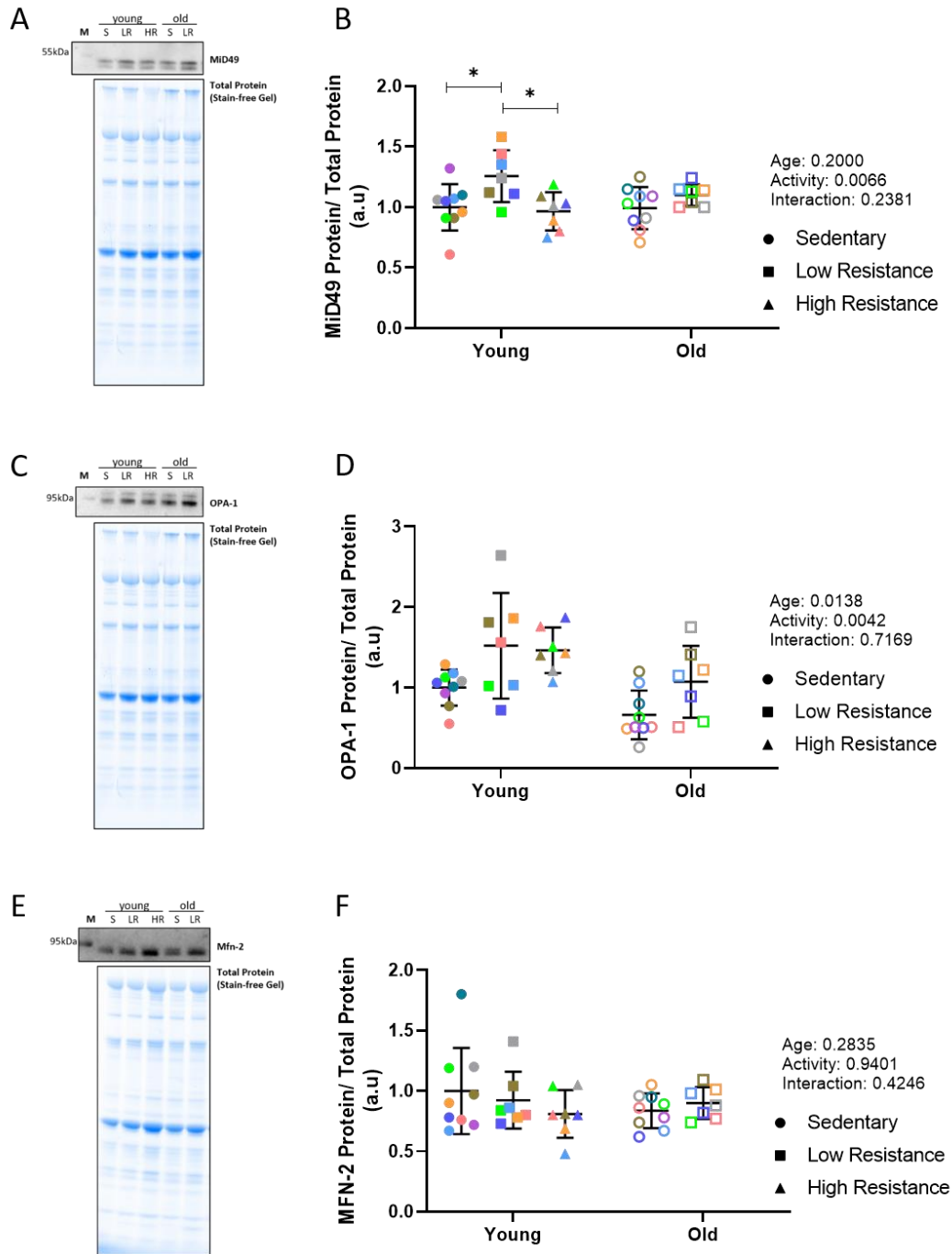


Figure 6.8: Mitochondrial fission and fusion. Representative western blots and stain-free gel images of total protein content for MiD49 (A), OPA-1 (C), and MFN-2 (E). A specific band for MiD49 was detected below 55 kDa (top band of representative blot, antibody generated by Prof. Mike Ryan – Monash University, expected molecular weight – 49 kDa). Doublet bands were detected for OPA-1 at ~95 kDa (BD Biosciences, expected molecular weight – 111 kDa). A single band just below 95 kDa was detected for MFN-2 (antibody generated by Prof. Mike Ryan, expected molecular weight – 86 kDa). (B) MiD49 showed an overall increase following low-resistance (LR) training relative to sedentary (S) controls (two-way ANOVA activity effect, $p = 0.0066$) that was not enhanced by high-resistance (HR) training in young mice. (D) OPA-1 was decreased in old mice (two-way ANOVA age effect, $p = 0.0042$) but increased following LR training (two-way ANOVA activity effect, $p = 0.014$). A linear trend was detected relative to increasing resistance levels in young mice (one-way ANOVA test for linear trend, slope = 0.02432, $p = 0.031$). (F) No overall effects were detected in MFN-2 due to ageing or exercise.

6.3.6. Autophagy

The total AMPK α and ULK proteins were measured as a general marker of autophagosome assembly (Figure 6.9). No effects of ageing and either LR or HR training were present for total AMPK α and ULK proteins.

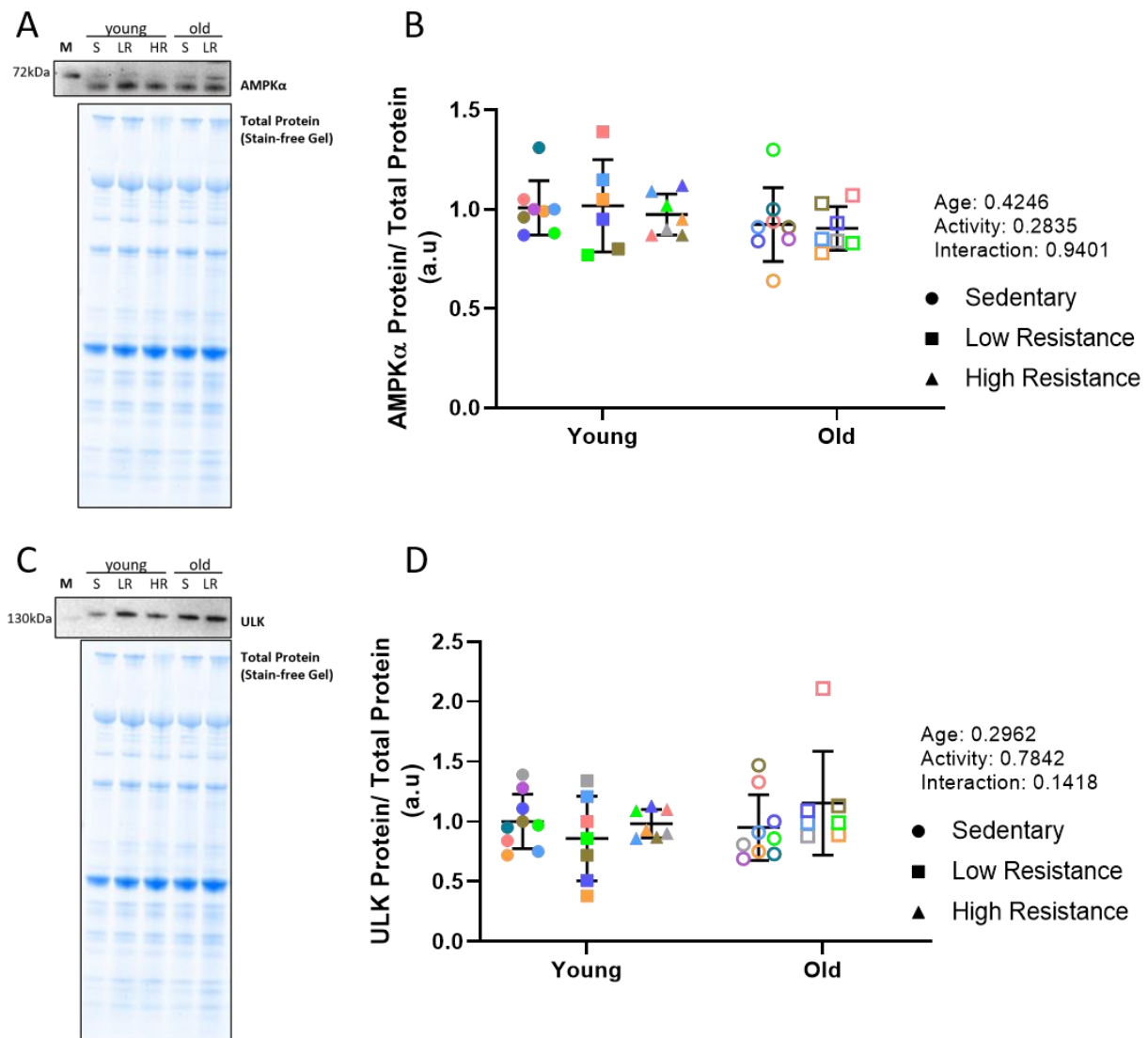


Figure 6.9: AMPK α and ULK. Representative western blots for AMPK α (A) and ULK (C) with stain-free gel image of total protein. AMPK α specific band was detected below 72 kDa (Cell Signaling Technology 2532, expected molecular weight – 63 kDa). Single band for ULK was detected above 130 kDa (Abcam 128859, expected molecular weight – 150 kDa). No effects of ageing or exercise were detected in AMPK α (B) or ULK (D).

Phosphorylation of AMPK α and ULK were not quantified as these antibodies did not produce consistent validated bands. A proxy of AMPK α and ULK activity was measured in the form of Acetyl-CoA phosphorylation (Figure 6.10). Normalised pAcetyl-CoA to total Acetyl-CoA was not altered due to ageing or training status (Figure 6.10A), however absolute measurement of pAcetyl-CoA relative to total protein (Figure 6.10B, C) was reduced in old mice (two-way ANOVA age effect, $p = 0.011$). Total Acetyl-CoA relative to total protein (Figure 6.10D, E) was trending lower in old mice but did not reach significance (two-way ANOVA age effect, $p = 0.056$).

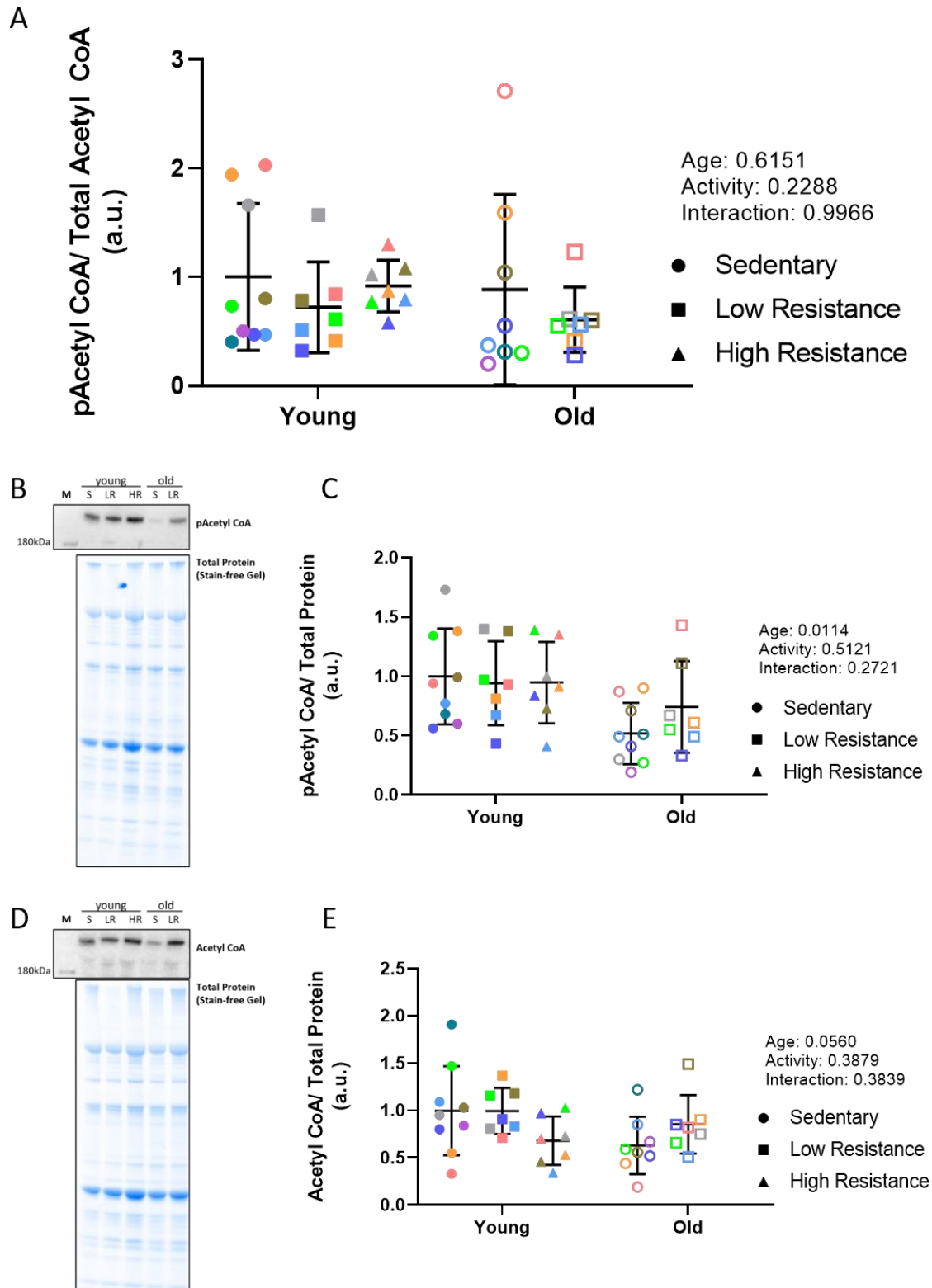


Figure 6.10: Phosphorylation of Acetyl-CoA. Representative western blots of pAcetyl-CoA (B) and Acetyl-CoA (D) with stain-free images of total protein content. A single band was detected above 180 kDa for both pAcetyl-CoA (Cell Signaling Technology 3661, expected molecular weight – 280 kDa) and Acetyl-CoA (Cell Signaling Technology 3676, expected molecular weight – 280 kDa). Whilst no overall changes were detected in pAcetyl-CoA/Acetyl CoA (A), absolute levels of pAcetyl-CoA (C) were reduced in old mice (two-way ANOVA age effect, $p = 0.011$). Absolute Acetyl-CoA (E) was approaching, but did not reach, significant reduction in old mice (two-way ANOVA age effect, $p = 0.0560$).

Processing of LC3BI to LC3BII as measured by both LC3BII:LC3BI ratio and total LC3BII were higher in old animals (two-way ANOVA age effect, $p = 0.014$; Figure 6.11). No effects of exercise were detected across age groups and resistance level.

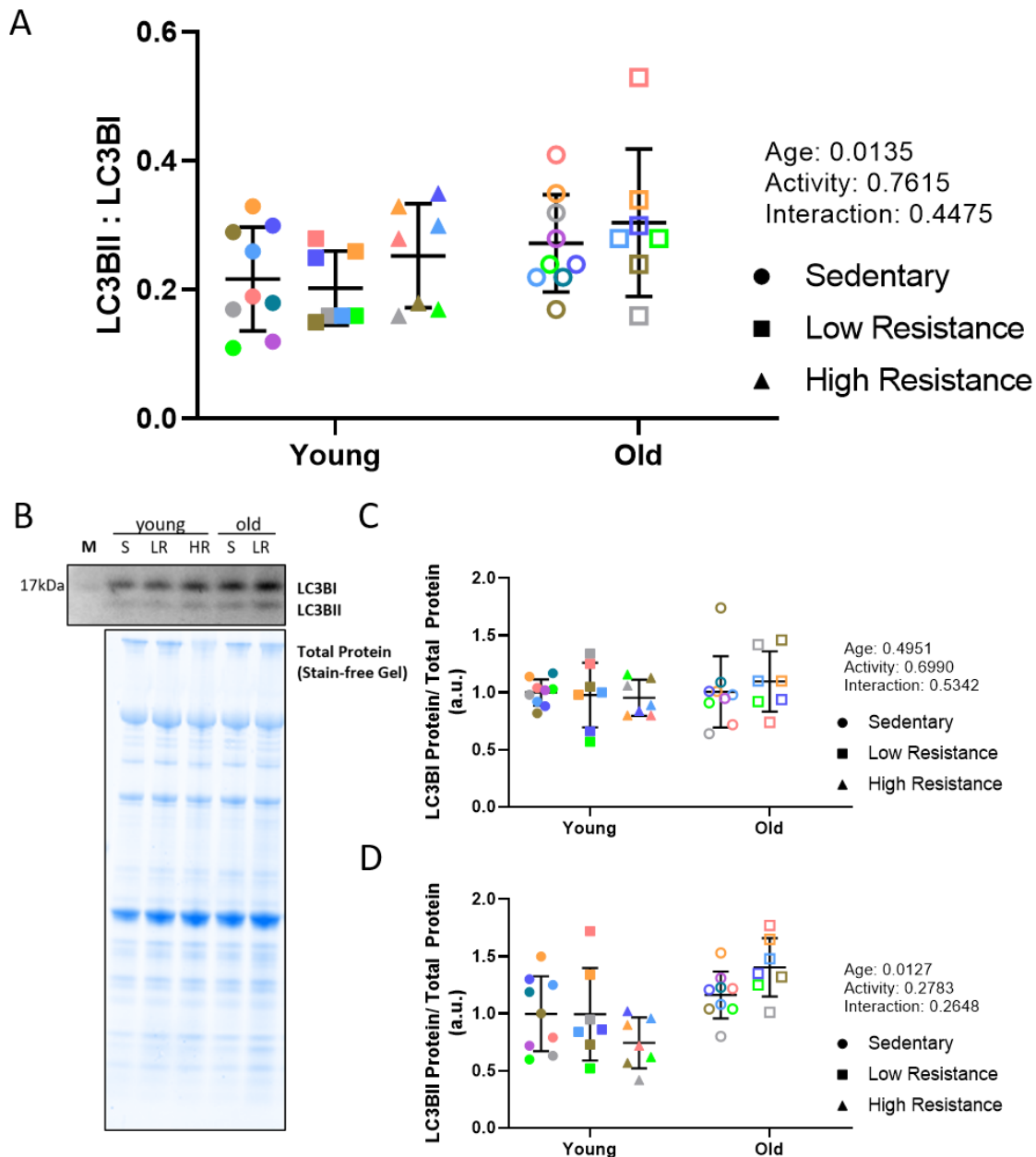


Figure 6.11: LC3B conversion. Representative western blot of LC3B (B) with stain-free images of total protein. LC3BI and LC3BII isoforms were detected as a doublet at ~17 kDa (Sigma L7543, expected molecular weight – 14 and 16 kDa). Conversion of LC3BI to LC3BII was measured as both a ratio of LC3BII:LC3BI (A) and absolute LC3BII (D). Both ratio and absolute measures showed an increase in old mice (two-way ANOVA age effect, $p = 0.014$ and 0.013 respectively). (C) LC3BI remained stable across age and exercise interventions.

Two forms of p62 were detected – a full length band at ~62 kDa and a shorter isoform at ~48 kDa. Accumulation of full length p62 showed no overall effects of age or exercise (Figure 6.12A, C). The suspected cleaved p62 product (Figure 6.12A, C) was significantly higher in old mice (two-way ANOVA age effect, $p = 0.0022$). A downward trend in cleaved p62 was observed in response to increased levels of resistance training in young mice only (one-way ANOVA test for linear trend, slope = -0.47, $p = 0.0013$).

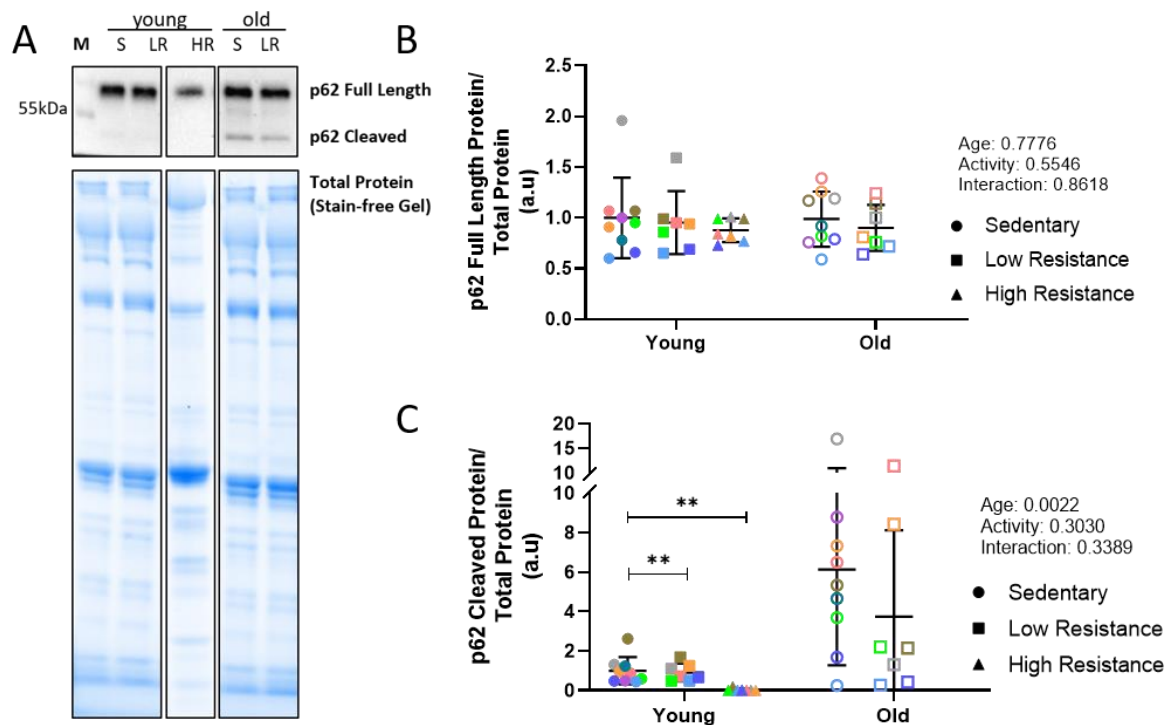


Figure 6.12: p62 accumulation and cleavage. Representative western blot of p62 (A) with stain-free images of total protein; representative blots taken from two separate blots due to later processing of young HR samples. A double band for p62 was detected above and below 55 kDa (Abcam 56416, expected molecular weight – 62 kDa, proposed cleavage product – 48 kDa (Sanchez-Garrido et al., 2018; Zhao et al., 2020)). No age or exercise effects were detected in full length p62 accumulation (B), however cleaved p62 (C) was significantly upregulated in old mice (two-way ANOVA age effect, $p = 0.0022$). A downward trend was also detected in cleaved p62 in young mice in response to increasing resistance level training (one-way ANOVA test for linear trend, slope = -0.47, $p = 0.0013$).

6.4. Discussion

6.4.1. Mitochondrial content and activity are not reduced in old mice

Mitochondrial content and activity as measured in the current study showed no differences in old mice relative to their younger counterparts. These results are congruent with the measured fibre-type proportions of the QUAD muscle, with predominantly type IIB in both young and old sedentary mice with comparable shifts towards faster IIA/X following low-resistance training. Our findings are largely consistent with the previous literature which posits that when young and old cohorts are matched for activity levels, apparent age-induced effects are negated (Lanza *et al.*, 2008).

PGC-1 α is notoriously difficult to reliably and accurately quantify at both the gene and protein level given its transient nature, lack of validated antibodies, and varying normalisation methods (discussed further in Section 6.4.2). In addition to this, claims regarding the role of PGC-1 α , particularly in ageing, are further confused by the wide citation of a since-retracted paper. Wenz *et al.* (2009) reported a protective effect of PGC-1 α overexpression in ageing which has since been retracted (National Academy of Science, 2016), but its inclusion in widely cited reviews mean that this assertion is still prevalent in the literature. PGC-1 α data is presented here for completeness and with acknowledgement of these limitations.

PGC-1 α transcript levels were lower in old compared with young mice in the current study. This trend was not reversed by low-resistance training, and overall did not reflect a change in muscle fibre type distribution or mitochondrial content. These results are somewhat unexpected but are not entirely at odds with previous literature. A review by Peterson *et al.* (2012a) indicates that whilst PGC-1 α is a key driver of mitochondrial biogenesis, it is not always linked with a change in fibre type composition. Implications of

reduced PGC-1 α in the old cohort in the wider context of this study are not clear, however higher mitochondrial content in the absence of greater PGC-1 α may indicate changes in mitochondrial turnover and stability, a possibility that is discussed at length below.

6.4.2. Old mice are metabolically responsive to low-resistance training

Old mice in the current study exhibited a reduced propensity for exercise and blunted hypertrophic response to chronic low-resistance training. Soffe *et al.* (2016) detailed the running habits of each cohort and noted both young exercise groups exhibited two running peaks throughout the night, whereas older mice showed only an initial activity peak and then ceased activity. The reasons for this distinct exercise pattern are not clear but it was suggested this is reflective of an overall reduced endurance capacity or blunted testosterone response, both of which are important considerations when prescribing exercise to aged humans. Despite this, these mice exhibited comparable metabolic adaptations to low-resistance training as their younger, more active counterparts. Extrapolation from younger high-resistance-trained mice suggests that resistance level is a key determinant in the higher COXIV content and fibre-type shifting. Citrate synthase instead shows a plateau, and in old mice correlates with volume rather than resistance level of training. Lack of correlation between cumulative running distance and citrate synthase activity in young mice may be explained by increased propensity for running in the younger cohort resulting in a plateau of citrate synthase adaptation.

A higher potential for mitochondrial fission in low-resistance-trained mice was indicated by upregulation of fission marker, MiD49, and suggests an enhanced turnover rate of damaged mitochondrial components. It is unclear whether this indicates an increase in mitochondrial damage necessitating higher turnover, or simply a more efficient machinery

with no overall increase in damage. This trend was not continued in high-resistance exercise, with comparable levels of MiD49 detected in sedentary and high-resistance-trained young mice. Wyckelsma *et al.* (2017) previously postulated that higher MiD49 in active older humans relative to younger counterparts was a compensatory mechanism in response to a less healthy aged mitochondrial pool, although that was seen along with an increase in MFN-2 also which was not the case in the current study. The subsequent decreased MiD49 following HIIT training of those active but untrained aged adults reported by Wyckelsma *et al.* (2017) may explain the high-resistance results shown in the current study. That is, a sufficiently high intensity exercise protocol may improve the overall health of the mitochondrial pool and reduce the need for fission and subsequent mitophagy.

Mitochondrial fusion proteins, MFN-2 and OPA-1, showed differential changes in the current study. No overall changes were detected in MFN-2 as a result of ageing or exercise. This finding is in contrast with previous studies of MFN-2 in aged mouse muscle. Sebastian *et al.* (2016) reported a lower MFN-2 in skeletal muscle of 22-month-old sedentary mice compared with muscle taken from 6-month-old controls. Studies of muscle biopsies taken from elderly sedentary humans have however shown no changes in MFN-2 protein compared with muscle from younger counterparts (Joseph *et al.*, 2012). One potential source of variation is the normalisation of prior measurements to the housekeeping protein, tubulin. Murphy and Lamb (2013) have previously raised concerns regarding the usage of apparently stable proteins which may in fact be altered with ageing or other confounding factors. Variability between model organisms and the target organism, as well as between similar model organisms, indicate the need to interpret and extrapolate independent results cautiously.

OPA-1 showed an overall lower content in old mice which was responsive to both low- and high-resistance training. It must be noted that OPA-1 is involved in distinct pathways other than mitochondrial fusion and the likelihood of these changes reflecting a true increase in fusion must be interrogated. A review of acute and chronic exercise interventions of varying intensity in both rodent and human subjects show no instance of increased OPA-1 in the absence of changes in MFN-2 (Trewin *et al.*, 2018). Further, Song *et al.* (2009) demonstrated that mitochondrial fusion is a sequential and distinct process wherein MFN-2 mediated fusion of the outer mitochondrial membrane precedes OPA-1 mediated fusion of the inner membrane. Changes in both MFN-2 and OPA-1 are more frequently reported in studies involving high-intensity exercise in both rodents and humans (Trewin *et al.*, 2018); it is plausible that the voluntary exercise utilised in the current study is below the intensity threshold to upregulate fusion. Taken in conjunction with the lack of changes detected in MFN-2, we suggest that OPA-1 variation in the current study is reflective of a distinct function outside of mitochondrial fusion. Frezza *et al.* (2006) describe a fusion-independent function of OPA-1 in the remodelling of mitochondrial cristae, which confers protection against apoptotic disassembly. Lower abundance of OPA-1 described in sedentary, but not active, aged humans have been correlated with muscle mass (Tezze *et al.*, 2017). It is possible that the lower OPA-1 we detected in old mice, and the subsequent higher content in low-resistance-trained mice, are reflective of changes in the fusion-independent remodelling of cristae. Whilst our intervention was not sufficient to restore muscle mass, the increased OPA-1 may indicate a shift towards a less atrophy-susceptible muscle phenotype in old mice and warrants further investigation.

Reduced susceptibility to atrophy is also supported by a reduction in the proportion of type IIB fibres. Fast and slow fibre types are differentially preserved, with fast fibres more

susceptible to wasting in most forms of muscle atrophy; the proposed underlying mechanisms of this are succinctly reviewed in Ciciliot *et al.* (2013). A shift towards slower muscle phenotypes in old active mice is an indication that old mice maintain their muscle plasticity, albeit without inducing anabolic remodelling. The lower abundance of faster fibre types may be beneficial in preserving muscle mass over a longer time course.

The changes in mitochondrial content, function, and turnover described here, whilst modest, provide an encouraging perspective on exercise interventions in ageing. Although previous studies have demonstrated similar responses in old rodents, the exercise interventions utilised have often relied on strenuous, exhaustive exercise (Young *et al.*, 1983) or were initiated prior to the onset of sarcopenia (White *et al.*, 2016). The ability for sarcopenic muscle to adapt to moderate levels of low intensity exercise provides a valid translational option for interventions in older, sedentary humans.

6.4.3. Mitochondrial content and activity are lower in sedentary mice

Changes observed due to LR and HR training in the current study are arguably best framed as changes observed due to sedentary behaviour. Both young and old sedentary mice in the current study exhibited lower COXIV protein abundance, citrate synthase activity, and faster fibre type distributions. Whilst it is encouraging to note that old mice maintain plasticity in their ability to adapt to low-resistance training, the key risk factor observed for impaired mitochondrial content and function is a sedentary lifestyle (Booth *et al.*, 2012; Whitham & Febbraio, 2016). The implications for this are two-fold. The work presented here adds support to the body of evidence that sedentary behaviour is a major risk factor for metabolic disease in all individuals, but particularly in the more vulnerable cohort of sarcopenic older adults. In addition to this, the dysregulation of mitochondrial content and activity observed in

sedentary young mice raise issues with the current standard housing option for experimental animals. Using sedentary mice as a baseline control, particularly when investigating muscle mass and metabolism, is overlooking the pathological dysregulation present in this model. Xu *et al.* (2018) additionally detail perturbations to calcium-handling and glycogen metabolism in sedentary rats versus rats housed with voluntary access running wheels.

Biological variability in the uptake of voluntary running was observed in this study and previous voluntary running models (Xu *et al.*, 2018). Whilst having to account for this confounding factor adds a level of complexity in study design, using a housing model which enables mice to partake in their natural running behaviours will likely have benefits in establishing a healthier metabolic baseline. Additionally, the conditions routinely imposed on experimental rodents are known to induce stress, with broad physiological implications which can be at least partially mediated by allowing rodents a perception of control over their environment (Gaskill & Garner, 2017). Enriching their environment with voluntary-access running wheels is thus an important ethical consideration which may also reduce confounding variables. It should be noted that exercised mice are often housed individually for data collection purposes, however this too poses behavioural changes and ethical concerns; markers of depression are evident in individually housed female mice (Martin & Brown, 2010) and male mice preference social contact over environmental enrichment, including nesting materials (Van Loo *et al.*, 2004). Experimental design should be adjusted to take these considerations into account.

6.4.4. Autophagy is altered in old mice

Compared to young, non-exercised mice, total AMPK and ULK were not different in old or exercised mice in the current study. The activation of each of these kinases was not directly

measured due to an inability to confidently validate antibodies for the phosphorylated form of each protein. Phosphorylation of Acetyl-CoA, a substrate of AMPK, was measured instead, as an indirect measure of AMPK activation. Whilst no overall changes were detected in the ratio of pAcetyl-CoA to total Acetyl-CoA across groups, there was significantly less pAcetyl-CoA relative to total protein in old mice. Total Acetyl-CoA relative to total protein was likewise approaching to be significantly less in old mice. Acetyl-CoA has been proposed as a master regulator of autophagy, with depletion of cytosolic Acetyl-CoA associated with induction of autophagy (Mariño *et al.*, 2014). The subcellular localisation of Acetyl-CoA was not measured in the current study but may provide further insight into the outcomes associated with reduced Acetyl-CoA and pAcetyl-CoA in old mice.

Both LC3BII:I ratio and total LC3BII relative to total protein were reduced in old mice. Measurements of LC3B as a marker of autophagic flux are notoriously difficult in models lacking adequate inhibitors, as was the case in the current retrospective study. Mizushima and Yoshimori (2007) provide a succinct review of the limitations and best practice for interpreting LC3B data in such a situation. Whilst it cannot be ascertained whether the increased LC3BII detected is due to an increase in autophagy or a block in the subsequent degradation of LC3BII itself, it can be said that there is an alteration of autophagic flux due to ageing. The accumulation of p62, a substrate of LC3B, occurs when there is suppression of autophagy and can be used to more accurately assess flux (Bjorkoy *et al.*, 2009). Two distinct isoforms of p62 were detected in the current study – both a full-length variant at ~62 kDa as expected, as well as a shorter isoform at ~48 kDa. This shorter p62 product has been described previously as a cleavage product following caspase-8 activation (Sanchez-Garrido *et al.*, 2018; Zhao *et al.*, 2020). Sanchez-Garrido *et al.* (2018) proposed that this cleaved form of p62 serves a differential function to full-length p62 in a human-donor derived skin fibroblasts cell model;

cleaved p62 was shown to enhance the ability of leucine-availability to stimulate cellular growth via the mTORC pathway. Whilst no overall changes were observed in full length p62 in old mice relative to young controls, the shorter isoform was significantly increased in muscle from old mice. It is unclear from the current study whether this indicates an accumulation of p62 due to defective autophagic flux or if it serves an ulterior purpose, such as an upregulation of the metabolic-sensing function described by Sanchez-Garrido *et al.* (2018). Interestingly, the mTORC pathway has been paradoxically implicated as a driver of sarcopenia in ageing rats (Joseph *et al.*, 2019); it is possible that accumulation of this cleaved p62 product may represent one mechanism by which mTORC is pathologically active in old rodents.

6.4.5. Low-resistance training is not sufficient to correct autophagy changes in old mice

Whilst the voluntary low-resistance training utilised in the current study was able to generate detectable changes in proteins related to mitochondrial content, function, and dynamics, it was unable to reverse the age-associated perturbations detected in autophagic intermediates. Although it is optimistic to observe preservation of mitochondrial plasticity in old mice, it is true that most of the baseline defects could be attributed to sedentary behaviour rather than an inherent mitochondrial dysfunction present in old mice. This was not the case with autophagic flux changes which were associated primarily with ageing. It is possible that a more intense or prolonged intervention is necessary to prevent or counteract these changes. White *et al.* (2016) describe such a study, wherein C57BL/6 mice were subject to voluntary resistance wheel exercise from the age of 15 months (approximate middle-age) and sustained for 34 weeks. Unlike the current study, these old mice showed preservation of muscle mass in the hindlegs. Autophagy was shown to be increased in that intervention as indicated by increased LC3BII:LC3BI ratios following exercise with no associated increase in

p62 accumulation (White *et al.*, 2016). Direct comparison between that and the current study are however complicated by slight variation in the assessment of these autophagic flux markers, e.g. soluble LC3B vs. total LC3B. Given the already complex and indirect nature of these measurements, we are hesitant to directly compare these autophagic flux changes, however given the hypertrophic response it is likely that this intervention that occurred at the earlier age has more widespread outcomes.

Although potential changes in autophagosome assembly and autophagic flux are evident in old mice, they do not appear to be strongly impacted by low-resistance training. Limitations of the current study design make it difficult to ascertain whether these changes are due to autophagic upregulation or impaired degradation of autophagic substrates (Mizushima & Yoshimori, 2007). A downward trend of p62 accumulation in younger mice in response to increased resistance levels suggests that higher resistance training may be necessary to counteract the age-associated changes seen in the current study.

6.5. Conclusions

Overall, the current study demonstrates that low-resistance exercise training initiated late in life following a history of sedentary behaviour is sufficient to induce adaptations in mitochondrial content, and fibre type, but not on markers of autophagy. These changes occur independently of muscle hypertrophy, which is blunted in old mice relative to their younger counterparts. Encouragingly, the changes observed in low-resistance-trained old mice are present despite a reduced capacity or willingness to partake in voluntary low-resistance training relative to young mice. This work highlights the necessity of adequate housing to enable experimental mice to partake in voluntary exercise, as current standards model pathological sedentary behaviour. Most importantly, this work has positive implications for

the efficacy of moderate exercise interventions in older sedentary humans, whom often have reduced exercise tolerance.

References

- Ashrafi G & Schwarz TL. (2013). The pathways of mitophagy for quality control and clearance of mitochondria. *Cell Death Differ* **20**, 31-42.
- Baehr LM, West DWD, Marcotte G, Marshall AG, De Sousa LG, Baar K & Bodine SC. (2016). Age-related deficits in skeletal muscle recovery following disuse are associated with neuromuscular junction instability and ER stress, not impaired protein synthesis. *Aging* **8**, 127-146.
- Bjorkoy G, Lamark T, Pankiv S, Overvatn A, Brech A & Johansen T. (2009). Monitoring autophagic degradation of p62/SQSTM1. *Methods Enzymol* **452**, 181-197.
- Booth FW, Roberts CK & Laye MJ. (2012). Lack of exercise is a major cause of chronic diseases. *Compr Physiol* **2**, 1143-1211.
- Brzeszczynska J, Meyer A, McGregor R, Schilb A, Degen S, Tadini V, Johns N, Langen R, Schols A, Glass DJ, Roubenoff R, Ross JA, Fearon KCH, Greig CA & Jacobi C. (2017). Alterations in the in vitro and in vivo regulation of muscle regeneration in healthy ageing and the influence of sarcopenia. *J Cachexia Sarcopenia Muscle* 10.1002/jcsm.12252.
- Chan DC. (2006). Dissecting mitochondrial fusion. *Dev Cell* **11**, 592-594.
- Chen H & Chan DC. (2004). Mitochondrial dynamics in mammals. *Curr Top Dev Biol* **59**, 119-144.
- Ciciliot S, Rossi AC, Dyar KA, Blaauw B & Schiaffino S. (2013). Muscle type and fiber type specificity in muscle wasting. *Int J Biochem Cell Biol* **45**, 2191-2199.
- Distefano G, Standley RA, Dubé JJ, Carnero EA, Ritov VB, Stefanovic-Racic M, Toledo FGS, Piva SR, Goodpaster BH & Coen PM. (2017). Chronological Age Does not Influence Ex-vivo Mitochondrial Respiration and Quality Control in Skeletal Muscle. *J Gerontol A Biol Sci Med Sci* **72**, 535-542.
- Egan DF, Shackelford DB, Mihaylova MM, Gelino S, Kohnz RA, Mair W, Vasquez DS, Joshi A, Gwinn DM, Taylor R, Asara JM, Fitzpatrick J, Dillin A, Viollet B, Kundu M, Hansen M & Shaw RJ. (2011). Phosphorylation of ULK1 (hATG1) by AMP-activated protein kinase connects energy sensing to mitophagy. *Science* **331**, 456-461.
- Frezza C, Cipolat S, Martins de Brito O, Micaroni M, Beznoussenko GV, Rudka T, Bartoli D, Polishuck RS, Danial NN, De Strooper B & Scorrano L. (2006). OPA1 controls apoptotic cristae remodeling independently from mitochondrial fusion. *Cell* **126**, 177-189.
- Gaskill B & Garner J. (2017). Stressed out: Providing laboratory animals with behavioral control to reduce the physiological effects of stress. *Lab Animal* **46**, 142-145.

- Glick D, Barth S & Macleod KF. (2010). Autophagy: cellular and molecular mechanisms. *J Pathol* **221**, 3-12.
- Hardie DG & Carling D. (1997). The AMP-activated protein kinase. Fuel gauge of the mammalian cell? *Eur J Biochem* **246**, 259-273.
- Herzig S & Shaw RJ. (2018). AMPK: guardian of metabolism and mitochondrial homeostasis. *Nat Rev Mol Cell Biol* **19**, 121-135.
- Holloszy JO. (1967). Biochemical adaptations in muscle. Effects of exercise on mitochondrial oxygen uptake and respiratory enzyme activity in skeletal muscle. *J Biol Chem* **242**, 2278-2282.
- Ji LL & Kang C. (2015). Role of PGC-1 α in Sarcopenia: Etiology and Potential Intervention - A Mini-Review. *Gerontology* **61**, 139-148.
- Joseph AM, Adihetty PJ, Buford TW, Wohlgemuth SE, Lees HA, Nguyen LM, Aranda JM, Sandesara BD, Pahor M, Manini TM, Marzetti E & Leeuwenburgh C. (2012). The impact of aging on mitochondrial function and biogenesis pathways in skeletal muscle of sedentary high- and low-functioning elderly individuals. *Aging Cell* **11**, 801-809.
- Joseph GA, Wang S, Zhou W, Kimble G, Tse H, Eash J, Shavlakadze T & Glass DJ. (2019). Inhibition of mTORC1 signaling in aged rats counteracts the decline in muscle mass and reverses multiple parameters of muscle signaling associated with sarcopenia. *bioRxiv* 10.1101/591891, 591891.
- Kim Y, Triolo M & Hood DA. (2017). Impact of Aging and Exercise on Mitochondrial Quality Control in Skeletal Muscle. *Oxid Med Cell Longev* **2017**, 3165396-3165396.
- Knutti D, Kressler D & Kralli A. (2001). Regulation of the transcriptional coactivator PGC-1 via MAPK-sensitive interaction with a repressor. *Proc Natl Acad Sci U S A* **98**, 9713-9718.
- Koshiba T, Detmer SA, Kaiser JT, Chen H, McCaffery JM & Chan DC. (2004). Structural basis of mitochondrial tethering by mitofusin complexes. *Science* **305**, 858-862.
- Lanza IR, Short DK, Short KR, Raghavakaimal S, Basu R, Joyner MJ, McConnell JP & Nair KS. (2008). Endurance exercise as a countermeasure for aging. *Diabetes* **57**, 2933-2942.
- Lee JW, Park S, Takahashi Y & Wang HG. (2010). The association of AMPK with ULK1 regulates autophagy. *PLoS One* **5**, e15394.
- Lin J, Wu H, Tarr PT, Zhang CY, Wu Z, Boss O, Michael LF, Puigserver P, Isotani E, Olson EN, Lowell BB, Bassel-Duby R & Spiegelman BM. (2002). Transcriptional co-activator PGC-1 alpha drives the formation of slow-twitch muscle fibres. *Nature* **418**, 797-801.

- Luo L, Lu AM, Wang Y, Hong A, Chen Y, Hu J, Li X & Qin ZH. (2013). Chronic resistance training activates autophagy and reduces apoptosis of muscle cells by modulating IGF-1 and its receptors, Akt/mTOR and Akt/FOXO3a signaling in aged rats. *Exp Gerontol* **48**, 427-436.
- Mariño G, Pietrocola F, Eisenberg T, Kong Y, Malik Shoib A, Andryushkova A, Schroeder S, Pendl T, Harger A, Niso-Santano M, Zamzami N, Scoazec M, Durand S, Enot David P, Fernández Álvaro F, Martins I, Kepp O, Senovilla L, Bauvy C, Morselli E, Vacchelli E, Bennetzen M, Magnes C, Sinner F, Pieber T, López-Otín C, Maiuri Maria C, Codogno P, Andersen Jens S, Hill Joseph A, Madeo F & Kroemer G. (2014). Regulation of Autophagy by Cytosolic Acetyl-Coenzyme A. *Mol Cell* **53**, 710-725.
- Martin AL & Brown RE. (2010). The lonely mouse: verification of a separation-induced model of depression in female mice. *Behav Brain Res* **207**, 196-207.
- Maruyama T & Noda NN. (2018). Autophagy-regulating protease Atg4: structure, function, regulation and inhibition. *J Antibiot* **71**, 72-78.
- Mizushima N & Yoshimori T. (2007). How to interpret LC3 immunoblotting. *Autophagy* **3**, 542-545.
- Murphy RM & Lamb GD. (2013). Important considerations for protein analyses using antibody based techniques: down-sizing Western blotting up-sizes outcomes. *J Physiol* **591**, 5823-5831.
- National Academy of Science. (2016). Retraction for Wenz et al., Increased muscle PGC-1 α expression protects from sarcopenia and metabolic disease during aging. *Proc Natl Acad Sci U S A* **113**, E8502-E8502.
- Palmer CS, Osellame LD, Laine D, Koutsopoulos OS, Frazier AE & Ryan MT. (2011). MiD49 and MiD51, new components of the mitochondrial fission machinery. *EMBO Rep* **12**, 565-573.
- Peterson CM, Johannsen DL & Ravussin E. (2012a). Skeletal muscle mitochondria and aging: a review. *J Aging Res* **2012**, 194821.
- Peterson CM, Johannsen DL & Ravussin E. (2012b). Skeletal muscle mitochondria and aging: a review. *J Aging Res* **2012**, 194821-194821.
- Pette D & Spamer C. (1986). Metabolic properties of muscle fibers. *Fed Proc* **45**, 2910-2914.
- Qaisar R, Bhaskaran S & Van Remmen H. (2016). Muscle fiber type diversification during exercise and regeneration. *Free Radic Biol Med* **98**, 56-67.
- Reznick RM, Zong H, Li J, Morino K, Moore IK, Yu HJ, Liu ZX, Dong J, Mustard KJ, Hawley SA, Befroy D, Pypaert M, Hardie DG, Young LH & Shulman GI. (2007). Aging-associated reductions in AMP-activated protein kinase activity and mitochondrial biogenesis. *Cell Metab* **5**, 151-156.

- Safdar A, Hamadeh MJ, Kaczor JJ, Raha S, Debeer J & Tarnopolsky MA. (2010). Aberrant mitochondrial homeostasis in the skeletal muscle of sedentary older adults. *PLoS One* **5**, e10778-e10778.
- Sanchez-Garrido J, Sancho-Shimizu V & Shenoy AR. (2018). Regulated proteolysis of p62/SQSTM1 enables differential control of autophagy and nutrient sensing. *Sci Signal* **11**, eaat6903.
- Sebastian D, Sorianello E, Segales J, Irazoki A, Ruiz-Bonilla V, Sala D, Planet E, Berenguer-Llargo A, Munoz JP, Sanchez-Feutrie M, Plana N, Hernandez-Alvarez MI, Serrano AL, Palacin M & Zorzano A. (2016). Mfn2 deficiency links age-related sarcopenia and impaired autophagy to activation of an adaptive mitophagy pathway. *EMBO J* **35**, 1677-1693.
- Soffe Z, Radley-Crabb HG, McMahon C, Grounds MD & Shavlakadze T. (2016). Effects of loaded voluntary wheel exercise on performance and muscle hypertrophy in young and old male C57Bl/6J mice. *Scand J Med Sci Sports* **26**, 172-188.
- Song Z, Ghochani M, McCaffery JM, Frey TG & Chan DC. (2009). Mitofusins and OPA1 mediate sequential steps in mitochondrial membrane fusion. *Mol Biol Cell* **20**, 3525-3532.
- Tezze C, Romanello V, Desbats MA, Fadini GP, Albiero M, Favaro G, Ciciliot S, Soriano ME, Morbidoni V, Cerqua C, Loeffler S, Kern H, Franceschi C, Salvioli S, Conte M, Blaauw B, Zampieri S, Salviati L, Scorrano L & Sandri M. (2017). Age-Associated Loss of OPA1 in Muscle Impacts Muscle Mass, Metabolic Homeostasis, Systemic Inflammation, and Epithelial Senescence. *Cell Metab* **25**, 1374-1389.e1376.
- Trewin AJ, Berry BJ & Wojtovich AP. (2018). Exercise and Mitochondrial Dynamics: Keeping in Shape with ROS and AMPK. *Antioxidants (Basel)* **7**, 7.
- Van Loo PL, Van de Weerd HA, Van Zutphen LF & Baumans V. (2004). Preference for social contact versus environmental enrichment in male laboratory mice. *Lab Anim* **38**, 178-188.
- Wenz T, Rossi SG, Rotundo RL, Spiegelman BM & Moraes CT. (2009). Increased muscle PGC-1alpha expression protects from sarcopenia and metabolic disease during aging. *Proc Natl Acad Sci U S A* **106**, 20405-20410. (Retraction published 20419 Dec 22016, Proc Natl Acad Sci U S A. 22016;20113(20452):E28502. doi:20410.21073/pnas.1619713114).
- White Z, Terrill J, White RB, McMahon C, Sheard P, Grounds MD & Shavlakadze T. (2016). Voluntary resistance wheel exercise from mid-life prevents sarcopenia and increases markers of mitochondrial function and autophagy in muscles of old male and female C57BL/6J mice. *Skelet Muscle* **6**, 45-45.
- Whitham M & Febbraio MA. (2016). The ever-expanding myokinome: discovery challenges and therapeutic implications. *Nat Rev Drug Discov* **15**, 719-729.
- Wyckelsma VL, Levinger I, McKenna MJ, Formosa LE, Ryan MT, Petersen AC, Anderson MJ & Murphy RM. (2017). Preservation of skeletal muscle mitochondrial content in older adults: relationship

between mitochondria, fibre type and high-intensity exercise training. *J Physiol* **595**, 3345-3359.

Xu H, Lamb GD & Murphy RM. (2017). Changes in contractile and metabolic parameters of skeletal muscle as rats age from 3 to 12 months. *J Muscle Res Cell Motil* **38**, 405-420.

Xu H, Ren X, Lamb GD & Murphy RM. (2018). Physiological and biochemical characteristics of skeletal muscles in sedentary and active rats. *J Muscle Res Cell Motil* **39**, 1-16.

Yang Y-p, Hu L-f, Zheng H-f, Mao C-j, Hu W-d, Xiong K-p, Wang F & Liu C-f. (2013). Application and interpretation of current autophagy inhibitors and activators. *Acta Pharmacol Sin* **34**, 625-635.

Young JC, Chen M & Holloszy JO. (1983). Maintenance of the adaptation of skeletal muscle mitochondria to exercise in old rats. *Med Sci Sports Exerc* **15**, 243-246.

Zhao Y, Zhu Q, Bu X, Zhou Y, Bai D, Guo Q, Gao Y & Lu N. (2020). Triggering apoptosis by oroxylin A through caspase-8 activation and p62/SQSTM1 proteolysis. *Redox Biology* **29**, 101392.

Chapter 7

Concluding Remarks and Future Directions

This thesis aimed to explore the role of TWEAK-Fn14 signalling in both acute and chronic damaged skeletal muscle. Chapter 3 showed the successful generation of a crosslinked α -Fn14 antibody which was characterised *in vitro* to act as an agonistic activator of Fn14 independently of TWEAK stimulation, a novel finding for Fn14 antibodies. A major limitation in characterising the activity profile of α -Fn14 001X was the inability to validate antibodies against substrates of the NF κ B pathway. Whilst this information would provide meaningful mechanistic insight into TWEAK-Fn14 signalling, the information which can be derived from *in vitro* characterisation is inherently limited in its translation to *in vivo* models, or more importantly, humans. Characterisation of signalling substrates associated with TWEAK-Fn14 would be best explored in *in vivo* models that were not as severely degraded as the ones obtained in the current thesis research.

Despite limitations in characterising the signalling pathway substrates, downstream utilisation of α -Fn14 001X, and to a lesser extent, α -Fn14 001, in the acute notexin-injury model served to demonstrate the positive-feedback regulation of Fn14 and a relationship with the master regulator of myogenesis, MyoD, as described in Chapter 5. Although the severity of the injury model examined precluded further conclusions on the ability of this antibody to alter the recovery timeline following notexin-injury, changes in MyoD expression and several muscle-specific structural proteins were sufficient to indicate that Fn14 is active in the skeletal muscle remodelling pathway following acute injury. This conclusion is in line with previous work on Fn14 in skeletal muscle remodelling (Raue *et al.*, 2012; Raue *et al.*, 2015; Pasiakos *et al.*, 2018).

The severity of the injury model itself raised important ethical and reproducibility questions regarding the use of animal injury models (Chapter 4). A simple PubMed search

shows that when compared to other myotoxic agents such as barium chloride or cardiotoxin, publications featuring notexin usage have tapered off in the last few years. The reasons for this are not clear from the literature but may be in part due to unpredictability in the injury model causing notexin to fall out of favour. Further work is warranted in this area to elucidate the precise cause of the unexpected adverse results and inform the selection of injury models in future research, as well as reconcile previous results obtained from varying models. Particular attention should be paid to the anaesthesia and analgesia utilised. Information on the use of anaesthesia and analgesia in animal models is currently limited by shortcomings in the reporting of methods used in animal research which often omit this crucial information. The findings in Chapter 6 also highlight the harmful impacts of sedentary behaviour which is frequently inadvertently modelled in experimental animals and argues for provisions for more suitable and natural housing, including access to voluntary exercise and social enrichment.

Examination of TWEAK and Fn14 in muscle taken from old and chronically low-resistance trained mice provided insight into the role of this pathway in aging-associated muscle atrophy. In the current study, no significant correlations were observed between either TWEAK or Fn14 and the muscle mass of the mice. We concluded that TWEAK-Fn14 was unlikely to play a major role in the loss of muscle mass in these animals and that TWEAK-Fn14 were not responsive to low-resistance exercise intervention. Chapter 6 therefore shifted focus and instead was an exploration of mitochondrial content and dynamics, as well as autophagy, as functions of aging and exercise intervention. Encouragingly, low-resistance exercise initiated late in life was shown to induce adaptations in fibre type, mitochondrial content, and mitochondrial dynamics similar to those observed in their younger and more active counterparts. Although independent of TWEAK-Fn14, this finding is relevant to the current thesis as a means of understanding how skeletal muscle remodelling occurs in chronic

atrophy, in this instance, aging. It also highlights the pathological outcomes of chronic sedentary behaviour which are likely to play a major role in what is often perceived or interpreted as aging-associated changes. Despite exhibiting adaptations in fibre type and mitochondria, old mice showed age-associated changes in autophagy markers which were not impacted by low-resistance exercise training. These findings are an important step towards optimising exercise prescription as intervention for aged and chronically sedentary humans. Future work should incorporate functional testing of muscle to determine how impactful these adaptations are.

Overall, this thesis demonstrated a role of Fn14 signalling in the remodelling of skeletal muscle following acute muscle injury. TWEAK and Fn14 were not determined to be major drivers of chronic aging-associated muscular atrophy in the context of this study, however the work shown here highlights sustained adaptability of aged skeletal muscle in response to low intensity interventions which may be missed when assessing muscle mass alone. The novel antibody intervention described in this thesis is capable of activating Fn14 independently of TWEAK. Whilst further work is needed to optimise this antibody and fully characterise the downstream myogenic outcomes, it provides valuable insight into the regulatory mechanisms of Fn14 *in vivo*, namely a positive feedback loop which may drive expression of key myogenic regulatory factors.

References

- Pasiakos SM, Berryman CE, Carbone JW, Murphy NE, Carrigan CT, Bamman MM, Ferrando AA, Young AJ & Margolis LM. (2018). Muscle Fn14 gene expression is associated with fat-free mass retention during energy deficit at high altitude. *Physiol Rep* **6**, e13801.
- Raue U, Jemiolo B, Yang Y & Trappe S. (2015). TWEAK-Fn14 pathway activation after exercise in human skeletal muscle: insights from two exercise modes and a time course investigation. *J Appl Physiol* **118**, 569-578.
- Raue U, Trappe TA, Estrem ST, Qian H-R, Helvering LM, Smith RC & Trappe S. (2012). Transcriptome signature of resistance exercise adaptations: mixed muscle and fiber type specific profiles in young and old adults. *J Appl Physiol* **112**, 1625-1636.

Appendix I

COVID-19 Impact Statement

This appendix details interruptions to working conditions in Melbourne, Victoria during the COVID-19 pandemic and acknowledges gaps in the thesis that resulted from restricted access to the laboratory during this time.

Stage 3 restrictions (stay at home orders, only four reasons to leave home including exercise, essential work or study, caregiving, and shopping for necessities) was imposed in Melbourne from 23rd March – 1st June and again from 9th July. I was granted limited access to the lab facilities starting 5th August, however this coincided with introduction of stage 4 restrictions (stay at home orders with 8pm-5am curfew and reduction in essential worker classifications) due to a second wave of infections in Melbourne with a proposed expiry date of 13th September, this stage of restrictions has since been extended to 28th September. At this time, it was decided that my return to the lab was classed as ‘not essential’ according to Department of Health and Human Services guidelines.

The gaps identified in this thesis represent incomplete data that could not be pursued further in a timely manner. Appendix II includes these preliminary findings which are absent from Chapter 3 and Chapter 5. These data are incomplete and under normal circumstances would warrant further exploration. It is presented here cautiously to illustrate the direction that was intended for this research. Whilst this data would present a more complete picture, we do not believe that the absence alters the overall findings of this thesis and does not justify a return to lab facilities during the COVID-19 pandemic.

Appendix II

Preliminary Data

Appendix Summary

This appendix outlines incomplete experiments or omitted data that could not feasibly be pursued in the current restrictions resulting from COVID-19 in Melbourne, Victoria (Appendix I). The data shown here is not suitable for inclusion in the main thesis but is presented here for context and completeness.

II.a. Introduction

These preliminary experiments attempt to characterise the distinct NF κ B signalling pathways in C2C12 myotubes treated with sTWEAK, α -Fn14 001, or the α -Fn14 001X mimetic (α -Fn14 001 plus Protein G), shown here in a western blot where n = 1. The data set of C2C12 cells differentiated with 500 ng of sTWEAK was not included on the initial blot due to space limitations and could not be repeated due to lab access restrictions. Whilst these data may provide a more complete picture of the activity of TWEAK-Fn14 signalling, it is unlikely to alter the outcomes observed *in vivo* in Chapter 5. It should also be noted that C2C12 myotubes and other *in vitro* skeletal muscle models are heterogenic in their transcriptomic and metabolic profiles (Abdelmoez *et al.*, 2020). For this reason, the insights provided would be at best an approximation and were determined not worth pursuing further at this time.

Also presented here is cell count data for C2C12 proliferation experiments from Chapter 3. These data represent an n of 1 and, as above, is inherently limited in its translation to *in vivo* models but is included for context and completeness. The cell count data could not be included in its current form in the main body of the thesis and is shown here as supplementary to the differentiation data presented in Chapter 3.

Finally, the lack of positive control on the representative blot of Fn14 protein in old and chronically exercised muscle (Chapter 5, Figure 5.3B) is acknowledged as an omission that could not be repeated due to restricted lab access.

II.b. Methods**II.b.i. C2C12 Proliferation Cell Count**

For proliferation assay, 1.5×10^5 cells were seeded in six-well tissue culture plates and cultured at 37°C under 5% CO₂ in DMEM containing 1% penicillin-streptomycin and 10% FBS and either 1 µg/ml 001, 1 µg/ml 001 plus 1 µg/ml Protein-G (ThermoFisher), 1 ng/ml sTWEAK, 100 ng/ml sTWEAK, or 500 ng/ml sTWEAK. Cells were harvested and cell numbers counted to measure proliferation rate at 24, 48, and 72 hours.

Proliferation was assessed using live and total cell count from each time point described in Chapter 3. Cell count was determined using a TC20 Automated Cell Counter (BioRad) with Trypan Blue stain. Live cell percentage was verified by visual inspection under light microscopy. Representative images of plated cells at each time point were also captured by light microscopy prior to harvesting (Figure II.1).

II.b.ii. NFκB Activation in C2C12 Cells

Involvement of non-canonical NFκB was assessed by western blotting of total p100-p52 relative to total protein in C2C12 homogenates described in Chapter 3. Activation of non-canonical NFκB was assessed by measuring conversion of p100 to p52. Canonical NFκB was assessed using p105/p50 in proliferating C2C12 homogenates described in Chapter 3. Lab access restrictions prevented assessment of p105/p50 in differentiating C2C12 homogenates, however given the limited translatability of C2C12-derived data to mouse models, and further, to humans, we determined that this data would be desirable however not essential (discussed further in Appendix II).

II.c. *Results*

II.c.i. Proliferation Assay

Semi-quantitative assessment of C2C12 proliferation cultured with varying concentrations of sTWEAK and/or α -Fn14 001 or α -Fn14 001X mimetic (α -Fn14 001 plus Protein G) was performed by light microscopy and automated cell counting with Trypan Blue (Figure II.1). All conditions showed time-dependent increases in cell density with 72h microscopy showing a mixture of proliferating myoblasts, apoptotic cells, and immature myotubes. A modest increase in proliferation was observed in α -Fn14 001 and α -Fn14 001 plus Protein G treated cultures.

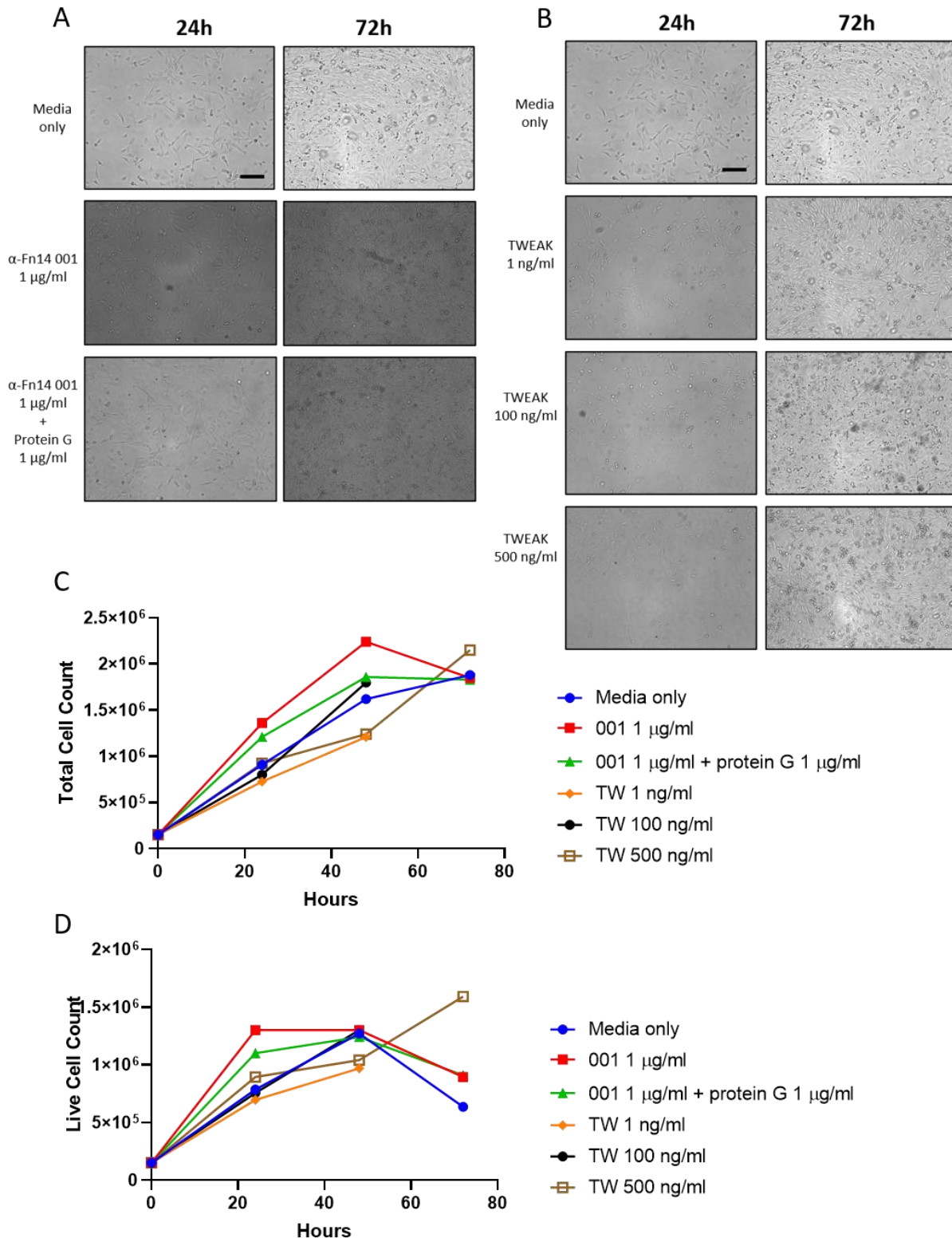


Figure II.1: Proliferation of C2C12 myotubes treated with α -Fn14 or soluble TWEAK (sTWEAK). Light microscopy images of myoblast proliferation in α -Fn14 (A) and sTWEAK (B) treated cell cultures. 24-hour images show scarce myoblasts whilst 72-hour cultures show densely packed myoblasts with immature myotubes beginning to form. 72-hour cultures in all conditions show non-adherent cells. (C) Cell count of total cells in cultures across time points for indicated treatments (001 = α -Fn14 001; TW = TWEAK) at indicated concentrations. (D) Live cell counts as determined by Trypan Blue stain. Scale bar 450 μ m.

II.c.ii. NF κ B Activation in C2C12 Model Cells

Involvement and activation of the non-canonical NF κ B pathway was assessed by measuring both total p100-p52 relative to total protein as well as p100 conversion to p52 (Figure II.2 and Figure II.3). Due to these experiments representing an n of 1, no statistical analyses have been performed.

In proliferating cells, a general trend of total p100-p52 decreasing in a time-dependent manner was detected. Total p100-p52 was highest in proliferating cells treated with 500 ng sTWEAK at all time points which did not decrease with incubation time. The conversion of p100 to p52 was likewise seen to decrease in a time-dependent manner with prolonged processing again seen in the 500 ng sTWEAK condition.

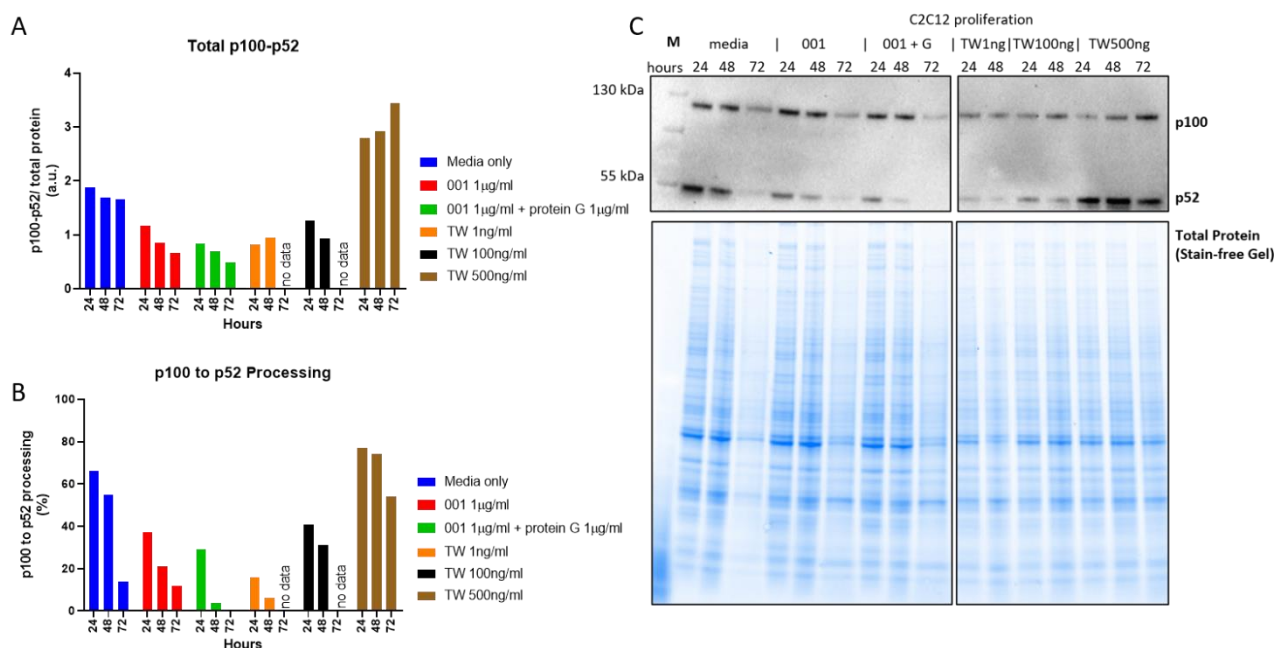


Figure II.2: p100-p52 in proliferation C2C12 myoblasts treated with soluble TWEAK (sTWEAK) and α -Fn14 antibodies. (A) Total p100-p52 expressed relative to total protein abundance. (B) Percentage of total p100-p52 converted to p52. (C) Representative blot of p100-p52 and Stain-Free UV image of total protein content. p100 was detected above below 130 kDa and p52 subunit was detected below the 55 kDa marker (CST 4882, expected molecular weight = 120 kDa and 52 kDa respectively). 001 = α -Fn14 001, 001X = α -Fn14 001X, TW = TWEAK, G = Protein G.

Differentiating cells showed a lower baseline of p100 to p52 conversion in media-only treated cells. A similar trend of increased total p100-p52 and increased p100 to p52 conversion was again seen in 100 ng sTWEAK cells. 500 ng sTWEAK treated differentiating cells were omitted from this blot

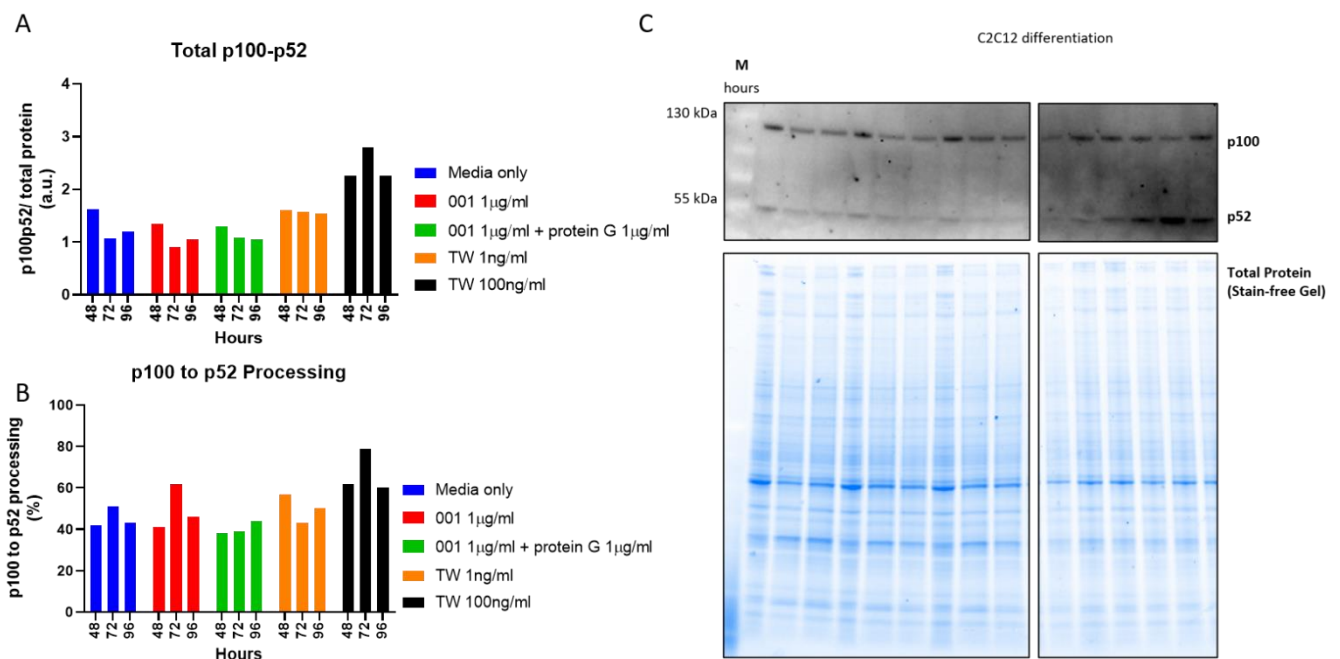


Figure II.3: p100-p52 in differentiating C2C12 myoblasts treated with soluble TWEAK (sTWEAK) and α -Fn14 antibodies. (A) Total p100-p52 expressed relative to total protein abundance. (B) Percentage of total p100-p52 converted to p52. (C) Representative blot of p100-p52 and Stain-Free UV image of total protein content. p100 was detected above below 130 kDa and p52 subunit was detected below the 55 kDa marker (CST 4882, expected molecular weight = 120 kDa and 52 kDa respectively). 001 = α -Fn14 001, 001X = α -Fn14 001X, TW = TWEAK, G = Protein G.

II.d. *Discussion*

II.d.i. *sTWEAK and α -Fn14 Treatments Do Not Prevent Proliferation*

These cell count data, though limited by lack of repetition, suggest that the ability of C2C12 myoblasts to proliferate is not impaired by the addition of either sTWEAK or α -Fn14 antibodies. This is relevant in establishing the pro- or anti-myogenic outcomes of these molecules endogenously or in the downstream *in vivo* treatment of mice. It cannot, however, be determined from this work whether these molecules have an enhancing effect on the proliferation rate of myotubes, as has often been asserted of exogenous TWEAK treatments on various tissues in the literature (Jakubowski *et al.*, 2005; Chen *et al.*, 2012; Zhu *et al.*, 2017).

II.d.ii. *Supraphysiological Dose sTWEAK Strongly Activates Non-Canonical NF κ B*

Whilst no antibody tested in this study could consistently detect the canonical NF κ B substrates, p105-p50, the non-canonical substrate, p100-p52 was able to be detected and measured in C2C12 lysates. The involvement of p100-p52 signalling appears to be greater in differentiated cells, as is expected given the apparent role of non-canonical NF κ B signalling in muscle homeostasis and mitochondrial biogenesis in mature muscle (Bakkar *et al.*, 2008).

Supraphysiological doses of sTWEAK, frequently utilised in the literature when assessing the outcomes of TWEAK-Fn14 activation, were able to strongly activate the non-canonical NF κ B arm. It should be noted that the delineation of canonical and non-canonical is not as straightforward as once postulated, with involvement of typically canonical and non-canonical substrates reported in both arms of NF κ B signalling (Shih *et al.*, 2011). Additional data on typically canonical substrates, p105-p50, may further elucidate detrimental effects of these treatments on myogenesis given the inhibition of differentiation associated with this

pathway (Straughn *et al.*, 2018). However, the value of pursuing the direct substrates to determine pathway involvement is limited without more robust mechanistic models.

What these data do suggest is that TWEAK-dependent activation of NF κ B, whether it be canonical or non-canonical, is robust when using supraphysiological doses of sTWEAK (> 100 ng/ml) when compared to the more physiologically relevant dose of 1 ng/ml (Pascoe *et al.*, 2020). This further highlights the need to critically assess the methodology of previous characterisation of TWEAK-Fn14 signalling when considering the physiological translation.

II.d.iii. α -Fn14 001 and α -Fn14 001X May Activate Fn14 Independently of sTWEAK

The data shown here, supplementary to that shown in Chapter 3, primarily aimed to illustrate that α -Fn14 001X is able to act as an agonistic antibody which can activate Fn14 signalling in the absence of TWEAK. The NF κ B activation data here is a preliminary attempt to measure this substrate activation as a following experiment to the reporter HEK293T NF κ B-GFP cells shown in Chapter 3. Although this was not fully achieved, the activation profile in C2C12 cells of both α -Fn14 001 and α -Fn14 001X appears similar to that of physiological levels of sTWEAK (1 ng/ml). Unlike the data generated from the reporter cells, where α -Fn14 001 behaved in a more inhibitory manner, both α -Fn14 001 and α -Fn14 001X show a similar profile in these preliminary experiments. This further suggests that α -Fn14 001 may naturally form multimeric antibodies *in vivo* which mimic the actions of α -Fn14 001X. These data, in combination with the data presented in Chapter 3, formed sufficient basis to proceed with *in vivo* use of this antibody as an agonist Fn14 antibody.

References

- Abdelmoez AM, Puig LS, Smith JAB, Gabriel BM, Savikj M, Dollet L, Chibalin AV, Krook A, Zierath JR & Pillion NJ. (2020). Comparative profiling of skeletal muscle models reveals heterogeneity of transcriptome and metabolism. *Am J Physiol Cell Physiol* **318**, C615-C626.
- Bakkar N, Wang J, Ladner KJ, Wang H, Dahlman JM, Carathers M, Acharyya S, Rudnicki MA, Hollenbach AD & Guttridge DC. (2008). IKK/NF-kappaB regulates skeletal myogenesis via a signaling switch to inhibit differentiation and promote mitochondrial biogenesis. *J Cell Biol* **180**, 787-802.
- Chen HN, Wang DJ, Ren MY, Wang QL & Sui SJ. (2012). TWEAK/Fn14 promotes the proliferation and collagen synthesis of rat cardiac fibroblasts via the NF-small ka, CyrillicB pathway. *Mol Biol Rep* **39**, 8231-8241.
- Jakubowski A, Ambrose C, Parr M, Lincecum JM, Wang MZ, Zheng TS, Browning B, Michaelson JS, Baetscher M, Wang B, Bissell DM & Burkly LC. (2005). TWEAK induces liver progenitor cell proliferation. *J Clin Invest* **115**, 2330-2340.
- Pascoe AL, Johnston AJ & Murphy RM. (2020). Controversies in TWEAK-Fn14 signaling in skeletal muscle atrophy and regeneration. *Cell Mol Life Sci* 10.1007/s00018-020-03495-x.
- Shih VF-S, Tsui R, Caldwell A & Hoffmann A. (2011). A single NFkB system for both canonical and non-canonical signaling. *Cell Res* **21**, 86-102.
- Straughn AR, Hindi SM, Xiong G & Kumar A. (2018). Canonical NF-kappaB signaling regulates satellite stem cell homeostasis and function during regenerative myogenesis. *J Mol Cell Biol* 10.1093/jmcb/mjy053.
- Zhu C, Zhang L, Liu Z, Li C & Bai Y. (2017). TWEAK/Fn14 interaction induces proliferation and migration in human airway smooth muscle cells via activating the NF-kappaB pathway. *J Cell Biochem* 10.1002/jcb.26525.

Appendix III

Antibodies and Primers

Appendix Summary

The following appendix includes a table of primers and antibodies utilised in this thesis. Troubleshooting efforts undertaken to improve the quality of muscle homogenates used in western blotting are outlined as well as detailing validation work on MyoD and TWEAK antibodies.

III.a. **Antibody details****Table III.1: Antibody details.** Full details of primary antibodies used for western blotting. CST, Cell Signaling Technologies; HRP, horse-radish peroxidase.

Protein	Product ID	Dilution	Secondary
Actin	Sigma A2066	1:300	Goat α -Rabbit HRP-conjugated (PIE31460, ThermoFisher) 1 in 20,000
Fn14	CST 4403	1:500	
MFN-2	Provided by Mike Ryan (Monash University)		
MiD49	Provided by Mike Ryan (Monash University)		
pAcetyl-CoA	CST 3661	1:1000	
Acetyl-CoA	CST 3676		
AMPK α	CST 2532		
CD68	Abcam 125212		
COXIV	CST 4844		
LC3B	Sigma L7543		
p100/p52	CST 4882		
ULK	Abcam 128859		
TWEAK	Abcam 37170	1:2000	
Calpain-3	Novocastra NCL- CALP2-12A2	1:100	Goat α -Mouse intact HRP-conjugated (ab97023, ThermoFisher) 1 in 20,000
Desmin	Novocastra NCL-L-DES- DERII	1:500	
Myosin	MF-20 DSHB	1:26	Goat α -Mouse HRP-conjugated (PIE31430, ThermoFisher) 1 in 20,000
OPA-1	BD Biosciences 612606	1:1000	
p62	Abcam 56416		

III.b. *Primer details***Table III.2: Primer sequences:** Primer sequence details used for qPCR. Primer Bank ID cited where applicable (Spandidos *et al.*, 2010)

Target	Primer Sequence		Source
Atrogin1	Forward	CGACCTGCCTGTGTGCTTAC	(Kweon, Lee et al., 2019)
	Reverse	CTTGCGAATCTGCCTCTCTG	
mFn14	Forward	AGAAGATGCCGCCGGAGAGAA	designed by Amelia Johnston
	Reverse	ATGAATGGACGACGAGTGGGC	
MRF4	Forward	AGAGGGCTCTCCTTTGTATCC	6678984a1
	Reverse	CTGCTTTCCGACGATCTGTGG	
MuRF1	Forward	AGCTGAGTAACTGCATCTCCATGC	(Nagarajan <i>et al.</i> , 2019)
	Reverse	TTCTCGTCCAGGATGGCGTA	
Myf5	Forward	AAGGCTCCTGTATCCCCTCAC	6678982a1
	Reverse	TGACCTTCTTCAGGCGTCTAC	
MyoD	Forward	CCACTCCGGGACATAGACTTG	6996932a1
	Reverse	AAAAGCGCAGGTCTGGTGAG	
Myogenin	Forward	GAGACATCCCCCTATTTCTACCA	13654247a1
	Reverse	GCTCAGTCCGCTCATAGCC	
PGC-1 α	Forward	TATGGAGTGACATAGAGTGTGCT	238018130c1
	Reverse	CCACTTCAATCCACCCAGAAAG	
TWEAK	Forward	GTGTTGGGATTCGGCTTGGT	7305059a1
	Reverse	GTCCATGCACTTGTCGAGGTC	

III.c. *Optimisation of muscle homogenates*

Initial western blotting showed extensive streaking of samples when viewed on UV Stain-free gel image with poor resolution of distinctive skeletal muscle homogenate bands (Figure III.1A). Removal of excessive OCT mounting media from frozen whole muscle samples and preparation of new homogenates vastly improved the appearance of UV Stain-free gels and eventual western blot images. After removal of excess OCT, several notexin-injured samples remained streaky on UV Stain-free gel image suggesting a widespread degradation of proteins which could not be improved with optimisation (Figure III.1B).

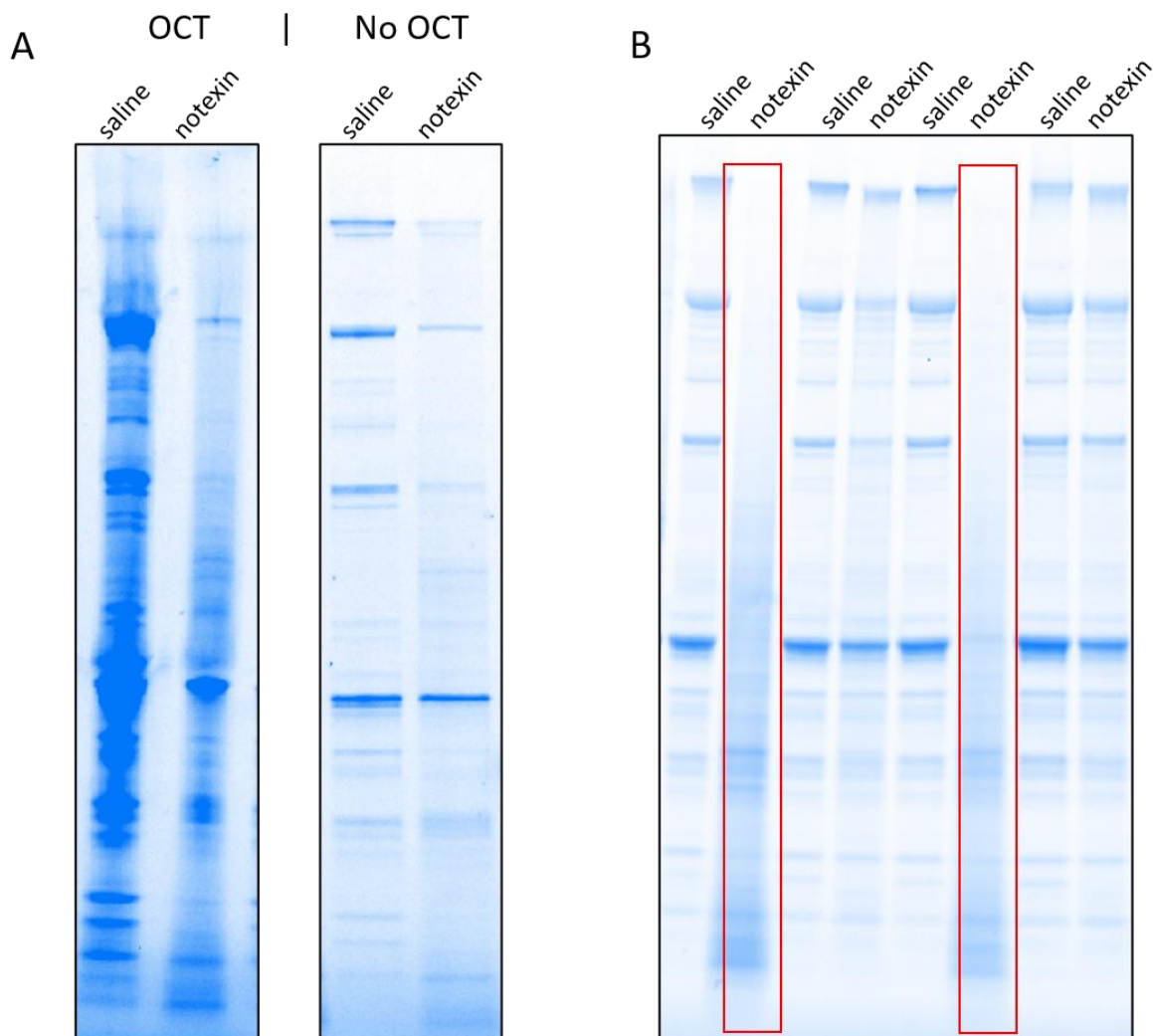


Figure III.1: Optimisation of whole muscle homogenates used for western blotting. (A) Before and after removal of OCT cutting media. (B) Whole muscle homogenates with excess OCT removed, notexin-injured samples showed streaking and loss of distinct protein banding after optimisation (highlighted in red boxes).

III.d. *Unsuccessful MyoD validation*

MyoD is a 34 kDa protein. Several MyoD antibodies were tested on a panel of skeletal muscle samples comprising human pre- and post-acute resistance exercise, *mdx* dystrophic mice at 28, or 70 days age, and 28-day old wild type mice. The only antibody which produced detectable bands was CST 138212 (Figure III.2). The band detected was at approximately 43 kDa and closely followed the appearance of the dense band on the stain-free total protein gel. This band is likely largely comprised of actin and is frequently detected as a non-specific band in our hands. For this reason we were unable to quantify MyoD at the protein level.

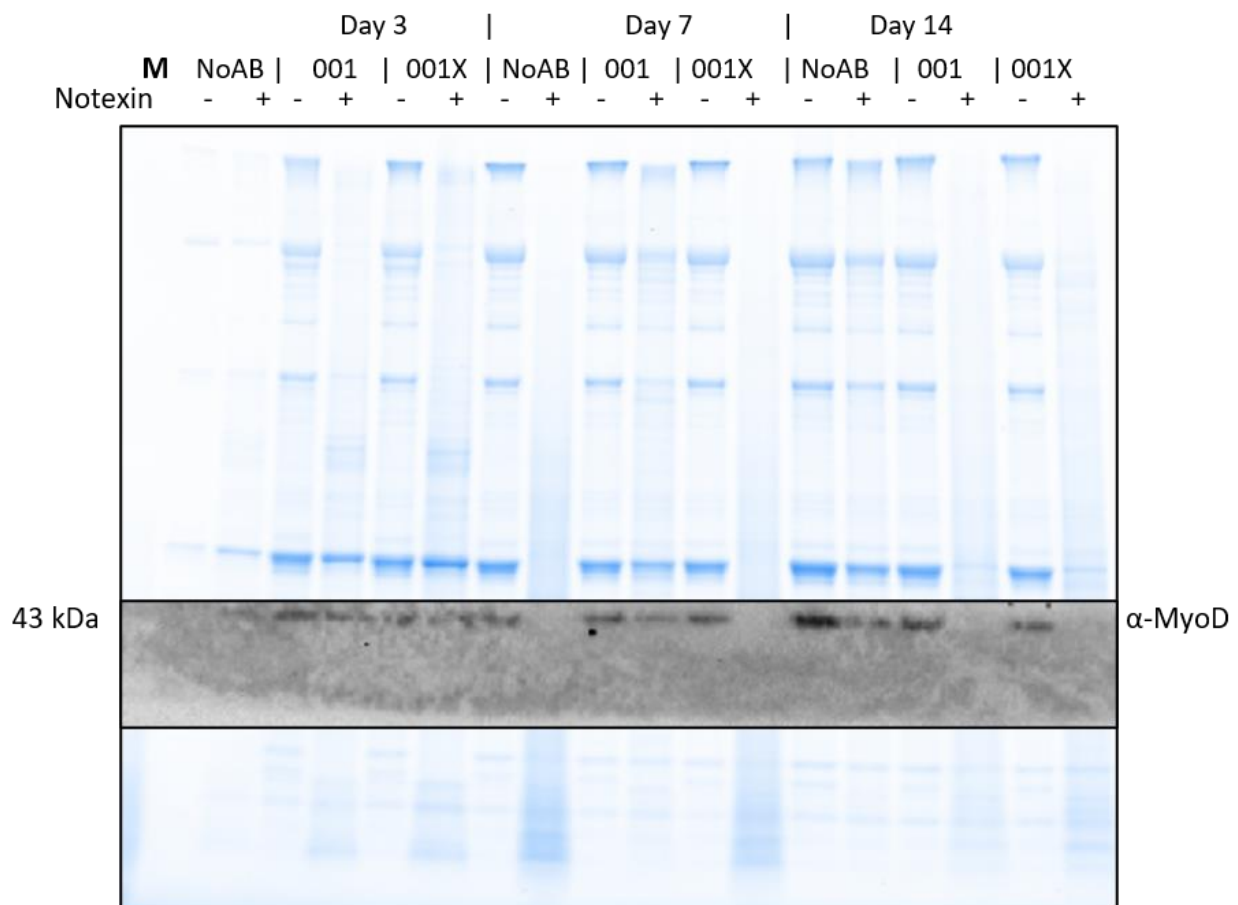


Figure III.2: Representative blot and stain-free UV image of Cell Signaling Technology 13812 α-MyoD antibody validation. A single band was detected at ~43 kDa in mouse tibialis anterior (TA) muscle treated with notexin or saline injection and either no antibody (NoAB), α-Fn14 001, or α-Fn14 001X at 3, 7, and 14 days post-injury (expected molecular weight = 34 kDa). Band was observed to mirror the size and appearance of the characteristic dense band apparent at ~43 kDa, comprised largely of actin protein, in whole skeletal muscle homogenates.

III.e. ***TWEAK antibody validation***

Successful validation of a TWEAK antibody was achieved and detailed below. Following this validation, both mTWEAK and sTWEAK were identifiable by western blot. Figure III.3 is representative of an initial western blot performed on notexin and saline injected TA muscle homogenates and probed for TWEAK (Abcam 37170, 1:2000 in 1% BSA/PBST + 0.2% sodium azide). Multiple bands were detected at approximately 26, 34, 55, and 130 kDa. Bands at 34- and 130 kDa were detected primarily in notexin-injured samples 3 days post-injury and are suspected to be multimeric TWEAK or non-specific binding associated with early inflammatory response. Band at 55 kDa was apparent primarily in saline controls and returned to notexin-injured TA late in the recovery timeline. It is possible that this band is indicative of non-specific binding to a protein, or proteins, which were degraded in the initial notexin injury. Expected molecular weight for TWEAK is 26 kDa for full-length membrane bound TWEAK (mTWEAK) and 18 kDa for cleaved soluble TWEAK (sTWEAK) (Chicheportiche *et al.*, 1997).

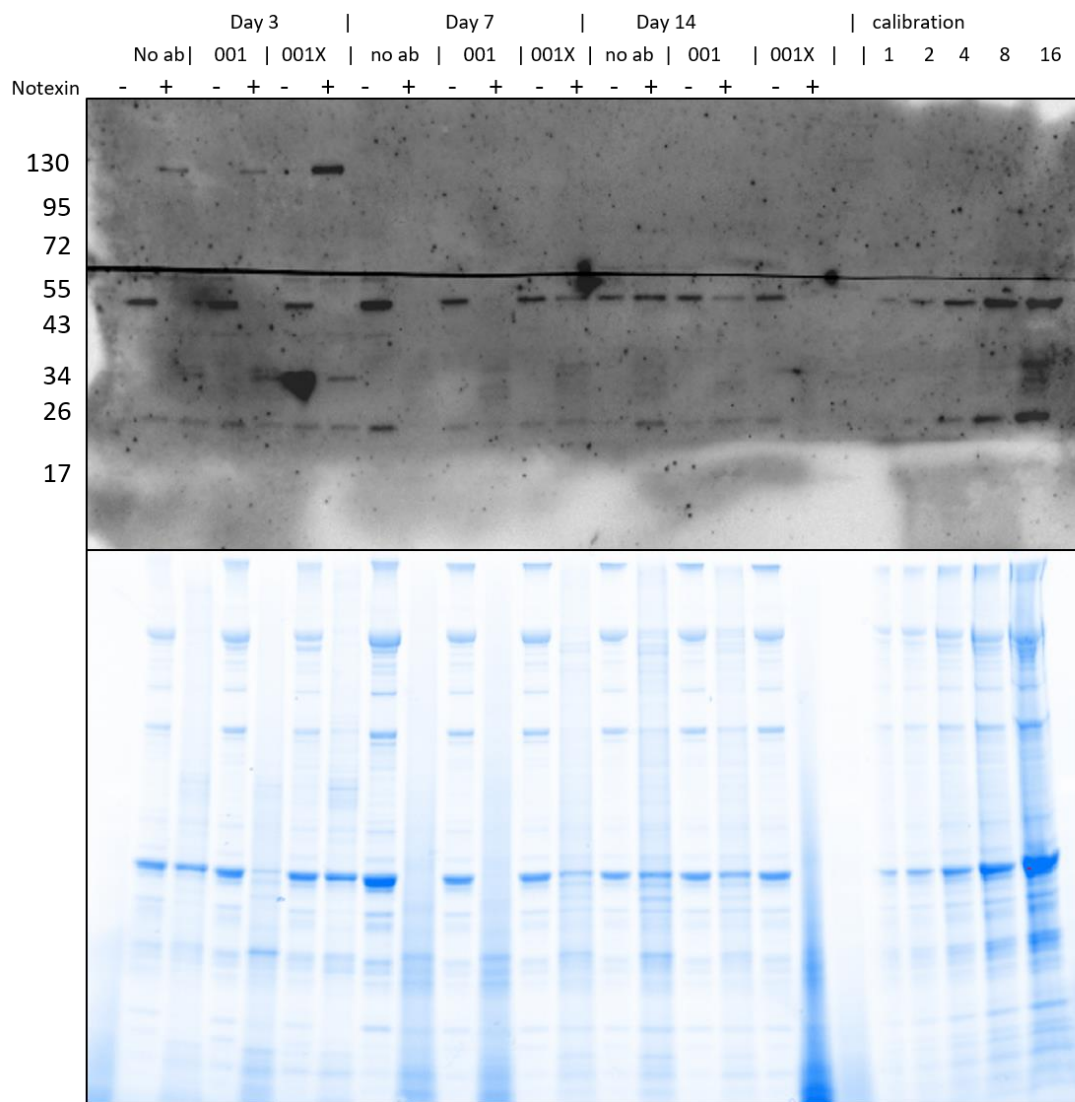


Figure III.3: Full western blot of TWEAK (Abcam 37170) in notexin-injured tibialis anterior (TA) mouse muscle. Multiple bands were detected at 26, 34, 55, and 130 kDa. Expected molecular weight for TWEAK is 18 and 26 kDa (soluble and membrane bound forms, respectively). 34, 55, and 130 kDa bands were selected as potential multimers for further investigation.

In order to better visualise potential bands at 26 and 18 kDa (the expected molecular weights for mTWEAK and sTWEAK respectively), membranes were cut between 34 and 43 kDa and imaged separately (Figure III.4). When imaged separately, an additional band was detected at ~18 kDa predominantly in notexin-injured samples and this was deemed to be sTWEAK.

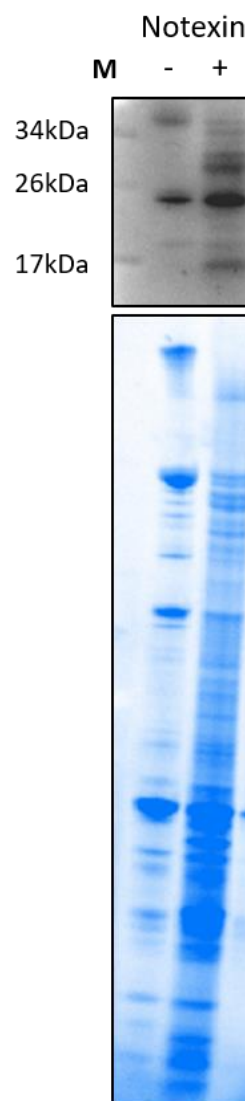


Figure III.4: Western blot of TWEAK (Abcam 37170) below 43 kDa in notexin-injured tibialis anterior (TA) mouse muscle. When probed and imaged separately, an additional band at 18 kDa was detected that appeared primarily in notexin-injured TA.

To confirm the identity of the above western blot results as either genuine multimeric forms of TWEAK or non-specific binding, bands were excised from a 4-15% criterion TGX gel. Samples were run in duplicate with one half of the gel processed for mass spectrometry by the La Trobe University Comprehensive Proteomics Platform and the duplicate samples processed as a confirmatory western blot. Western blot of the excised bands and their corresponding molecular weight is shown in Figure III.5. Results from mass spectrometry identified numerous muscle-specific proteins but failed to identify TWEAK (TNFSF12 *Mus musculus* NCBI Gene ID: 21944). It was determined that the overall abundance of TWEAK in whole muscle homogenate was below the detection limits of mass spectrometry and as such it was decided to proceed only with western blot validation.

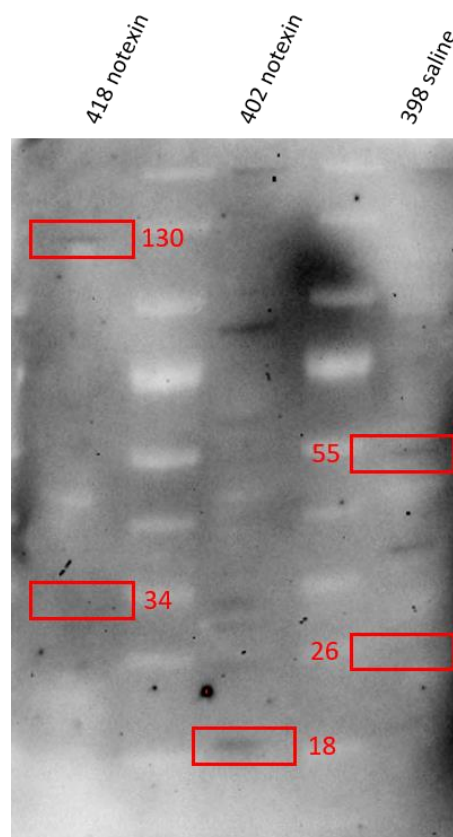


Figure III.5: Western blot of suspected TWEAK bands excised for mass spectrometry. Bands of interest to be excised and analysed by western blot are indicated in red.

Further validation was performed using samples provided by Dr Stefan Wette (La Trobe University). Figure III.6 shows the lower portion of western blot performed on C57BL/6 mouse skeletal muscle and liver homogenates. A prominent band at 26 kDa is observed in the skeletal muscle sample, believed to be mTWEAK, whilst a band at 18 kDa believed to be sTWEAK is the predominant isoform in liver. Furin, the enzyme responsible for the conversion of mTWEAK to sTWEAK (Brown *et al.*, 2010) is abundant in the liver (Dubois *et al.*, 2001). This provides support to these two bands representing mTWEAK and sTWEAK.

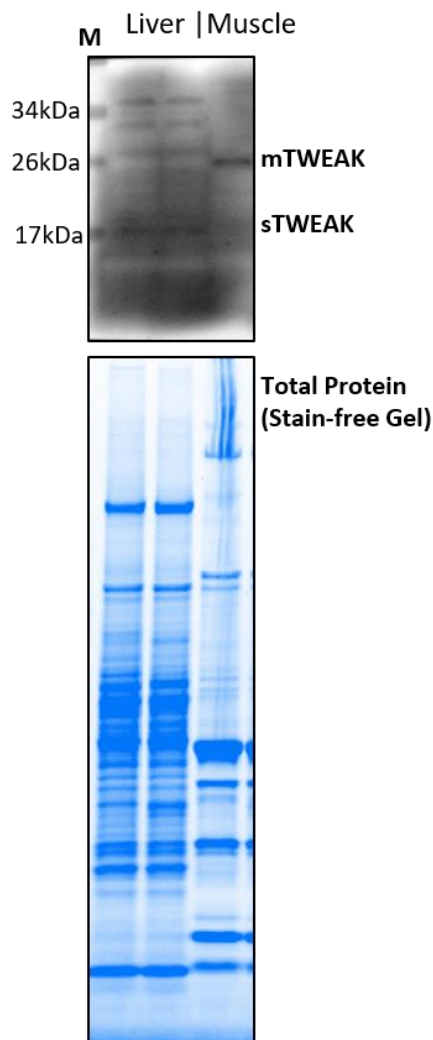


Figure III.6: TWEAK (abcam 37170) validation in mouse liver and skeletal muscle homogenates. Representative western blot and stain-free UV image of total protein. 26 kDa band believed to be mTWEAK was detected strongly in skeletal muscle homogenate, 18 kDa band believed to be sTWEAK was the predominant isoform in liver.

Finally, fractionation of the mouse whole muscle homogenate into its soluble and insoluble components (fractionation performed by Dr Stefan Wette, technique described previously in Wette *et al.* (2017)). Figure III.7 shows bands indicative of mTWEAK and sTWEAK at 26 and 18 kDa, respectively in whole muscle (W). Insoluble fraction (I) shows the vast majority of the 26 kDa band, as is expected of mTWEAK whilst the 18 kDa band is present only in the soluble (S) fraction. Notably this fractionation is not completely clean with some mTWEAK detected in the soluble portion, however this in conjunction with the other validation data provides reasonable confidence to go forward with this antibody when characterising TWEAK.

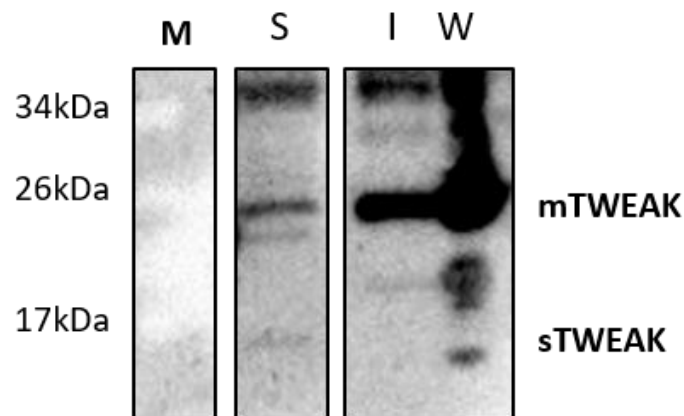


Figure III.7: TWEAK (abcam 37170) antibody testing in fractionated mouse skeletal muscle. W = whole muscle homogenate with multiple bands detected including both 26 kDa (mTWEAK) and 18 kDa (sTWEAK), I = insoluble portion shows primarily 26 kDa band, S = soluble portion shows some residual 26 kDa band as well as the 18 kDa sTWEAK band.

References

- Brown SAN, Ghosh A & Winkles JA. (2010). Full-length, Membrane-anchored TWEAK Can Function as a Juxtacrine Signaling Molecule and Activate the NF- κ B Pathway. *J Biol Chem* **285**, 17432-17441.
- Chicheportiche Y, Bourdon PR, Xu H, Hsu YM, Scott H, Hession C, Garcia I & Browning JL. (1997). TWEAK, a new secreted ligand in the tumor necrosis factor family that weakly induces apoptosis. *J Biol Chem* **272**, 32401-32410.
- Dubois CM, Blanchette F, Laprise MH, Leduc R, Grondin F & Seidah NG. (2001). Evidence that furin is an authentic transforming growth factor-beta1-converting enzyme. *Am J Pathol* **158**, 305-316.
- Nagarajan P, Agudelo Garcia PA, Iyer CC, Popova LV, Arnold WD & Parthun MR. (2019). Early-onset aging and mitochondrial defects associated with loss of histone acetyltransferase 1 (Hat1). *Aging Cell* **18**, e12992-e12992.
- Spandidos A, Wang X, Wang H & Seed B. (2010). PrimerBank: a resource of human and mouse PCR primer pairs for gene expression detection and quantification. *Nucleic Acids Res* **38**, D792-D799.
- Wette SG, Smith HK, Lamb GD & Murphy RM. (2017). Characterization of muscle ankyrin repeat proteins in human skeletal muscle. *Am J Physiol Cell Physiol* **313**, C327-c339.

Appendix IV

Validation of Injury Timeline

Appendix Summary

The following appendix details the selection of notexin injury timeline points using samples provided by Dr Brad Launikonis (University of Queensland) and the validation of injury regenerative markers using barium chloride (BaCl₂) injured samples provided by Dr Chris van der Poel (La Trobe University) and Dr Alex Addinsall (Karolinska Institutet).

IV.a. Notexin Timeline Assessment

The following samples were kindly provided by Dr Brad Launikonis and are published in Head *et al.* (2014). Mice (C57BL/10, 6 m.o., n = 5) were anaesthetised with ketamine (0.1 mg/ g body weight) and xylazine (20 µg/ g body weight) and the *extensor digitorum longus* (EDL) muscle was exposed with a 1 cm incision. Notexin (0.2 µg) was administered directly into the EDL via intramuscular injection. Contralateral EDL was surgically exposed but not injected as an internal control. Injection site was sutured, and mice were returned to individual housing for 21 days prior to euthanasia and tissue collection. Muscles were frozen over liquid nitrogen and stored at -80°C prior to use.

EDL samples were prepared in accordance with western blotting technique described in Chapter 2. Total protein and actin content were assessed by Coomassie staining and western blotting respectively (Rabbit α-Actin antibody, Sigma A2066) as an overall measure of muscle regeneration (Figure IV.1). Notexin-injured EDL protein content was determined to be comparable to contralateral controls at 21 days post-injury. From this observation and previously published time-points, mice in the present study were collected at a final time-point of 14 days post-injury with the intention of capturing muscle which is just approaching full regeneration.

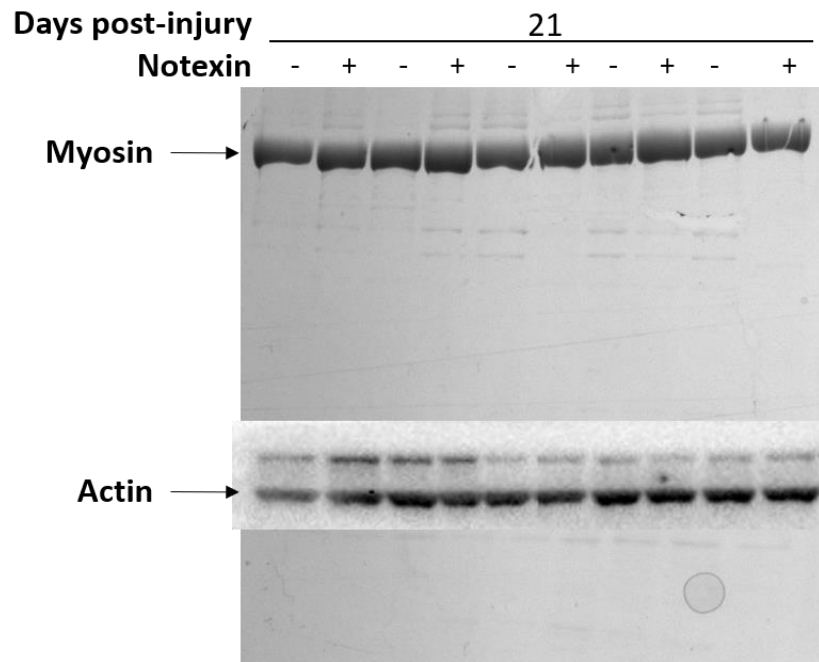


Figure IV.1: Actin and myosin content in notexin-injured tibialis anterior (TA) mouse skeletal muscle 21 days post-injury. Both myosin, visualised by Coomassie stain of post-transfer gel, and actin, visualised by western blot, show comparable levels in notexin-injured TA and saline-treated contralateral control leg.

IV.a.i. Validation of Regenerative Markers

Following the development of unexpected adverse events (detailed in Chapter 4), additional injured muscle samples using an alternative injury mechanism were acquired from Dr Chris van der Poel (La Trobe University) and Dr Alex Addinsall (Karolinska Institutet). C57BL/6 mice were injected with BaCl₂ intramuscularly in the *tibialis anterior* (TA) muscle. Mice were culled and TA muscles were collected at 3 (n = 2), 7 (n = 3), and 14 (n = 4) days post-injury. TA muscles were prepared for western blotting and qPCR as described in Chapter 2.

Expression of Fn14 was assessed at both the protein and mRNA level to confirm upregulation and return to baseline following acute injury (Figure IV.2). Fn14 mRNA was measured in SV40 H-Ras^{V12} Ms6 mouse embryonic fibroblast (MEF) Fn14 knock outs (Fn14-) and wild-type controls (Fn14+), as well as uninjured C57BL/6 TA controls (n = 3), and the three

post-injury time points (3D, 7D, and 14D). Fn14 transcripts were detected at negligible levels in Fn14⁻ cells relative to Fn14⁺. Uninjured TA muscle showed low baseline Fn14 mRNA which was increased ~6-fold at 3 days post-injury. Fn14 transcripts had returned to baseline by 7 days post-injury. Fn14 protein was similarly temporally regulated. Uninjured TA showed non-detectable levels of Fn14 with a sharp induction by 3 days post-injury. Fn14 protein abundance gradually decreased over 7- and 14 days post-injury without fully returning to uninjured levels. From these results it was determined that Fn14 could be transcriptionally and translationally upregulated within 3 days following an acute necrotic injury and that mRNA would return towards baseline with protein expression persisting for longer.

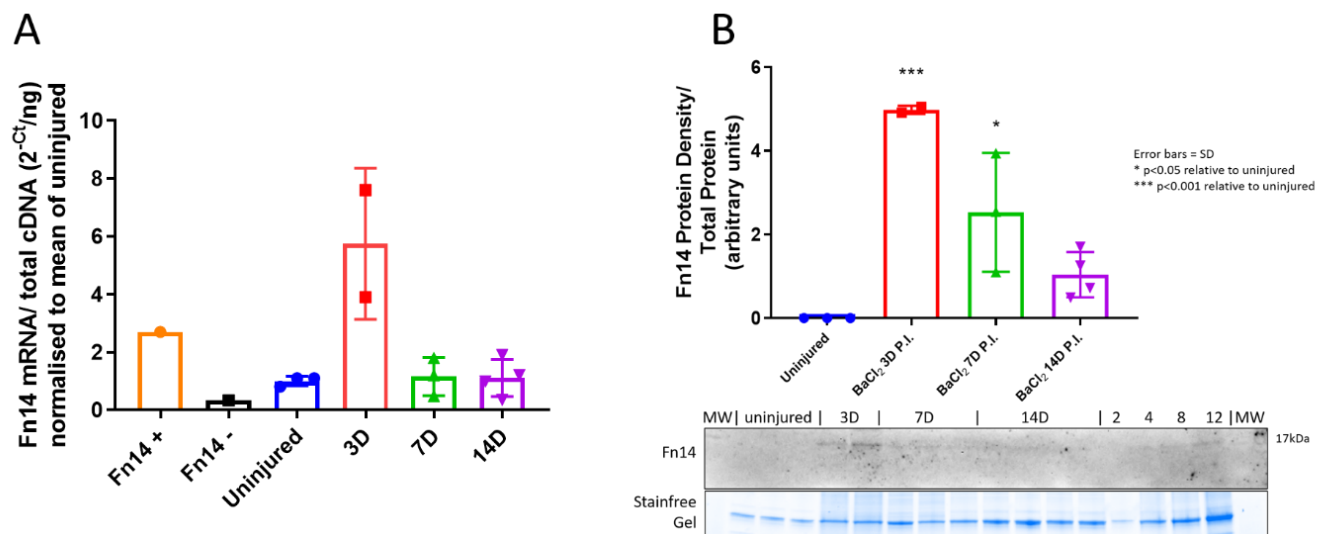


Figure IV.2: Fn14 mRNA and protein abundance following barium chloride (BaCl₂)-induced skeletal muscle injury in mouse tibialis anterior (TA). (A) Fn14 mRNA abundance in uninjured (UI), 3-, 7-, and 14 days post-injury with Fn14 positive and negative control cell lines. (B) Representative blots of Fn14 and stain-free total protein.

Structural proteins, actin and desmin, were measured using quantitative western blotting as described in Chapter 2 (Figure IV.3). Actin was shown to be degraded at 3 days post-injury with a gradual return to baseline levels by day 14. Desmin was expressed at low abundance in uninjured controls and not detectable at 3 days post-injury. Upregulation of desmin beyond baseline was observed at day 7, with a gradual decline at day 14 without returning to baseline. These results were used as a comparative study to assess recovery progression in notexin-injured samples.

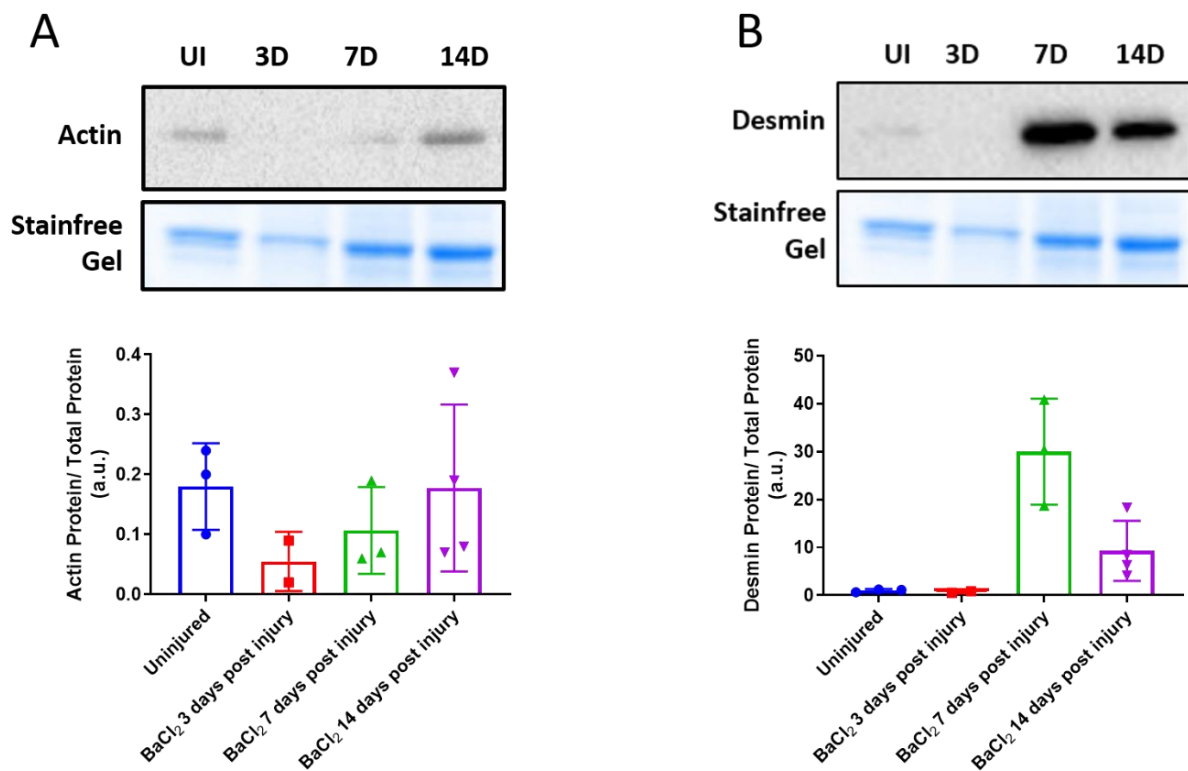


Figure IV.3: Structural protein recovery following barium chloride (BaCl₂)-induced skeletal muscle injury in mouse tibialis anterior (TA). Representative blot and stain-free gel image of Actin (A) and Desmin (B) in uninjured (UI), 3-, 7-, and 14 days post-injury.

E3 ubiquitin-ligases, Atrogin-1 and MuRF-1, were measured at the mRNA level using qPCR as described in Chapter 2 (Figure IV.4). Both Atrogin-1 and MuRF-1 were expressed at low levels in uninjured TA. Transcriptional upregulation was observed in 3 and 7-day post-injury samples for both ligases with peak upregulation at day 14. As this was the latest time point available it was not determined how long transcripts remained upregulated in acutely injured muscle.

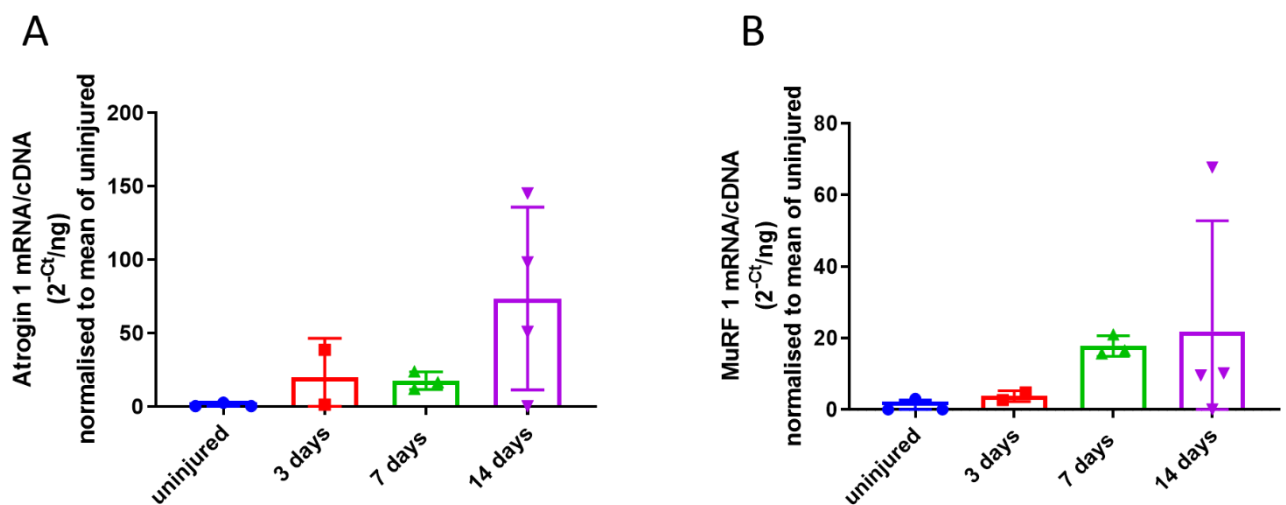


Figure IV.4: Atrogin1 and MuRF1 expression following barium chloride (BaCl₂)-induced skeletal muscle injury in mouse tibialis anterior (TA). mRNA levels of Atrogin1 (A) and MuRF1 (B) normalised to total cDNA in uninjured, 3-, 7-, and 14 days post-injury.

References

Head SI, Houweling PJ, Chan S, Chen G & Hardeman EC. (2014). Properties of regenerated mouse extensor digitorum longus muscle following notexin injury. *Exp Physiol* **99**, 664-674.

Appendix V

Statistical Correlation Tests

Appendix Summary

This appendix shows the statistical correlation tests between TWEAK-Fn14 and *quadriceps* muscle mass performed on the muscle from old and chronically low-resistance trained mice described in Chapter 5 and Chapter 6. These correlations showed that the TWEAK-Fn14 axis was not correlated with muscle mass in these mice and was not responsive to exercise intervention. For this reason, Chapter 6 focuses on the role of mitochondria and autophagy in old and exercised mice.

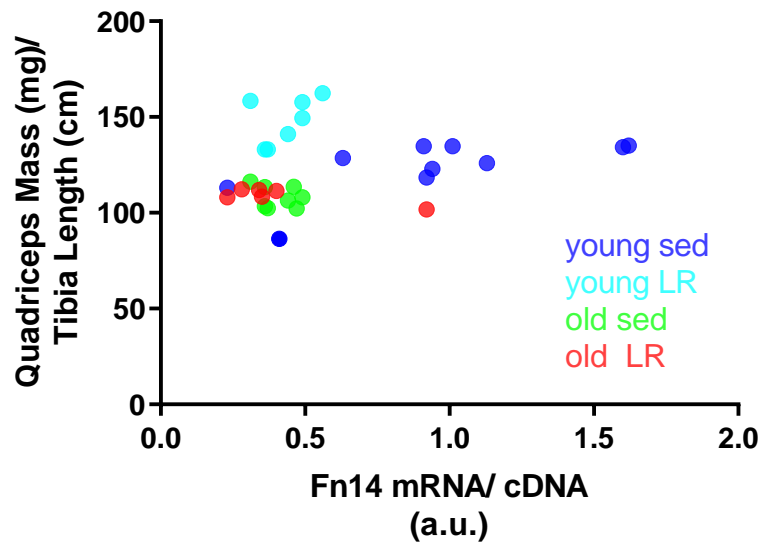
V.a. Fn14 mRNA correlation with quadriceps mass

Figure V.1: Correlation between Fn14 mRNA and normalised quadriceps muscle mass in old and chronically low-resistance (LR) trained mice.

Table V.1: Pearson co-efficient tests of Fn14 mRNA correlation normalised quadriceps muscle mass in old and chronically low-resistance (LR) trained mice. Significant but weak correlation was seen only in Young Sedentary (SED) mice.

	Young SED	Young LR	Old SED	Old LR
Pearson r				
r	0.6988	0.4857	-0.2863	-0.3108
95% confidence interval	0.06473 to 0.9309	-0.4215 to 0.9070	-0.8246 to 0.5241	-0.8621 to 0.5774
R squared	0.4883	0.2359	0.08198	0.09660
P value				
P (two-tailed)	0.0362	0.2692	0.4918	0.4975
P value summary	*	ns	ns	ns
Significant? (alpha = 0.05)	Yes	No	No	No
Number of XY Pairs	9	7	8	7

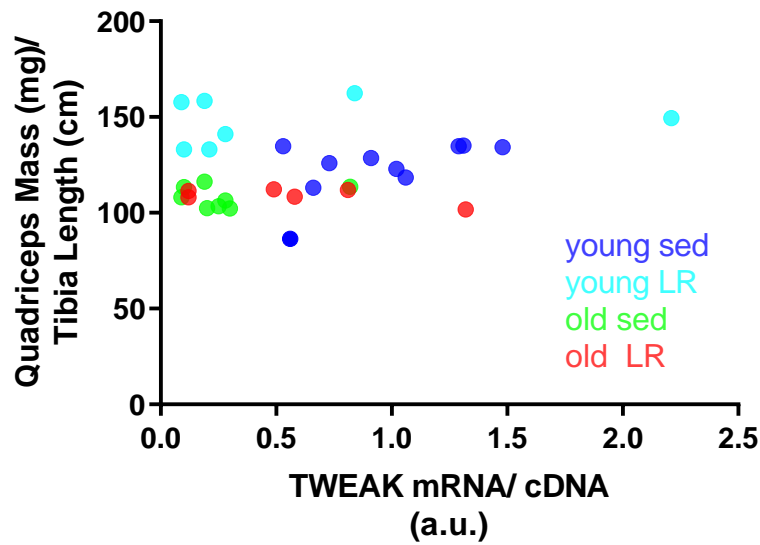
V.b. TWEAK mRNA correlation with quadriceps muscle mass

Figure V.2: Correlation between TWEAK mRNA and normalised quadriceps muscle mass in old and chronically low-resistance (LR) trained mice.

Table V.2: Pearson co-efficient tests of TWEAK mRNA correlation normalised quadriceps muscle mass in old and chronically low-resistance (LR) trained mice. No significant correlations were detected.

	Young SED	Young LR	Old SED	Old LR
Pearson r				
r	0.4235	0.2110	0.1976	-0.2350
95% confidence interval	-0.3348 to 0.8489	-0.6444 to 0.8319	-0.5891 to 0.7920	-0.8395 to 0.6294
R squared	0.1794	0.04454	0.03903	0.05525
P value				
P (two-tailed)	0.2560	0.6496	0.6391	0.6119
P value summary	ns	ns	ns	ns
Significant? (alpha = 0.05)	No	No	No	No
Number of XY Pairs	9	7	8	7

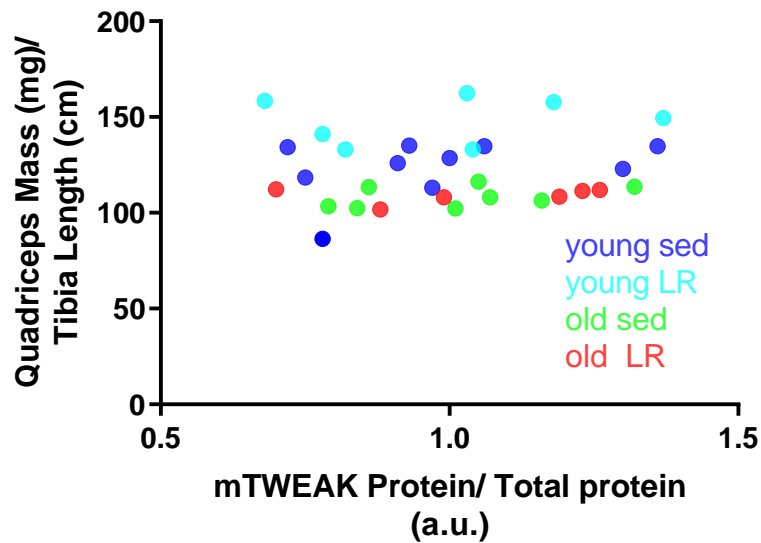
V.c. TWEAK protein correlation with quadriceps muscle mass

Figure V.3: Correlation between membrane-bound TWEAK (mTWEAK) protein and normalised quadriceps muscle mass in old and chronically low-resistance (LR) trained mice.

Table V.3: Pearson co-efficient tests of membrane-bound TWEAK (mTWEAK) protein correlation normalised quadriceps muscle mass in old and chronically low-resistance (LR) trained mice. No significant correlations were detected.

	Young SED	Young LR	Old SED	Old LR
Pearson r				
r	0.1495	0.1672	0.4334	0.4895
95% confidence interval	-0.5713 to 0.7401	-0.6702 to 0.8174	-0.3906 to 0.8718	-0.4174 to 0.9079
R squared	0.02235	0.02797	0.1878	0.2396
P value				
P (two-tailed)	0.7010	0.7201	0.2834	0.2649
P value summary	ns	ns	ns	ns
Significant? (alpha = 0.05)	No	No	No	No
Number of XY Pairs	9	7	8	7